EFFECTS OF HYDROCARBON FOULING

ON

REVERSE OSMOSIS MEMBRANES

M. Hassan Owadally BEng (Hons)

Submitted in fulfilment of the requirements for

the Degree of MSc by Research

Department of Mechanical Engineering

Faculty of Engineering

University of Glasgow

October 2008

To my Mother and Father.

ABSTRACT

Organic fouling in reverse osmosis (RO) has been studied using model hydrocarbons such as hexane and diesel. A large number of countries that use reverse osmosis to obtain drinking water also are producers and exporters of hydrocarbons. This makes seawater RO units particularly susceptible to damage from oil spills. This project is focused on the repercussions of such an incident on the performance of the above-mentioned modules. The study has concentrated on the lower molecular weight hydrocarbons present in contaminated seawater feed as it can be safely assumed that organics of higher molecular weight will have already been dealt by passage through the RO pre-treatment processes.

The organic foulants chosen for investigation are: diesel (a likely constituent arising from spillages) and hexane (chosen as a model low-molecular-weight hydrocarbon). The study has investigated the effects of the presence of these contaminants in both water-soluble and emulsion form. The membranes tested are brackish water membranes and seawater membranes of different structures polyamide based and CTA (cellulose triacetate). These membranes were tested in saline water mainly at the salinity, 5500 ppm NaCl.

The performance of the RO unit, in terms of salt passage and permeate flux through the membranes, were assessed before and after fouling. These results have been correlated with microscopic examinations of the surface of the membranes. Substantially different effects of exposure to hydrocarbons have been monitored between different membranes and also in terms of the active and support layers of a particular membrane.

CONTENTS

INDEX OF FIGURES

TABLES

ACKNOWLEDGEMENTS

I wish to extend my thanks and gratitude to my supervisor Dr. Trevor Hodgkiess for his advice and guidance throughout the course of this work.

I would also like to express my thanks to the Faculty of Engineering and the Department of Mechanical Engineering for having granted me the opportunity to carry out this research.

DECLARATION

I declare that this thesis has been composed by me and is a record of work performed by me unless otherwise stated. It has not been previously submitted for any other degree. The work described in this thesis was carried out under the supervision of Dr. Trevor Hodgkiess in the Department of Mechanical Engineering at the University of Glasgow.

M. Hassan Owadally

NOTATION

Symbol	Representing	Units
C_b	Salt concentration in feed tank	g/cm^3
C_d	Salt concentration in permeate flow	g/cm^3
C_s	Salt concentration	g/cm^3
ΔC_s	Salt concentration across the membrane	g/cm^3
J_1	Water flux through the membrane	$g/cm^2/sec$
J_2	Salt flux through the membrane	$g/cm^2/sec$
k_1	Water permeability of the membrane	$g/cm^2/sec/bar$
k_2	Salt permeability of the membrane	cm/sec
m_d	Permeate flow rate	kg/sec
N_{Re}	Reynolds number	-
P	Pressure	bar
ΔP	Pressure differential across the membrane	bar
R	Universal gas constant	kJ/kg-mol/K
T	Absolute Temperature	K
X_s	Salt mole fraction	-
ν	Number of ions per molecule of solute	-
ν_w	Molar volume of water	$m^3/kg\text{-}mol$
Π_f	Osmotic Pressure of feed	bar
Π_p	Osmotic Pressure of permeate	bar
$\Delta\Pi$	Osmotic pressure difference across the membrane	bar

Table 1 Notation

CHAPTER 1 INTRODUCTION

1.1 Setting the Scene

Water is crucial for human survival and development, the human body is made up of a very high proportion of water. In a modern society water is needed not only for consumption and agriculture but also for many other industrial processes.

There are numerous sources of fresh water such as rivers, lakes, underground sheets and also manmade reservoirs and dams. These all depend on rain to be replenished. Rain is due to solar energy evaporating water from oceans, lakes, soil and vegetation surfaces. The water then condenses to form clouds that return the water to the surface in the form of rain and snow. This overall process is referred to as the water cycle and is depicted in Figure 1-1.

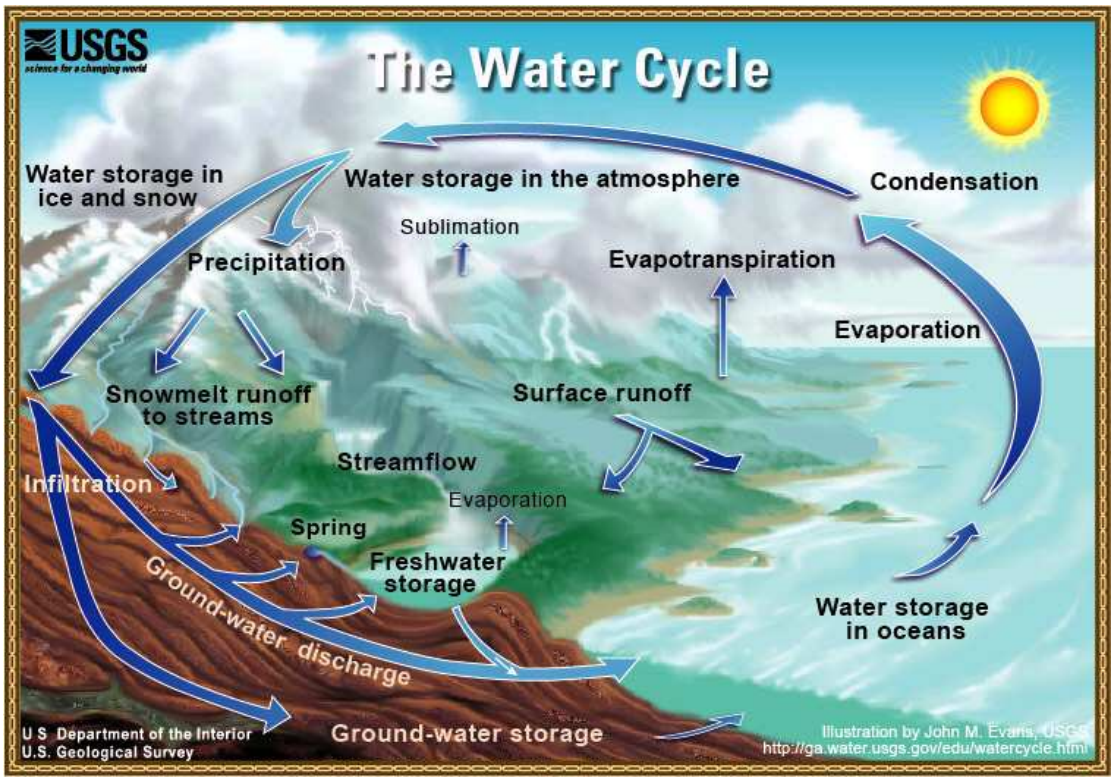

Figure 1-1 Hydro Cycle Diagram.[1]

This cycle under ideal circumstances should provide an adequate source of fresh water to the whole of the earth's inhabitants. Unfortunately the distribution of rain and fresh water bodies is not uniform. This means that some parts of the planet receive very little rain and have no other readily available fresh water sources. These countries have to turn to other means of obtaining water if they want to sustain a viable economic development Figure 1-2.

Most of the earth's water is locked in the form of seawater in the oceans; these cover approximately 75 % of the earth's surface. Many of the dry regions have borders with the sea, so finding a way to process the seawater at a reasonable cost would partially if not completely solve their water problems.

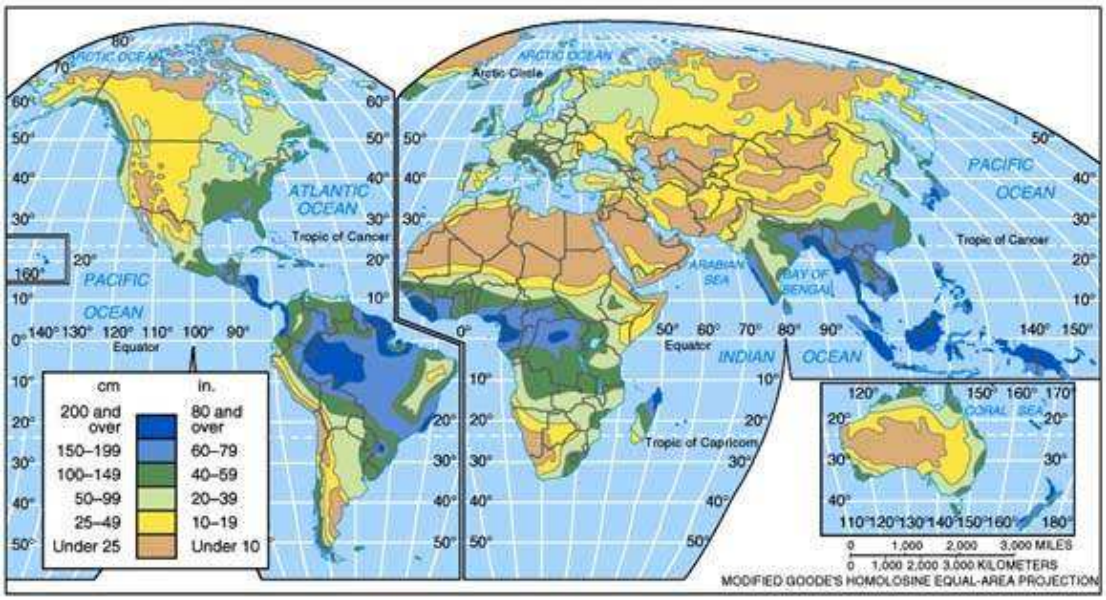

Figure 1-2 Global Rain Distribution Diagram.[2]

1.2 Why the Work is being Done

The process by which seawater or brackish water is processed to produce fresh water which is suitable for human consumption is called desalination. This result can be achieved by numerous methods ranging from freezing, distillation to reverse osmosis. The World Health Organisation recommended maximum total dissolved solids (TDS) in water for human consumption is 500 ppm.

A number of countries that suffer from a shortage of fresh water are located in oil rich parts of the world. This increases the risk of an oil spill. Any other coastal region could also be affected by an oil spill, as oil-carrying tankers have been known to have shipwrecks and send many thousands of tonnes of petroleum product into the sea. This is then carried to the shores and the intake of any desalination plants that may be nearby. Fortunately the heavier fractions are likely to be taken care of by pre-treatment. The only fractions that would be expected to get through to the membrane would most likely be in the form of dissolved hydrocarbons and emulsions with the seawater.

This takes us to the need to investigate the repercussions of such products on the performance of the plant. The type of plant that is being concentrated on is the reverse osmosis one.

Reverse osmosis is the process by which fresh water moves from a solution of higher salt concentration to one of lower concentration, the two being separated by a semi-permeable membrane. This is achieved by applying pressure on the more saline side with higher pressure to overcome the osmotic pressure to force the water to flow in the opposite direction that it would normally do if no pressure was applied.

The part of this process that is most prone to be affected by any form of contamination is the membrane. In the research described in this thesis a number of membranes were tested to access their performances before and after being exposed to different hydrocarbons. This should help model what would happen in such an incident in reality.

The overall objective was to study the effect of fouling on commercial reverse osmosis membrane when exposed to hydrocarbon based fluids. The detailed objectives were as follows:-

- To compare the performance, in terms of, water flux and salt rejection, before and after exposure to hydrocarbons of varying concentrations.
- To focus on the effects of a model hydrocarbon, hexane, but some attention is directed to the effect of fouling in a diesel environment.
- To investigate the susceptibility to hydrocarbon fouling of a range of commercial reverse osmosis membranes: a polyamide seawater membrane, a polyamide brackish water membrane and a cellulose triacetate brackish water membrane.
- To ascertain the mechanism of any fouling phenomenon, principally by the use of light optical and scanning electron microscopy.

1.3 Outline of the Thesis

This thesis will look at desalination in general and will include an over view of the desalination methods that are available just now. These can be classified in two categories, thermal processes and membrane processes. While membrane processes are a relatively new (50 years) invention, thermal processes have been around for centuries. There even are references to thermal processes in the bible.

Membrane processes are considered in more detail and especially the process of reverse osmosis. Special attention is given to reverse osmosis membranes and to the two following types:

a) Asymmetric Membrane

b) Thin film Composite (Cellulose TriAcetate)

The thesis then goes on to consider the susceptibility of reverse osmosis membranes to different types of fouling. The main categories of fouling are colloidal and organic. This part of the thesis includes a review of the literature on organic fouling by hydrocarbons.

There follows a description of the experimental protocol used in this study of fouling of reverse osmosis membranes by hydrocarbons. The main series of experimental findings are then presented; these determine the effects of fouling on the performance of the membranes in terms of change in flux and salt passage. The discussion of the experimental results includes some observations made by microscopy aimed at identifying the fundamental mechanism of any deterioration processes.

The thesis concludes with a summary of the main findings and their relevance to operational aspects of hydrocarbon fouling together with some recommendations for future work.

CHAPTER 2 DESALINATION PROCESSES

2.1 The Availability of Water

Earth, or the blue planet as it has been called, is very rich in water, this factor has enabled life to flourish on its surface. The absence of water on the other planets has made them inhospitable for any life form. Water is the very essence of life and is part of every living organism. Not only has water enabled this planet to sustain life but as we can see it has also enabled this life and more particularly mankind to evolve. Throughout the ages the location of human settlement has been guided by the availability of fresh water. Therefore it is no wonder that many important cities of the developed world are located on the banks of rivers or near to a fresh water source. That has allowed man to develop a growing agricultural sector and with easy access to water, thus in time man has been able to develop industry and advanced technologies. The growth of human civilisation has been dependent on the reliability of water sources. Throughout history it can be seen how civilisations have evolved and prospered while they had plenty of water but when water became scarce this such prosperous civilisation suffered a sharp decline.

However much modern man has progressed and mastered much of the environment, we are still very dependent on water for our survival and future advancement. So it makes sense that we manage the fresh water resources we have and also look for new ways of guaranteeing reliable water sources for the future. As the world population increases, the available water resources, if not expanded, will be stretched more and more to cater for that population reaching points where the lack of water will hamper further development.

Even though it may not seem to be the case in the western world, fresh water is a scarce resource in many parts of the world but on the other hand seawater is plentiful even in regions described as arid. Figure 2-1 below is an indication of how water can be found on the planet.

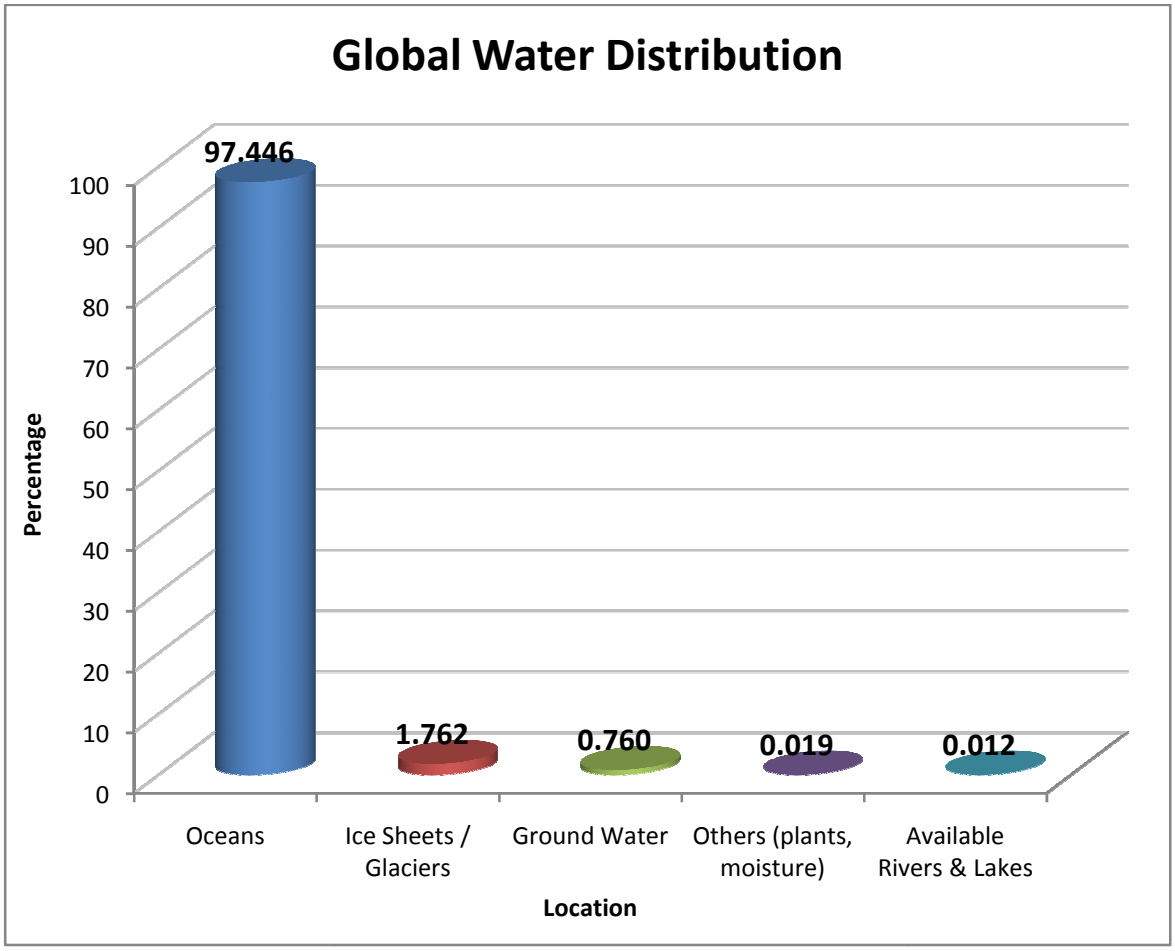

Figure 2-1 Global Water Distribution.[3]

Seawater is a plentiful resource, about 75 % of the planet is covered by it. This is also where most of the surface water is trapped. Unfortunately this water is not usable as is, as on average it is constituted of 3.5 % by mass of dissolved mineral salt. It makes sense that humans find ways to tap into this large reserve. The water cycle is a way by which nature performs desalination, the water is heated up by the sun and it evaporates leaving the non-volatile salts behind. This evaporated water forms clouds, which in turn fall, as rain. Unfortunately only a very small percentage (about 1 %) of

that rain falls on land. This rainfall, if evenly distributed, may be adequate for mankind. That is not the case, which means that some inhabited regions of the planet receive little or no rain at all. The lack of water in other uninhabited regions means that humans cannot settle there, hence reducing the possibility of expansions in these areas, which in turn may adversely affect the economy of that region, thus the need for an alternate source of fresh water. The most economical and reliable alternative must be found. In regions that are within reasonable range of sources of brackish water or seawater, desalination turns out to be a viable option.

2.2 Summary of Historical Development of Desalination

Desalination is the removal of salt from fluids such as brackish water and seawater.

The concept of producing fresh water from seawater is rather antique. There are some allusions to water treatment in the Bible. In his writings Aristotle explains how Greek Sailors from the 4th century BC evaporated seawater. He [4] also speculates "*If one plunges a water-tight vessel of wax into the ocean, it will hold, after 24 hours, a certain quantity of water, which filtered into it through the waxen walls, and this water will be found to be potable, because the earthy and salty components have been sieved off*".

This could not be achieved at that time because of the logistics involved; vessel capable of withstanding a great deal of pressure and it would have to be immersed to depths of approximately 500m.

Other ingenious methods were devised usually by sailors who were faced with the threat of thirst on their voyages. One such method was to place a sponge over a jar of boiling seawater to collect the steam.

There is another mention of desalination in the 8th century AD by an Arab scholar and so on. 1869 saw the award of the first patent for desalination in England. The first commercial still was built in Aruba, near Venezuela, in 1930.[5]

In the 20th century AD, the two main commercial desalination processes to be developed and refined are thermal processes and membrane processes.

2.3 Thermal Desalination Processes

2.3.1 Introduction

The available thermal processes involve changing the seawater from one state to another. There are two choices

1. Evaporation → Condensing.
2. Freezing → Melting.

Evaporation is more obvious as while water evaporates at a relatively low temperature salts do not, the steam thus obtained is then condensed to form pure water. This is referred to as **distillation**.

Freezing is the crystallisation of water by cooling. In the same way as above when the seawater is cooled to a low temperature ice forms. The ice is virtually free from salt. An example of this in nature is the iceberg. It is in theory more efficient than boiling, and corrosion and scaling are less of an issue. But it takes more time and is not as practical on a large scale due to the difficulty involved in separating liquid and ice mixtures. The other problem that arises is that of keeping the process at such low temperatures, as these plants would mainly be located in rather hot regions.

2.3.2 Distillation

There are a number of distillation methods that have been developed but the two predominant ones are

- Multi effect evaporation
- Multi-stage flash distillation (MSF)

MULTI EFFECT EVAPORATION (ME)

Multi effect evaporation was developed to be used by the chemical industry and was also used in the production of sugar. It was the first process to be used to produce water from the sea on a large scale. This method of distillation remains an important desalination process but, for the largest plants, it has been largely superseded by Multi-stage flash distillation (MSF).

The Multi effect evaporation process consists of evaporating seawater to form vapours which are in turn passed into a condenser, which also serves as a secondary evaporator. This can be repeated, and each such unit is called an effect. For this to work, pressure and hence the boiling temperature of the second evaporator cannot be the same as the first, this is achieved by connecting the second evaporator to a vacuum pump.

As the number of effects is increased the volume of water produced per unit of the initial steam also increases proportionally. Usually up to 20 effects are used for an optimum yield.

MULTI-STAGE FLASH DISTILLATION (MSF)

Multi-stage flash distillation (MSF) is a very simple process. It consists of causing seawater to evaporate and condense in a series of chambers, hence the term multi. Seawater is heated up and then introduced in a chamber at a lower pressure, this causes some of the water to evaporate (flash). This vapour then condenses on cooler tubes which contain the feed seawater that will be heated even more as it passes in the heater. A plant will be made up of a number of such units that are connected in series and have progressively less pressure. The feed seawater input is connected to the last unit where the temperature and pressure are lowest and it progresses toward the hottest unit thus being heated on the way. The rest of the heat is imparted to it in the heater. The product water that is formed on the cooler tubes is trapped on trays that are installed under the tubes. The salt exits with the remaining un-evaporated water. This method of desalination is not efficient, for example an evaporation of 7.1 % of the water causes the temperature to drop from 100 ^{o}C to 60 ^{o}C i.e. by 40 ^{o}C. However this method has a very simple design, which makes it rather attractive where larger plants are required.

SOLAR DISTILLATION

Solar radiation is a very abundant source of energy, and is more particularly so in dry coastal regions where it can be used to extract fresh water from seawater throughout the year. Solar distillation has been used for more than a thousand years though in the early applications it was to produce salt rather that water. The principle is very simple, solar energy is used to heat the seawater or brackish water and make it change to vapour which is then collected and stored to be used.

For an efficient process the unit must be able to achieve a high temperature for the feed and there must be as high as possible a temperature difference between the feed and the condensing surface. It is also very desirable to have very low or no vapour leakages.

To achieve a high feed temperature, a large amount of the solar energy needs to be absorbed by the water, this can be achieved by using a good radiation absorbing base and low radiation absorbing glazing. The level of water must also be kept low.

Having a low absorbing glazing also ensures that the condensing surface is at a low temperature.

2.4 Membrane Processes

2.4.1 Introduction

Separation processes involving selectively permeable membranes of one sort or another have become quite popular during the past 25 years. Membrane based processes have numerous advantages. For one they require much less energy [6] which reflects well on the cost of production considering the rising cost of energy. The underlying technology is also rather simple.

The selectively permeable membrane is the heart of the process, and its properties determine the result of the process. The membrane acts as a selective barrier and theoretically allows only certain substances to pass. This selective behaviour depends on the type of membrane used. To achieve this some membranes use pore sizes whilst others use electric charge. Some important membrane processes are listed below

- Micro-filtration
- Ultra-filtration
- Nano-filtration
- Electrodialysis
- Reverse Osmosis

Electrodialysis produces separation on the basis of charge. Micro-filtration, Ultra-filtration, Nano-filtration, and Reverse Osmosis are all pressure driven processes. The main difference is in the size of the particles they allow through. Figure 2-2 (based on 'The Osmonics Filtration Spectrum' [7]) is an indication of what they can be used to remove and the sizes of the particles that are let through.

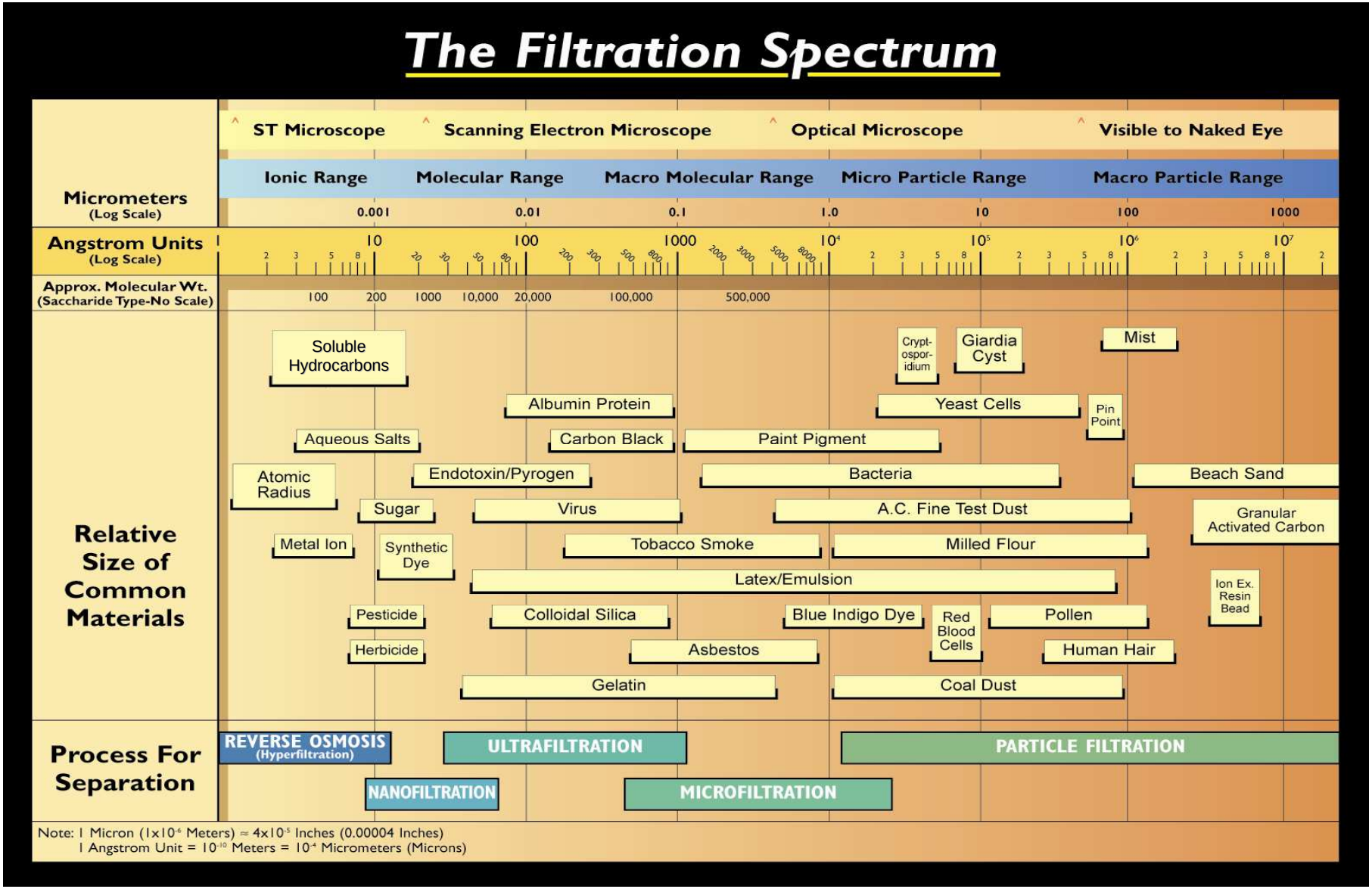

Figure 2-2 Filtration Spectrum (based on ref [7])

2.4.2 Electrodialysis

Electrodialysis is an electrically driven membrane process. It makes use of an electric field to drive ions through ion-exchange membranes as depicted in Figure 2-3. A single cell contains two selective membranes, one that allows cations through while the other only allows anions to pass. When a current is applied to the cell the positively charged ions will flow in one direction and through a cation exchange membrane while the negatively charged ion will migrate in the opposite direction and through the anion exchange membrane. The result is that the solution in the initial chamber will be depleted of ions. The adjacent chambers will contain the concentrated liquids of anions and the other of cations. Electrodialysis is favoured in situations where a high recovery rate of the feed is required.

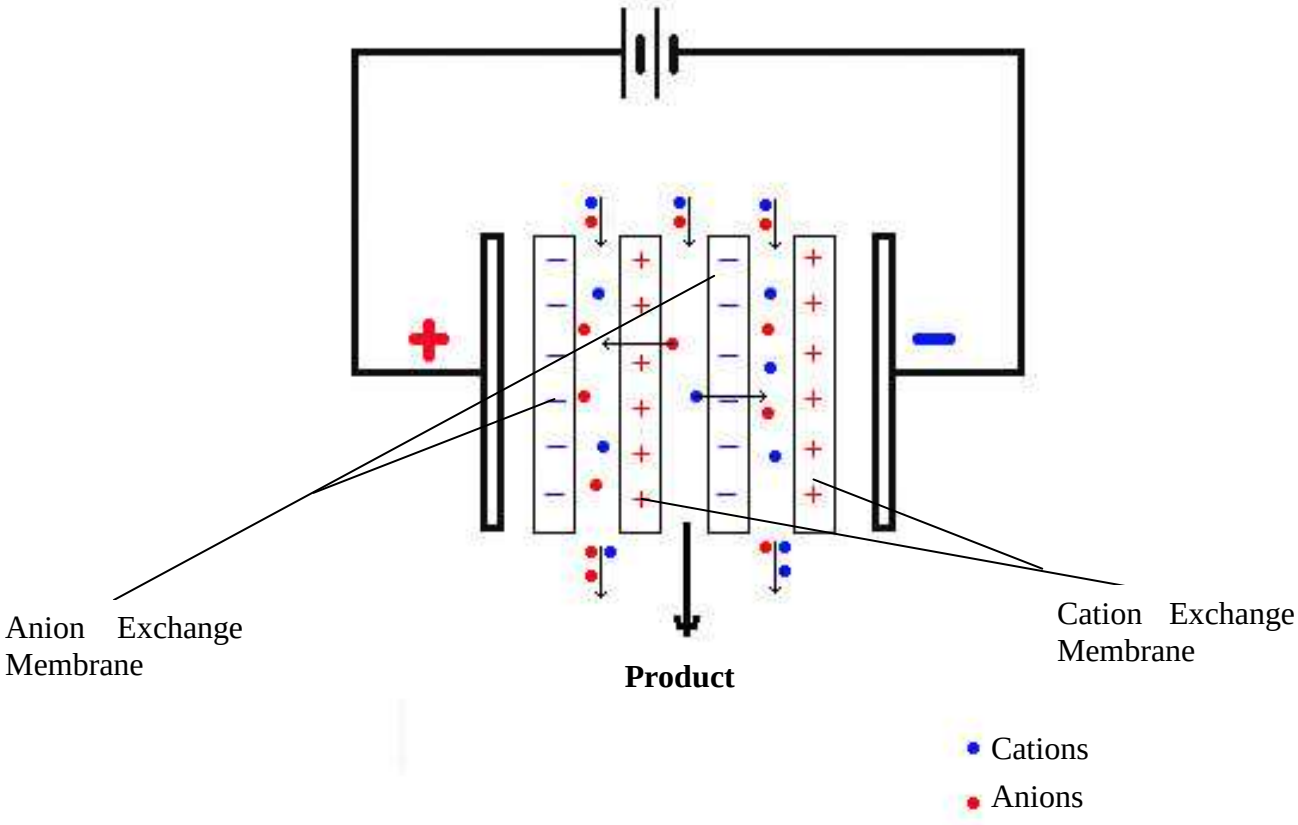

Figure 2-3 Electrodialysis

2.4.3 Micro-filtration and Ultra-filtration

Micro filtration and ultra filtration both use the same principles except for the fact that the pores in an ultra filtration membrane are much tighter. These membranes (Figure 2-4) act as physical selective barriers and they only allow particles of sizes smaller that the pores to pass. Suspended solids and microorganisms together with dissolved solids will be retained on the surface of these membranes. Larger dissolved organics are also rejected by ultra filtration membranes.

Process	**Pore size** Micron/µm
Microfiltration	0.1 to 10
Ultrafiltration	0.1 to 0.01

Table 2 Membrane Pore size.[8]

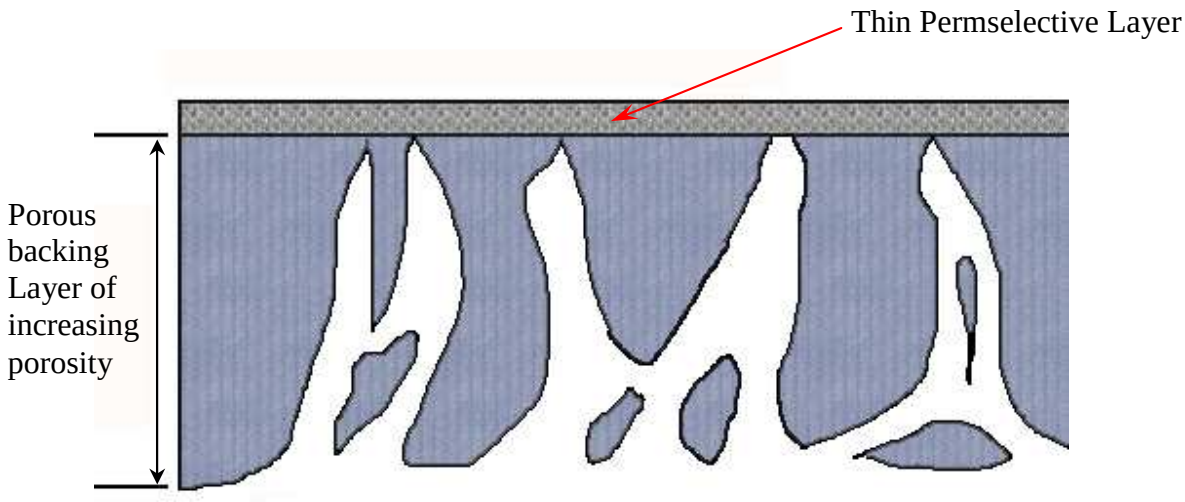

Figure 2-4 Cross-section of a typical Ultra-filtration Membrane

The extent to which suspended solids, turbidity and micro organisms are removed is determined by the size of the pores in the membranes. Substances that are larger than the pores in the membranes are fully removed. Substances that are smaller

than the pores of the membranes are partially removed, depending on the formation of a gel layer on the membrane during filtration.

Micro filtration and ultra filtration are pressure-dependent processes, which remove suspended solids and other substances from water to a lesser extent than nano filtration and Reverse Osmosis.

MICRO FILTRATION

Membranes with a pore size of 0.1 – 10 µm perform micro filtration. Micro filtration membranes will remove all bacteria. Part of the viral contamination is caught up in the process; this is because even though viruses are smaller than the pores of a micro filtration membrane, viruses can attach themselves to bacterial biofilm.

Examples of micro filtration applications are:

- Cold sterilisation of beverages and pharmaceuticals
- Clearing of fruit juice, wines and beer
- Separation of bacteria from water (biological wastewater treatment)
- Effluent treatment
- Separation of oil/ water emulsions
- Pre-treatment of water for nano filtration or Reverse Osmosis
- Solid-liquid separation for pharmacies or food industries

ULTRA FILTRATION

Ultra filtration will remove viruses completely. The pores of ultra filtration membranes can remove particles of 0.01 – 0.1 µm from fluids.

Examples of fields where ultra filtration is applied are:

- The dairy industry (milk, cheese)
- The food industry (proteins)
- The metal industry (oil/ water emulsions separation, paint treatment)
- The textile industry

2.4.4 Nano filtration (NF)

The nano filtration is a technique mainly used for the removal of molecules (divalent ions e.g. Ca^{2+}, Mg^{2+}, $(SO_4)^{2-}$) and the larger single ions such as heavy metals. Nanofiltration membranes are charged, which means the ions rejected by the membrane depend to some extent on their charge. This technique is often described as a coarse reverse osmosis process.

Because nano filtration uses less fine membranes, the feed pressure of the nano filtration system is generally lower compared to reverse osmosis systems. Importantly the fouling rate is lower compared to reverse osmosis systems.

Process	**Pore size** Micron
NF, REVERSE OSMOSIS	0.001 (theoretical)

Table 3 Membrane Pore size. [8]

Examples of fields where nanofiltration is applied are:

- Hardness removal
- Colour removal
- Demineralise cheese (salt removal)

2.4.5 Reverse Osmosis (RO)

Reverse Osmosis (RO) uses a semi-permeable membrane to separate and remove dissolved solids, organics, pyrogens, submicron colloidal matter, viruses, and bacteria from water. Reverse Osmosis is capable of removing 95-99% of the total dissolved solids (TDS) and 99% of all bacteria, thus providing safe and pure water. Pressure, 4000-8000 kPa (40-80 bars), is applied to the seawater and it is passed through the semi-permeable membrane (Figure 2-5), this process allows only the solvent to pass and not the dissolved solids.

Seawater is pumped into a closed vessel where it is pressurized against the membrane. As a portion of the pure water passes through the membrane, the remaining feed water now has a larger salt content. This because there is less water to contain the same total amount of dissolved solids (salt). At the same time, a portion which varies between 20% and 70% of this feed water is discharged without passing through the membrane. Without this controlled discharge, the pressurized feed water would continue to increase in salt concentration, creating problems such as precipitation of supersaturated salts and increased osmotic pressure across the membranes.

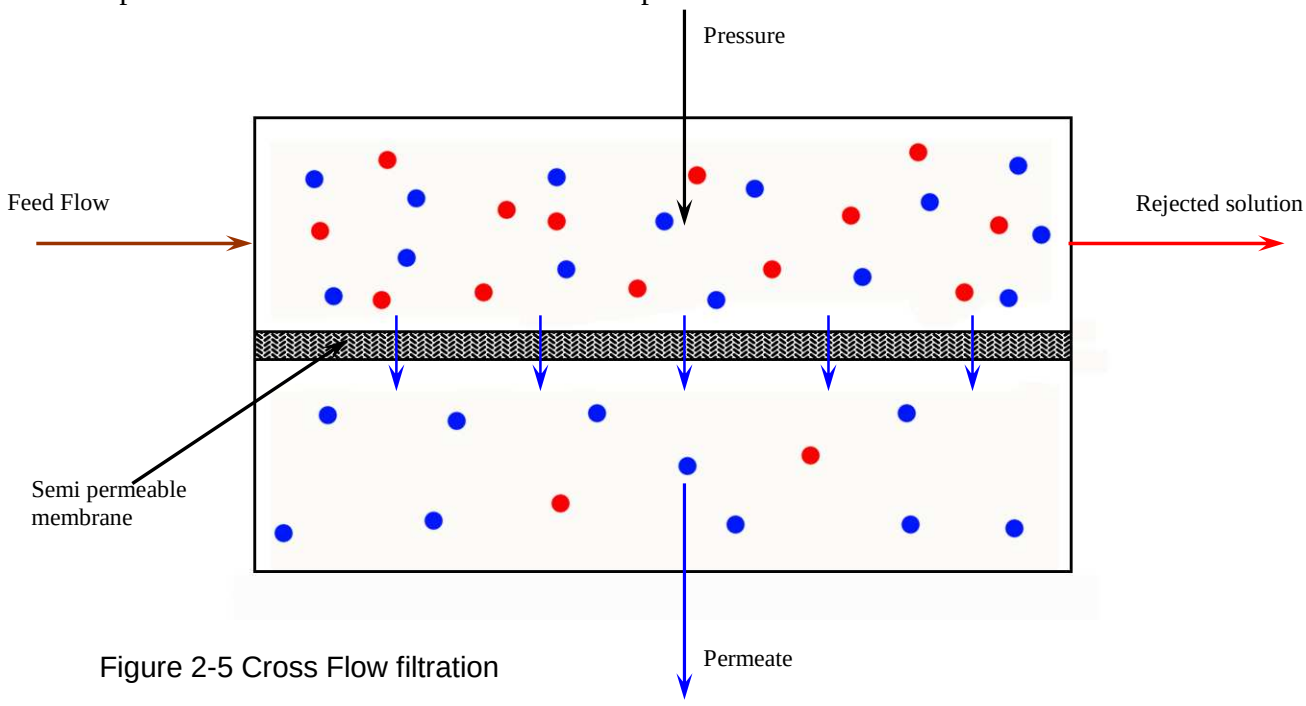

Figure 2-5 Cross Flow filtration

Since this project focuses on Reverse Osmosis, the main features of this process are described in more detail in Chapter 3.

CHAPTER 3 REVERSE OSMOSIS

3.1 Principle of Osmosis/Reverse Osmosis

Osmosis denotes the spontaneous flow of pure water from an aqueous solution of low salt concentration to a solution of higher salt concentration, provided the two solutions are divided by a semi-permeable membrane. The driving force for this process is the difference in chemical potential of H_2O, μ_{H_2O}, between the dilute and more concentrated regions. As the pure water permeates through the membrane the pressure in the dilute region drops and that in the more concentrated region rises. This flow will continue until there is an equilibrium between the fluids on each side of the membrane. Osmosis is seen in nature, for example plants roots use this method to absorb water from the ground.

Figure 3-1 below shows a laboratory demonstration of osmosis in action

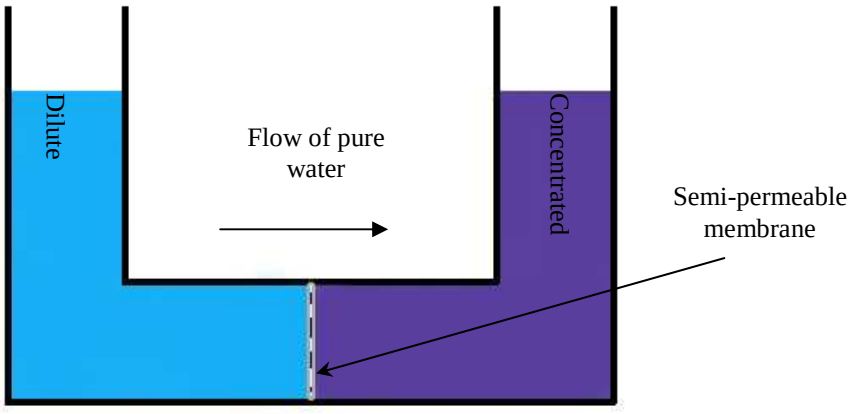

Figure 3-1 Osmosis

As H_2O flows from left arm to the right arm, the water level falls and rises in the two arms and equilibrium is attained (i.e. H_2O flow ceases) when the differential water level has attained a certain value which is known as the osmotic pressure differential between two solutions (Figure 3-2).

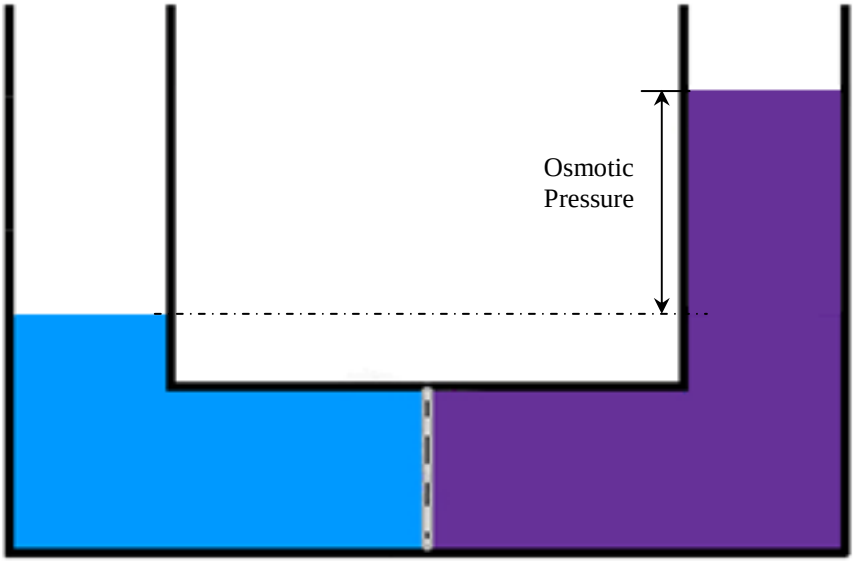

Figure 3-2 Osmotic Pressure

Now, consider the original situation with the two water levels equal, if a pressure equal to the osmotic pressure differential is applied in the right column until the pressure in both columns were the same, this will produce an equilibrium, so the net flow of water from one side of the membrane to the other would be zero (Figure 3-3).

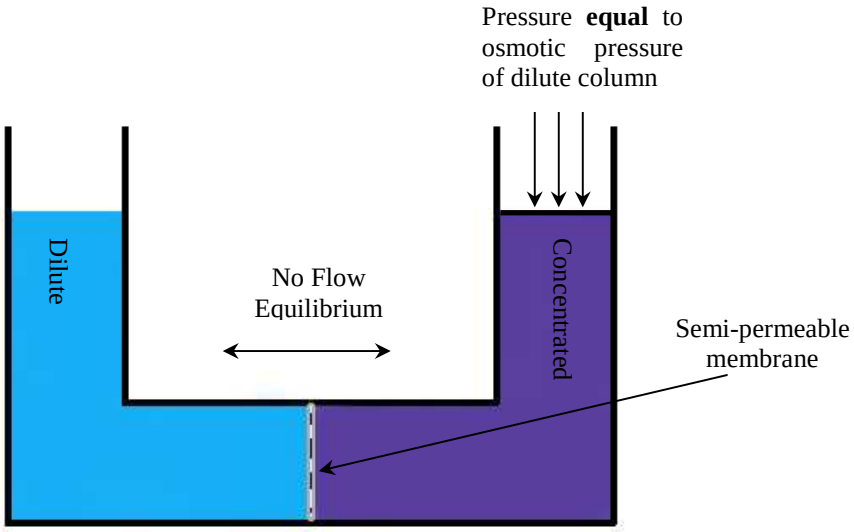

Figure 3-3 Equilibrium

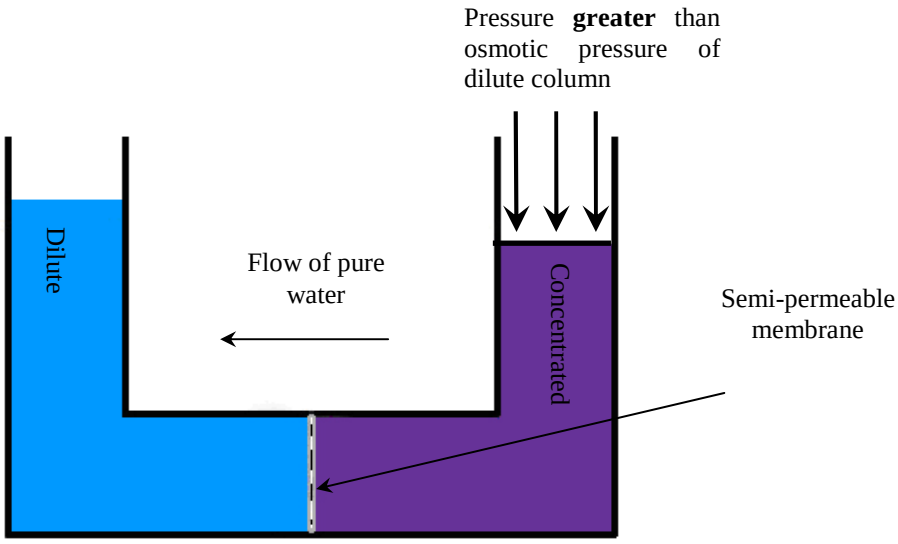

Figure 3-4 Reverse Osmosis

When pressure greater than that of the osmotic pressure differential is applied to the right column the flow of pure water will go in the opposite direction to that of the first case. This reversal of pure water flow is called reverse osmosis. This phenomenon can be used to extract pure water from seawater.

For any given solution the osmotic pressure is defined as the pressure necessary required to stop the osmotic flow through a semi permeable membrane separating the solution from pure solvent.

3.2 Development of Reverse Osmosis as a Technique of Desalination.

This technique was conceived and named by Reid at the University of Florida in the 1950s. Reid experimented with a number of synthetic polymeric films and found some of them to be selectively permeable to saline solution. He came across cellulose acetate and obtained very good salt rejections using it under reverse osmosis conditions. The salt rejections were up to 98.4 percent. For his experiments he used isotropic membranes and was able to manufacture membranes no thinner than 6 μm. But even at this low thickness the permeate flux was too low for commercial application.

At around the same time at the University of California, Los Angeles Sourirajan was experimenting with commercially available porous cellulose acetate sheets. Here again the permeate flux was quite low. Later he was joined by Loeb and they repeated the experiments using porous cellulose acetate sheets from Schleicher and Schuell Co.[9] These sheets gave high fluxes but no salt rejection. But when these same sheets were heated to 80-90 ^{o}C in water the results obtained were very promising. The salt rejection of these membranes, with a thickness of around 100 μm was of the order of 90 % and a much higher permeate flux that which Reid obtained. The big difference between the membranes was that the ones used by Soorirajan were anisotropic (asymmetric).

Reverse osmosis was first successfully applied to desalinate brackish water. The late 1960s saw the appearance of large scale plants. During the next ten years new and higher performance membranes were developed which were suitable for seawater desalination as they had higher salt rejections with higher permeability and can be operated at higher pressures.

By the 1980s reverse osmosis became a serious competitor to classical desalination techniques. Further advances in membrane technology have produced membranes that can be operated at lower pressures and still produce the same permeate flux as the older membranes that were operated at high pressures. For instance the pressures required for seawater reverse osmosis were in the order of 120 bar for the earlier membranes but now seawater membranes operate at around 50-70 bar and brackish membranes at 20 bar.

Examples of fields where reverse osmosis is applied are:

- Seawater desalination
- Effluent water reuse from various industries such as chemical, mining, paper
- Production of ‘ultra pure’ water for the integrated circuit manufacturing industry
- Food processing – soft drinks, beer and wine production, dairy processing
- Fermentation products recovery and purification.
- Production of drinking water.
- Humidification.
- Ice making
- Rinse waters
- Photography
- Pharmaceuticals

- Kidney dialysis
- Chemical process water
- Cosmetics
- Semi-conduction industry
- Waste water treatment

A typical layout of a commercial reverse osmosis plant is shown in Figure 3-5

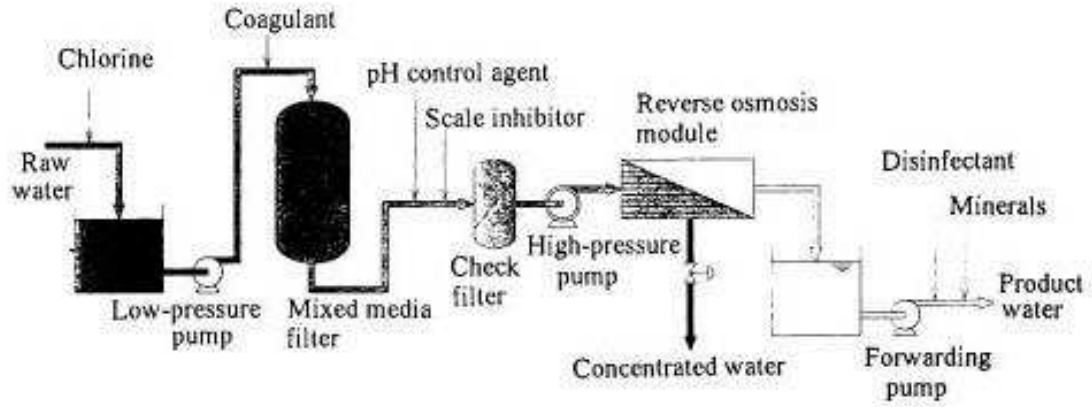

Figure 3-5 Commercial Reverse Osmosis Plant

In an ideal case the only energy required for reverse osmosis to occur is the pressure applied to overcome the osmotic pressure of the seawater. This would require an ideal membrane, which only allows the flow of pure water. Unfortunately in real life such membranes do not exist, what we get is a membrane that allows a constant amount of salt to pass independent of pressure applied and pure water to pass proportionally to the pressure applied. The minimum pressure required to produce any water is the osmotic pressure, but the production rate is infinitely low and it will not yield water of good quality; so the higher the pressure applied the better the water quality. The maximum pressure is determined by the strength of the membrane.

3.3 Reverse Osmosis Membrane Materials

There are a number of different reverse osmosis membranes available today; each type has some different properties that make it more appropriate to be used in a particular situation.

The characteristics that are looked for in membranes are the following:

- Good salt rejection (allows negligible amounts of salt through)
- High water flux (allows water to flow though with considerable ease)
- Resistant to a large range of environmental conditions (physical, chemical and thermal)
- Resistant to high pressures and wear (is durable)
- Inexpensive and easy to manufacture
- Resistant to fouling

The earlier membranes were made using cellulose acetate (CA), which is still used even now. Other materials such as cellulose triacetate and a number of polyamides are also being used now.

3.3.1 Cellulose Acetate

Cellulose acetate (CA) performed adequately when treating brackish water, but not with seawater because unfortunately the membrane suffered compression at the higher pressures that were required. Nowadays even more, its pH, temperature and performance limitations have reduced its overall use. CA membranes are limited to an upper operating temperature of approximately 35°C. However, it is interesting to note that CA has a superior chlorine [10] and fouling resistance. This makes it quite useful for certain applications.

3.3.2 Cellulose Triacetate

Cellulose triacetate (CTA) is an improvement on the cellulose acetate membrane, it was very popular in home plants and was also used in industry.

The main reason for CTA membranes becoming so popular in the home market is the fact that they are comparatively cheap and readily available. Generally, domestic CTA membranes are used on chlorinated water supplies with a total dissolved solid content below 800 ppm.[11] Furthermore they are fairly tolerant to oxidising chemicals such as chlorine.[12] This is particularly relevant as chlorine is used to disinfect and treat drinking water in most of the world.

CTA membranes unfortunately have some major disadvantages. They only have a low flux. Flux is defined as the volume of water that can be passed through unit area of membrane. This means that a larger area of membrane is needed to produce a comparable flux as a thin film membrane.

CTA membranes also have a low tolerance to high pH. If feed water pH is higher than 8.5, CTA membranes begin to quickly degrade and lose total dissolved solids (TDS) rejection performance. When this happens, the CTA membrane is said to hydrolyze, a

condition characterized by high output and poor rejection. Lastly, CTA is more sensitive to high feed water temperatures. A typical CTA-RO system has an upper limit of 30°C for feed water temperature. And feed water temperatures approaching 40°C are not uncommon in many parts of the world.

3.3.3 Polyamide

During the 1980s when the thin film membrane was invented, it provided a means to achieve flux and salt rejection suitable for seawater desalination. Typically composite membranes are made up of two layers; one a very thin layer (e.g. polyamide) and the second a tougher supportive layer typically made of polysulfone. For cases where higher durability and performance is needed three layered membranes can be used. Figure 3-6 shows the layout of the different layers.

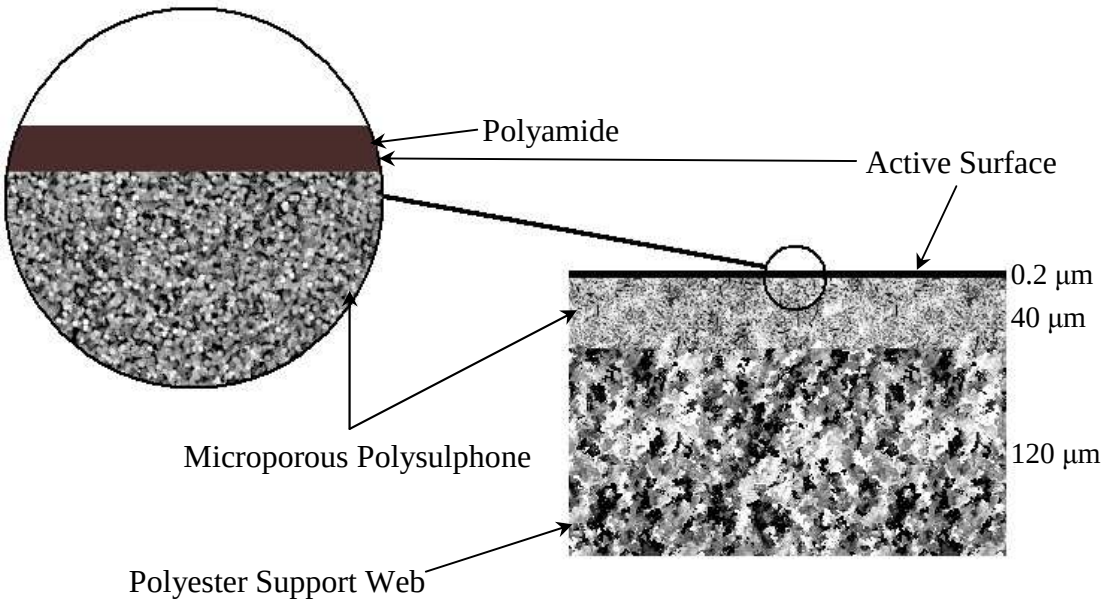

Figure 3-6 Detail of Layers of Polyamide Membrane (based on [13])

Thin film membranes have other useful characteristics. They have a good resistance to environmental factors such as temperature and pH, but have poor tolerance to oxidizing environments particularly where chlorine is concerned.

Thin Film composite membranes (TFM) are ideally used on non chlorinated water supplies with a higher TDS content. They are also used on chlorinated supplies where a faster water production is required or a higher water purity is needed. When used on chlorinated water supplies it is crucial to include a means to remove the chlorine prior to it entering the membrane. The part of the chemical structure of the polyamide layer is shown in Figure 3-7 below; the exact chemical structure is a close guarded industrial secret.

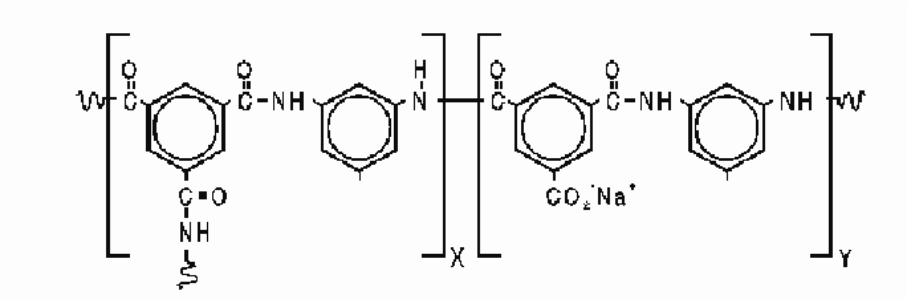

Figure 3-7 Partial chemical structure of membrane showing cross-linked polyamide containing carboxylate groups.[14]

CHAPTER 4 REVIEW OF FOULING PHENOMENON IN MEMBRANE PROCESSES

4.1 Overview of all types of Membrane Fouling

The main ailment [15] that membranes suffer from in operation is fouling. As the membranes are the determining component of the separation process it is important that their health is a priority. Any fouling issues with the membrane will reduce their useful lifespan. Fouling will lead to a loss of membrane performance, this often results in the reduction of flow and the increase in salt passage and eventually leads to ruination of the membrane.

Fouling is the term used to describe the accumulation of unwanted material on the surface of the membranes. Fouling is seen in processes involving fluids (gas and liquid) and foulants are diverse. These can be in various forms such as suspended matter, dissolved solids, living organisms, chemical and other substances present in the flow. They form deposits on the membrane that sometimes damage the membrane but mostly interfere with the proper operation of the process.

In certain, highly specialised circumstances [16] fouling is actually encouraged; for example in waste water treatment processes biofilms are utilised. In all other cases, including the ones studied in this project, fouling of any kind is counter productive.

Fouling in the separation process is due to many factors. Depending on the composition of the liquid there is sometimes precipitation of dissolved solids or the deposition of suspended solids. These suspended solids may be already present in the feed or be the result of the corrosive effect of the feed particularly on steel parts of the

system. The membranes also provide a surface for micro and macro biological organisms to thrive. Eventually the build up of a layer of foulant will interfere with the flow across the membrane.

The different agents in water that can be involved in the fouling of a membrane are:

- Particulates including colloids.
- Low solubility salts such as $CaCO_3$.
- Biological organisms.
- Corrosion products.
- Organic Substances including
    i. Humic Acids.
    ii. Hydrocarbons.

The focus of this project has been on organic fouling; hence the other types of fouling are only briefly summarised below.

4.2 Particulates

This involves [17] the formation of a thin layer of particulates on the surface of the membrane which causes the plugging of the 'pores'. This layer consists of suspended solids, and colloids. This layer affects the passage of water through the membrane. This accumulation can be removed by regular cleaning of the membrane or the setup of an adequate pre-treatment stage.

4.3 Low Solubility Salts

Low solubility salts are usually of inorganic nature, for example $CaCO_3$, $CaSO_4$ and SiO_2. Figure 4-1 is a photograph of a reverse osmosis membrane with calcium carbonate ($CaCO_3$) deposits. These minerals are present in most water feeds. They form hard scales as they precipitate on the surface of the membrane. Scale formation depends on crystallisation and hydrodynamic transport mechanisms. There are two ways for crystallisation to occur, these are [18],[19] surface (heterogeneous) crystallisation and bulk (homogeneous) crystallisation. Heterogeneous crystallisation is the more harmful of the two. The energetics of the crystallisation process are such as to favour the nucleation of a solid on the surface as opposed to the bulk of the water. The consequences are reduced permeate flow rate and also damage to the membrane surface.

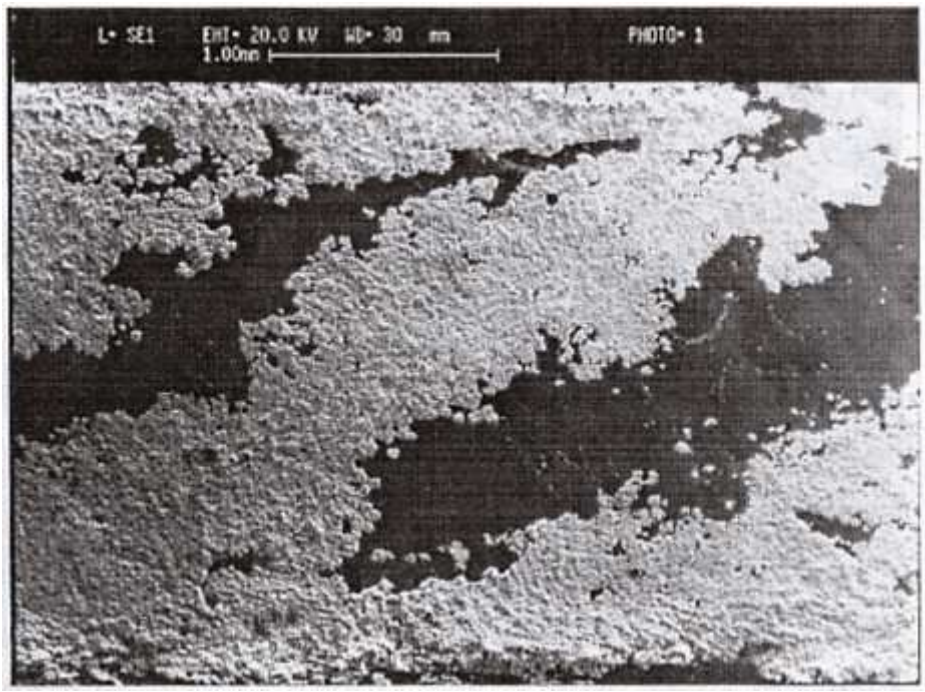

Figure 4-1 Calcium Carbonate Scale Deposition on Reverse Osmosis Membrane (Courtesy Dr. T. Hodgkiess)

4.4 Biological Organisms

Fouling caused by biological organisms [20] is usually described as biofouling. The organisms can be of different sizes and species, and can be plants or animals. Some examples are :

Bacteria, Fungi, Algae, Mussels, Barnacles, and Hydroids.[21]

But membranes are mostly prone to fouling from bacteria, fungi and algae. The bigger organisms tend to affect other parts of the desalination plant such as the pipe work and pre-treatment processes.

Unlike the other types of fouling discussed above, biofouling cannot be totally prevented by pre-treatment. Even chlorination will not completely get rid [22] of the micro organisms that are responsible of biofouling. This is even more so in reverse osmosis plants as chlorine cannot be present in the feed to the membrane as it will damage many types of commercial membranes. For example if 99 % of these micro organisms have been killed or removed in the pre-treatment stage, the remaining 1 % will start multiplying again feeding on any form of biodegradable substance they can find in the system and form a new colony. As the micro organisms travel in the pipe work they eventually reach the membranes and attach to them forming a biofilm.[23] This biofilm has very adverse effects on both the membranes durability and performance.[24]

The first effect of the biofilm will be to restrict the flow of water in the system as the biofilm layer will increase the surface roughness of the system, this will mean that more power will be required to achieve the same flowrate. As the microbial colony grows, the effect will be more acute and will eventually lead to the plugging of the membrane causing severe drop in permeate flux.

Secondly, increasing pressure applied across the membrane to counteract the effect of increased surface roughness will reduce the lifespan of the membranes as they are not designed to withstand excessive pressure for extended periods of time.

The third effect is a decrease in salt rejection. This occurs because the roughness of the biofilm on the membrane surface promotes concentration polarisation.

And finally the worse that can happen is that the micro-organisms can attack the membrane itself. Figure 4-2 shows bacteria growing on a hollow fibre membrane. As part of their metabolisms, micro-organisms excrete acids and enzymes, some of which can corrode the membrane or its support. Cellulose acetate is particularly vulnerable to these sorts of attack.

Figure 4-2 SEM of Biofouling of Hollow Fibre (Courtesy Dr. T. Hodgkiess)

4.5 Corrosion Products

These are usually the product of water becoming in contact to various metal objects. During that time depending on the pH of the water and ionic content there are varying degrees of corrosion that occur. As the water is collected and treated, the metal ions can be deposited on the membrane. This will occur in conditions where corrosion is prevalent. The only way to stop this from happening is to use corrosion resistant metal or materials. The cost of such modifications can be justified as they result in a longer membrane life. This factor results in very extensive use of polymer material throughout the pre-treatment system of the reverse osmosis plant.

4.6 Organic Substances

According to the literature [25] available from the manufacturer of the SW 30 membranes the adsorption of organic substances on the surface of the membrane will cause a loss in flux that can be irreversible in serious cases.

In this thesis, organic substances involved in fouling are divided into two categories, these are :

- Humic acids (since these represent the major proportion of natural organic substances present in natural water.)
- Hydrocarbons. (since these represent a particular type of organic substance that can be introduced into water as a pollutant and these form the basis of the experimental work undertaken in this project.)

4.6.1 Humic Acid

Humic substances can be found pretty much anywhere. They are the products of both chemical and biological breakdown of plant and animal residues and the by-products of micro-organisms synthesis [27]. Figure 4-3 is a picture of a humic acid seen under a scanning electron microscope.

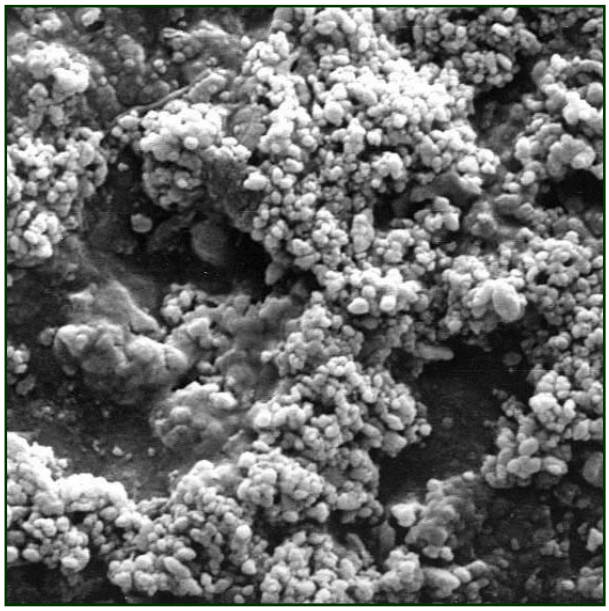

Figure 4-3 Humic Acid (Approx 2000x)[26]

Humic substances form a large proportion of the total dissolved organic matter of any aquatic system.[28],[29] Very often they are present in equal or even larger proportions than inorganic ions in aquatic systems such as rivers and lakes.[30]

Humic substances can be divided in three main categories.

- Fulvic acids tend to be between light yellow and yellow brown in colour. They are soluble in water irrespective of pH. They contain both aliphatic and aromatic functional groups.[31]
- Humic acids are the fraction of humic substances that are not soluble in water under acidic conditions (pH < 2) but are soluble at higher pH values.[32] These are usually obtained from the soil.

Humic acids are the major extractable component of soil humic substances. They are dark brown to black in colour.

Humic acids have a negative charge as they are naturally oxidized. In Figure 4-4 the humic acid has attached itself to a sugar molecule which is delimited by the red box.

- Humins are black in colour and make up the fraction of humic substances that are not soluble in water of any pH.[33],[34]

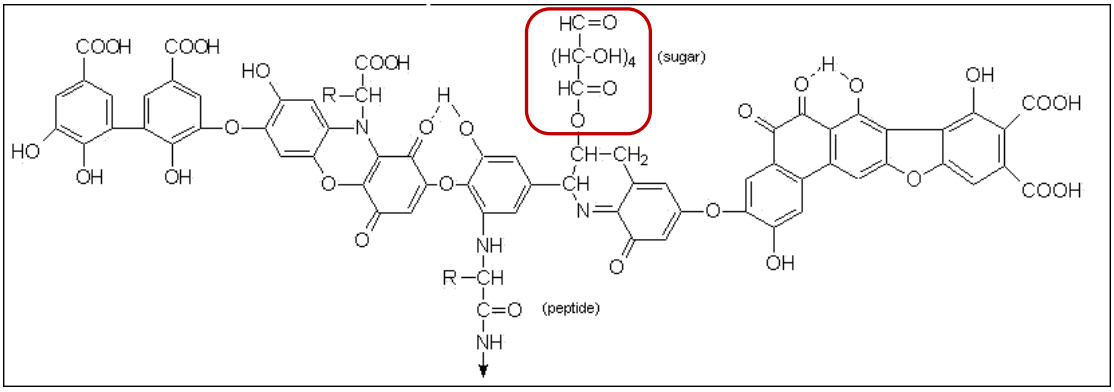

Figure 4-4 Model structure of Humic Acid.[35]

Humic substances can interact with a large number of elements (approx 50). As seen in Figure 4-5, they also give an unpleasant colouring to the water and induce photo-chemical transformation of both chemical compounds and trace metals.[36] A major concern is the fact that humic substances react with halogens to produce carcinogenic substance [37] such as chloroform and bromoform. These would prove to be a serious health hazard if found in the drinking water supply.[38],[39]

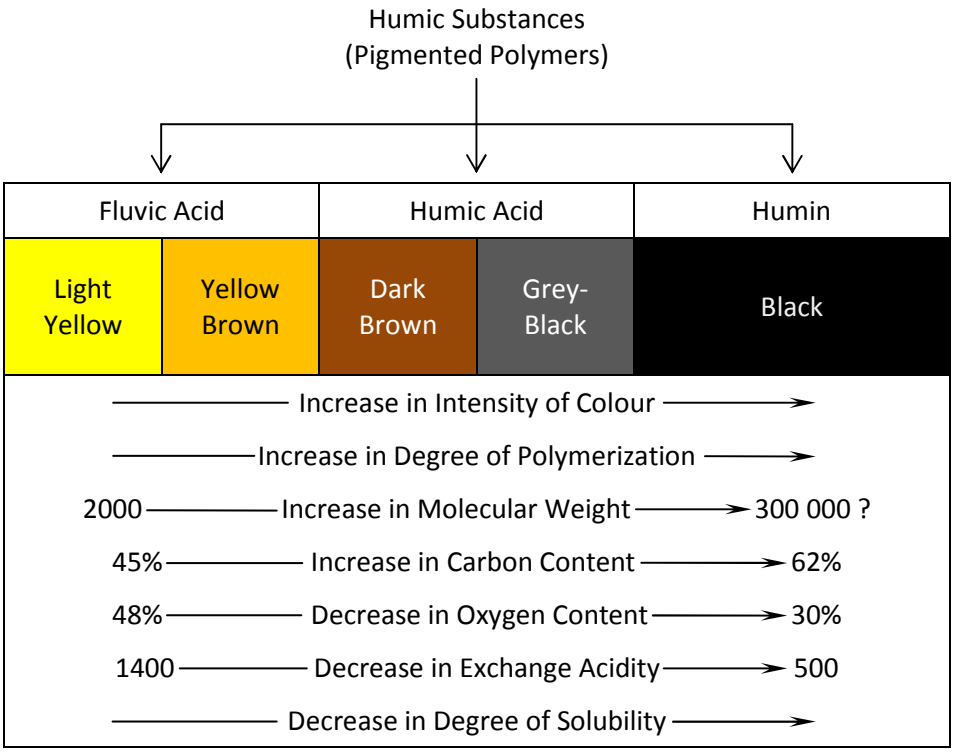

Figure 4-5 Properties of Humic Substances.[40]

Humic substances have structures [41] that can vary between rigid spherocolloidal and flexible linear. These molecules (humic acid and fulvic acid) have a compact form in the following conditions: high sample concentration, low pH and if an appreciable amount of neutral electrolyte is present.

These molecules will have a relatively linear structure when ionic strength is relatively low, pH is neutral to alkaline and there is a low sample concentration.

These organic substances are extremely complex (see Figure 4-4) with molecular weights [42] of humic acid varying between 700 and more than $2x10^6$ g/mol and that of fulvic acid less than 1000 g/mol. The weighted average molecular mass of commercially available Aldrich humic acid is 50 000 g/mol.[43]

More studies of fouling by humic acids of microfiltration and ultrafiltration membranes have been undertaken than of nanofiltration [44],[45],[46] and reverse osmosis membranes.[47] For example, ultrafiltration membranes were found [48] to experience humic acid fouling from drinking water and this caused significant reduction in water flux.

Some researchers have considered the influence of charge interactions on humic acid fouling of membranes. One study [49] on the interaction between humic acids and ultra-filtration and reverse osmosis membranes reports that when these membranes are exposed to humics they become more negatively charged. This phenomenon is observed over a wide range of pH. This leads to the conclusion that humics are easily adsorbed by the membrane surface and the negatively charged functional groups of the humic acids give the membrane surface its new charge. Humic acids with higher molecular weights are more readily adsorbed by the surface. In contrast, another paper [50] has discussed the potential limitation (by electrostatic charge repulsion) of humic acid fouling on those membranes that exhibit negative surface charge. Addition of divalent cations is said [49],[50] to promote adsorption of the humics.

Experiments [51] indicated that asymmetric cellulose acetate membranes were mostly unaffected by humic acid. The performance drop, both in terms of flowrate and salt passage, of these membranes, was almost indiscernible. But when a thin film composite polyamide membrane was exposed to the same humic acids it suffered from a drop in water flux. This indicates that humic acids affect the polyamide membranes. This fouling behaviour can be explained by the affinity of humic acids to bond with multivalent ions forming a gel layer on the membrane which causes a reduction in the flux. This layer fortunately cannot pass through the pores and cause irreversible damage to the membrane, though if left to accumulate this cake layer will

greatly affect the flux. This layer should be cleaned to restore the properties of the membrane.

Another work [52] demonstrated that polyamide hollow fibre membranes were vulnerable to fouling in circumstances where the humic acid coagulates out of the seawater.

4.6.2 Hydrocarbons

Hydrocarbons are found in fossil fuel reserves under the earth's surface. Hydrocarbons are made of carbon and hydrogen atoms that bond together to form chains, for example hexane, or cyclic molecules, for example benzene. These chains can be either straight or branched.

The effect of oil spills on the performance of Multi-stage flash distillation plants have received some consideration.[53] It was reported that seawater polluted by oil would cause a number of negative effects that would overall impact the performance and efficiency of the plant.

What is of specific interest to the present work is whether hydrocarbons can affect the different reverse osmosis membranes and, if that is the case, what kind of the impact do they have on the performance of the membrane.

There have been previous studies that have looked at some effects of different hydrocarbons on reverse osmosis membranes, while others have investigated if such membranes could be used to remove different hydrocarbons from contaminated water. In one of these former studies [54] the effect of passing oily water through a polyamide membrane on the permeate flux was investigated. The oil used in the mixture was Iranian crude oil which contains long chain hydrocarbons and the membrane was a

FilmTec FT 30 polyamide membrane. The following four parameters were varied during the experiment

(a) Transmembrane pressure

(b) Oil concentration

(c) Temperature

(d) Crossflow velocity

The findings are summarised in the table below.

Increasing	Impact on Permeate Flux
Pressure	Increase
Oil concentration	Decrease
Temperature	Increase
Velocity	Increase

Table 4 Impact of Parameters on Permeate Flux

The authors concluded that fouling occurred mainly through concentration polarisation and the formation of a gel layer on the membrane as opposed to the blocking of the membrane pores by the oil molecules.

Another study [55] that was closely related to the current work looked at two different polyamide membranes. Membrane samples were exposed on both sides to crude oil, diesel, hexane and emulsions of the mentioned substances and water. Diesel contamination is especially dangerous with a capacity to reduce membrane fluxes to zero if present in large concentrations for even short periods of time. Hexane, which is one of lighter crude oil fractions also caused serious deterioration of the performance of reverse osmosis membranes when in contact in pure or emulsified form. The

damage was worse in more concentrated hydrocarbon mixtures and at longer exposure times. Within the scope of the experiments conducted in this previous project, hydrocarbons retained in solution in water were not found to exhibit damaging effects of the performance of the reverse osmosis membranes. The damaging effects of the hydrocarbon contaminants were found to be different on the two types of membrane studied. The brackish water membrane suffered substantial reductions in flux and roughly proportionate increases in salt passage. The seawater membrane underwent larger deleterious effects on salt passage and much lower reductions in permeate flux. It appears that the damage caused by exposure to hydrocarbons is difficult to reverse. The study did not differentiate between the effects of hydrocarbons on the upper and lower membrane surface and was largely focused on the performance characterization and did not yield any clear evidence of the mechanisms of the fouling phenomena.

Another study [56] was on nanofiltration membranes rather than reverse osmosis membrane but it is still relevant. The membranes used in the experiments were NF 70 from Dow and UTC-20 from Toray Ind. Inc. and they were contaminated using a wide range of hydrocarbon derivatives. The membranes were more susceptible to some compounds than others and the UTC-20 membranes were more robust. On the whole the authors concluded that molecular size of the compound played a large role on the flux decline. This was due to the fact that those molecules were adsorbed on the surface of the membrane or inside the pores of the membranes. Also the flux decline was said to be due to the following two factors. The molecules were a size that filled the membrane pores and the adsorption was exacerbated by the fact that the component was hydrophobic.

It is clear that not much work has been done of the effects of hydrocarbons on reverse osmosis membranes. Without such knowledge it is not possible to predict what would happen if contamination by hydrocarbon was to occur at one of these facilities. The work done in this project is aimed at increasing the knowledge and understanding in this specific fouling topic.

	Operating Parameters	**Fouling Procedure**	**Concentration**	**Time**	**Impact on Membrane**	
Membrane					BW 30 [55]	SW 30 [55]
Material					polyamide with polysulfone backing	polyamide with polysulfone backing
Hexane	For BW 30 – 30 bar at 25 ^{o}C		Pure	5 h	Flux 90 % ▼ and % salt passage 3X ▲	Flux 87 % ▼ and % salt passage 5X ▲
Diesel			Pure	60 mins	Zero flux	Zero flux
Hexane water		Stirring	1 : 10	24 h	75 % fall in flux	
Hexane water		Stirring	1 : 5	5 h		Flux 87 % ▼ and % salt passage 5X ▲
Diesel water	For SW 30 – 65 bar at 30 ^{o}C		1 : 100	30 mins	Flux 89 % ▼ and % salt passage 4X ▲	Flux - 60 % and % salt passage 12X ▲
Hexane solution						Flux 5 % ▼ and % salt passage 1.8X ▲
Emulsified Crude Oil			1:3	6 days		No measurable effect on flux, % salt passage 0.2X ▲

Table 5 Tabulation of Membrane Susceptibility to Hydrocarbons.

	Operating Parameters	Fouling Procedure	Concentration	Time	Impact on Membrane		
Membrane					FT 30* [54]	Nanofiltration membrane [56] (NF-70, NF-45, UTC-20, NTR-7450)	SR-90 [59] Sulphate Reducing membrane
Material					polyamide	polypiperazine amide	polyamide with polysulfone backing
Crude Oil	20 ^{o}C / 13 bar	present in flux	5 % Vol	100 mins	80 % fall in flux		
Hexane	20 ^{o}C / 20 bar	Active layer	Pure	6 days			Flux 64 % ▼
		Both layer					No Flux
Pesticide						Flux ▼(9-27%) membrane dependent	
▲ - Increase ▼ – Decrease							

Table 5 Contd.

* Note FT30 is a generic name for a range of seawater, brackish water and tap water membranes from DOW. Detail type not stated in paper.

CHAPTER 5 EXPERIMENTAL PROCEDURES

5.1 Introduction

The focus of this thesis is to look at the effects hydrocarbons have on reverse osmosis membranes.

Two model hydrocarbons were selected for the experiments. These were Hexane and Diesel. Also a variety of membranes were selected and subjected to a number of fouling treatments as described below. The three membranes used for the experiments were :

1. Polyamide brackish water membrane Filmtec BW 30.
2. Polyamide seawater membrane Filmtec SW 30.
3. Cellulose triacetate membrane Ametek CTA B - 2 – 10 HF

5.2 Membranes under Investigation.

The polyamide membranes came in large sheets from the manufacturer, while the cellulose triacetate one came in the form of a module. The membranes-containing module was bought from Fileder Filter Systems. The actual membrane was obtained after disassembling an Ametek CTAB2-10 cartridge (Figure 5-1). This was done carefully in many steps as described below.

Figure 5-1 Membrane Module and Module Cross Section.

The module was placed on a clean work top and the structure on the left was pulled out. Then the protective and sealing skin was pealed off. This reveals a spiral wound membrane that is wrapped around a central conduit. Wrapped together with the membrane is a plastic spacer which allows the feed to enter the membrane when the module is in normal use. The membrane wrap consists of two membranes that have had three of their edges glued together to form an envelope. The fourth side is left open and connected to the conduit via a slit to allow the filtrate to be collected.

Figures 5-2 and 5-3 show the module from the side.

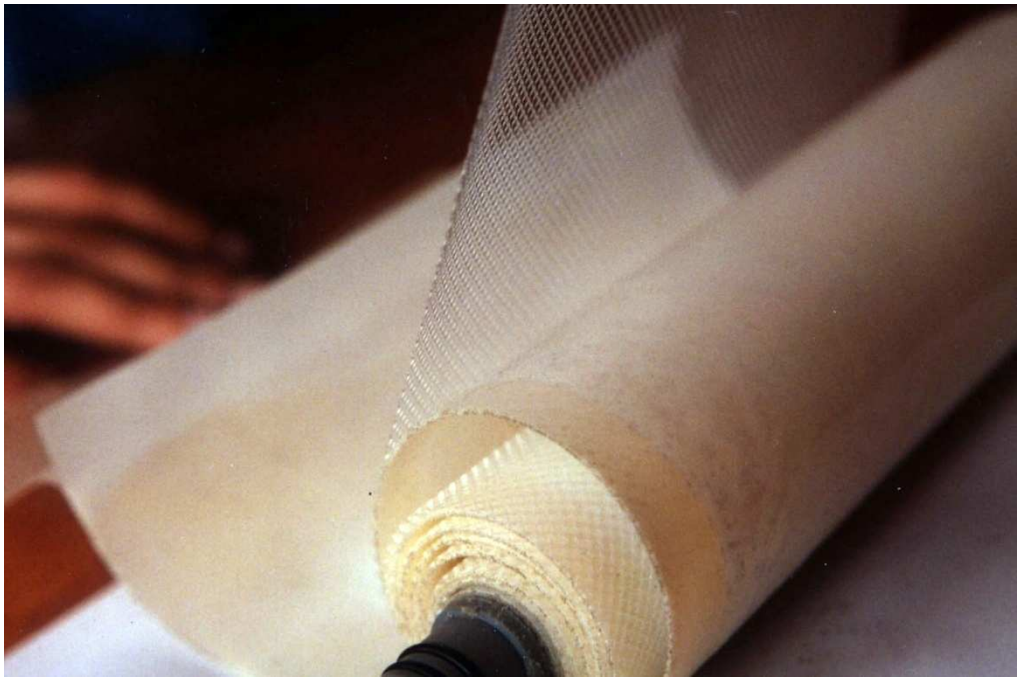

Figure 5-2 Side view of Module and Plastic Spacer

In Figure 5-3, which is a cross section of the module, the red arrows show the flow of the feed and the blue arrow shows the flow of the permeate.

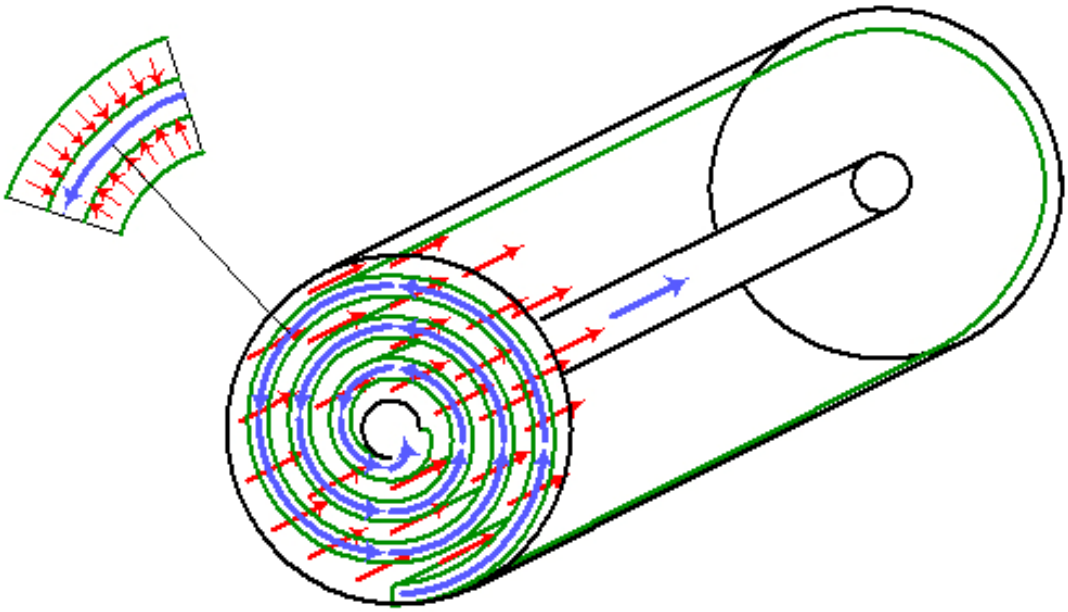

Figure 5-3 Membrane Packing and Water Flow in Membrane Unit

A purpose built hollow circular punch shown in Figure 5-4 was used to stamp out samples of membranes. A mechanical press was used to provide a high enough impact to produce a clean cut.

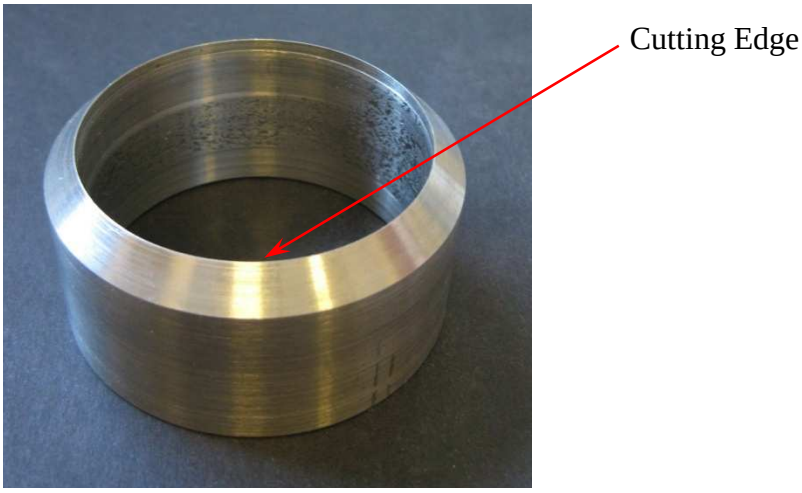

Figure 5-4 Hollow Circular Punch

This method was used to obtain samples of both polyamide and cellulose triacetate membranes.

The membranes samples (Figure 5-5) were thus cut in to disks to fit in the desalination rig. The disc has a diameter of 5 cm and of an area covering 19.63 cm^2

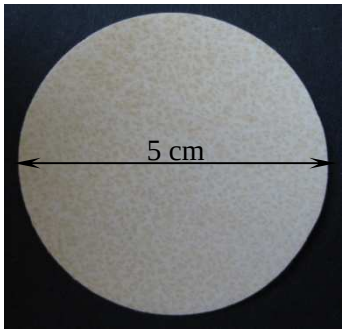

Figure 5-5 Membrane Disk

5.3 Fouling Procedure

The experimental protocol in this study comprised exposing membrane samples to various hydrocarbon-containing liquids for selected periods of time, followed by measuring their performances in the Reverse Osmosis Rig.

5.3.1 Seawater / Hydrocarbon Mixture

The membranes were exposed to a hydrocarbon seawater mixture using either of two apparatus depending on whether one or both surfaces of the membrane were being exposed.

The very simple apparatus shown in Figure 5-6 was used for exposing both membrane surfaces, it consisted of a glass jar containing a magnetic stirrer. The jar was filled with a seawater and hydrocarbon mixture, these were in the 10:1 ratio.

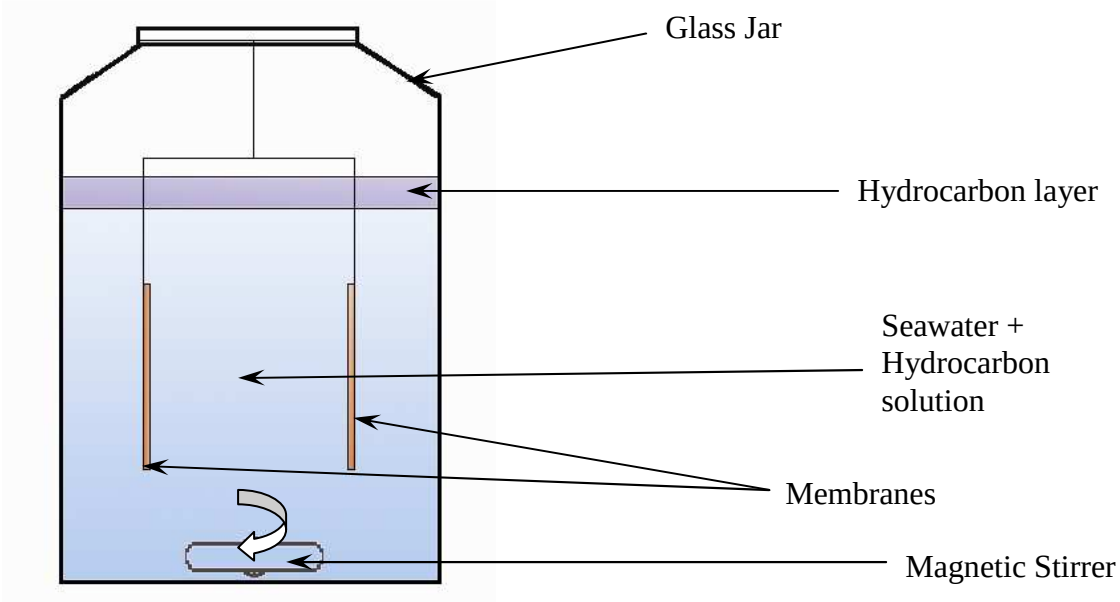

Figure 5-6 Apparatus for Fouling of Both Surfaces

Table 6 shows the respective solubility of hexane and diesel in water.

Hydrocarbon	**Solubility in water, g/100 ml at 20°C**
Hexane	0.0013 [57]
Diesel	0.0005 [58]

Table 6 Solubility of Hydrocarbons

The solubility of these hydrocarbons is very low, so in a 10:1 seawater, hydrocarbon mixture two distinct layers can be observed. A top layer consisting of the less dense hydrocarbon and a main lower layer consisting of a solution of seawater and dissolved hydrocarbon.

In some experiments the membrane was kept in the main lower layer during the exposure period as shown in the above diagram.

In a number of experiments the stirrer was switched on. This turned the two layers into just one layer of emulsion.

A different apparatus was used in the experiments where only one layer of the membrane was exposed to the fouling substance. Figure 5-7 shows the layout of this apparatus.

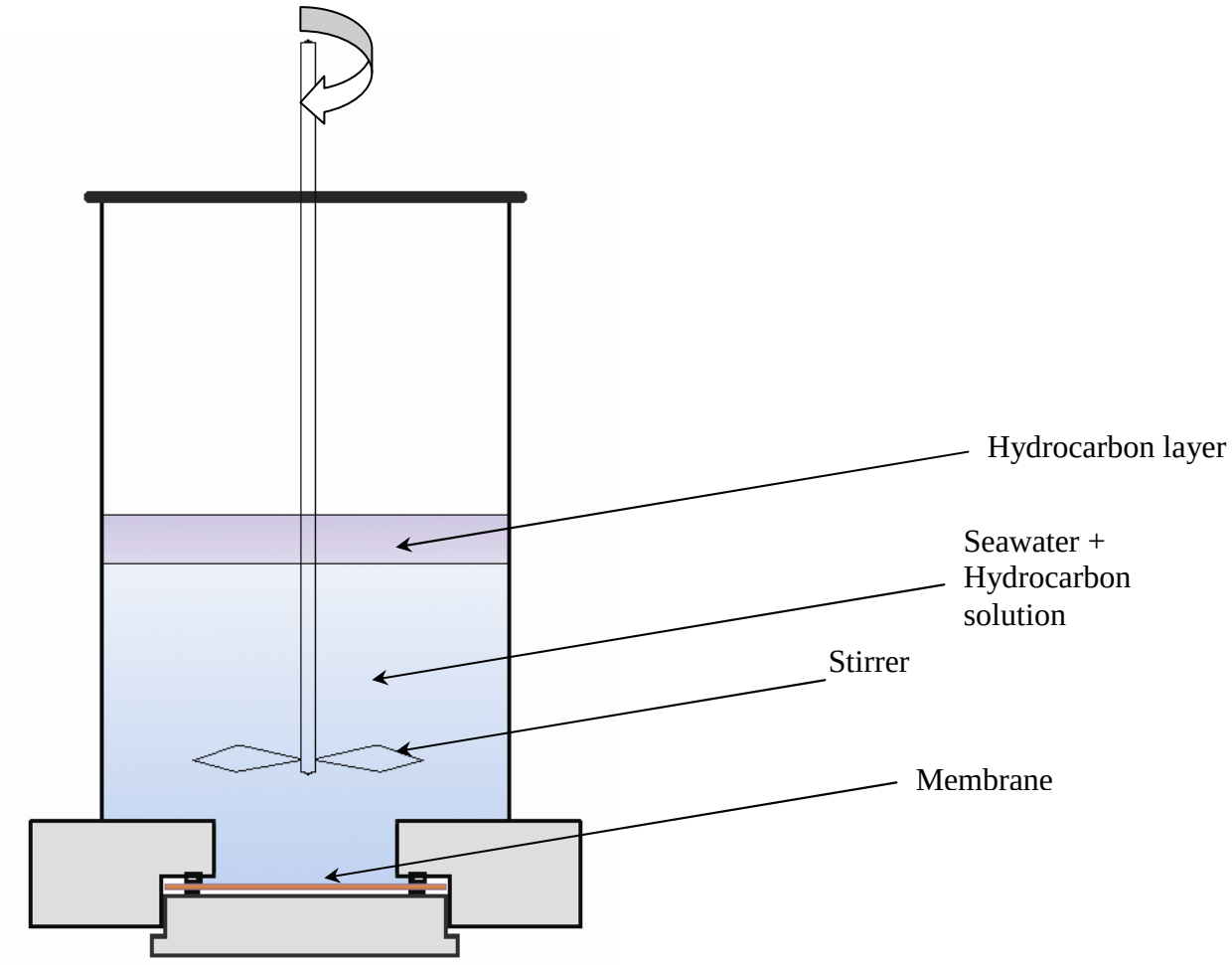

Figure 5-7 Apparatus for Fouling of Single Membrane Surface

The membrane lies at the bottom of a column of liquid, the membrane is sandwiched between two o-rings to make sure that there is no leakage of the liquid around the edges of the membrane. In this apparatus only the desired surface is exposed to the fouling agent. Thus it can be determined what effect the hydrocarbon is having on either the active surface or the backing (passive) layer.

5.3.2 Pure Hydrocarbon

In some experiments where the membrane is only exposed to the hydrocarbon, the liquid is replaced by the pure hydrocarbon either hexane or diesel, hence there is no need for stirring. For the experiments where both layers of the membrane are exposed to the pure hydrocarbon, the membrane sample is placed in a sealed jar with the liquid. When only one side of the membrane needs to be exposed to the hydrocarbon, the apparatus in Figure 5-7 is used without the stirrer with the relevant side of the membrane facing the hydrocarbon.

5.4 Rig Layout

The main experiments were carried out on a purpose built Reverse Osmosis rig (Figures 5-8 to 5-17) in the laboratory. The structure and working of the rig is described below.

The rig is made up of five different sections that are interlinked. They can be described as

1. Storage
2. Pumping
3. Control
4. Membrane Test Cells
5. Monitoring

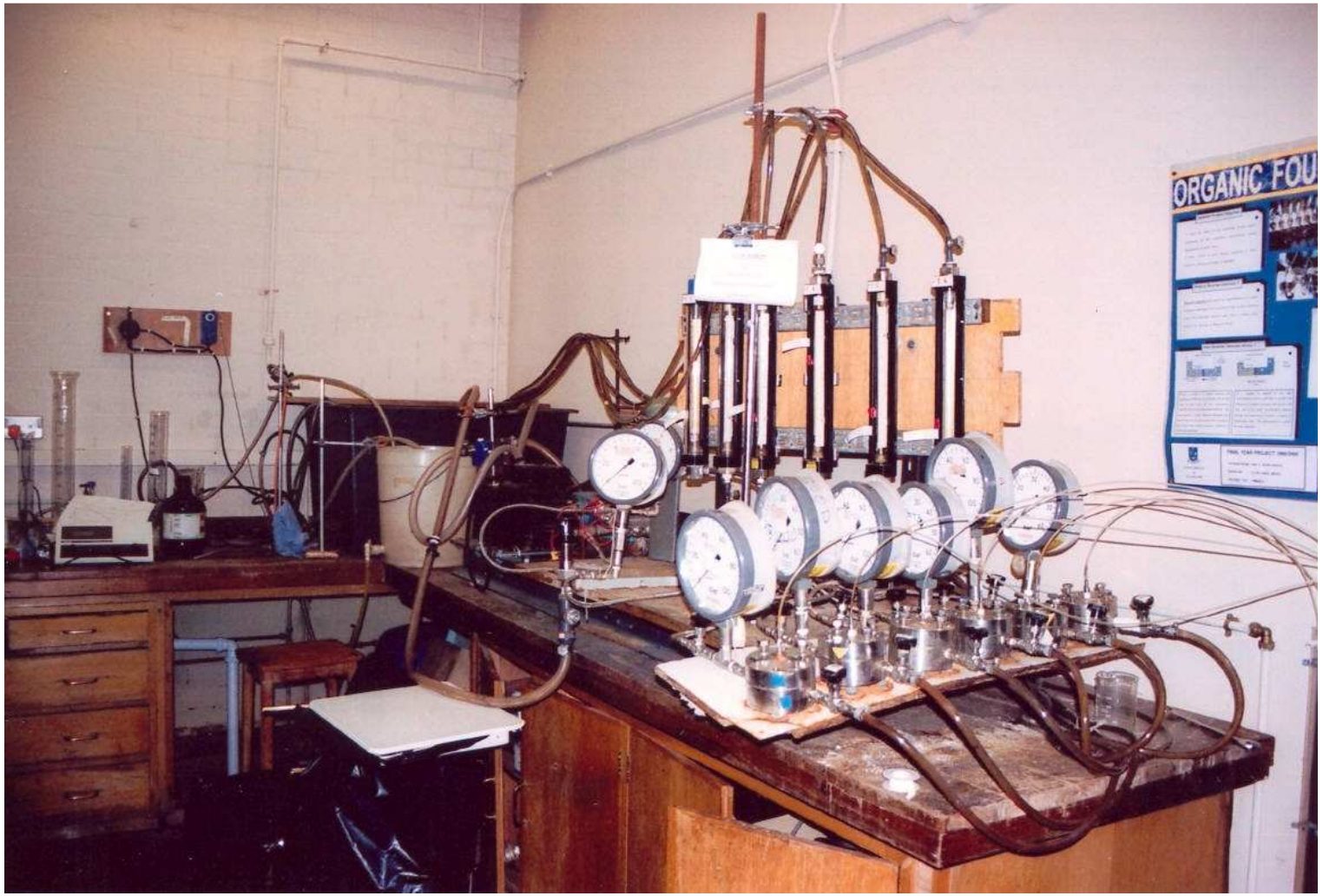

Figure 5-8 Rig

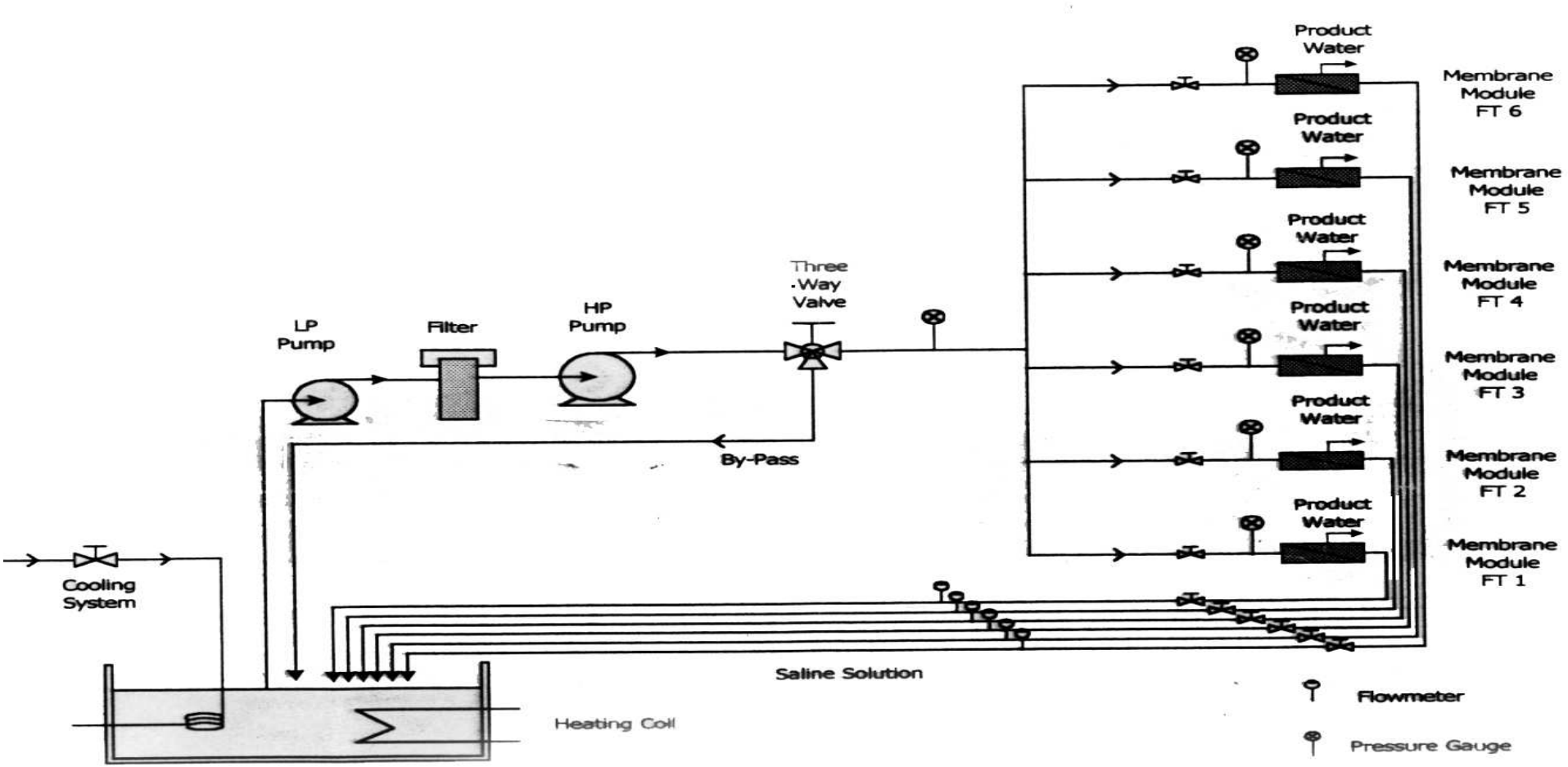

Figure 5-9 Illustration of the Layout of the Rig

5.4.1 Storage

The storage section contains the feed solution and consists of a 200 litre tank (Figure 5-10) that is fitted with a cooling device and a heating element. These two thermal devices are used to maintain the contents of the holding tank at a predetermined temperature. The temperature of the liquid in the tank is measured with a thermometer that is also in the tank. The thermometer is part of the monitoring section. The rejected flow from the rig is also returned to that holding tank. Considering that the volume of permeate is very small this does not affect the short term salinity of the tank water which is checked before and after each run.

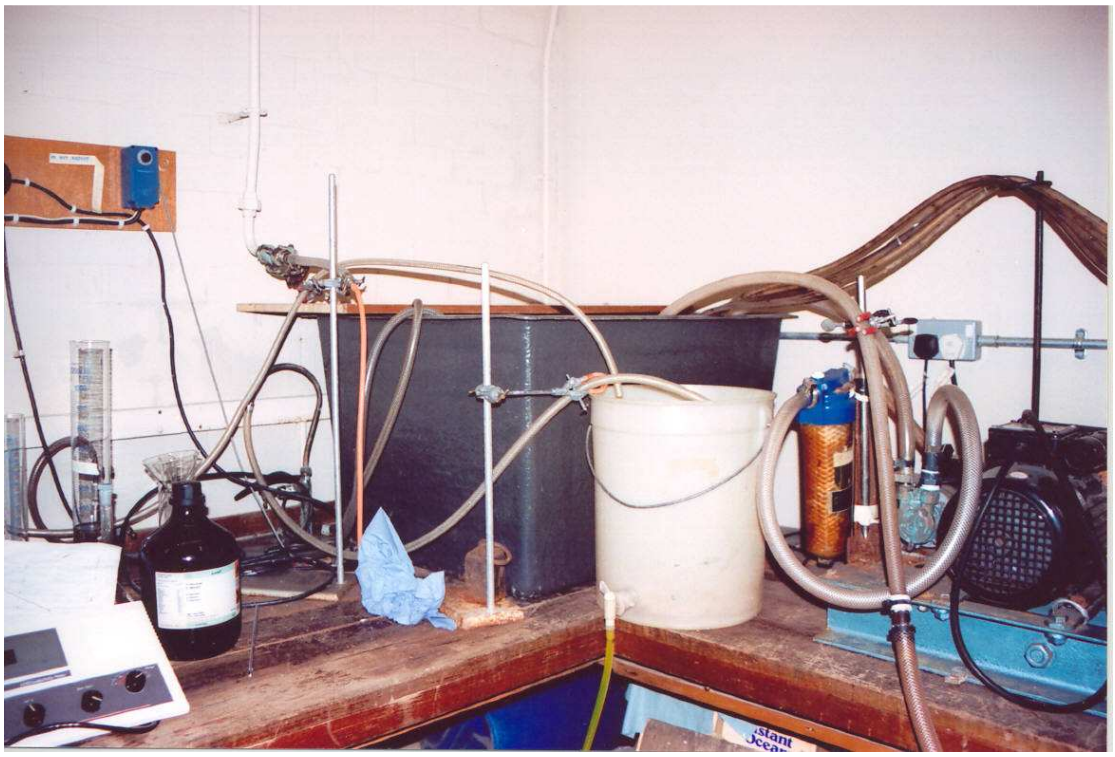

Figure 5-10 Holding Tank

5.4.2 Pumping

This section is made up of two pumps and an inline filter. The first pump is a low pressure pump that takes liquid from the holding tank and passes it through the inline filter to the high pressure pump that is responsible for feeding the membrane process section. The pumping module can produce pressure upwards of 85 bar.

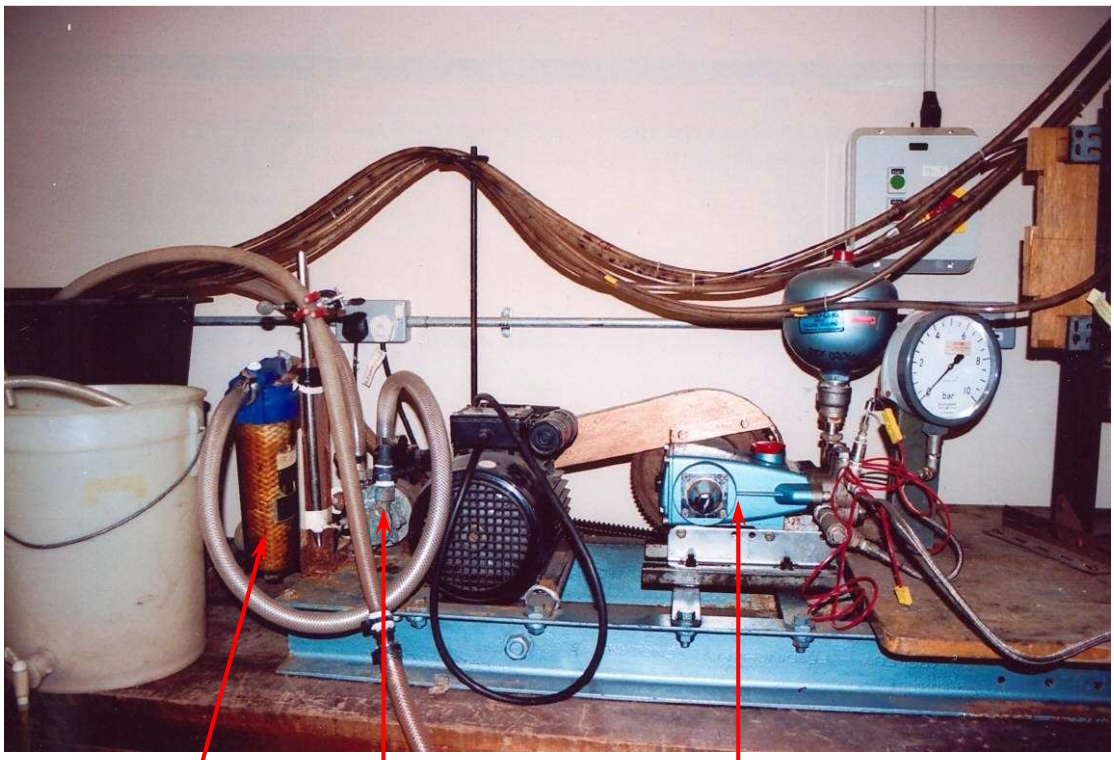

Figure 5-11 Pumps

5.4.3 Control

The control section is split into three parts.

The first part is the thermal devices in the holding tank that are used to maintain the temperature of the liquid in the rig.

The second part consists of a three way valve that can be adjusted to regulate the pressure and flow rate of the liquid that is the feed to the bulk of the membrane process.

And the third one consists of two pressure taps present before and after each individual membrane pressure cell (Figure 5-12). These are used to control the pressure and flow rate of the liquid through each membrane.

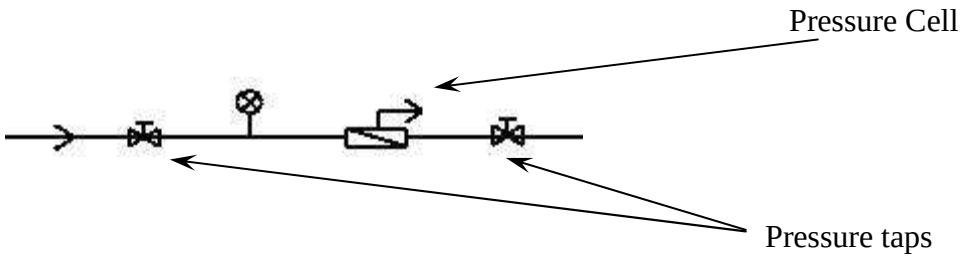

Figure 5-12 Layout of Pressure Taps

5.4.4 Membrane Test Cells.

The membrane process encompasses six identical pressure cells that are in a parallel configuration (Figure 5-13 and 5-14). Each pressure cell consists of six distinct sets of components.

Figure 5-13 Shows 6 Pressure Cells

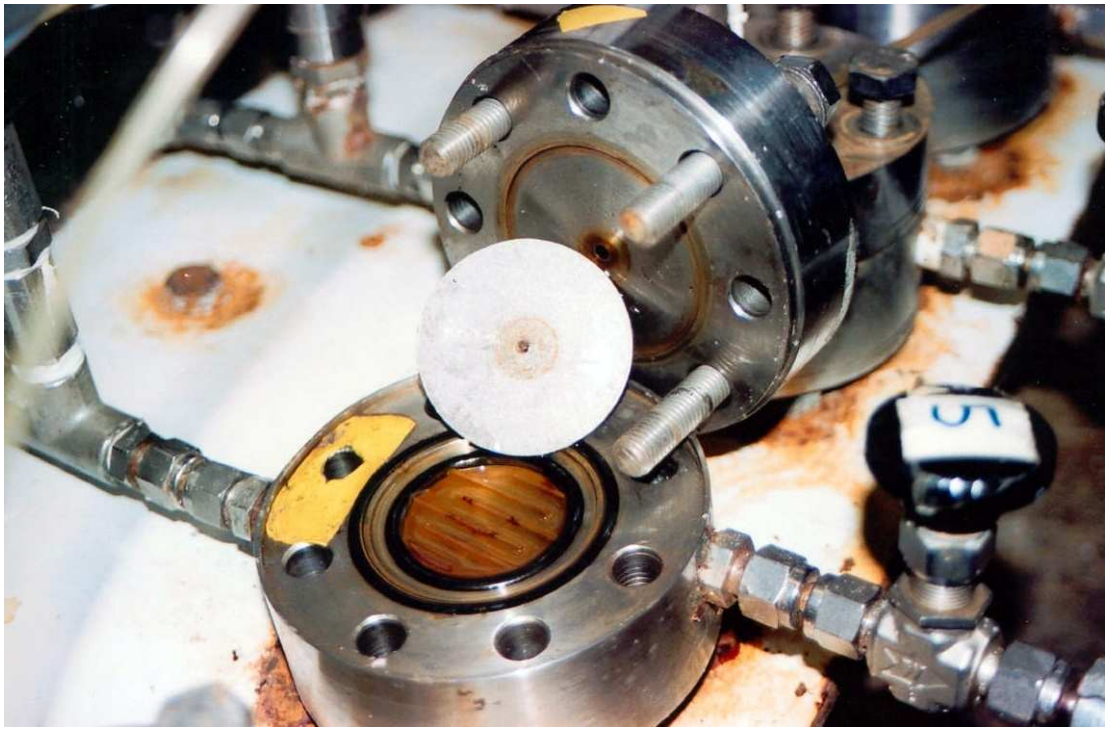

Figure 5-14 Pressure Cell Opened

- The base, made of stainless steel, allows the liquid to come in and leave in a crossflow pattern (Figure 5-15).

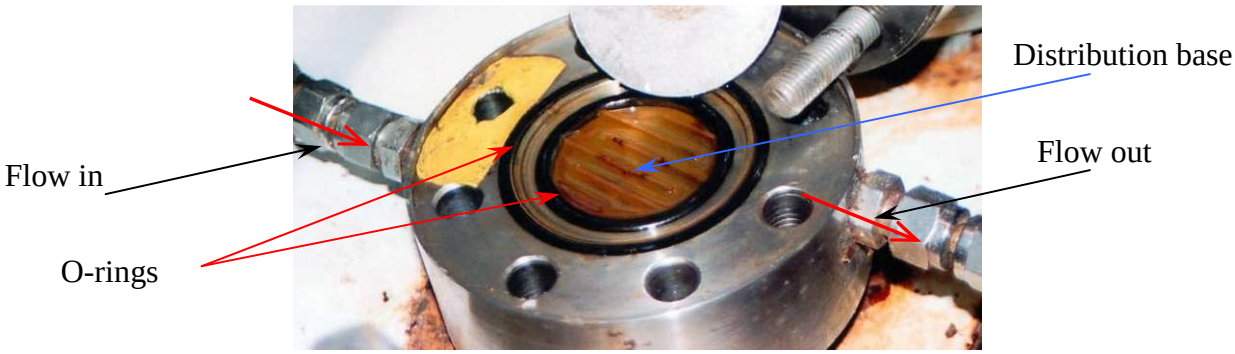

Figure 5-15 Flow in Cell

- The distribution base that shapes the incoming liquid for maximum flow against the membrane surface.

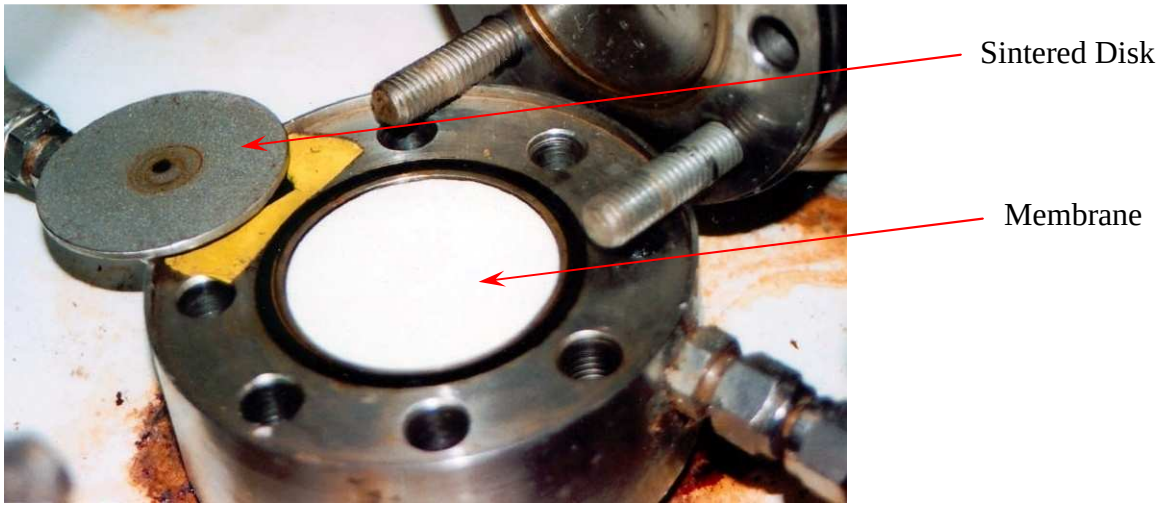

Figure 5-16 - Membrane Disc in Pressure Cell

- The membrane

The membrane disc has a diameter of 5 cm and of an area covering 19.63 cm^2.

The membrane shown in Figure 5-16 is a Filmtec SW30 membrane. Under optimal conditions it can yield a permeate flow rate of 34 m^3/d.

- A porous metallic disk that acts as backing surface for the membrane while allowing the filtrated liquid to pass through.

- A pair of O-rings to make the cell water tight as shown in Figure 5-15.

- The cover made of stainless steel that provides the top part of the cell. This cover has a small tube in the middle that allows the filter liquid to be collected.

And finally four bolts that are used to seal the base and the cover together. turning the device into a pressure cell.

5.4.5 Monitoring

This section provides the data from the experiments carried out on the rig. There are four types of data that are produced in this module.

- Pressure. There are 8 different readings here. One for the pump module, one after the three way valve for the membrane process and another six, one for each individual pressure cell. The first two readings are there to monitor the health of the various parts of the rig they are attached to and are not used in experimental calculations.

- Flowrate. There are six meters to read from, one for every pressure cell (Figure 5-17).

-Volume. This is the volume of filtrate collected in burettes (Figure 5-18) for each pressure cell. That is six values.

-Temperature. This is from the thermometer in the holding tank (Figure 5-10), it gives the temperature of the liquid flowing in the rig.

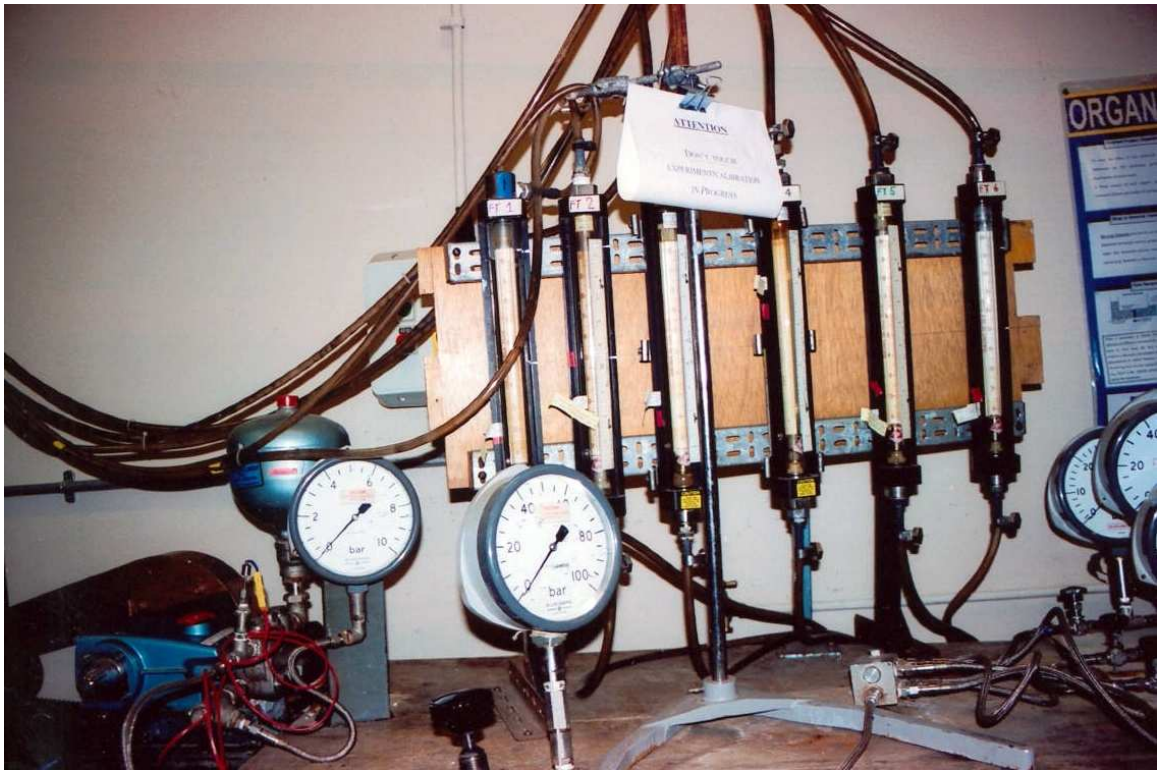

Figure 5-17 - Flow-meters

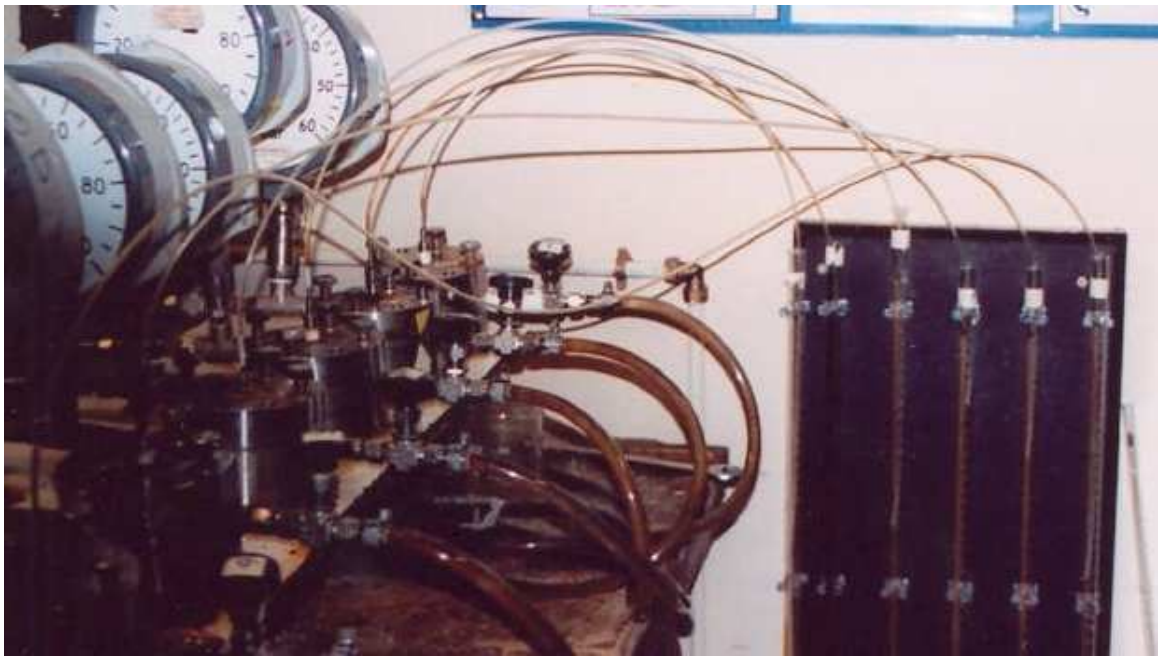

Figure 5-18 - Permeate collection in burettes

5.5 Calibration and Rig Commissioning

EXPERIMENTS

To start with, the conductivity meter was calibrated using five different known concentrations of NaCl. A concentration curve was plotted over the range of values obtained.

NaCl	50 ppm	100 ppm	300 ppm	2 000 ppm	10 000 ppm	35 000 ppm
Conductivity	0.13	0.24	0.655	3.80	16.55	50.3

Table 7 Results of Calibration experiment

This concentration curve can be used to find the corresponding salt concentration for each conductivity reading taken.

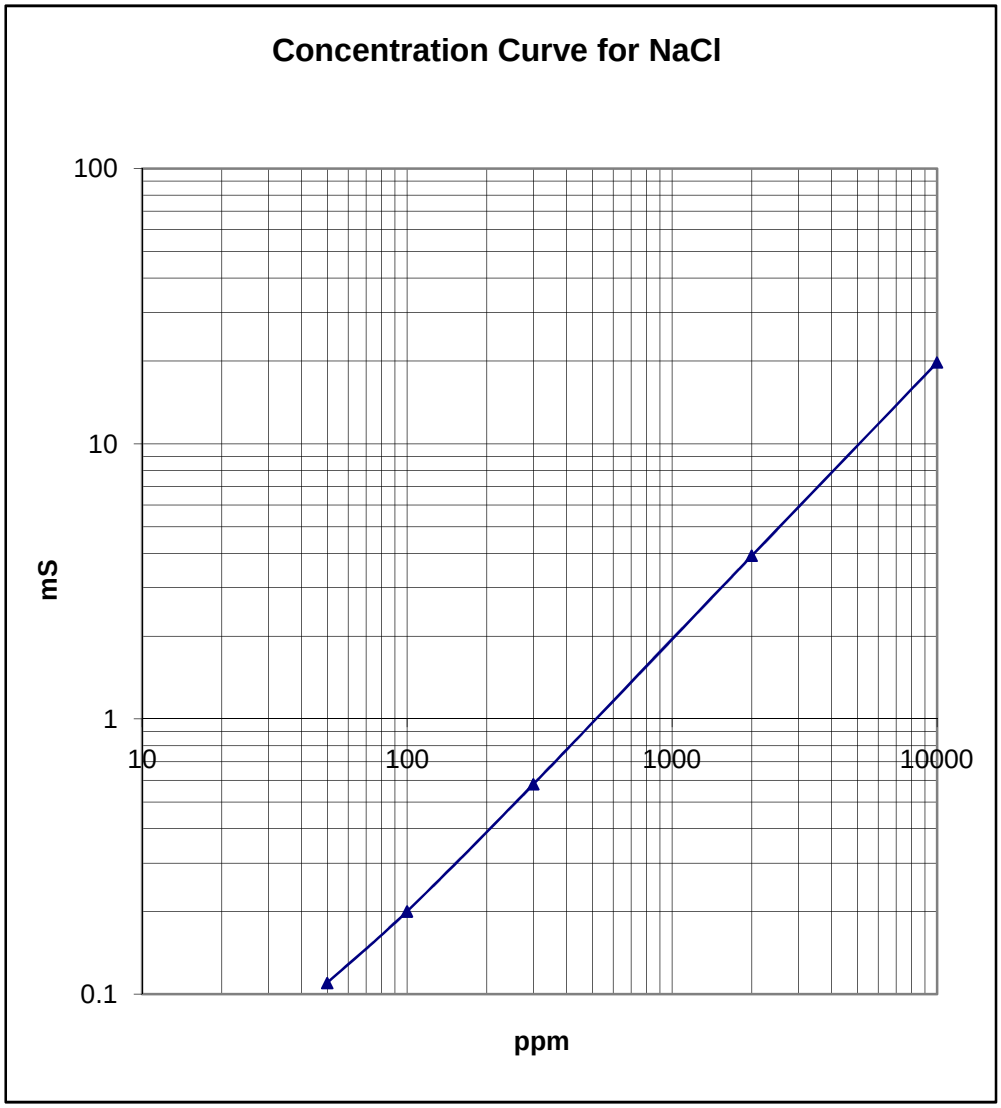

$y = 0.002x - 0.0049$

Figure 5-19 Calibration Curve for NaCl

$$y = 0.002x - 0.0049$$

This equation is used in the spreadsheet to continue the calculations. y represents conductivity in mS/cm and x is the concentration in ppm.

The curve above in Figure 5-19 is now used for calculation and can be approximated to the above linear equation.

5.6 Rig Integrity

Four samples of the same membrane were used for the following experiment to re-check the integrity of the rig and also determine the active surface of the membrane. The active surface was found by alternating the samples such that 2 cells would have the membrane with a particular surface facing the flow and the other 2 would have the other face in contact with the flow.

The results of the experiment are as follows:

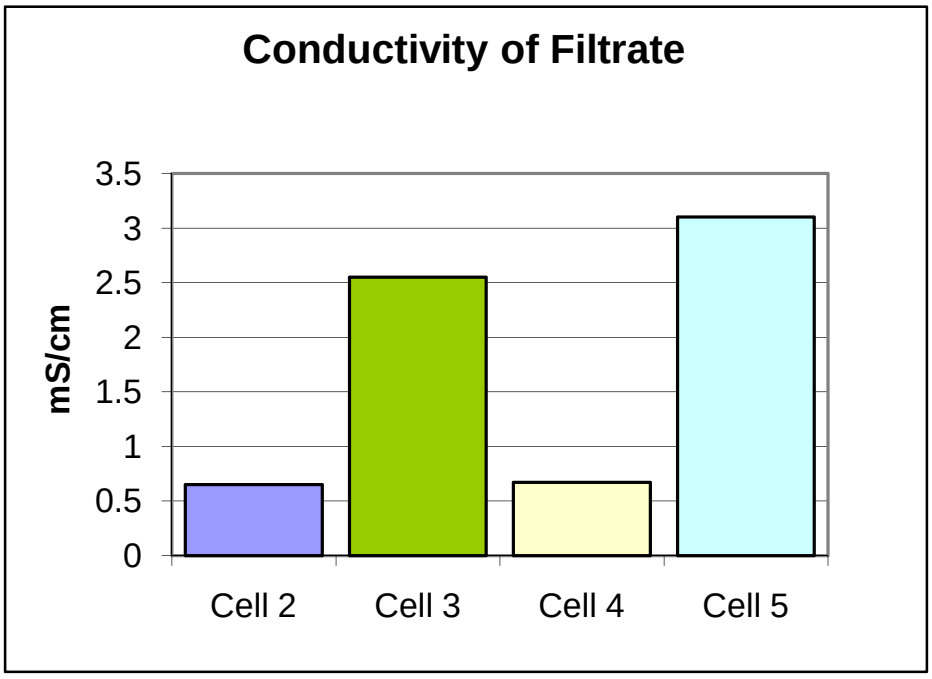

Figure 5-20 Conductivity of filtrate

CELLS	Cell 2	Cell 3	Cell 4	Cell 5
Conductivity mS/cm	0.65	2.55	0.67	3.10

Table 8 Conductivity of Cells 2-5

From table 8 it can be seen that cells 2 and 4 have lower conductivity compared to the two others, so this test confirmed which surface was the active surface in the membrane sheet. It turned out that the glossy side of the membrane is the active surface.

The next experiment was used to check for leaks and have an idea of the working of the rig. Miscellaneous membranes were used including a nanofiltration membrane and three reverse osmosis membranes with different side facing the flow.

The results from that experiment are summarised below and in Figure 5-21.

Time	**Conductivity in Cell mS/cm**			
	2	**3**	**4**	**5**
1250	**8.79**	**1.24**	**0.61**	**0.52**
1415	**8.70**	**1.12**	**0.58**	**0.51**
1515	**8.63**	**1.07**	**0.54**	**0.48**

Table 9 Conductivity in Cells

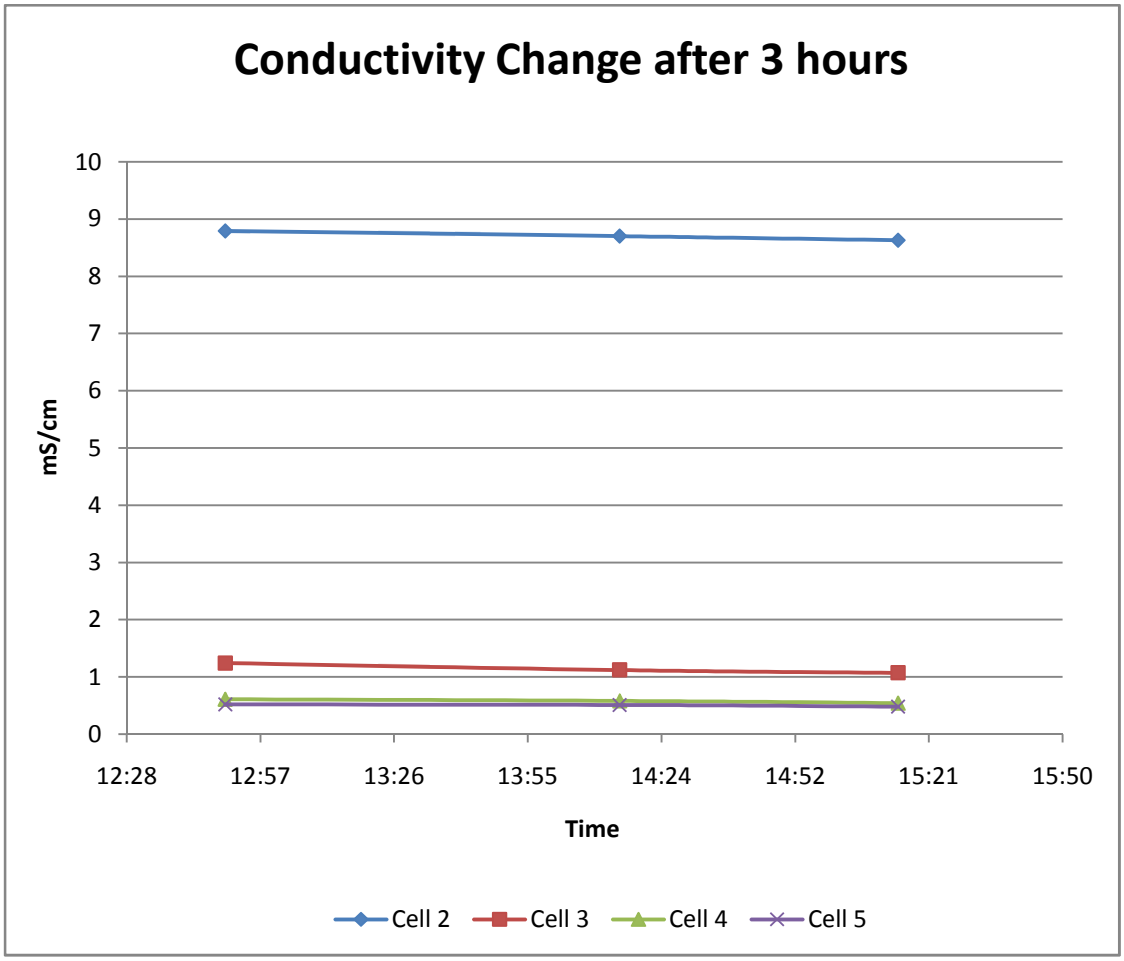

Figure 5-21 Conductivity in Cells after 3 hours

The cells, which had the higher filtrate flux, would have the samples in the proper set-up. From the two sets of experiments performed it was ascertained which surface of the membrane was the active one and needed to be exposed to the flow.

For the rest of the experiments the following procedures were used unless stated otherwise.

The tank was filled with 150 litres of 5500 mg/l NaCl and distilled water solution. This was achieved by weighing and adding 825 g NaCl to the tank containing 150 litres of distilled water

A spreadsheet was created to perform the routine calculation and graph plotting. The spreadsheet produced values for the following:

Salinity of the filtrate in ppm

- J_1 - k_1 - J_2 - k_2
- Percentage salt passage
- Percentage salt rejection

The following is an example of the formula used and the calculation made by the spreadsheet.

Typical results from a polyamide brackish water membrane

Molecular weight of water	= 18 kg
Molecular weight of salt	= 58.5 kg
Concentration of salt	= 2×10^{-3} kg/l
Volume of solution in tank	= 150 l
Measured conductivity	= 4.2 mS/cm
Temperature of feed	= 298 K

1 kg of solution contains 0.998 kg of H_2O and 2 x 10^{-3} kg of NaCl.

Hence

No. of kmoles of H_2O = mass/ molar mass

= 0.998 / 18

= 5.54 x 10^{-2}

No. of kmoles of NaCl = mass / molar mass

= 2 x 10^{-3} / 58.2

= 3.42 x 10^{-5}

Mole fraction of salt X_s = 3.42 x 10^{-5} / (5.54 x 10^{-2} + 3.42 x 10^{-5})

= 6.16 x 10^{-4}

Area of membrane = Πr^2

= Π $(2.5)^2$

= 19.63 cm^2

Osmotic pressure of feed Π_f = $\nu RTX_s / \nu_w$

= 2 x 8.314 x 298 x 6.16 x 10^{-4} / 1.8 x 10^{-4}

= 170 KJ/m^3

= 1.70 x 10^2 KN/m^2

= 1.70 x 10^5 N/m^2

Π_f = 1.70 bar

Pressure differential across the membrane ΔP **= (P – P_o)**

= 30 -1

ΔP = 29 bar

Permeate Conductivity = 30 μS

Salt concentration in Permeate = 60 ppm

= 60 mg/l

So

1 kg of Permeate contains 0.9994 kg of H_2O and 6 x 10^{-5} kg of NaCl.

No. of kmoles of H_2O = mass/ molar mass

= 0.9994 / 18

= 5.56 x 10^{-2}

No. of kmoles of NaCl = mass / molar mass

= 6 x 10^{-5} / 58.2

= 1.026 x 10^{-6}

Mole fraction of salt X_s = 1.026 x 10^{-6} / (5.56 x 10^{-2} + 1.026 x 10^{-6})

= 18.48 x 10^{-4}

Osmotic pressure of permeate Π_p = $\nu RTX_s / \nu_w$

$= 2 \times 8.314 \times 298 \times 18.48 \times 10^{-4} / 1.8 \times 10^{-4}$

$= 5.08\ KJ/m^3$

$= 5.08\ KN/m^2$

$= 0.0508 \times 10^5\ N/m^2$

Π_p = 0.051 bar

Difference in osmotic pressure across the membrane $\Delta\Pi$ = $\Pi_f - \Pi_p$

$= 1.70 - 0.051$

$\Delta\Pi$ = 1.65 bar

Calculations for J_1 and k_1

Permeate flow $= 3.8 \times 10^{-5}$ l/s

Membrane area $= 19.63\ cm^2$

Water flux through the membrane J_1 = (Density x Water flowrate) / Area

$= 1\ g/cm^3 \times 0.038\ cm^3/s / 19.63\ cm^2$

$J_1 = 1.94 \times 10^{-6}\ g/cm^2/sec$

$J_1 = k_1 (\Delta P - \Delta\Pi)$

Water permeability constant of the membrane k_1 **$= J_1 / (\Delta P - \Delta \Pi)$**

k_1 $= 1.94 \times 10^{-6} / (29 - 1.65)$

k_1 **$= 7.08 \times 10^{-5}$ g/cm^2/sec/bar**

Calculations for J_2 and k_2

Permeate flow $= 3.8 \times 10^{-5}$ l/s

Salt concentration in feed tank **C_b** $= 2315$ ppm

Salt concentration in permeate flow **C_d** $= 60$ mg/l

Salt concentration across the membrane ΔC_s **$= (C_b - C_d)$**

$= 2316 - 60$

$= 2255$ mg/l

ΔC_s **$= 2.26 \times 10^{-3}$ g/cm^3**

1 litre of permeate is collected in $= 1 / (3.8 \times 10^{-5})$s

$= 2.63 \times 10^4$ s

1 litre of permeate contains 60 mg of NaCl

Therefore 60 mg of NaCl passes through the membrane in 2.63×10^4 s

Salt flux through the membrane **J_2** **$= k_2 (\Delta C_s)$**

J_2 **$= (60 \times 10^{-3}) / (2.63 \times 10^4 \times 19.63)$**

J_2 **$= 1.16 \times 10^{-6}$ g/cm^2/sec**

Salt permeability constant of the membrane k_2 **= J_2 / (ΔC_s)**

= 1.16×10^{-6} / (2.26×10^{-3})

k_2 **= 5.15 x 10-5 cm/s**

The percentage salt passage of membrane **= (C_d / C_b) x 100**

= (60 / 2315) / x 100

= **2.59 %**

The percentage salt rejection of membrane **= 100 x (C_b – C_d) / C_b**

= 100 x (2315 – 60) / 2315

= **97.4 %**

The following set of experiments (Cells 1 to 5 of experiment BW/1) was used to investigate the effect of different feed pressures.

The 5 membranes used in this experiment are all BW 30 membranes provided by Filmtec. They were used to process a water/salt solution of 8.81 mS/cm (approx 44 mg/l). The experiment was used to find out the properties of that membrane and how they changed with an increase in pressure. The membranes were run at three different pressures 10, 20, and 30 bar.

The pressure in the individual cells was distributed as follows.

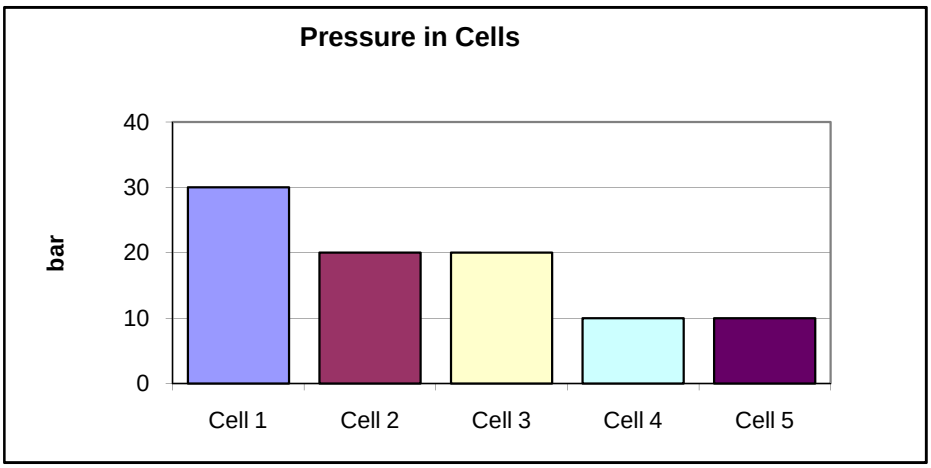

Figure 5-22 Pressure in Cells

Cell **1** → **30** bar

Cells **2** → **20** bar

Cells **3** → **20** bar

Cells **4** → **10** bar

Cells **5** → **10** bar

The conductivity of the product water was measured at different time intervals depending on the volume of permeate collected. The Bulk Conductivity of feed is 8.81 mS/cm (approx 44 mg/l) and all readings were taken at a feed temperature of 20 ^{o}C

The table below shows the conductivity of the permeate flux. These were measured using the conductivity meter.

Cell	**1**	**2**	**3**	**4**	**5**
Pressure (bar)	30	20	20	10	10
Time	**Conductivity of Product From Cell (mS/cm)**				
1140	Start	Start	Start	Start	Start
1210	0.655	1.03	0.91	1.42	1.755
1240	0.51	0.61	0.64	0.90	0.91
1340	0.51	0.57	0.60	0.90	0.88
1440	0.50	0.55	0.59	0.90	0.88
1510	0.50	0.54	0.58	0.90	0.88
1540	0.50	0.54	0.58	0.85	0.88
1640	0.49	0.54	0.58	0.83	0.87
1710	0.49	0.54	0.58	0.83	0.87

Table 10 Conductivity of Product Water from Cells

The Figure 5-23 below shows the trend for the conductivity against time.

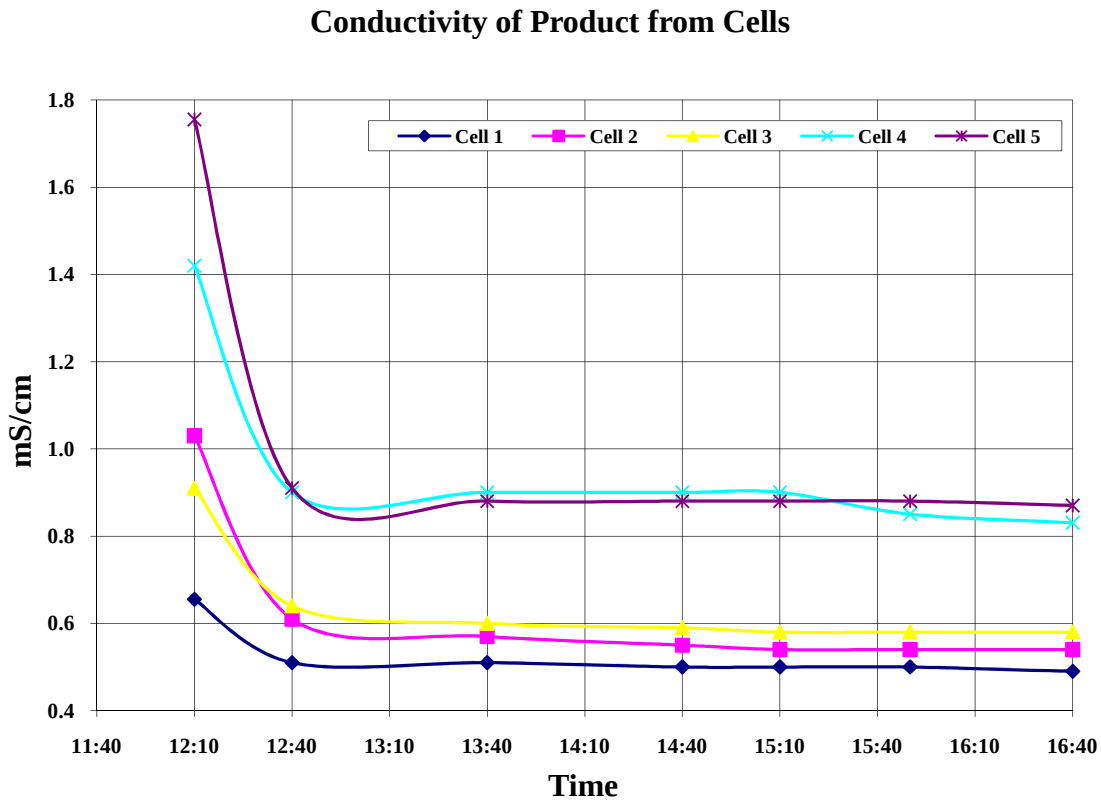

Figure 5-23 Conductivity of Product Water from Cells 1 to 5

The results are displayed in the following graphs. The results show that at higher pressures the membrane performs better. This improvement in performance is seen in both permeate flux and percentage salt passage.

The increase in permeate flux is very visible as the pressure increases. Whereas for percentage salt passage there is not as much improvement when the pressure is increased from 20 bar to 30 bar. But the percentage salt passage drops by about 4 % when the pressure is increased from 10 bar to 20 bar.

Overall it was observed that, as expected, an increase in pressure improves the performance of the membrane as indicated in the following graphs Figures 5-24 and 5-25.

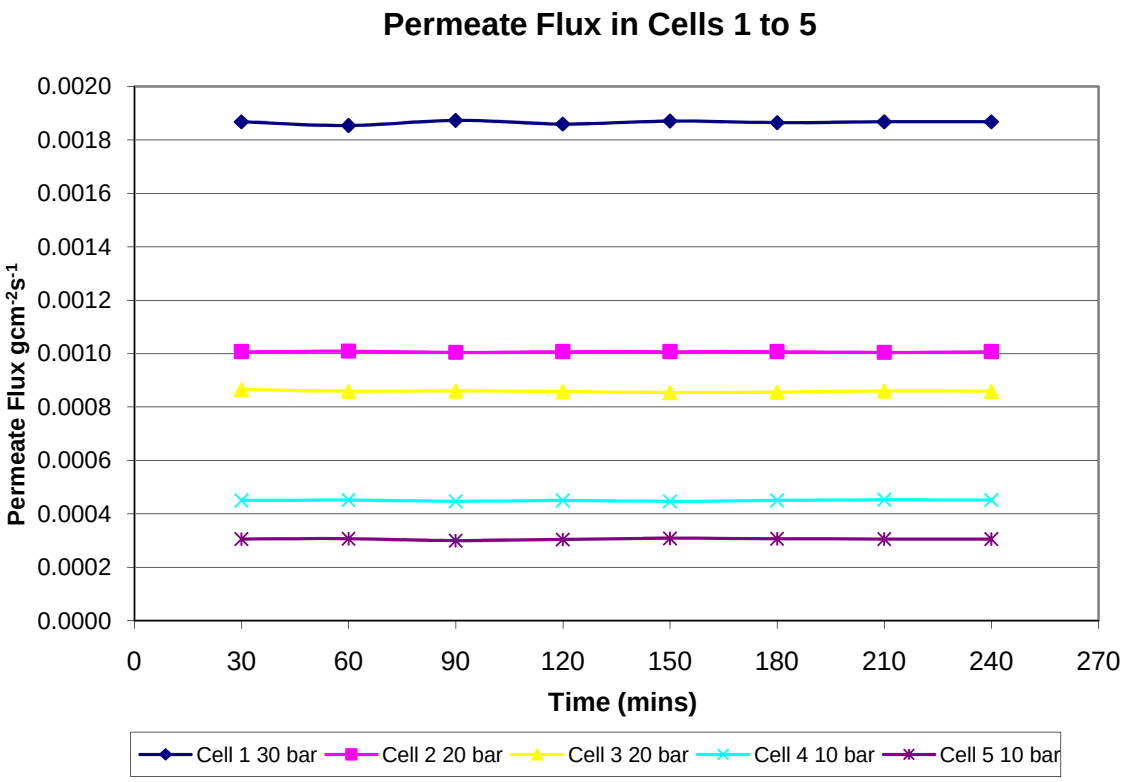

Figure 5-24 Permeate Flux in Cells 1-5

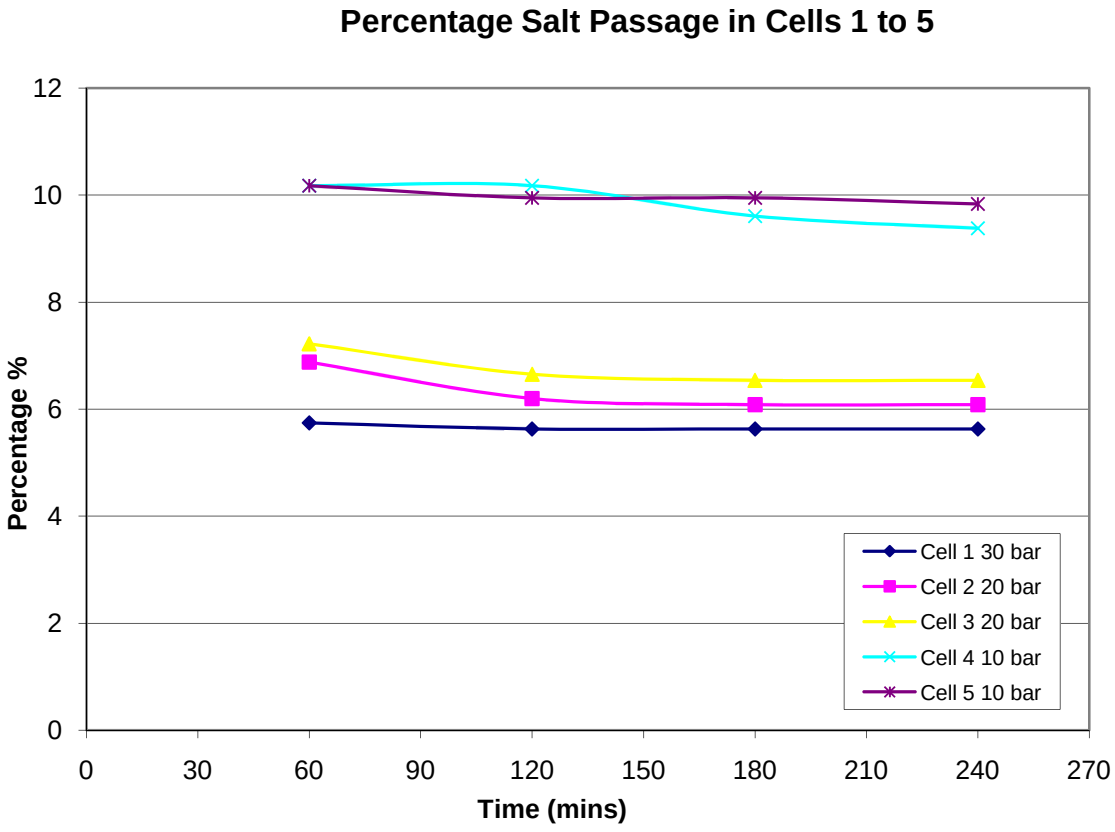

Figure 5-25 Percentage Salt Passage in Cells 1-5

From this set of experiments a number of factors emerged.

1. It takes three hours for the rig to stabilise and produce a constant flow rate and salt rejection.
2. It takes 30 minutes for the cell to produce a reasonable volume of water.
3. The expected trend of increasing performance was obtained with increasing operating pressure.

In summary, the work described in this chapter was successful in the familiarisation with the equipment and this enabled the initiation of the main project investigation described in the following chapter.

CHAPTER 6 RESULTS: HYDROCARBON FOULING OF POLYAMIDE MEMBRANES

6.1 Introduction

The experiments on polyamide membranes can be divided into the following two sets as two distinct types of membranes were used.

1. Seawater membrane polyamide SW 30.
2. Brackish water membrane polyamide BW 30.

Each experiment involved utilising a new set of membrane samples under the following parameters.

Feed TDS	5500 ppm NaCl
Pressure	30 bar
Temperature	23 ± 1 ^{o}C

The experimental protocol was generally as follows.

- Two membranes samples tested in the Reverse Osmosis rig without prior exposure to hydrocarbon contaminated liquid.
- Other membranes samples investigated as follows
    - Tested in Reverse Osmosis rig
    - Then removed from Reverse Osmosis rig, placed in separate vessels (see 5.3.1) and exposed to various hydrocarbon contaminated liquids per selected periods of time
    - Then returned to the Reverse Osmosis rig to measure their performance to assess any effect of the hydrocarbon exposure.

6.2 Seawater Membrane Polyamide SW 30

6.2.1 Summary of Experiments Undertaken

Table 11 provides a summary of the experiments that were carried out on the Seawater membranes polyamide SW 30.

Experiment	Cells	Stirring	Duration of exposure to hydrocarbon (h)	Membranes exposure to hydrocarbon-contaminated liquid.
Exp SW/1	1 & 2	-	-	None (Control)
	3 & 4	Y	24	Both sides of the membrane were exposed to a hexane water mixture
	5 & 6	Y	1	Both sides of the membrane were exposed to a Diesel water mixture
Exp SW/2	1 & 2			None (Control)
	3 & 4	Y	24	Both sides of the membrane were exposed to a hexane water mixture
	5 & 6	Y	2	Both sides of the membrane were exposed to a Diesel water mixture
Exp SW/3	1 & 2			None (Control)
	5 & 6	N	1	Both sides of the membrane were exposed to Pure Diesel

Table 11 Experiments on SW 30 Polyamide Membranes.

Experiment	Cells	Stirring	Duration of exposure to hydrocarbon (h)	Membranes exposure to hydrocarbon-contaminated liquid.
Exp SW/4	1 & 2			None (Control)
	3 & 4	Y	3	Both sides of the membrane were exposed to a hexane water mixture
	5 & 6	N	1	Both sides of the membrane were exposed to Pure hexane
Exp SW/5	1 & 2			None (Control)
	3 & 4	Y	3	The active side was exposed to a hexane water mixture
	5 & 6	Y	3	The active side was exposed to a Diesel water mixture
Exp SW/6	1 & 2			None (Control)
	3 & 4	Y	3	The active side was exposed to a hexane water mixture
	5 & 6	Y	6	The active side was exposed to a Diesel water mixture
Exp SW/7	1 & 2			None (Control)
	3 & 4	Y	3	The passive side was exposed to a hexane water mixture
	5 & 6	N	X	Both sides of the membrane were exposed to the aqueous phase of a hexane water mixture

Table 11 Contd.

6.2.2 Results of Experiments on SW 30 Membrane

EXPERIMENT SW/1

The layout of this experiment was as follows:

Cells 1 & 2 no exposure to hydrocarbon (Control)

Cells 3 & 4 --> 24 hours exposure in a hexane / water mixture (1:10) with stirring and both sides of the membrane exposed.

Cells 5 & 6 --> 1 hour exposure in a Diesel / water mixture (1:10) with stirring and both sides of the membrane exposed.

Figures 6-1 to 6-6 show a comparison of the flowrate and percentage salt passage before and after treatment for each pair of cells.

Note that the captions ‘Before’ and ‘After’ in Figure 6-1 simply relate to the performance of the control samples when monitored in the Reverse Osmosis Ring at the same times as the other samples before and after the hydrocarbon exposure of the latter.

Cells 1 & 2

As expected, there was some minor experimental scatter but no significant difference in the fluxes and salt passages in the two phases of testing.

Cells 3 & 4

The membranes of cells 3 and 4 were completely blocked i.e. no permeate flux was detectable. They were left in the rig for 3 hours and that did not change. So it can be

seen that long exposure to a hexane water mixture has disastrous consequences for the SW 30 membrane.

Cells 5 & 6

The membranes of cells 5 and 6 were exposed to the diesel water mixture for only one hour. Their performance showed some deterioration. There was a reduction in flux and also an increase in salt passage.

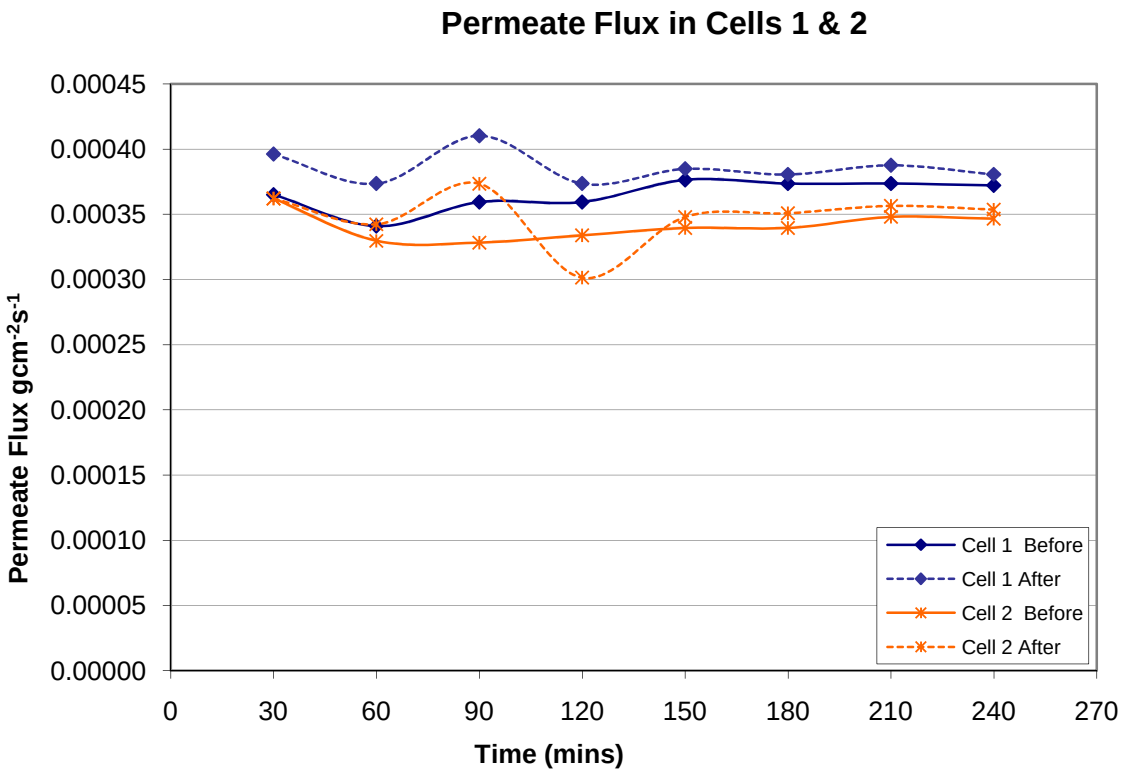

Figure 6-1 Permeate Flux in cells 1 & 2 of Exp. SW/1

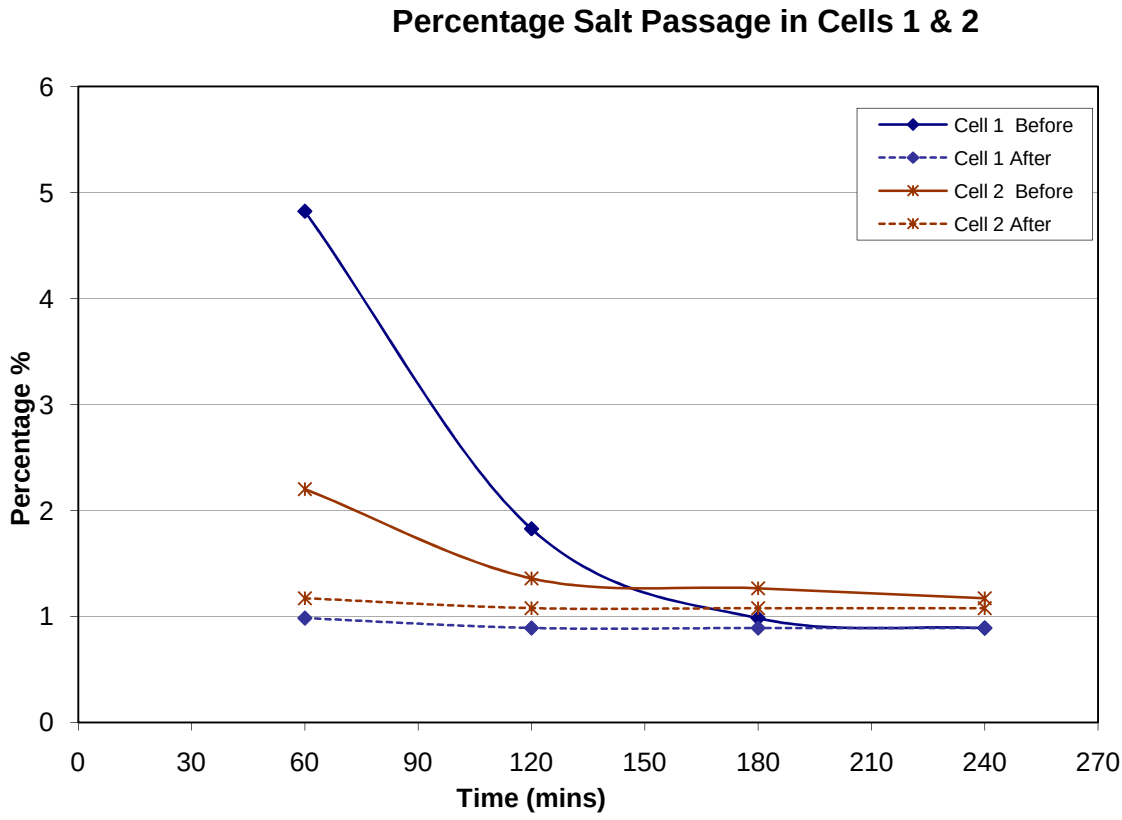

Figure 6-2 Percentage Salt Passage in Cells 1 & 2 of Exp. SW/1

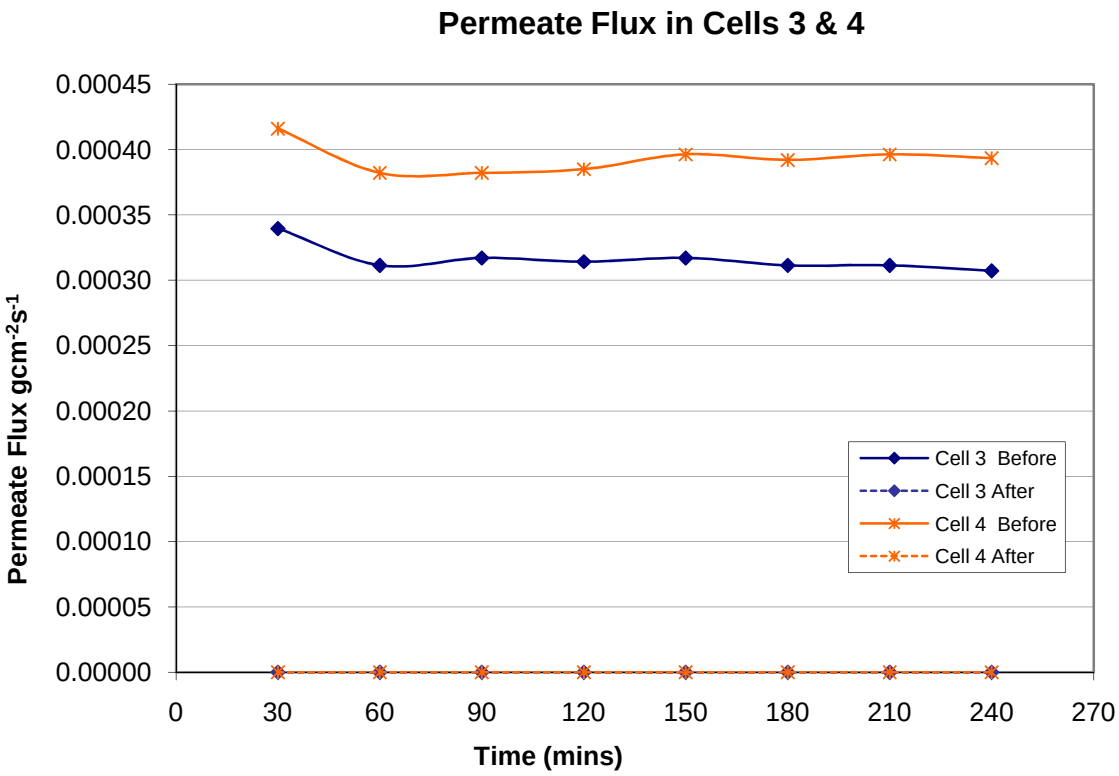

Figure 6-3 Permeate Flux in cells 3 & 4 of Exp. SW/1

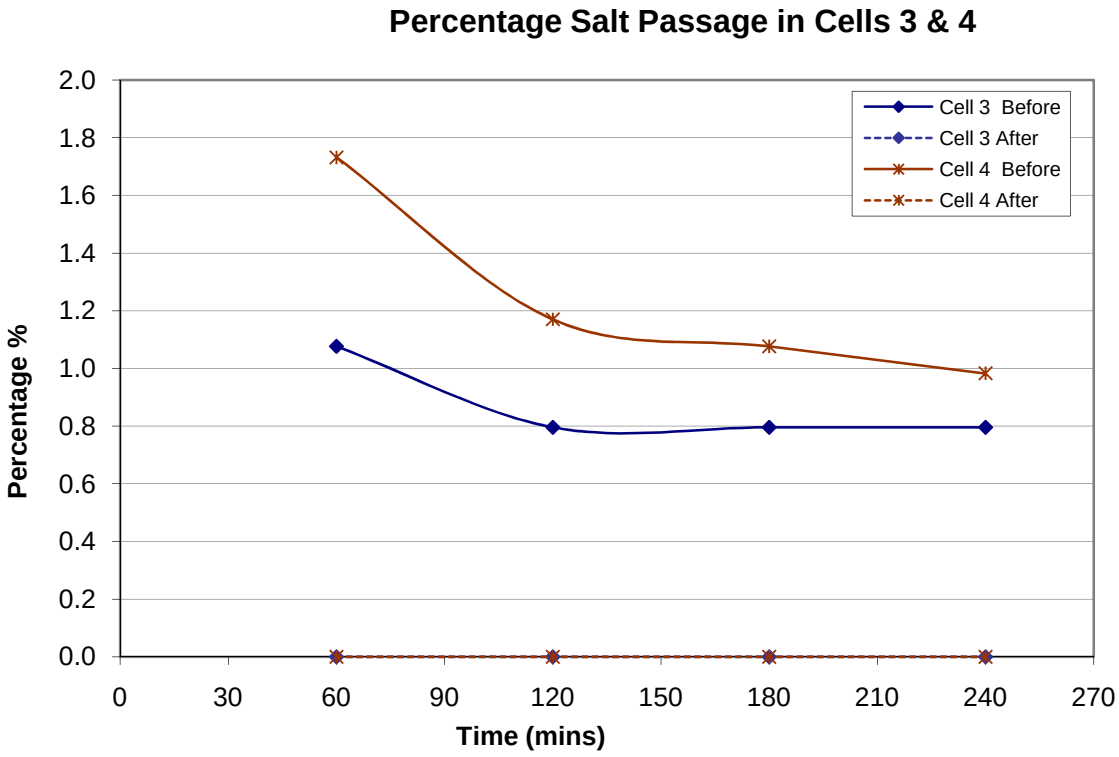

Figure 6-4 Percentage Salt Passage in Cells 3 & 4 of Exp. SW/1

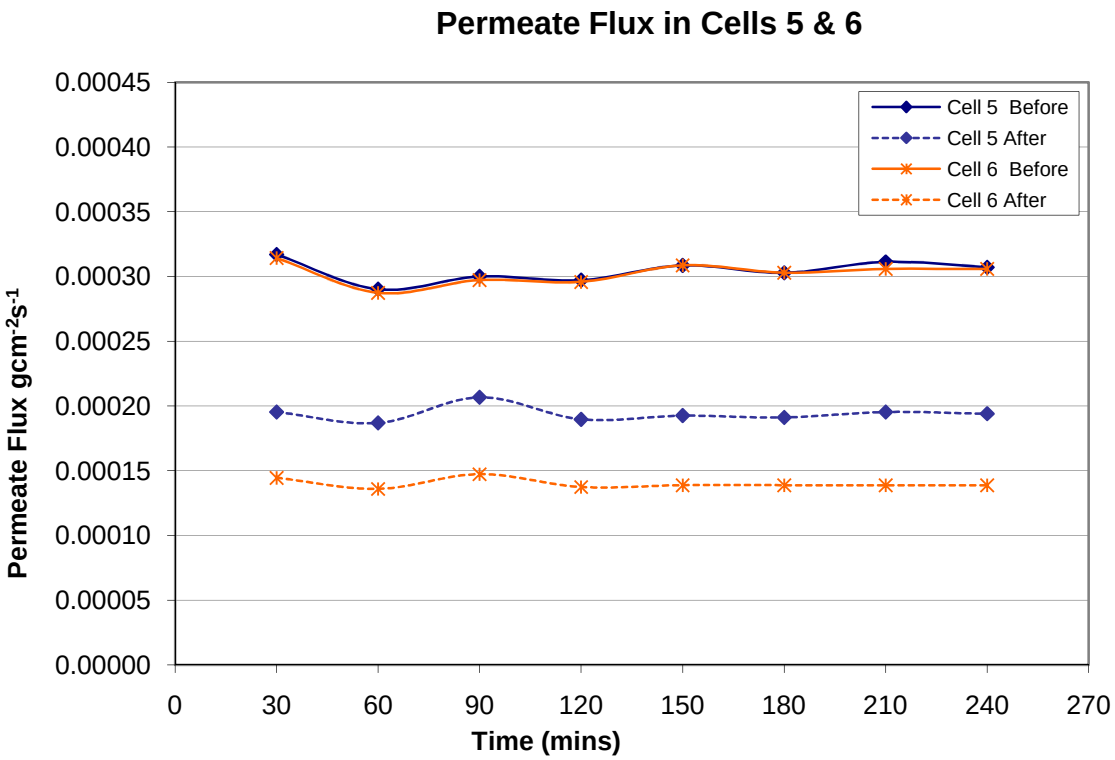

Figure 6-5 Permeate Flux in cells 5 & 6 of Exp. SW/1

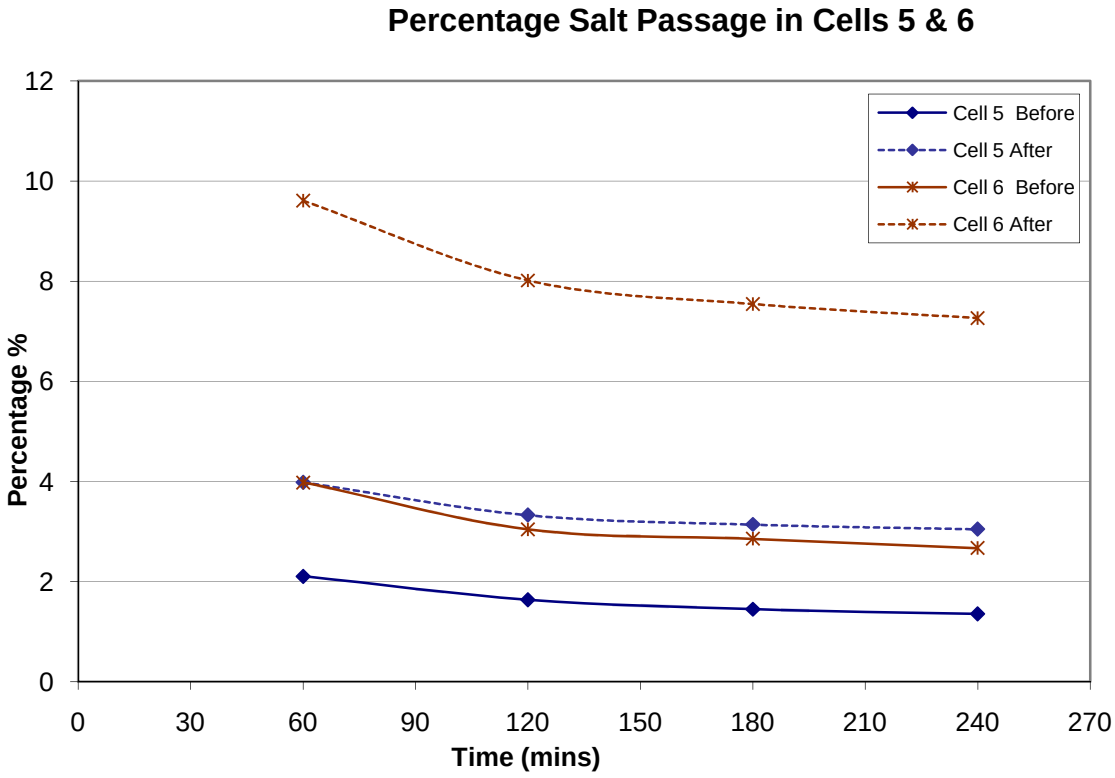

Figure 6-6 Percentage Salt Passage in Cells 5 & 6 of Exp. SW/1

EXPERIMENT SW/2

The detailed graphical results can be found in Appendix I

The layout of this experiment is as follows

Cells 1 & 2 no exposure to hydrocarbon (Control)

Cells 3 & 4 --> 24 hours exposure in a hexane / water mixture (1:10) with stirring and both sides of the membrane exposed. (i.e. replication of experiment 1)

Cells 5 & 6 --> 2 hours exposure in a Diesel / water mixture (1:10) with stirring and both sides of the membrane exposed.

Cells 1 & 2

As expected, there was some minor experimental scatter but no significant difference in the fluxes and salt passages in the two phases of testing.

Cells 3 & 4

These produced the same behaviour as in Experiment 1. Their measured fluxes were about 2.5 $x10^{-4}$ $gcm^{-2}s^{-1}$ and percentage salt passage about 2% in the first phase of testing prior to hydrocarbon exposure but, after the hexane / water treatment the membranes of cells 3 and 4 were found to be completely blocked (zero permeate production over the 3 hour monitoring period) similarly to what was seen in cells 3 and 4 of experiment 1. This confirmed that long exposure to a hexane water mixture has disastrous consequences for the SW 30 membrane.

Cells 5 & 6

The membranes of cells 5 and 6 provided the usual performances (flux 3.2 $x10^{-4}$ $gcm^{-2}s^{-1}$, percentage salt passage 1.6%) in the first phase of the test but, after being exposed to the diesel water mixture for two hours this time, they were rendered completely unusable. They were completely blocked (zero permeate production).

EXPERIMENT SW/3

The detailed graphical results can be found in Appendix I

The layout of this experiment is as follows:

Cells 1 & 2 no exposure to hydrocarbon (Control)

Cells 5 & 6 --> 1 hour exposure to Pure Diesel without stirring and both sides of the membrane exposed.

Cells 5 & 6

The membranes were exposed to pure diesel to confirm that it is not just the mixture but diesel that causes the damage to the membranes. As expected from the indications in the previous experiment, the membrane was rendered unusable (i.e. zero permeate production) after having been in contact with pure diesel for just one hour.

EXPERIMENT SW/4

The detailed graphical results can be found in Appendix I

The layout of this experiment is as follows:

Cells 1 & 2 no exposure to hydrocarbon (Control)

Cells 3 & 4 --> 3 hours exposure to a hexane water mixture (1:10) with stirring both sides of the membrane exposed with stirring

Cells 5 & 6 --> 1 hour exposure to Pure hexane without stirring both sides of the membrane exposed.

Cells 1 & 2

As expected, there was some minor experimental scatter but no significant difference in the fluxes and salt passages in the two phases of testing.

Cells 3 & 4

The membranes in cells 3 and 4 were exposed to the hexane 1:10 mixture for just 3 hours this time as opposed to 24 hours in the previous experiments. Even though the time of exposure was considerably less, the negative result was the same. The membranes were totally blocked (zero permeate production).

Cells 5 & 6

The membranes in cells 5 and 6 were exposed to pure hexane this time to confirm that it is not just the mixture but also hexane that causes the damage to the membranes. As expected from the indications in the previous experiment, the membrane was rendered

unusable after (zero permeate production) having been in contact with pure hexane for just one hour.

EXPERIMENT SW/5

The layout of this experiment is as follows:

Cells 1 & 2 no exposure to hydrocarbon (Control)

Cells 3 & 4 --> 3 hours exposure to a hexane / water mixture (1:10) with stirring and only the active side of the membrane exposed with stirring

Cells 5 & 6 --> 3 hours exposure to a diesel / water mixture (1:10) with stirring and only the active side of the membrane exposed.

Figures 6-7 to 6-12 show a comparison of the flowrate and percentage salt passage before and after treatment for each pair of cells.

This set of experiments involved the exposure of only the active surface, as in most cases it is the only surface that will be affected by any fouling. This is because the fouling agent which has larger molecules than water will be stopped by the active surface and will not get to the backing material.

Cells 1 & 2

As expected, there was some minor experimental scatter but no significant difference in the fluxes and salt passages in the two phases of testing.

Cells 3 & 4

The membranes of cells 3 and 4 were exposed to the hexane water mixture for three hours. Their performances showed an increase in permeate flux and percentage salt passage. There was a reduction in flux and also an increase in salt passage

Cells 5 & 6

The membranes of cells 5 and 6 were exposed to the diesel water (1:10) mixture for three hours. Their performances showed small changes in permeate flux and increase in salt passage. There was an increase in salt passage, though in this case the flux did not seem to suffer.

The following graphs (Figures 6-7 to 6-12) show a comparison of the flowrate and percentage salt passage before and after treatment for each pair of cells.

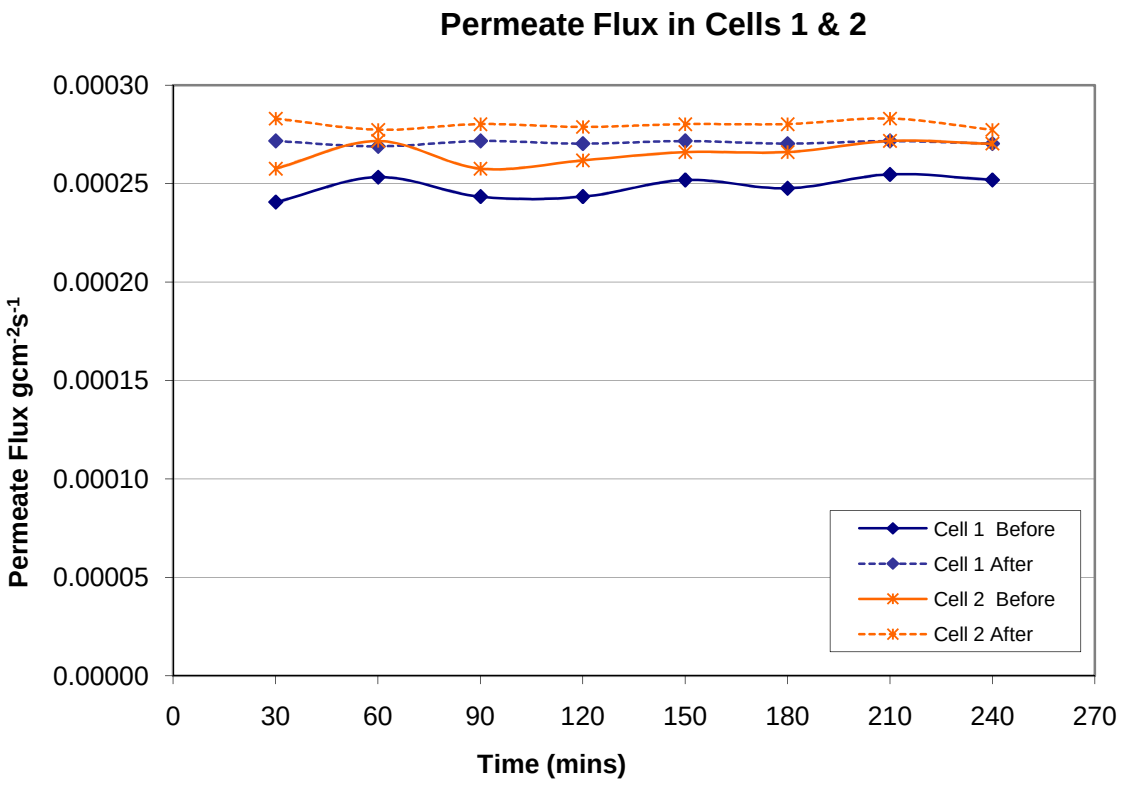

Figure 6-7 Permeate Flux in Cells 1 & 2 of Exp. SW/5

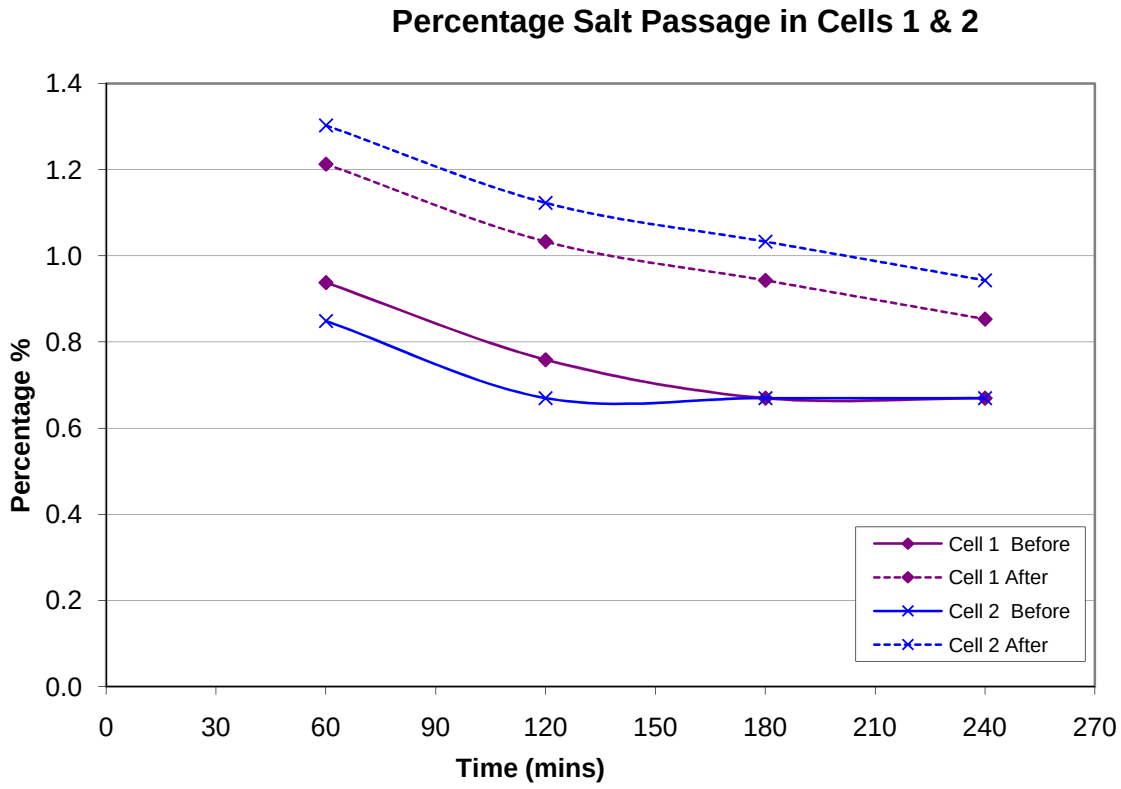

Figure 6-8 Percentage Salt Passage in Cells 1 & 2 of Exp. SW/5

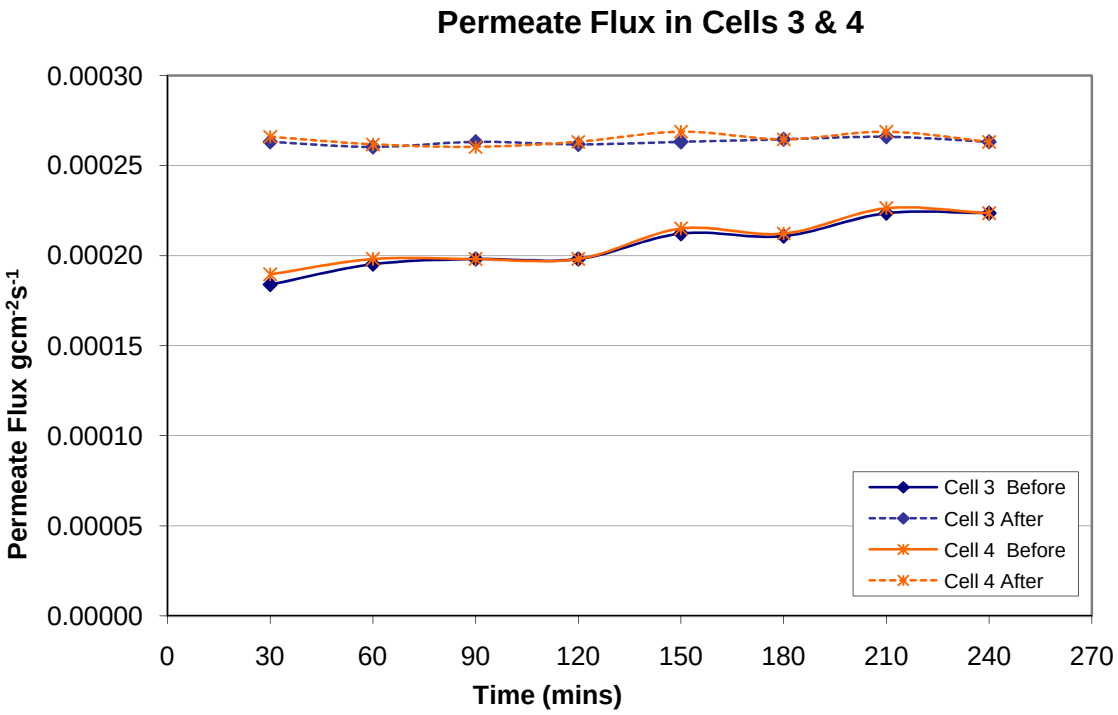

Figure 6-9 Permeate Flux in Cells 3 & 4 of Exp. SW/5

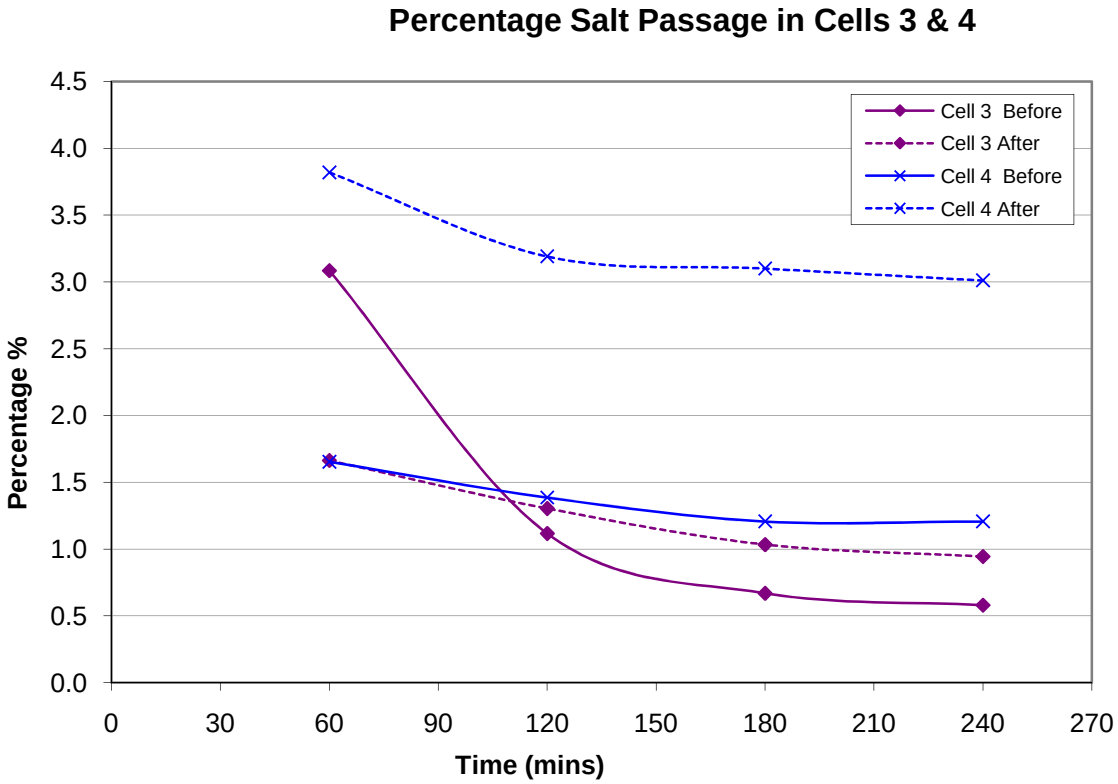

Figure 6-10 Percentage Salt Passage in Cells 3 & 4 of Exp. SW/5

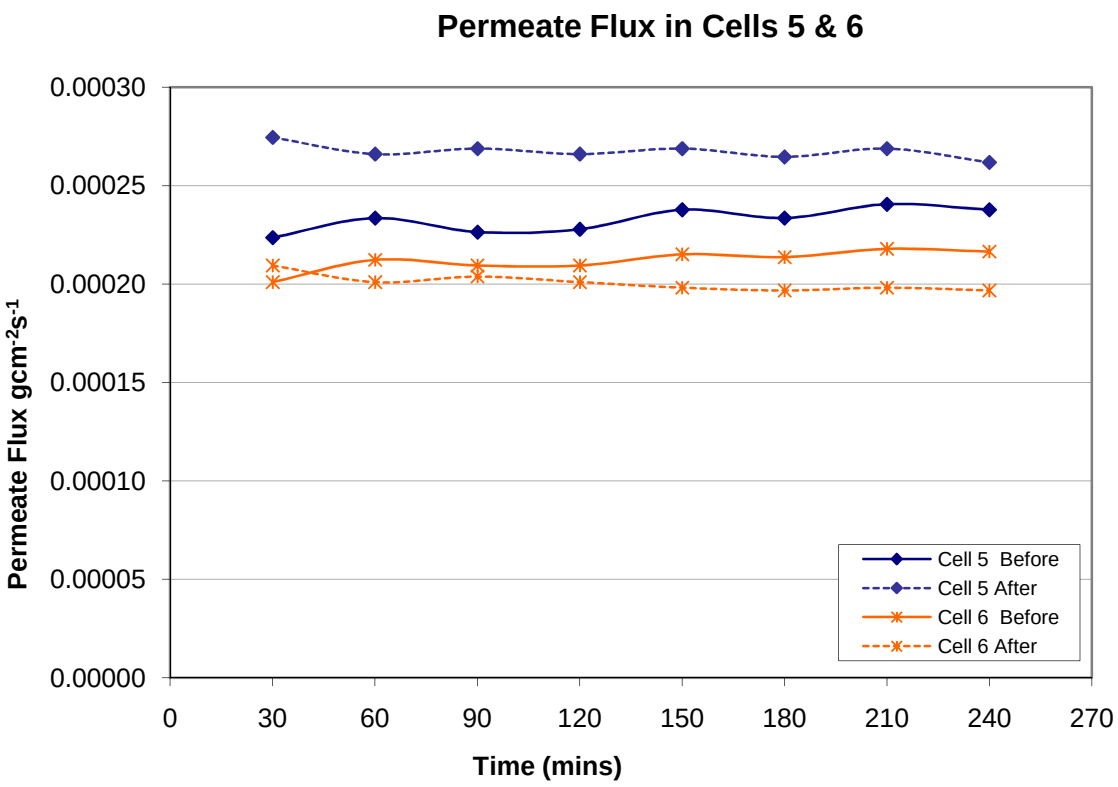

Figure 6-11 Permeate Flux in Cells 5 & 6 of Exp. SW/5

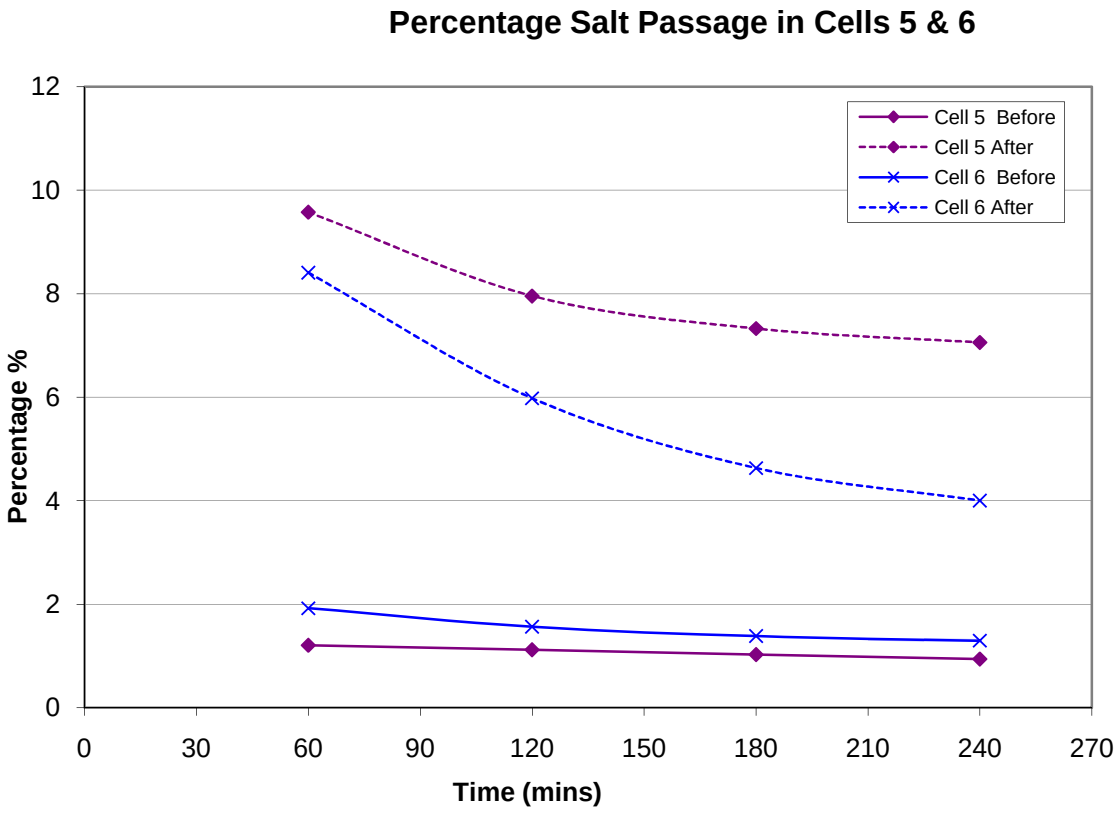

Figure 6-12 Percentage Salt Passage in Cells 5 & 6 of Exp. SW/5

EXPERIMENT SW/6

The layout of this experiment is as follows:

Cells 1 & 2 no exposure to hydrocarbon (Control)

Cells 3 & 4 --> 6 hours exposure to a hexane / water mixture (1:10) with stirring and only the active side of the membrane exposed with stirring

Cells 5 & 6 --> 6 hours exposure to a diesel / water mixture (1:10) with stirring and only the active side of the membrane exposed.

Cells 1 & 2

As expected, there was some minor experimental scatter but no significant difference in the fluxes and salt passages in the two phases of testing.

Cells 3 to 6

As in the experiment 5 (cells 3-6) only the active surface was exposed to the fouling agent. This time the length of the exposure was doubled to six hours. But this did not cause any substantially greater effects on the membrane performance than the shorter exposures in that, again there were small increases in flux and in percentage salt passage.

Figures 6-13 to 6-18 show a comparison of the flowrate and percentage salt passage before and after treatment for each pair of cells.

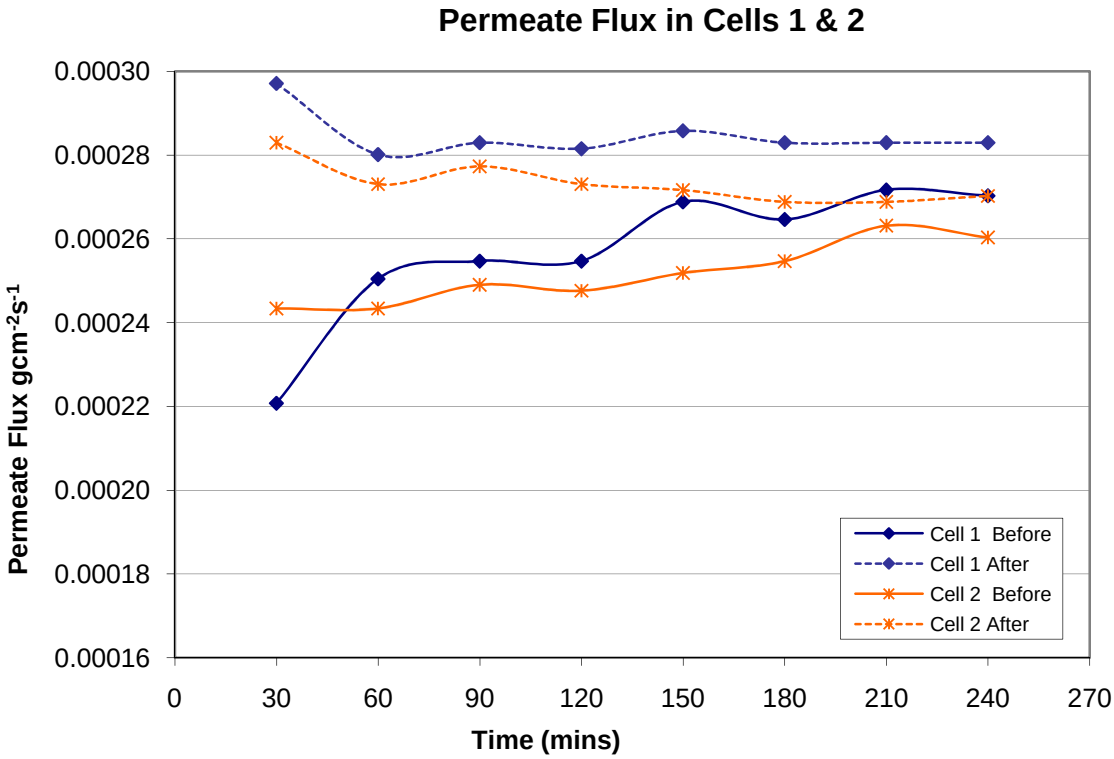

Figure 6-13 Permeate Flux in Cells 1 & 2 of Exp. SW/6

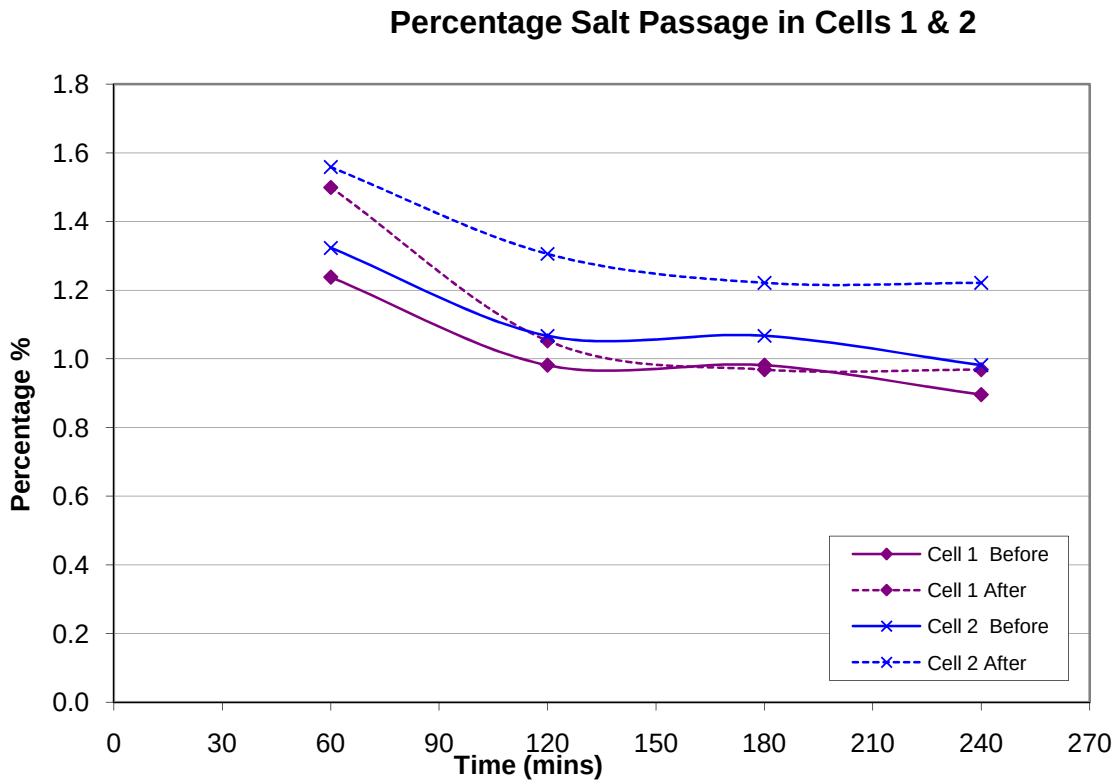

Figure 6-14 Percentage Salt Passage in Cells 1 & 2 of Exp. SW/6

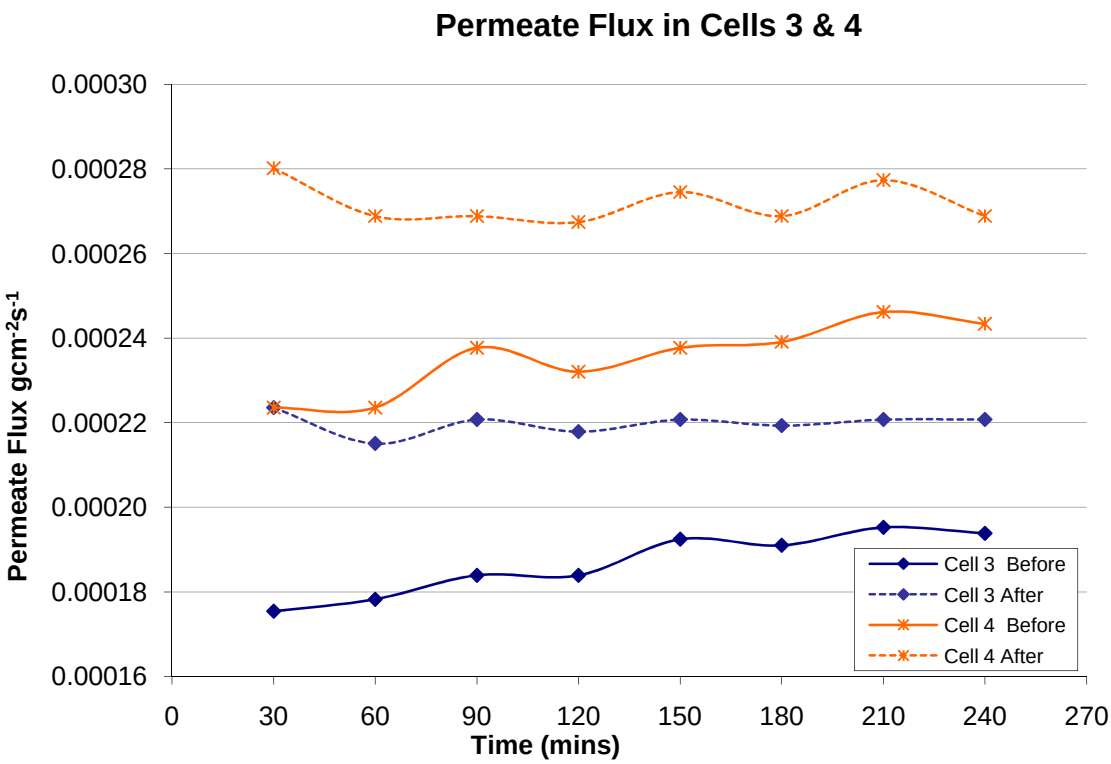

Figure 6-15 Permeate Flux in Cells 3 & 4 of Exp. SW/6

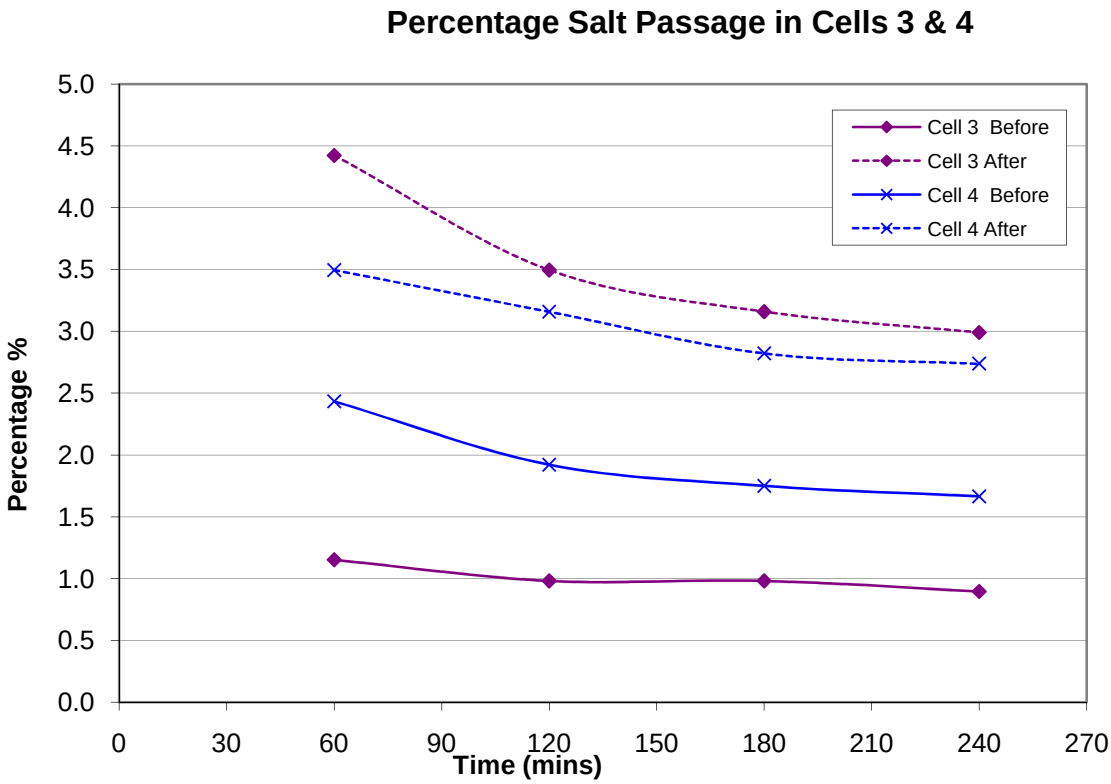

Figure 6-16 Percentage Salt Passage in Cells 3 & 4 of Exp. SW/6

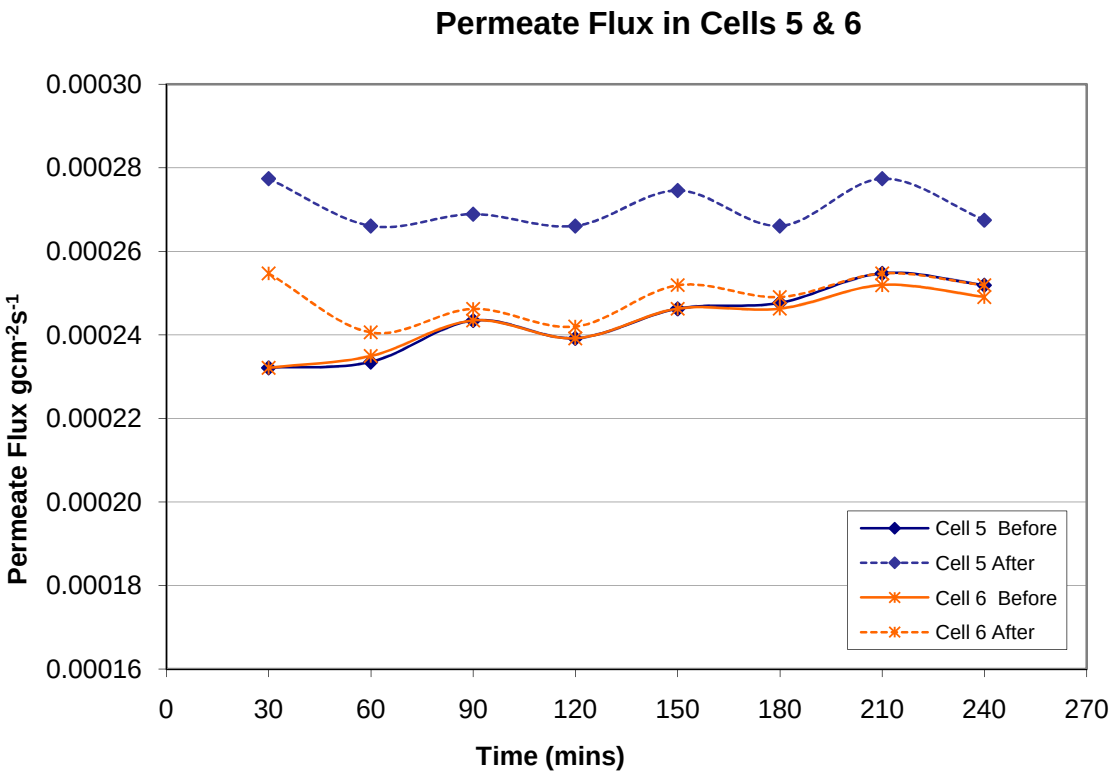

Figure 6-17 Permeate Flux in Cells 5 & 6 of Exp. SW/6

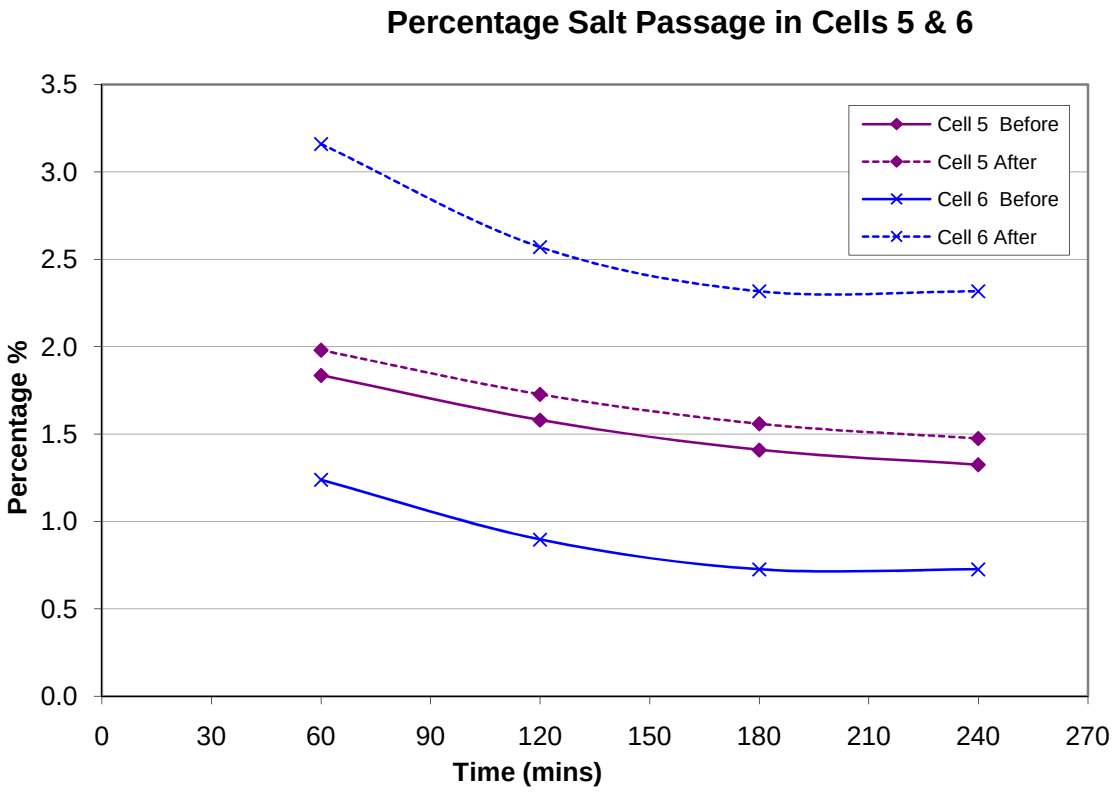

Figure 6-18 Percentage Salt Passage in Cells 5 & 6 of Exp. SW/6

EXPERIMENT SW/7

The layout of this experiment is as follows:

Cells 1 & 2 no exposure to hydrocarbon (Control)

Cells 3 & 4 --> 4 weeks fouling in the aqueous phase of a hexane water mixture without stirring and only the both sides of the membrane exposed

Cells 5 & 6 --> 3 hours fouling in a hexane water mixture (1:10) with stirring and only the passive side of the membrane exposed with stirring.

Cells 1 & 2

As expected, there was some minor experimental scatter but no significant difference in the fluxes and salt passages in the two phases of testing.

Cells 3 & 4

The membranes of cells 3 and 4 were exposed to the aqueous phase of a hexane water mixture for four weeks. The result was a change in performance. The salt passage increased. The permeate flux also showed a very slight increase.

Cells 5 & 6

From the previous experiments it was observed that the damage to the membranes were not as pronounced when the passive (backing) surface was not exposed to the fouling agent. To confirm the susceptibility of the passive surface to fouling in this experiment only that particular surface was exposed.

As suspected the membranes from cells 5 and 6 were completely blocked after the membranes' passive surface was contaminated. This shows that the material that is used as the backing surface does not tolerate hydrocarbon fouling.

The following graphs (Figures 6-19 and 6-20) show a comparison of the flowrate and percentage salt passage before and after treatment for cells 3 and 4.

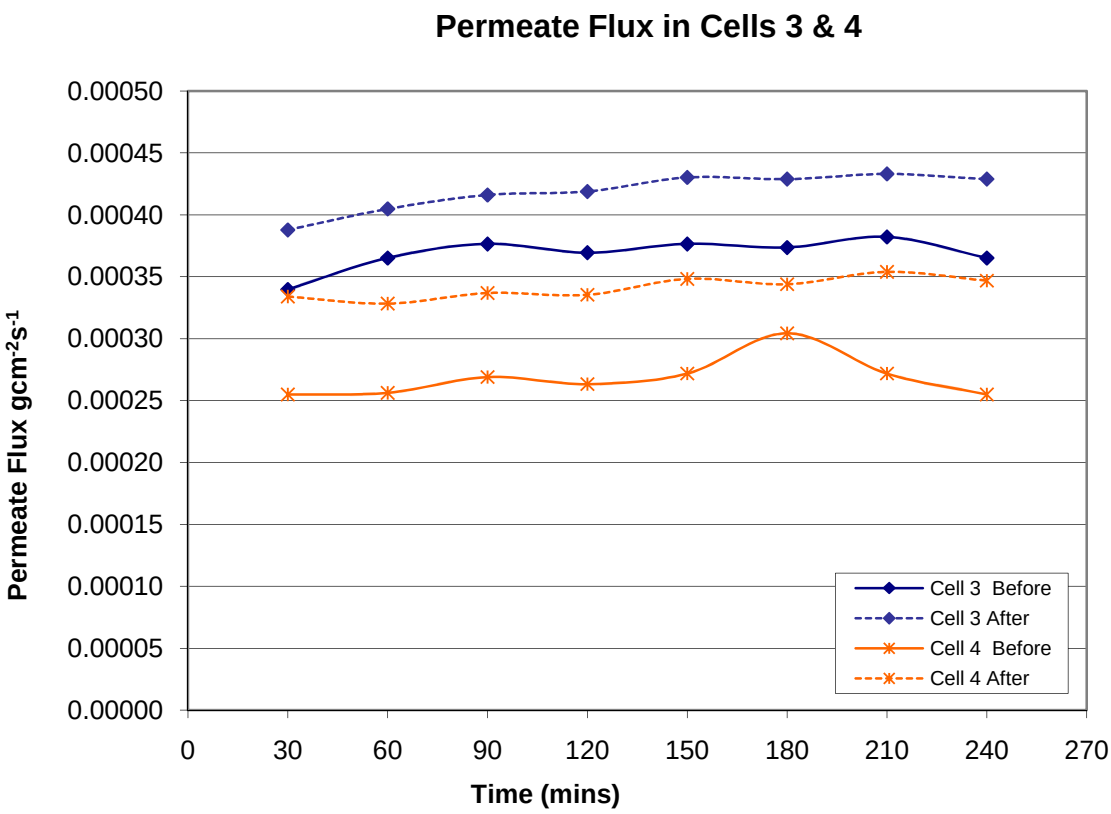

Figure 6-19 Permeate Flux in Cells 5 & 6 of Exp. SW/7

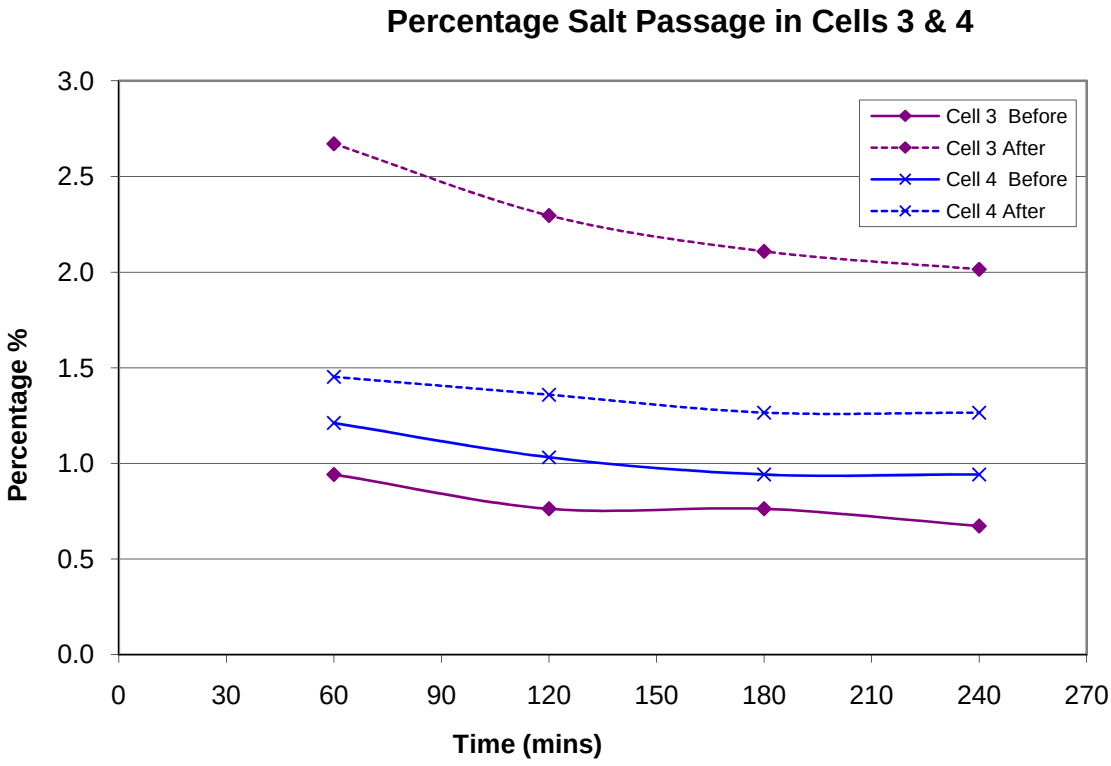

Figure 6-20 Percentage Salt Passage in Cells 5 & 6 of Exp. SW/7

6.3 Overview of Result of Tests on SW 30 Membranes

Table 12 represents a summary (on several pages) of the findings from all the experiments on the Seawater polyamide membranes SW 30; those described in this chapter and those presented in Appendix I.

Experiment	Cells	Exposure to hydrocarbon	Surface Exposed	Duration of treatment/ Stir	Change in Performance	
SW 30				**Hours**	**% Salt passage**	**Flux (x10^{-4}) [% change]**
Exp SW/1	1	Control			1.2 – 0.9 ▼	3.65 – 3.86 [6 % ▲]
	2	Control			1.2 – 1.1 ▼	3.41 – 3.49 [2 % ▲]
	3	Hexane water mixture (1:10)	Both	24 hrs + Stirring	No flux	No flux
	4				No flux	No flux
	5	Diesel water mixture (1:10)	Both	1 hrs + Stirring	1.5 – 3.2 ▲	3.04 – 1.94 [36 % ▼]
	6				2.8 -7.6 ▲	3.02 – 1.40 [54 % ▼]

Table 12 Results of Experiments on SW 30 Polyamide Membranes.

Experiment	Cells	Exposure to hydrocarbon	Surface Exposed	Duration of treatment/ Stir	Change in Performance	
SW 30				**Hours**	**% Salt passage**	**Flux (x10^{-4}) [% change]**
Exp SW/2	1	Control			1.0 – 0.8 ▼	2.79 – 2.91 [4 % ▲]
	2	Control			1.2 – 1.0 ▼	3.25 –3.53 [9 % ▲]
	3	Hexane water mixture (1:10)	Both	24 hrs + Stirring	No flux	No flux
	4				No flux	No flux
	5	Diesel water mixture (1:10)	Both	2 hrs + Stirring	No flux	No flux
	6				No flux	No flux

Table 12 Contd.

Experiment	Cells	Exposure to hydrocarbon	Surface Exposed	Duration of treatment/ Stir	Change in Performance	
SW 30				**Hours**	**% Salt passage**	**Flux (x10^{-4}) [% change]**
Exp SW/3	1	Control			1.0 – 0.9 ▼	3.12 –3.86 [24 % ▲]
	2	Control			0.6 – 0.6 ▲	3.18 – 3.54 [11 % ▲]
	5	Pure Diesel	Both	1 hr +NO Stirring	No Flux	No Flux
	6				No Flux	No Flux
Exp SW/4	1	Control			0.9 – 0.8 ▼	3.49 – 3.94 [13 % ▲]
	2	Control			0.9 – 0.7 ▼	3.02 – 3.42 [13 % ▲]
	3	Hexane water mixture (1:10)	Both	3 hrs + Stirring	No flux	No flux
	4				No flux	No flux

Table 12 Contd.

Experiment	Cells	Exposure to hydrocarbon	Surface Exposed	Duration of treatment/ Stir	Change in Performance	
SW 30				**Hours**	**% Salt passage**	**Flux ($x10^{-4}$) [% change]**
Exp SW/4	5	Pure Hexane	Both	1 hr + NO Stirring	No flux	No flux
	6				No flux	No flux
Exp SW/5	1	Control			0.7 – 0.9 ▲	2.48 – 2.71 [9 % ▲]
	2	Control			0.7 – 1.0 ▲	2.65 – 2.80 [6 % ▲]
	3	Hexane water mixture (1:10)	Active	3 hrs + Stirring	0.6 - 1.0 ▲	2.06 – 2.63 [28 % ▲]
	4				1.2 -3.1 ▲	2.08 – 2.65 [27 % ▲]
	5	Diesel water mixture (1:10)	Active	3 hrs + Stirring	1.0 – 7.2 ▲	2.33 – 2.67 [15 % ▲]
	6				1.3 – 4.3 ▲	2.12 – 2.01 [5 % ▼]

Table 12 Contd.

Experiment	Cells	Exposure to hydrocarbon	Surface Exposed	Duration of treatment/ Stir	Change in Performance	
SW 30				**Hours**	**% Salt passage**	**Flux ($x10^{-4}$) [% change]**
Exp SW/6	1	Control			0.9 – 1.0 ▲	2.57 – 2.85 [11 % ▲]
	2	Control			1.0 – 1.3 ▲	2.52 – 2.73 [9 % ▲]
	3	Hexane water mixture (1:10)	Active	6 hrs + Stirring	1.0 – 3.2 ▲	1.87 – 2.20 [18 % ▲]
	4				1.8 – 3.0 ▲	2.35 – 2.72 [15 % ▲]
	5	Diesel water mixture (1:10)	Active	6 hrs + Stirring	1.4 – 1.6 ▲	2.44 – 2.70 [11 % ▲]
	6				0.8 – 2.4 ▲	2.43 – 2.49 [3 % ▲]

Table 12 Contd.

Experiment	Cells	Exposure to hydrocarbon	Surface Exposed	Duration of treatment/ Stir	Change in Performance	
SW 30				**Hours**	**% Salt passage**	**Flux ($x10^{-4}$) [% change]**
Exp SW/7	1	Control			1.0 – 0.9 ▼	3.12 –3.86 [24 % ▲]
	2	Control			0.6 – 0.6 ▲	3.18 – 3.54 [11 % ▲]
	3	aqueous phase of a hexane water mixture	Both	Long term 4 weeks	0.7 – 2.3 ▲	3.68 – 4.19 [14 % ▲]
	4				1.0 – 1.3 ▲	2.68 – 3.41 [27 % ▲]
	5	Hexane water mixture (1:10)	Passive	3 hrs + Stirring	No flux	No flux
	6				No flux	No flux
▲ – Increase ▼ – Decrease			Note: in the ‘Change in Performance’ columns x – y means that the value changes from x to y			

Table 12 Contd.

6.4 Brackish Water Membrane Polyamide BW 30

This is a summary of the experiments that were carried out on the Brackish water membranes polyamide BW 30.

Experiment	Cells	Stirring	Duration of exposure to hydrocarbon (h)	Treatment
Exp BW/1	1 to 5	-	-	Five samples were used with pressure increasing from 10 to 20 and then 30 bar
Exp BW/2	1 & 2	-	-	Control
	3 & 4	N	17	Both sides of the membrane were exposed to hexane water mixture
	5 & 6	Y	17	Both sides of the membrane were exposed to hexane water mixture
Exp BW/3	1 & 2	-	-	Control
	3 & 4	Y	14 + 21	Both sides of the membrane were exposed to hexane water mixture
	5 & 6	Y	14 + 21	The active side was exposed to hexane water mixture

Table 13 Experiments on BW 30 Polyamide Membranes

Experiment BW/2

In this set of experiments, in between phases 1 & 2 of the tests the membranes were divided as follows.

Feed TDS	5500 ppm
Pressure	30 bar
Temperature	23 ± 1 ^{o}C

Cells 1 & 2 --> Dipped in a sample of reverse osmosis feed solution for 17 hours.

Cells 3 & 4 --> Kept in container with tank solution and hexane 10 : 1 proportion **without** stirring, both sides of the membranes exposed for 17 hours.

Cells 5 & 6 --> Kept in container with tank solution and hexane 10 : 1 proportion with stirring, both sides of the membranes exposed for 17 hours.

The results are shown in Figures 6-21 to 6-26

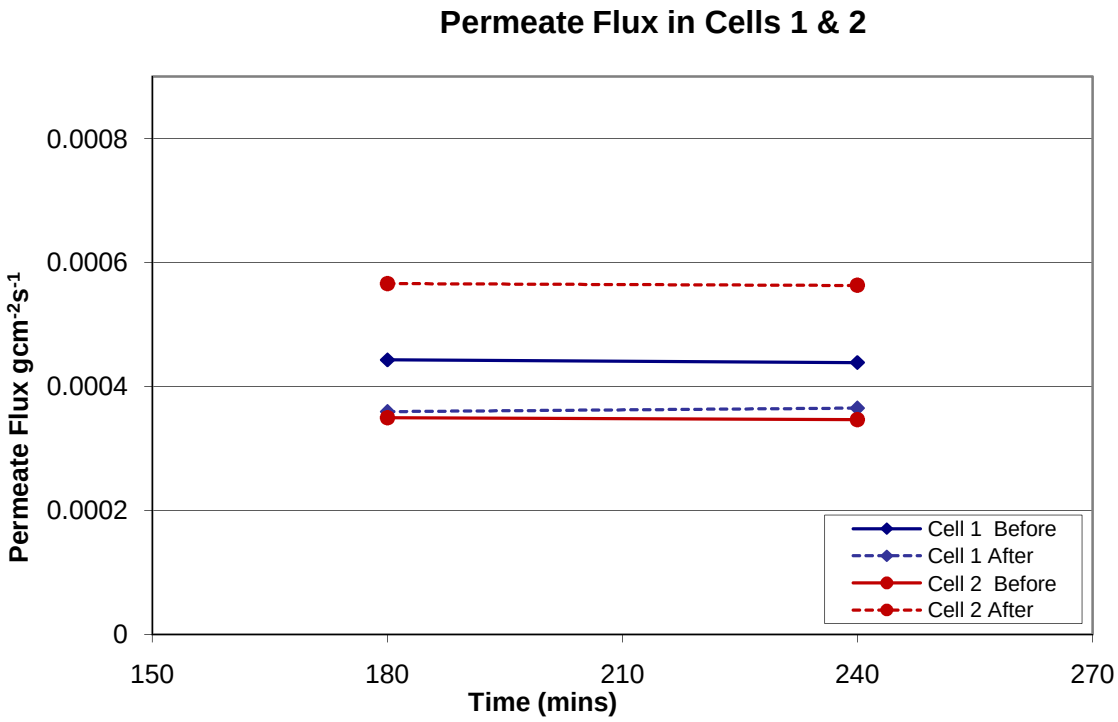

Figure 6-21 Permeate Flux in Cells 1 & 2 of Exp. BW/2

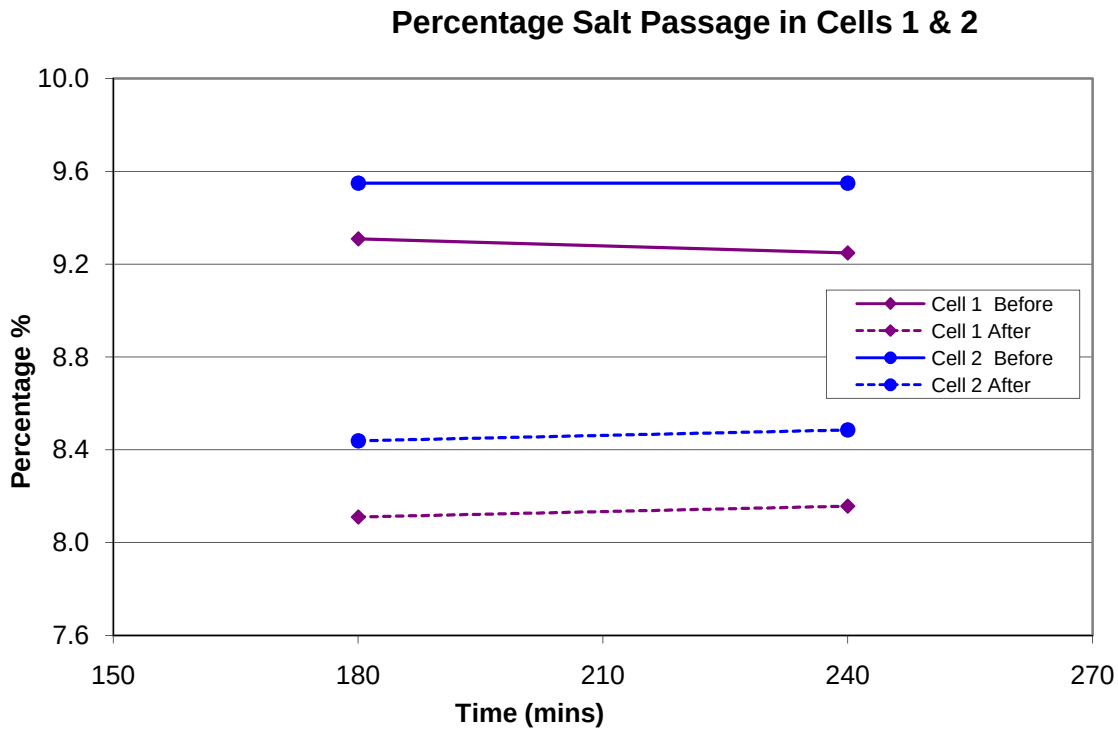

Figure 6-22 Percentage Salt Passage in Cells 1 & 2 of Exp. BW/2

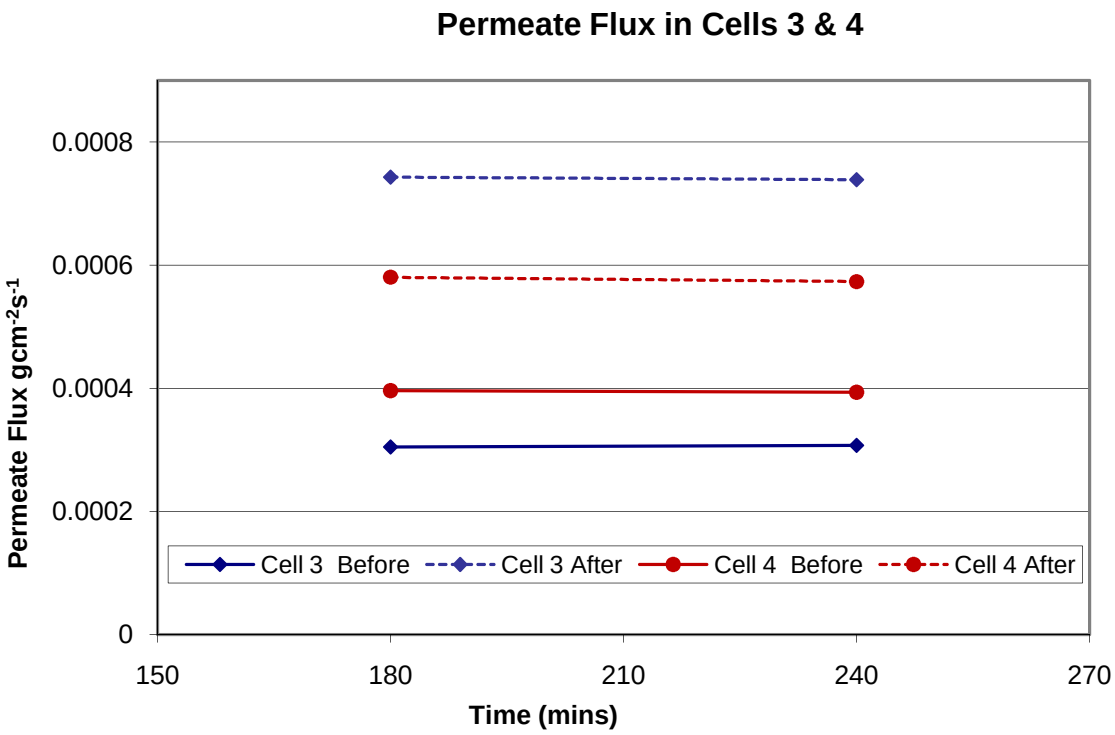

Figure 6-23 Permeate Flux in Cells 3 & 4 of Exp. BW/2

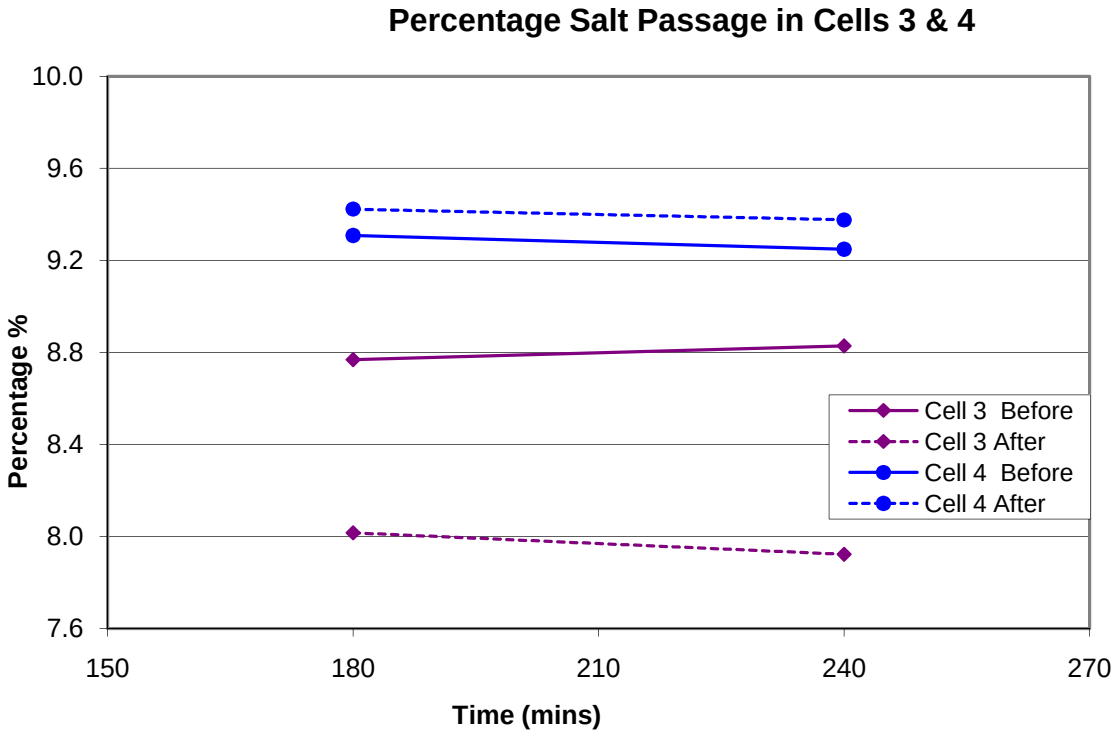

Figure 6-24 Percentage Salt Passage in Cells 3 & 4 of Exp. BW/2

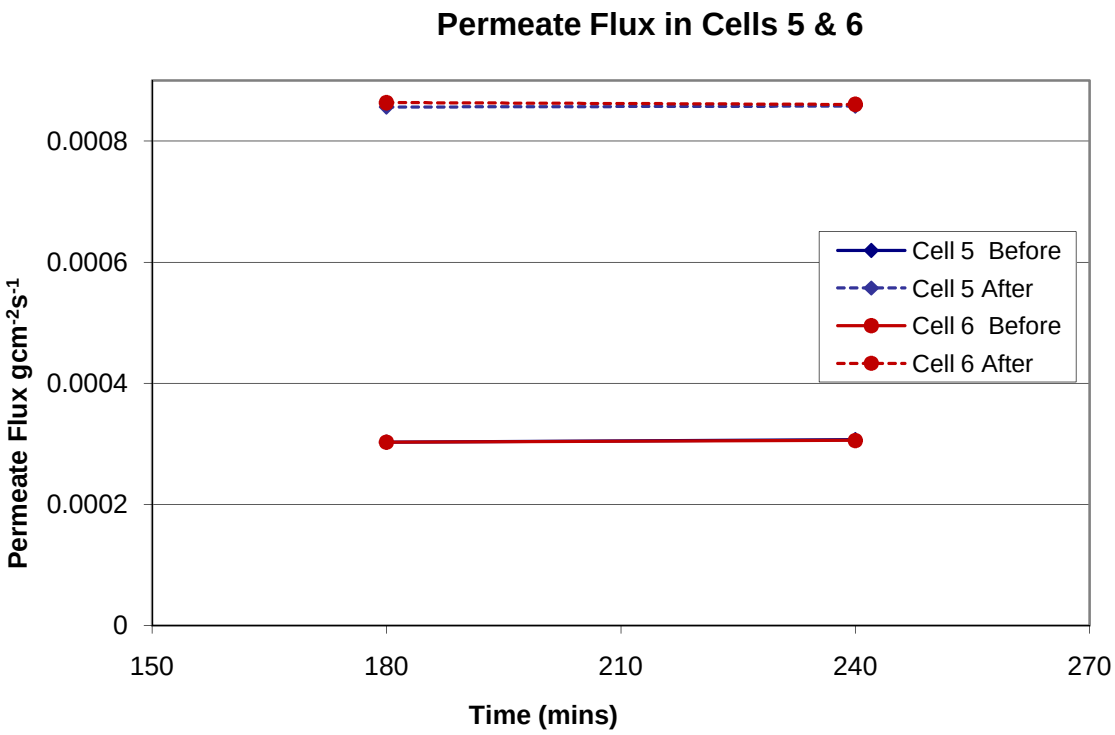

Figure 6-25 Permeate Flux in Cells 5 & 6 of Exp. BW/2

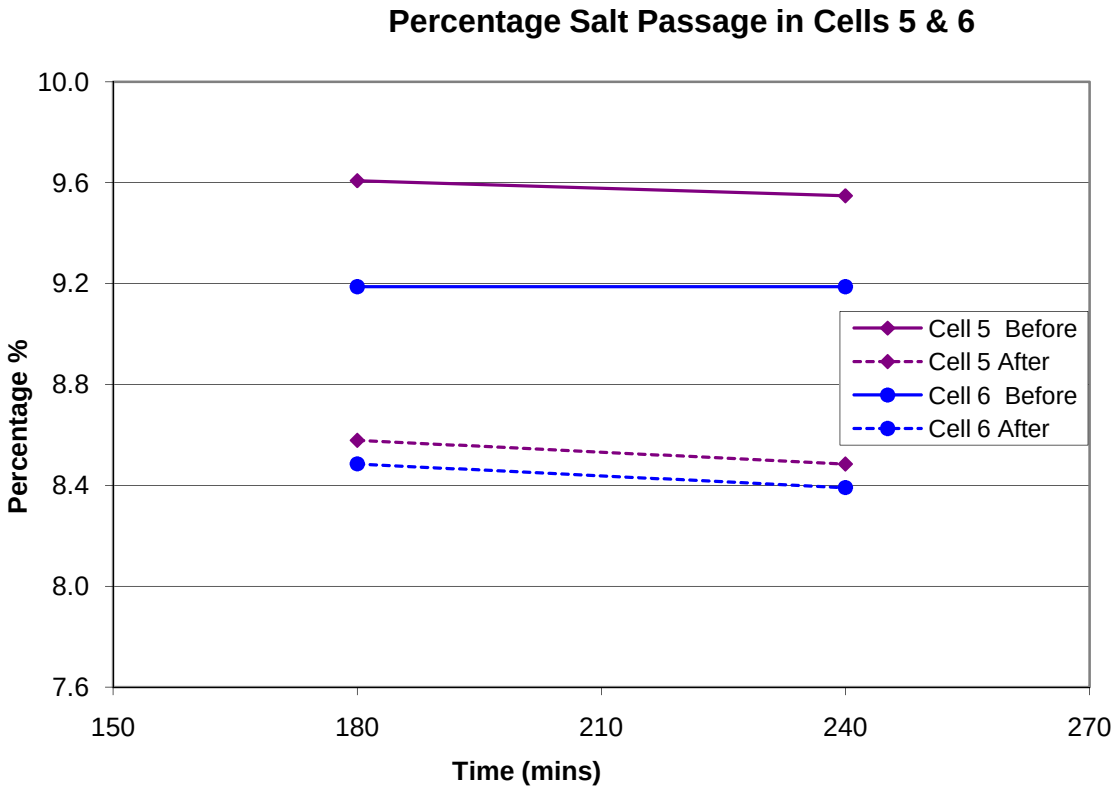

Figure 6-26 Percentage Salt Passage in Cells 5 & 6 of Exp. BW/2

The BW 30 membranes were affected by the fouling, both layouts; stirring and no stirring. The permeate flux was seen to increase, the increase was slightly more in the case where stirring was applied. The data on percentage salt passage was mostly inconclusive.

Experiment BW/3

In the next set of experiments all membranes were initially exposed for 14 hours

Feed TDS	5500 ppm
Pressure	30 bar
Temperature	23 ± 1 ^{o}C

The membranes were divided as follows:

Cells 1 & 2 --> Dipped in a sample of tank solution

Cells 3 & 4 --> Kept in container with tank solution and hexane 10 : 1 proportion with stirring. Both sides of the membranes are being contaminated.

Cells 5 & 6 --> Kept in container with tank solution and hexane 10 : 1 proportion with stirring. Only the active sides of the membranes are being contaminated.

The membranes were dipped for a further 21 hours

The additional 21 hours of fouling was done to make the effects of fouling more visible.

The permeate flux was seen to increase, but the fouling has a comparatively more negative effect on the salt passage. The salt passage increased in both layouts i.e. when both sides of the membrane were exposed and where only the active side was exposed.

6.5 Overview of Result of Tests on BW 30 Membranes

Table 14 is a summary of the results obtained for the experiments carried out on the Brackish water membranes polyamide BW 30. The detailed graphical results can be found in Appendix II

Membrane	**Cells**	**Exposure to hydrocarbon**	**Surface Exposed**	**Duration of Treatment / Stir**	**Change in Performance**	
BW 30				**Hours**	**% Salt passage**	**Flux**
Exp BW/1	1 to 5	Five samples were used with pressure increasing from 10 to 20 and then 30 bar			Percentage Salt passage decreased as pressure increased	Flux increased as pressure increased
Exp BW/2	1				9.5 – 8.4 ▼	22 %▲
	2				9.2 – 8.0 ▼	57 %▲
	3	Hexane water mixture (1:10)	Both	17 hours + No Stirring	8.7 – 7.9 ▼	150 %▲
	4	Hexane water mixture (1:10)	Both	17 hours + No Stirring	9.2 – 9.3 ▲	50 %▲

Table 14 Results of Experiments on BW 30 Polyamide Membranes

Membrane	Cells	Exposure to hydrocarbon	Surface Exposed	Duration of treatment / Stir	Change in Performance	
BW 30				**Hours**	**% Salt passage**	**Flux**
Exp BW/2	5	Hexane water mixture (1:10)	Both	17 hours + Stirring	9.5 – 8.4 ▼	180 %▲
	6	Hexane water mixture (1:10)	Both	17 hours + Stirring	9.1 – 8.3 ▼	183 %▲
Exp BW/3	1			14	9.4 – 8.4 ▼	18 %▲
				21	9.1 – 8.2 ▼	21 %▲
	2			14	8.5 – 8.4 ▼	20 %▲
				21	8.5 – 8.0 ▼	24 %▲
	3	Hexane water mixture (1:10)	Both	14 hours + Stirring	8.2 – 8.5▲	74 %▲
				35 hours + Stirring	8.2 – 8.7 ▲	91 %▲

Table 14 Contd.

Membrane	Cells	Exposure to hydrocarbon	Surface Exposed	Duration of treatment / Stir	Change in Performance	
BW 30				**Hours**	**% Salt passage**	**Flux**
Exp BW/3	4			14 hours + Stirring	8.5 – 8.4 ▼	45 %▲
				35 hours + Stirring	8.5 – 8.9 ▲	100 %▲
	5	Hexane water mixture (1:10)	Active	14 hours + Stirring	7.9 – 8.6 ▲	80 %▲
				35 hours + Stirring	7.9 – 8.8 ▲	110 %▲
	6			14 hours + Stirring	8.8 – 9.4 ▲	58 %▲
				35 hours + Stirring	8.8 –9 7. ▲	70 %▲
▲ - Increase ▼ - Decrease		Note: in the ‘Change in Performance’ columns x – y means that the value changes from x to y				

Table 14 Contd.

CHAPTER 7 RESULTS: CELLULOSE TRIACETATE (CTAB2-10) MEMBRANE

7.1 Test Protocol

Each experiment involved utilising a new set of membrane samples under the following parameters.

Feed TDS	5500 ppm
Pressure	30 bar
Temperature	23 ± 1 ^{o}C

7.1.1 Protocol for Tests on Control Membranes

For the experiments carried out in cells 1 and 2, the membranes were not exposed to hydrocarbon.

Step 1

The membranes were placed in the cells at the beginning of the experiment. For the first three hours the rig and membranes were allowed to stabilise, the next four hours were used to record the properties of the membranes.

Step 2

After the first stage, the membranes were removed from the rig. The membranes were stored in a container filled with salt water from the feed tank so that they would not dry up. This was done for the duration that the other membranes i.e. from cells 3-6 were being exposed to hydrocarbon.

Step 3

The membranes were put back in the rig. The same process as the one at the beginning, i.e. step 1, was repeated. The rig was allowed to stabilise for three hours and the next four hours were used to obtain the properties of the membranes. The volume of permeate collected every 30 minutes was measured and the conductivity of the collected permeate was measured every hour.

In two of the experiments there was an additional treatment after step 3, this is described below.

Step 4

This is the same as step 2, the membranes were removed from the cells and stored in salt water from the tank.

Step 5

Step 5 is the same as step 3. The membranes were put back in the rig and allowed to stabilise for three hours and tested for another four hours where the flux and conductivity of the permeate were recorded.

7.1.2 Protocol for Tests on Membranes exposed to Hydrocarbons

For most of the experiments carried out, the membranes in cells 3 to 6 were exposed to hydrocarbons, either hexane or diesel.

Step 1

The membranes were placed in the cells at the beginning of the experiment. For the first three hours the rig and membranes were allowed to stabilise, the next four hours were used to record the properties of the membranes.

Step 2

After those two stages the membranes were removed from the rig. The membranes were then carefully transferred into a vessel containing the hydrocarbon. There were different methods of exposure. The membrane could have both sides or just one surface in contact with the hydrocarbon. This was done with or without stirring. The stirring was to make the hydrocarbon / water fluid into an emulsion. The membranes were left in the fouling mixture for a predetermined number of hours.

Step 3

When the pre-determined time per hydrocarbon exposure treatment was over, all the membranes were put back in the rig. The same process as the one at the beginning, i.e. step 1, was repeated. The rig was allowed to stabilise for three hours and the next four hours were used to obtain the properties of the membranes. The volume of permeate collected every 30 minutes was measured and the conductivity of the collected permeate was measured every hour.

In two experiments there was an additional treatment after step 3, this is described below.

Step 4

This is the same as step 2, the membranes were removed from the cells and treated with the hydrocarbon containing mixture.

Step 5

Step 5 is the same as step 3. The membranes were put back in the rig and allowed to stabilise for three hours and tested for another four hours where the flux and conductivity of the permeate were recorded.

Steps 4 and 5 are only done in some of the experiments to accentuate any effects of the contact with the hydrocarbon.

7.2 Overview of Tests on CTA Membranes

Table 15 is a summary of the experiments that were carried out on the cellulose triacetate membranes (CTA).

Experiment	Cells	Stirring	Duration of exposure to hydrocarbon (h)	Treatment
Exp CTA/1	1	-		Membrane with passive surface against flow for 1 hour *
	2	-		The membrane was checked for compaction by being in the operating rig for 30 hours
	3&4	Y	16	Both sides of the membrane were exposed to a 1:10 hexane / water mixture
	5&6	Y	16	The active side was exposed to a 1:10 hexane / water mixture
* **Note** : This was the **only** test in which the membrane was positioned in the Reverse Osmosis rig with the passive surface against the feed. In all other tests including those on the polyamides (chapter 6) the membranes were tested in the Reverse Osmosis rig in the correct configuration, i.e. the active surface facing the feed.				
Exp CTA/2	1			The membrane was checked for compaction by being in the operating rig for 4 intervals of 7 hours each
	2			The membrane was checked for compaction by being in the operating rig for 30 hours
	3&4	Y	16	Both sides of the membrane were exposed to a 1:10 hexane / water mixture
	5&6	Y	16	The active side was exposed to a 1:10 hexane / water mixture

Table 15 Experiments on CTA Cellulose Triacetate Membranes

Experiment	Cells	Stirring	Duration of exposure to hydrocarbon (h)	Treatment
Exp CTA/3	1&2			Control
	3&4	Y	14 +21	Both sides of the membrane were exposed to a 1:10 hexane / water mixture
	5&6	Y	14 +21	The active side was exposed to a 1:10 hexane / water mixture
Exp CTA/4	1			Control
	2			Empty
	3&4	Y	2	Both sides of the membrane were exposed to a 1:10 diesel / water mixture
	5&6	Y	1	Both sides of the membrane were exposed to a 1:10 diesel / water mixture
Exp CTA/5	1			Control
	2			Empty
	3&4	Y	21	Both sides of the membrane were exposed to a 1:10 diesel / water mixture
	5&6	N	X	The membranes were left in the aqueous phase of a 1:10 hexane / water solution for 6 weeks

Table 15 Experiments on CTA Cellulose Triacetate membranes.

Experiment	Cells	Stirring	Duration of exposure to hydrocarbon (h)	Treatment
Exp CTA/6	1&2			Control
	3&4	N	2	Both sides of the membrane were exposed to the aqueous phase of a 1:10 diesel / water solution
	5&6	Y	2	Both sides of the membrane were exposed to a 1:10 diesel / water mixture
Exp CTA/7	1&2			Control
	3&4	Y	6	Active surface of the membrane was exposed to a 1:10 diesel / water mixture
	5&6	N	6	Both sides of the membrane were exposed to pure diesel

Table 15 Contd.

7.3 Aspects of Basic Performance of CTA Membranes

7.3.1 Experiment CTA/1 Cells 1 and 2

The following experiment was used to find out how this particular membrane reacts in different situations.

In Cell 1 the membrane was used with the passive surface facing the flow. After an hour it was turned back to the proper configuration.

During the first hour, when the membrane in cell 1 was placed with the passive surface facing the flow, the membrane did not stop the salt passage and it offered very little resistance to the permeate flow. This was done to find out what would happen if the membrane was accidentally reversed. This would be very unlikely in practice as in most cases these membranes come in a sealed pre-assembled module. Nevertheless it is interesting to see how this membrane works in such an abnormal condition. After one hour in this configuration the membrane was taken out of the pressure cell and put back in the proper configuration i.e. the active side facing the flow and the performances in this phase of the test are shown in Figures 7-1 and 7-2.

In Cell 2 the membrane was left in the cell for 30 consecutive hours. A reason for this ‘compaction test’ was that cellulose acetate membranes are known to be relatively vulnerable to compaction and it was important to assess if the CTA membrane is subject to compaction during the entire time frame of the experiments (including tests involving exposure to the hydrocarbons). In the tests that have been carried out a membrane would be in the operating rig for a maximum of 21 hours, i.e. the membrane was placed in the rig for three intervals of seven hours. The first interval

would be to check the behaviour of the membrane and the next two intervals would be after exposing the membrane to a hydrocarbon containing liquids. Figures 7-1 and 7-2 show the performance during the final, three hour period in the reverse osmosis rig.

During the hour when the passive side of the membrane was against the feed in Cell 1, it did not stop the passage of salt and there was very little resistance to the flux. The membrane was then put back in the proper configuration. The results in the graphs (Figures 7-1 & 7-2) show that the performance of the membrane has been noticeably impacted upon. The permeate flux showed a 50 % increase compared to an expected value from cell 2 and the percentage salt passage was of the order of 75 % when it was expected to be about 4 %. Though with time the permeate flux seems to return to the expected value the percentage salt passage does not recover.

Note: The test in cell 1 was completed after a few hours, but the test using cell 2 had still many hours to go. So for the sake of efficiency a new membrane was inserted in cell 1. This is the membrane used in exp CTA/2 cell 1.

Explanations of the Legend of Figures 7-1 and 7-2.

Cell 1 A – First run for Cell 1 with unused membrane.
Cell 1 B – Run after the membrane has been in the operating rig for 1 hour with the back surface facing the feed for Cell 1.
Cell 2 R – First run for Cell 2 with unused membrane.
Cell 2 T – Run after the membrane has been in cell 2 of the operating rig for 30 hours.

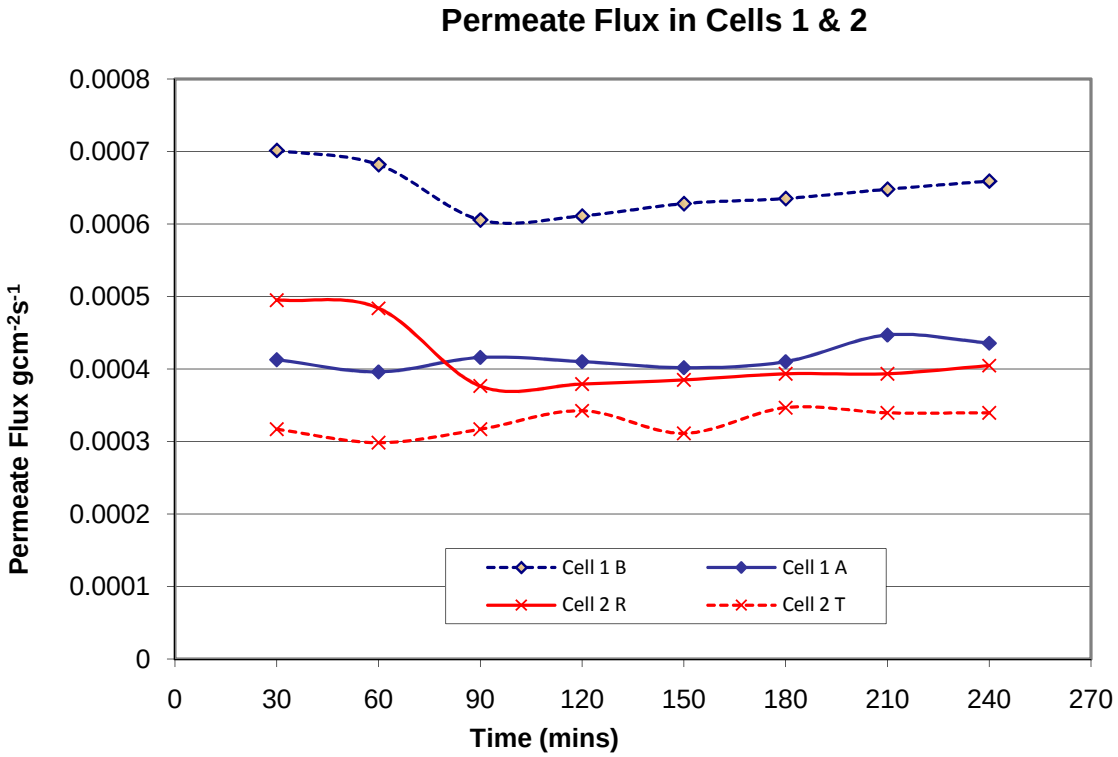

Figure 7-1 Permeate Flux in Cells 1 & 2 of Exp.CTA/1

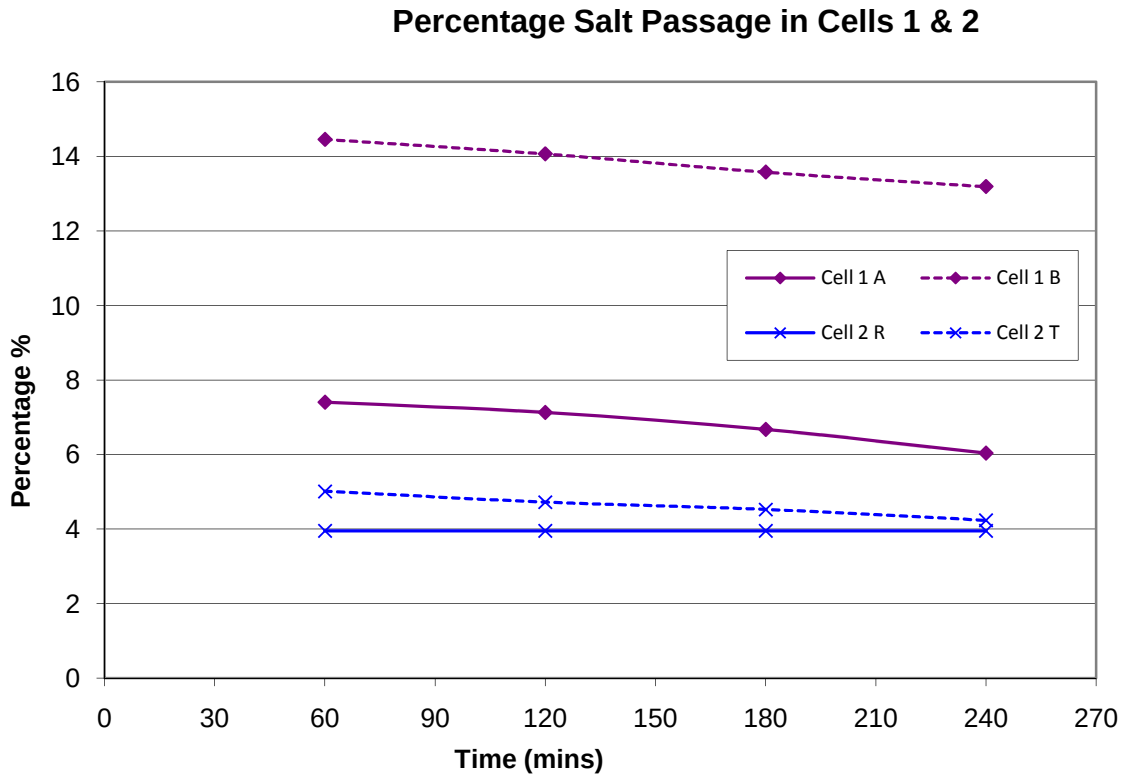

Figure 7-2 Percentage Salt Passage in Cells 1 & 2 of Exp. CTA/1

7.3.2 Experiment CTA/2 Cells 1 and 2

Cells 1 and 2 of experiment CTA/2 further tests were done to check for compaction.

The membrane in Cell 1 was obtained from cell 1 of experiment CTA/1 (the second membrane used in that experiment) i.e. this test represented an extended period of exposure to the saline solution.

The membrane in Cell 2 was left in the cell continuously for 30 hours under operating conditions. The aim was to find if there was any compaction.

Explanations of the Legend of Figures 7-3 and 7-4

Cell 1 R – First run for Cell 1 with unused membrane.

Cell 1 T – Run after the membrane has been in cell 1 of the operating rig for 4 intervals of 7 hours each.

Cell 2 R – First run for Cell 2 with unused membrane.

Cell 2 T – Run after the membrane has been in cell 2 of the operating rig for 30 hours.

Figures 7-3 and 7-4 show a comparison of the flowrate and percentage salt passage before and after treatment for each pair of cells.

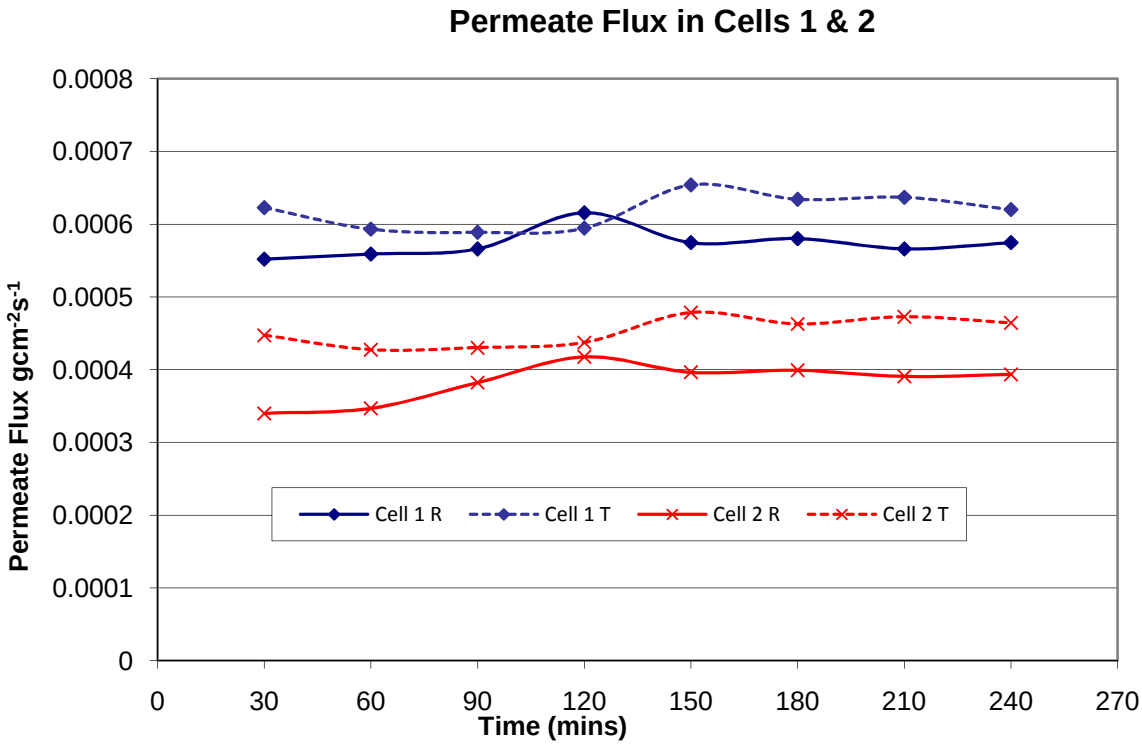

Figure 7-3 Permeate Flux in Cells 1 & 2 of Exp.CTA/2

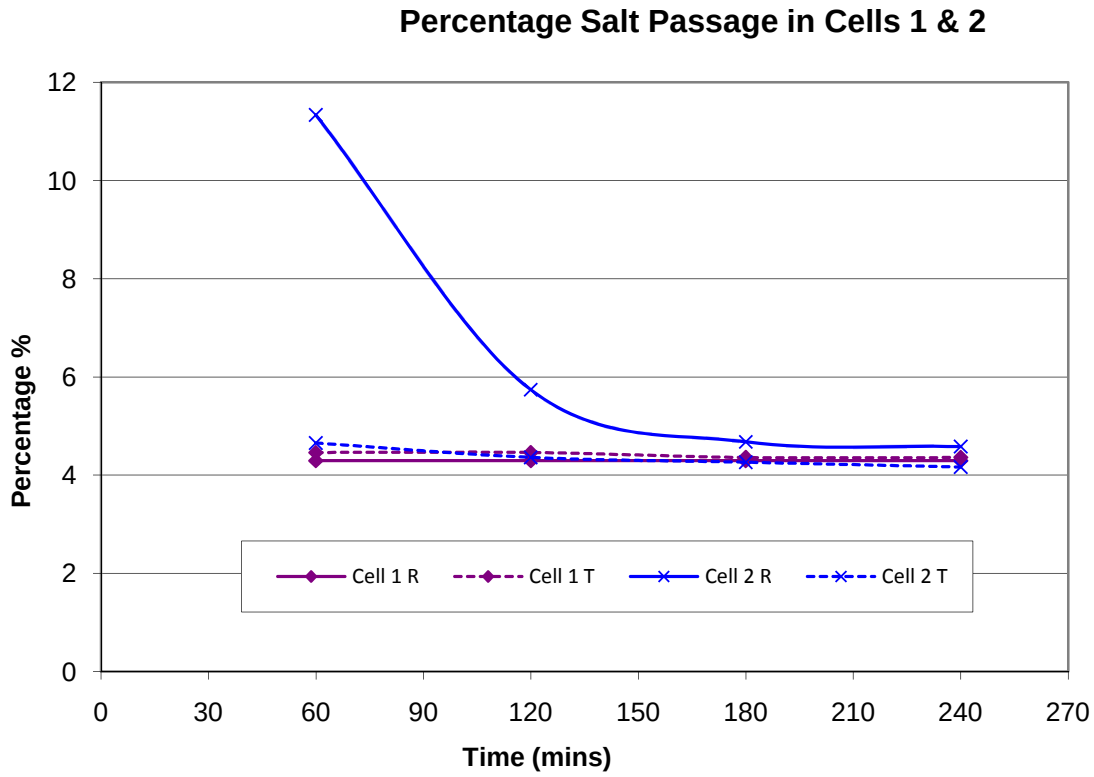

Figure 7-4 Percentage Salt Passage in Cells 1 & 2 of Exp. CTA/2

The membrane used in cell 1 was taken from the previous experiment (CTA/1). It was the second membrane used in cell 1 and in experiment CTA/1 it was exposed to the feed for two separate 7 hours intervals and it was not subjected to any fouling. In the current experiment the membrane was placed in the rig for a further two intervals of 7 hours.

In total the membrane was in the active rig for 28 hours. The result here is a very small increase of 7 % in the permeate flux and very small decrease in salt passage. This indicates that the performance of the membrane is not being degraded by the normal operation of the rig; so we can conclude that no compaction of the membrane occurs during the experiment.

The membrane in cell 2 was left in the cell for the duration of the experiment which was a total of thirty continuous hours. Even though the parameters for cell 2 were slightly different, the membrane was exposed to four intervals of 7 hours, the results mirrored the one obtained in cell 1: small increase of 8 % in the permeate flux and very small decrease in salt passage. This confirms that no significant compaction of the membranes occurred during the experiments.

7.4 Effects of Hydrocarbon Exposure on performance of CTA Membranes

As outlined in Table 15, a number of experiments, CTA/1 to CTA/7, were carried out to investigate the effects of hydrocarbon exposure on this membrane. The detailed results are shown in Appendix III and are summarised in Table 16, but the results of one experiment (CTA/6) are displayed as a typical example in Figure 7-5 to 7-10 and described below.

Cells 1 & 2 no exposure to hydrocarbons
Cells 3 & 4 --> 2 hours exposed to a diesel water mixture (1:10) without stirring, both sides of the membrane exposed.
Cells 5 & 6 --> 2 hours exposed to a diesel water mixture (1:10) with stirring, both sides of the membrane exposed.

During the two hours the membranes from cells 3 to 6 were being exposed, the control membranes from cells 1 & 2 were stored in a vessel containing feed water (see 7.1.1).

The permeate flux in cell 1 displayed a 2 % increase between the initial run and the second run. While the percentage salt passage increased from 2.8 % to 3 % during that same period. In cell 2 the permeate flux showed a 1 % increase and the percentage salt passage increased from 3.1 % to 3.2 %.

After exposure to the hydrocarbon, the permeate flux in cell 3 showed a 0.2 % increase and the percentage salt passage increased from 3.1% to 3.7%. In cell 4 the permeate flux increased by 3% and the percentage salt passage increased from 3.0% to 3.8 %.

The permeate flux in cell 5 showed an increase of 2% and the percentage salt passage increased from 3.2% to 3.9%. In cell 6 the permeate flux decreased by 3% and the percentage salt passage increased from 3.1% to 4.3 %.

The results in this experiment for cells 3 to 6 generally indicated that there are no substantial effects on the membrane from exposure to hydrocarbons either in the case of aqueous solution or the emulsion.

Explanations of the Legend of Figures 7-5 to 7-10

Cell 1 Before – Initial Run for Cell 1.
Cell 1 After – Second run of Cell 1, after membrane was stored in a container of feed water while membranes from cells 3 to 6 were being exposed to hydrocarbon fluid.
Cell 2 Before – Initial Run for Cell 2.
Cell 2 After – Second run of Cell 2, after membrane was stored in a container of feed water while membranes from cells 3 to 6 were being exposed to hydrocarbon fluid.
Cell 3 Before – Initial Run for Cell 3.
Cell 3 After – Second run of Cell 3, after membrane was exposed to hydrocarbon fluid under the parameters specified in the experiment.
The legend for cells 4 to 6 follows the same pattern as cell 3.

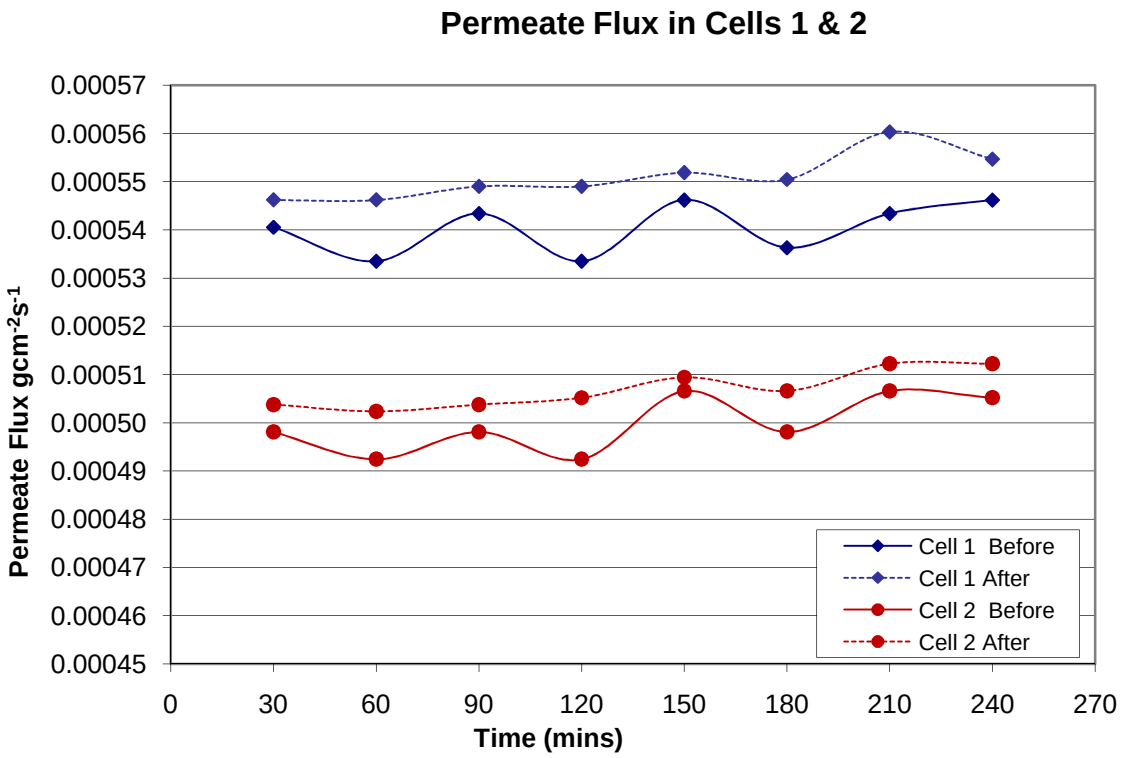

Figure 7-5 Flux in Cells 1 & 2 of Exp.CTA/6

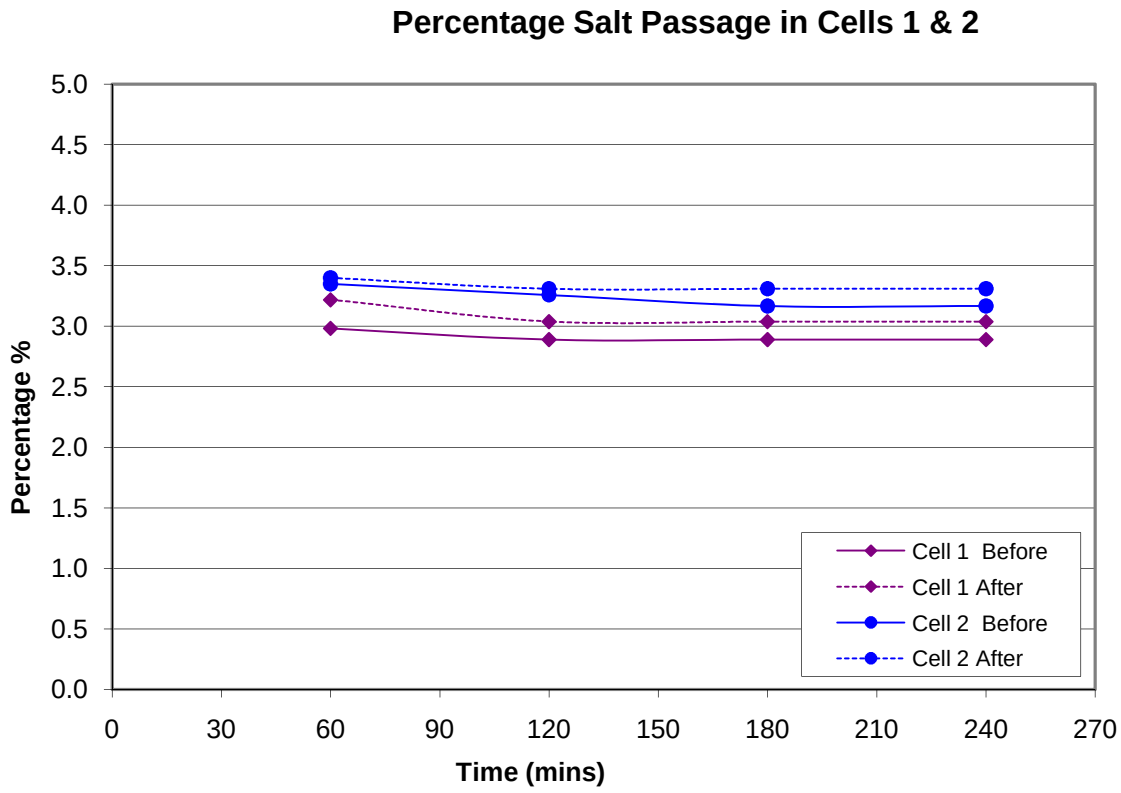

Figure 7-6 Percentage Salt Passage in Cells 1 & 2 of Exp. CTA/6

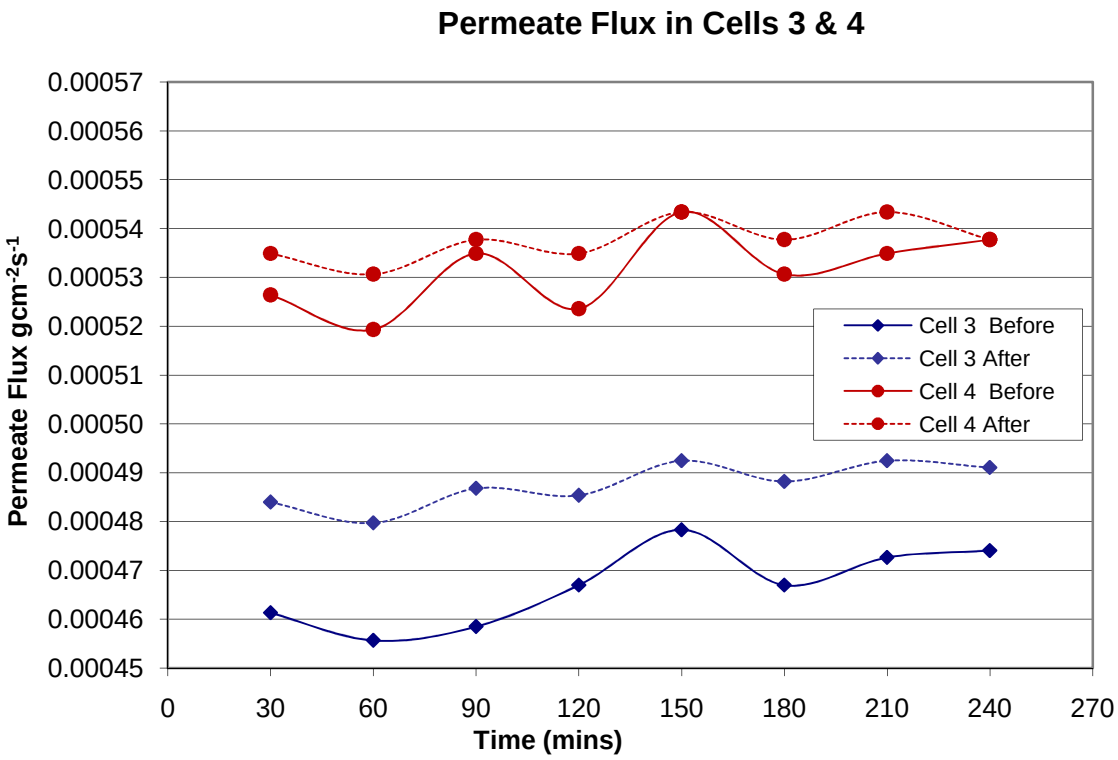

Figure 7-7 Flux in Cells 3 & 4 of Exp.CTA/6

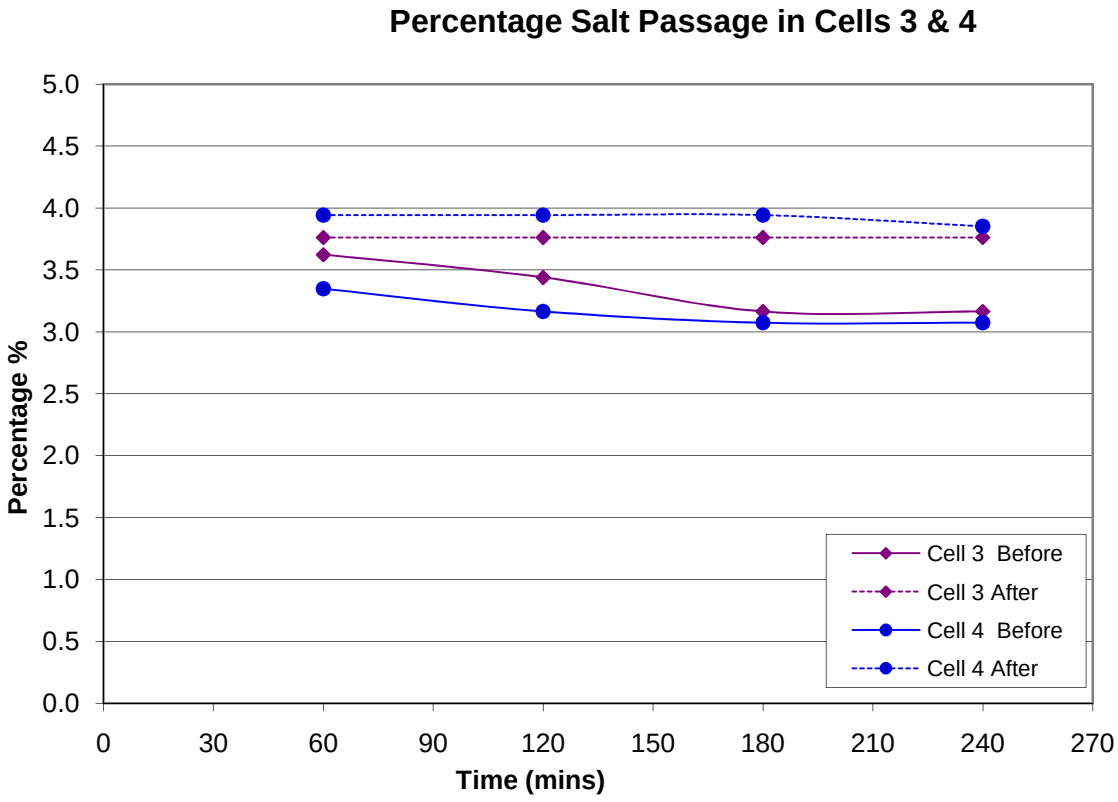

Figure 7-8 Percentage Salt Passage in Cells 3 & 4 of Exp. CTA/6

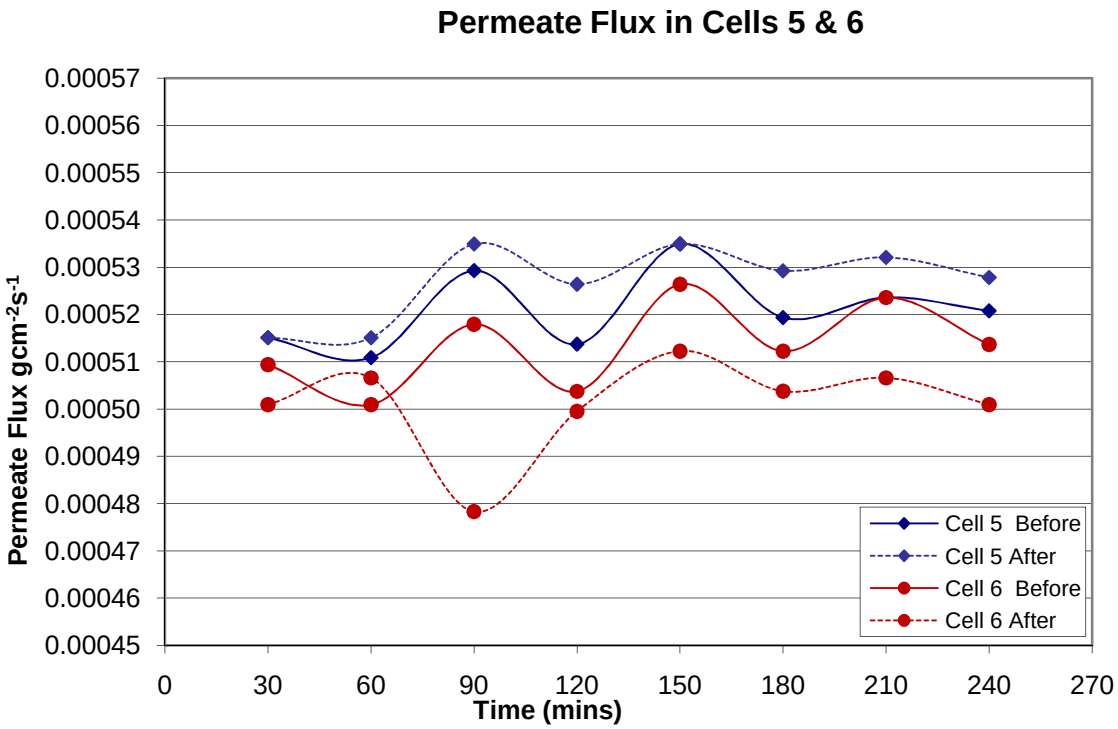

Figure 7-9 Flux in Cells 5 & 6 of Exp.CTA/6

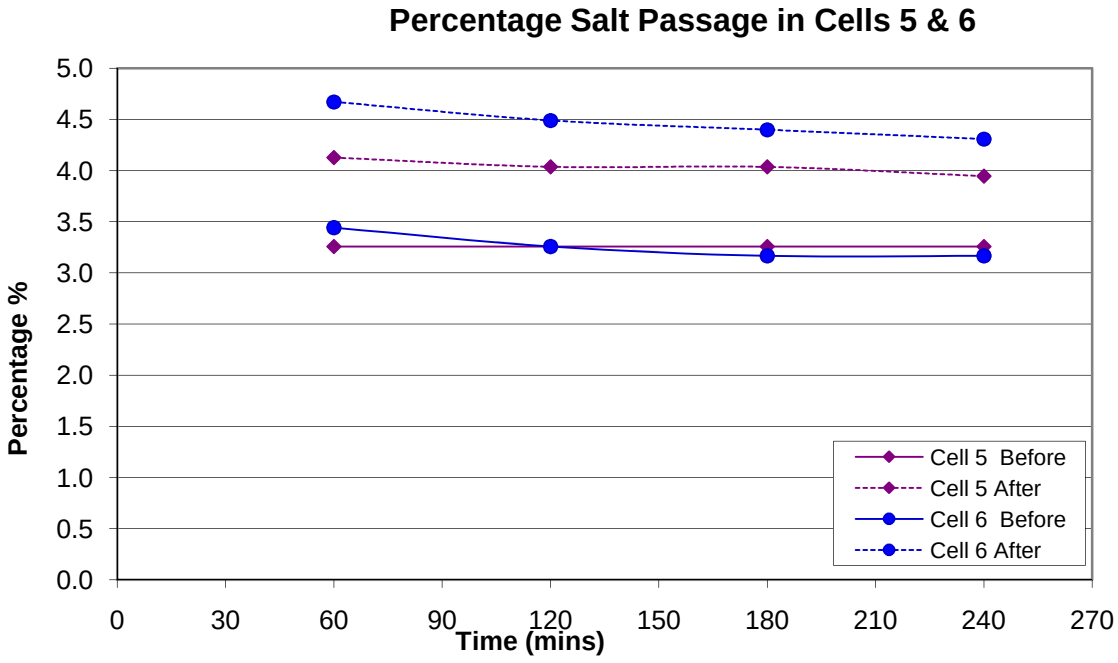

Figure 7-10 Percentage Salt Passage in Cells 5 & 6 of Exp. CTA/6

7.5 Overview of Result of Tests on CTA Membranes

Table 16 is a summary of the results obtained for the experiments carried out on the cellulose triacetate membranes (CTA). Although the main focus of this table is to reveal the effects of exposure to hydrocarbon, the findings from the basic performance of membranes (section 7.2) are also included for completeness.

Experiment	Cells	Exposure to hydrocarbon	Surface Exposed	Duration of treatment / Stir	Effect on	
CTA				**Hours**	**% Salt passage**	**Flux ($x10^{-4}$) [% change]**
Exp CTA/1	1			Passive surface facing feed for 1 hour		
	2			Ran for 30 hours to check for compaction	Remains constant	Slight Increase
	3	Hexane water mixture (1:10)	Both	16 hours + Stirring	3.8 – 4.5 ▲	4.78 – 3.93 [13 % ▼]
	4				3.6 – 3.5 ▼	5.68 – 4.62 [14 % ▼]
	5	Hexane water mixture (1:10)	Active	16 hours + Stirring	3.3 - 3.6 ▲	4.66 – 4.23 [6 % ▼]
	6				3.4 – 4.4 ▲	5.02 – 2.98 [40 % ▼]

Table 16 Results of Experiments on CTA Cellulose Triacetate

Experiment	Cells	Exposure to hydrocarbon	Surface Exposed	Duration of treatment / Stir	Effect on	
CTA				Hours	% Salt passage	Flux (x10^{-4}) [% change]
Exp CTA/2	1			Compaction		
	2			Ran for 22 hours to check for compaction		
	3	Hexane water mixture (1:10)	Both	16 hours + Stirring	3.2 – 16.0 ▲	5.03 – 5.58 [12 % ▲]
	4				4.8 – 13.0 ▲	5.96 – 6.72 [13 % ▲]
	5	Hexane water mixture (1:10)	Active	16 hours + Stirring	3.8 – 9.4 ▲	5.43 – 5.31 [3.6 %▼]
	6				5.0 – 6.2 ▲	5.72 - 6.24 [12 % ▲]

Table 16 Contd.

Experiment	Cells	Exposure to hydrocarbon	Surface Exposed	Duration of treatment / Stir	Effect on	
CTA				Hours	% Salt passage	Flux ($x10^{-4}$) [% change]
Exp CTA/3	1	Control	-	14	5.7 - 4.7 ▼	3.67 – 4.16 [14 % ▲]
				21	4.7 – 5.5 ▲	Overall 3.67 – 3.78 [7 % ▲]
	2	Control	-	14	4.6 – 3.9 ▼	2.60 – 3.27 [24 % ▲]
				21	3.9 – 3.6 ▼	Overall 2.60 – 2.39 [7 % ▼]
	3	Hexane water mixture (1:10)	Both	14	5.5 – 4.9 ▼	3.54 -3.93 [11 % ▲]
				21	4.9 –7.5 ▲	Overall 3.54 – 3.60 [2 % ▲]

Table 16 Contd.

Experiment	Cells	Exposure to hydrocarbon	Surface Exposed	Duration of treatment / Stir	Effect on	
CTA				**Hours**	**% Salt passage**	**Flux ($x10^{-4}$) [% change]**
Exp CTA/3	4	Hexane water mixture (1:10)	Both	14	4.1 – 3.1 ▼	3.63 – 4.62 [5.7 % ▲]
				21	4.0 – 3.2 ▼	Overall 3.63 – 3.86 [6 % ▲]
	5	Hexane water mixture (1:10)	Active	14	5.3 – 5.5 ▲	3.54 – 4.23 [20 %▲]
				21	5.5 – 5.9 ▲	Overall 3.54 – 4.17 [18 % ▲]
	6	Hexane water mixture (1:10)	Active	14	5.0 – 7.0 ▲	3.15 – 2.98 [6 % ▼]
				21	7.0 – 9.0 ▲	Overall 3.15 – 2.20 [30 % ▼]

Table 16 Contd.

Experiment	Cells	Exposure to hydrocarbon	Surface Exposed	Duration of treatment / Stir	Effect on	
CTA				**Hours**	**% Salt passage**	**Flux ($x10^{-4}$) [% change]**
Exp CTA/4	1	Control			4.4 – 4.8 ▲	5.63 - 6.05 [5 % ▲]
	3	diesel water mixture (1:10)	Both	2 hours + Stirring	4.1 – 4.9 ▲	5.34 – 4.96 [9% ▼]
	4				5.7 – 6.0 ▲	6.56 – 5.83 [11 % ▼]
	5	diesel water mixture (1:10)	Both	1 hour + Stirring	5.3 – 5.4 ▲	5.82 – 5.75 [8 % ▼]
	6				4.5 – 4.9 ▲	6.02 - 5.48 [5 % ▼]

Table 16 Contd.

Experiment	Cells	Exposure to hydrocarbon	Surface Exposed	Duration of treatment / Stir	Effect on	
CTA				Hours	% Salt passage	Flux (x10^{-4}) [% change]
Exp CTA/5	1	Control			4.4 – 4.8 ▲	5.63 - 6.23 [5 %▲]
	3	diesel water mixture (1:10)	Both	19 + 2 hours + Stirring	4.2 – 6.0 ▲	5.38 - 5.28 [2 %▼]
	4				5.7 – 6.7 ▲	6.56 – 5.62 [14 %▼]
	5	Aqueous phase hexane / water	Both	Long term 6 weeks	3.9 – 5.0 ▲	5.76 – 4.76 [17 %▼]
	6				3.6 – 4.5 ▲	5.93 – 4.92 [18 %▼]

Table 16 Contd.

Experiment	Cells	Exposure to hydrocarbon	Surface Exposed	Duration of treatment / Stir	Effect on	
CTA				**Hours**	**% Salt passage**	**Flux ($x10^{-4}$) [% change]**
Exp CTA/6	1	Control			2.8 – 3.0 ▲	5.40 - 5.51 [2 %▲]
	2	Control			3.1 – 3.2 ▲	5.00 – 5.07 [1 %▲]
	3	diesel water mixture (1:10)	Both	2 hours + NO Stirring	3.1 – 3.7 ▲	4.67 – 4.87 [4 %▲]
	4				3.0 – 3.8 ▲	5.31 – 5.38 [3 %▲]
	5	diesel water mixture (1:10)	Both	2 hours + Stirring	3.2 – 3.9 ▲	5.12 -5.27 [2 %▲]
	6				3.1 – 4.3 ▲	5.13 – 5.01 [3 %▼]

Table 16 Contd.

Experiment	Cells	Exposure to hydrocarbon	Surface Exposed	Duration of treatment / Stir	Effect on	
CTA				**Hours**	**% Salt passage**	**Flux ($x10^{-4}$) [% change]**
Exp CTA/7	1	Control			3.7 – 4.2 ▲	5.42 – 5.33 [4 %▼]
	2	Control			3.6 – 4.1 ▲	5.21 – 5.06 [4 %▼]
	3	diesel water mixture (1:10)	Active	6 hours + Stirring	3.6 – 4.6 ▲	4.36 – 3.65 [16 %▼]
	4				3.4 – 4.4 ▲	5.68 – 4.94 [14 %▼]
	5	Pure Diesel	Both	6 hours + no Stirring	3.8 – 4.4 ▲	5.16 – 4.74 [13 %▼]
	6				4.2 – 7.7 ▲	5.57 – 4.85 [14 %▼]
▲ - Increase ▼ - Decrease		Note: in the 'Effect on columns' x – y means that the value changes from x to y				

Table 16 Contd.

CHAPTER 8 MICROSCOPY

8.1 Introduction

The major impetus of this project was to investigate the effects of exposure to hydrocarbons upon the operating performance of a range of commercial membranes. In addition, attempts were made to see if microscopical examination of membranes would provide any evidence of the mechanisms by which the hydrocarbons might be affecting the performance.

8.2 Light Optical Microscopy

8.2.1 Polyamide Membranes

The three distinct parts of the SW 30 membrane can be seen in Figure 8-1 where the polyester support web has been pealed from the rest of the membrane. Examination of the active surface of the polyamide (SW 30 and BW 30) membranes under the light microscope did not reveal any distinguishing features both before and after exposure to hydrocarbons. This is due to the low magnification factor provided by the light microscope.

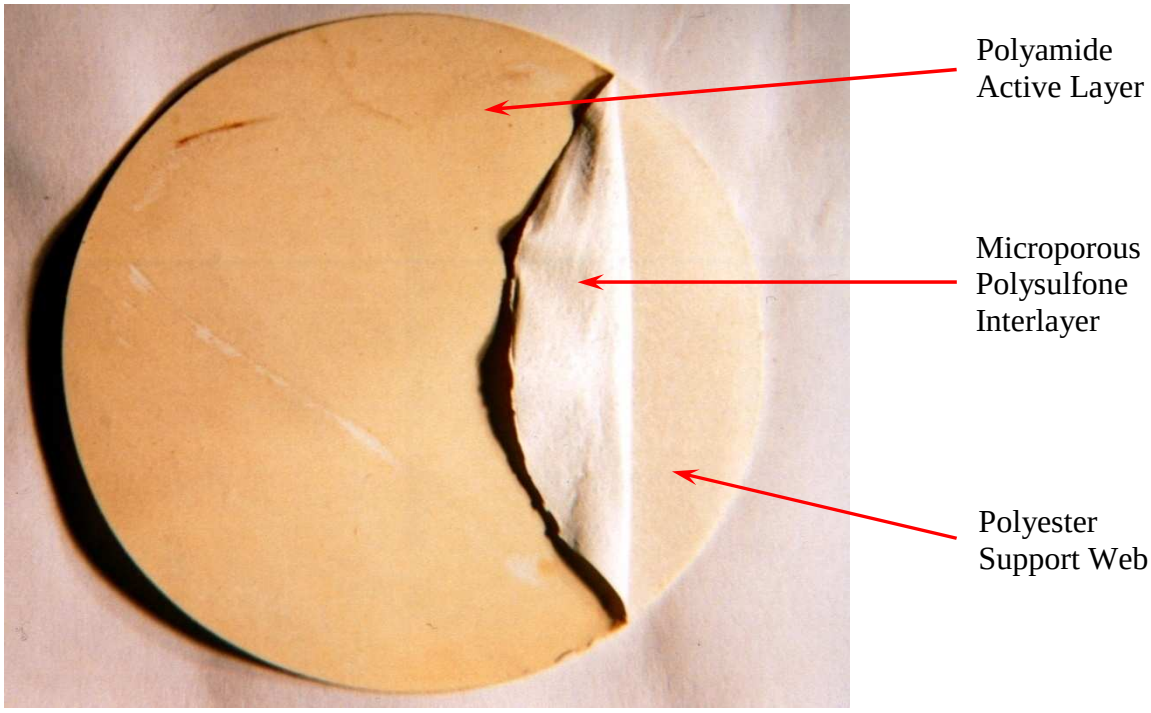

Figure 8-1 Three Layers of SW 30 Membrane

However the structure of backing support web of those membranes was visible under this microscope. Figure 8-2 is a photograph of the backing support web of a SW 30 membrane.

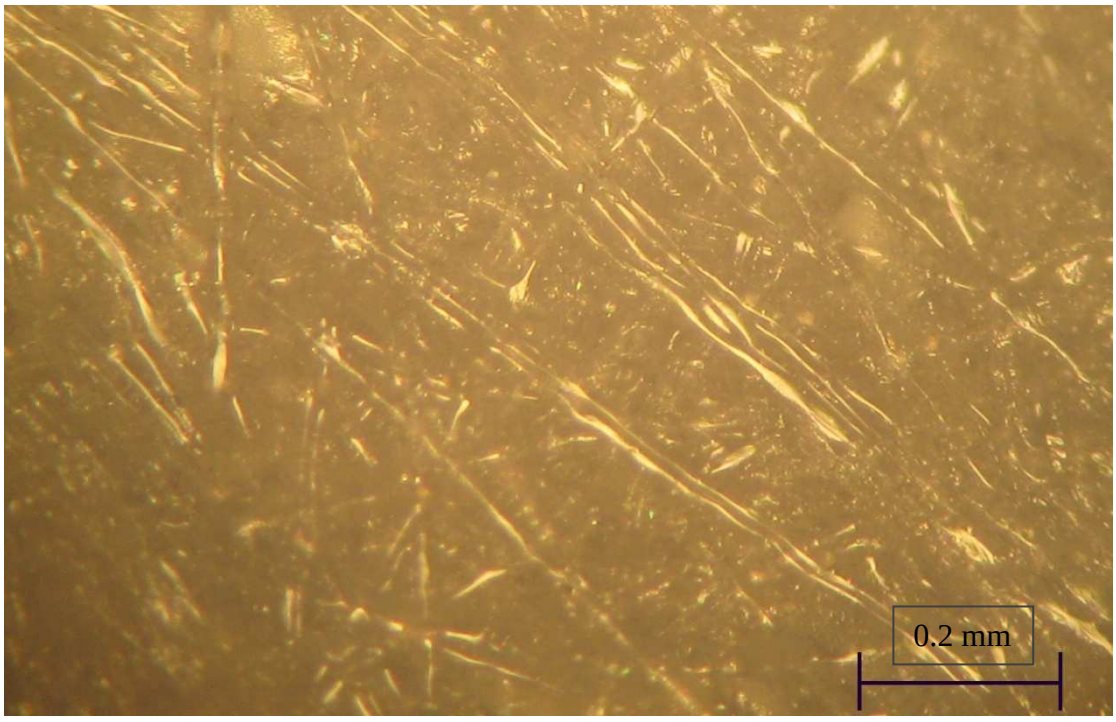

Figure 8-2 Support Web of SW 30 Membrane

8.2.2 Cellulose Triacetate Membranes

The CTA membrane-containing cartridge was bought from Fileder Filter Systems. The actual membrane was obtained after disassembling an Ametek CTAB2-10 cartridge.

Figure 8-3 is a photograph of the CTA membrane. It shows the active layer and the support web and the porous CTA where a section of the active layer has been peeled off.

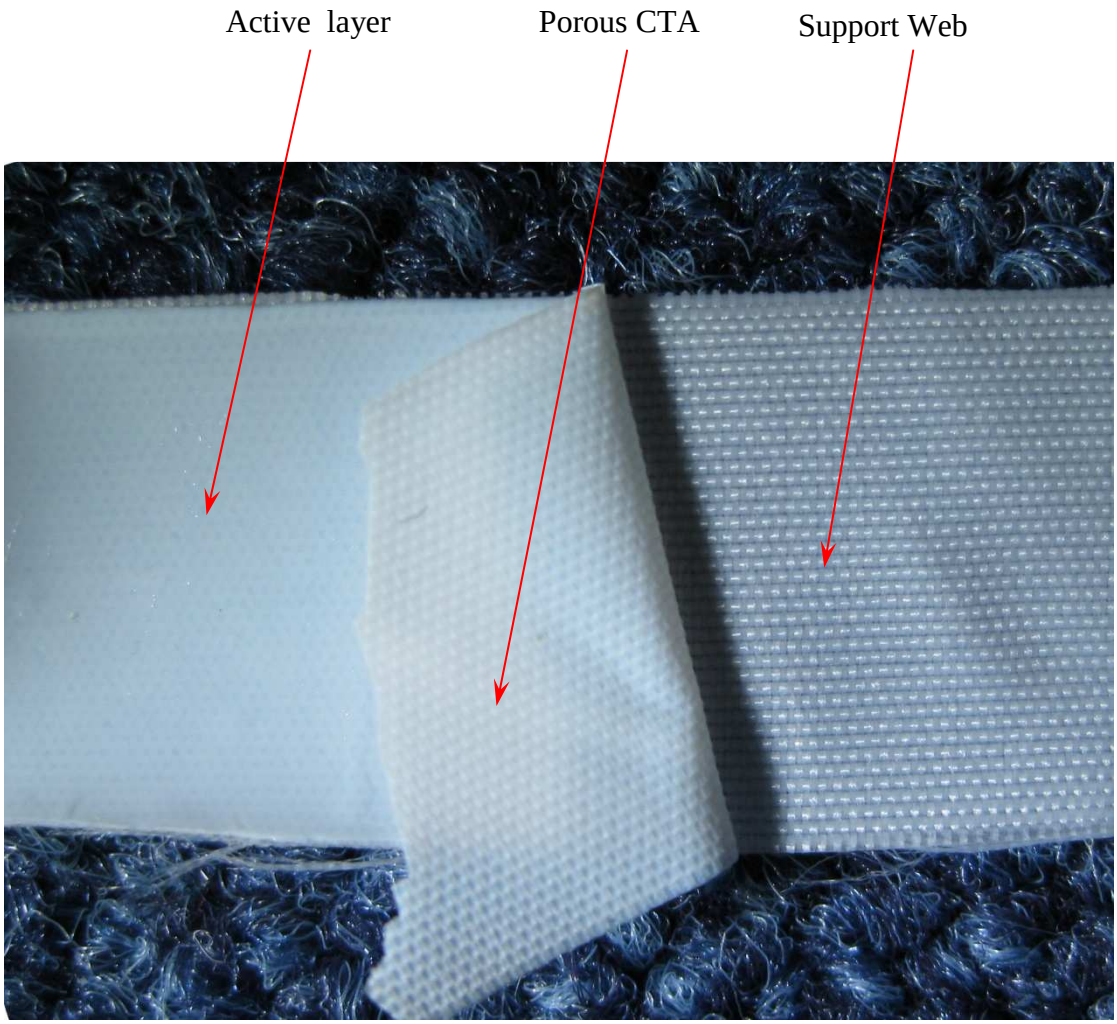

Figure 8-3 Three Layers of CTA Membrane

Initially the active surface of **unused** CTA membranes was examined under the light microscope at different magnifications. Several samples of the membrane were examined and Figures 8-4, 8-5 and 8-6 show typical membrane landscapes.

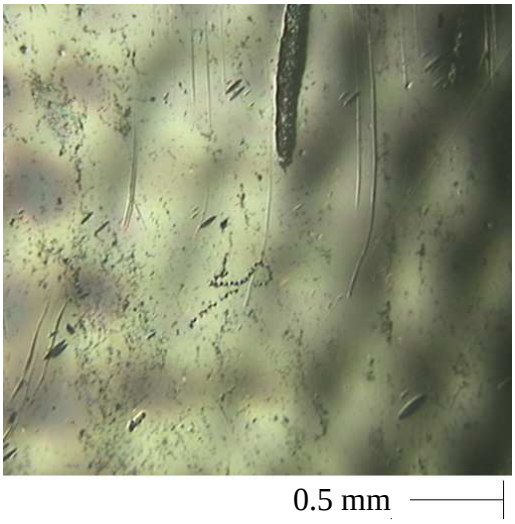

Figure 8-4 Active side of Unused CTA Membrane

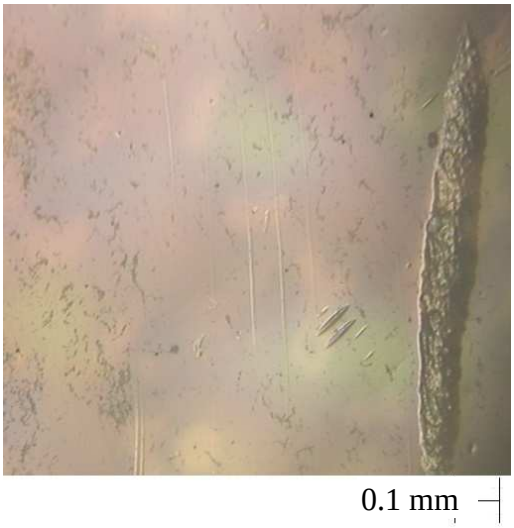

Figure 8-5 Active side of Unused CTA Membrane

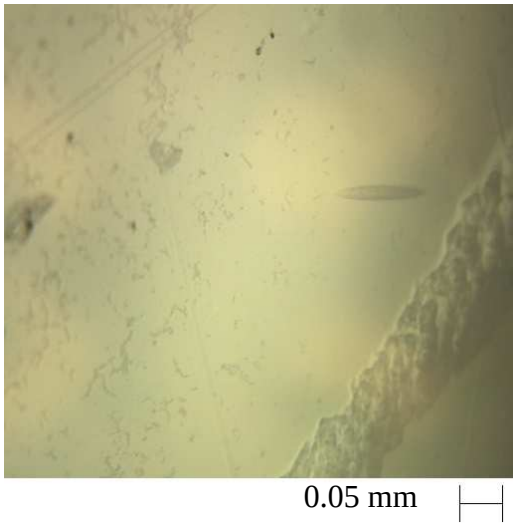

Figure 8-6 Active side of Unused CTA Membrane

It can be observed from the Figures 8-4, 8-5 and 8-6 that the active surface of the CTA membrane is not totally flat. There is a regular cellular-like pattern of depressions on the surface and what looks like a scar on the bottom right of Figure 8-4 is in fact a regular indentation that is all over the membrane. It was probably made during the rolling and assembling of the cartridge. Figure 8-5 is a photo of another part of the same membrane at the same magnification and shows the same kind of landscape as in Figure 8-4. Figure 8-5 and 8-6 are at higher magnifications from which not much can be distinguished.

The next set of pictures is taken from another sample of the CTA membrane.

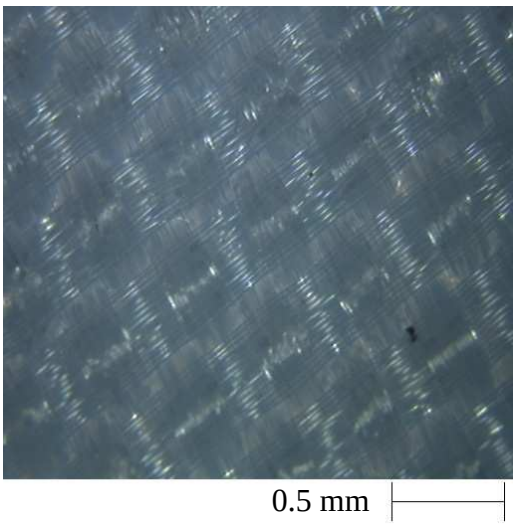

Figure 8-7 Underside of Unused CTA Membrane

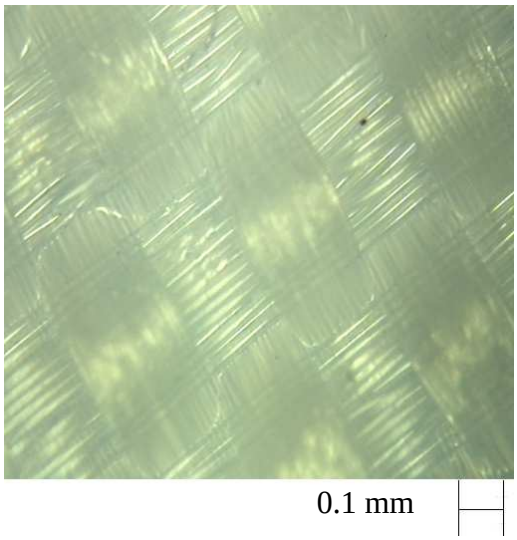

Figure 8-8 Underside of Unused CTA Membrane

Figures 8-7 & 8-8 are of the passive surface at different magnifications. The criss-cross pattern is that of the supportive web behind the CTA membrane and it is clearly the impression of this web that is visible on the photographs of the active surface (Figures 8-4, 8-5)

Figure 8-9 is a photograph of the back of the CTA membrane.

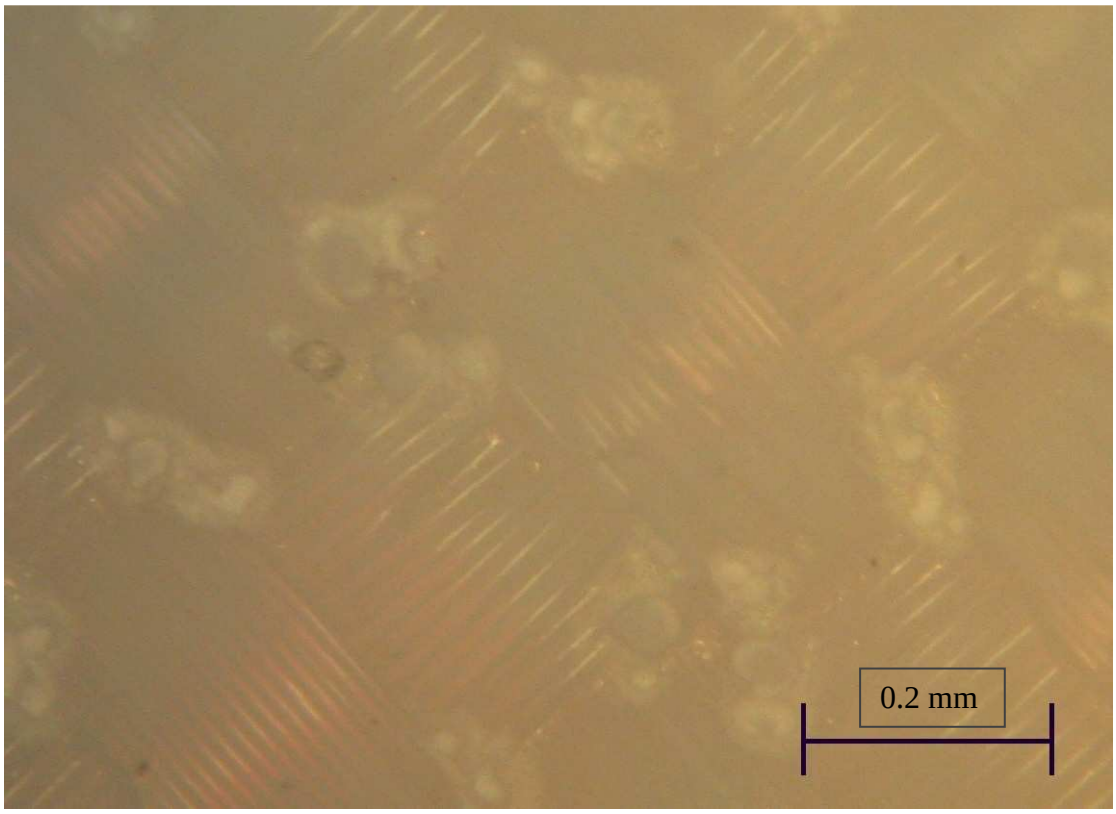

Figure 8-9 Back of CTA Membrane

The membrane from cell 1 in experiment CTA/3 was also examined under microscope. It had only been exposed to saline feed water. The aim was to see if there were any distinct changes caused by exposure to the feed solution at elevated pressure.

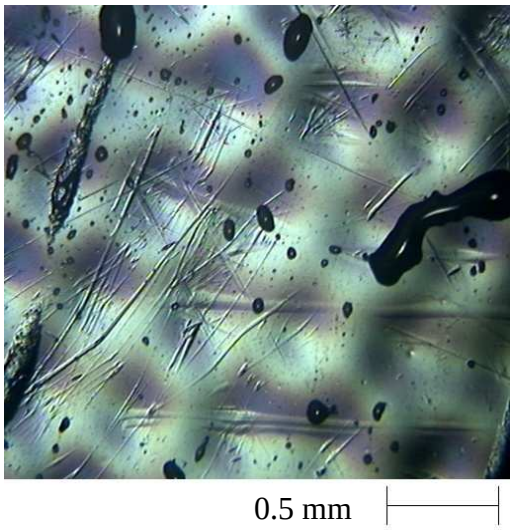

Figure 8-10 Active side of Used CTA Membrane

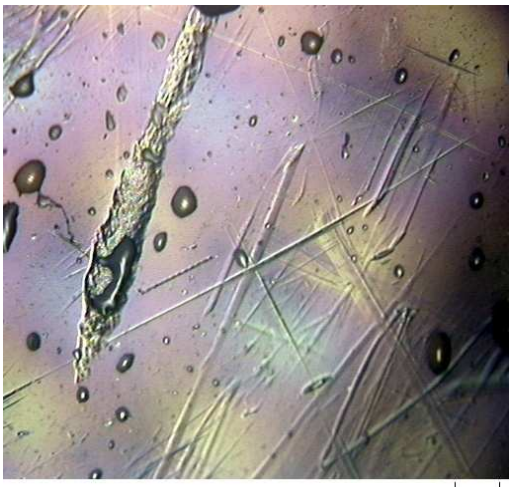

Figure 8-11 Active side of Used CTA Membrane

Figure 8-12 Active side of Used CTA Membrane

Figures 8-10 to 8-12 reveal that, except for a more pronounced impression of the support web, the texture of the membrane has not much changed from the original state when compared to Figures 8-4, 8-5 and 8-6.

The membrane from experiment CTA/1 cell 1 was then examined under the microscope, Figures 8-13 and 8-14 show what was seen.

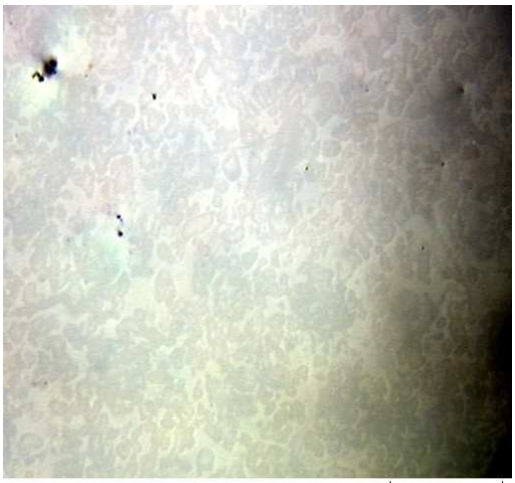

Figure 8-13 Active side of Used CTA Membrane placed against the feed

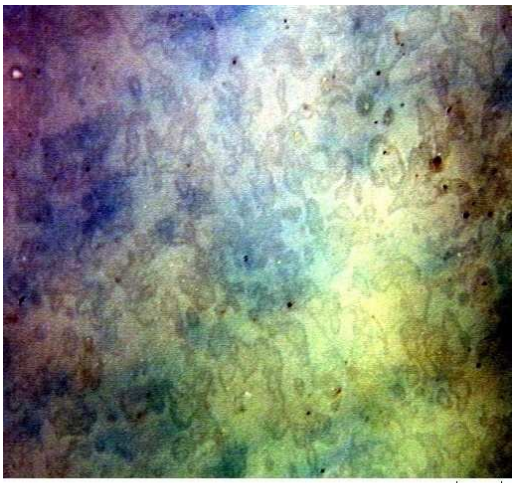

Figure 8-14 Active side of Used CTA Membrane placed against the feed

The texture of the surface is very different to what was expected (e.g. Figure 8-10) this indicates that the membrane sustained some damage; the texture seen here has many similarities to the texture of the sintered metal disk that is used as backing surface. The active layer was probably compacted against the uneven surface of the sintered disc and detached from the passive surface. This probably caused micro-tears to form on the active layer. When the membrane was placed in the proper configuration these tears were partially closed due to the compaction effect caused by the pressure of the feed inducing a gradual improvement in performance. But the membrane was irrevocably damaged.

Membranes that had experienced contact with hydrocarbon fluid were also examined under the light microscope. Figures 8-15 to 8-17 show the membrane from cell 4 of experiment CTA/1 involving exposure to a hexane / water emulsion. In Figures 8-15 and 8-16 a distinct pitting can be seen on the surface of the depressions.
Figures 8-18 and 8-19 show the membrane from cell 3 while Figures 8-20 and 8-21 show that of the membrane in cell 4 in both cases coming from experiment CTA/5 exposed for 2 hours to a diesel / water emulsion. In Figures 8-18 to 8-21 the pitting is more widespread and can be seen on the whole of the membrane surface rather than only in the depressions as in the case of exposure to the hexane / water emulsion.

This pitting effect is not present on used membranes (Figures 8-10 and 8-11) that have not been exposed to any hydrocarbon. This is an indication that the hydrocarbons are having a physical effect on the surface of the CTA membranes. From the results of the experiments it can be concluded that those changes do not have any bearing on the membranes at the level of exposure used in the experiments. It may be the case that if the CTA membrane is exposed for a longer period of time (6 months) there may be noticeable effects on the performance of the membrane.

Cell 4

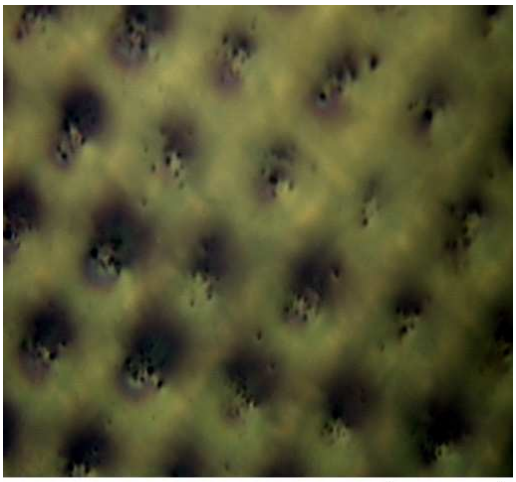

Figure 8-15 Active side of Used CTA Membrane exposed to hexane water mix

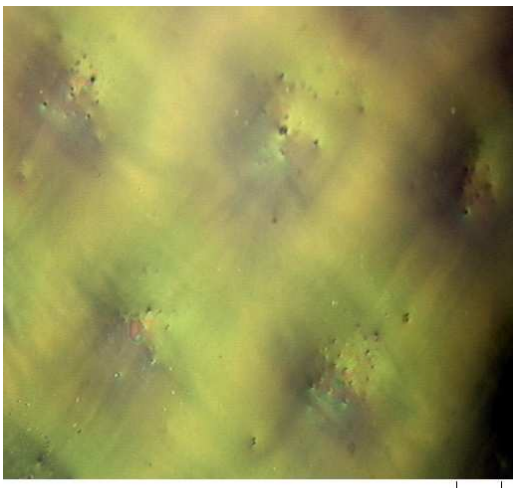

Figure 8-16 Active side of Used CTA Membrane exposed to hexane water mix

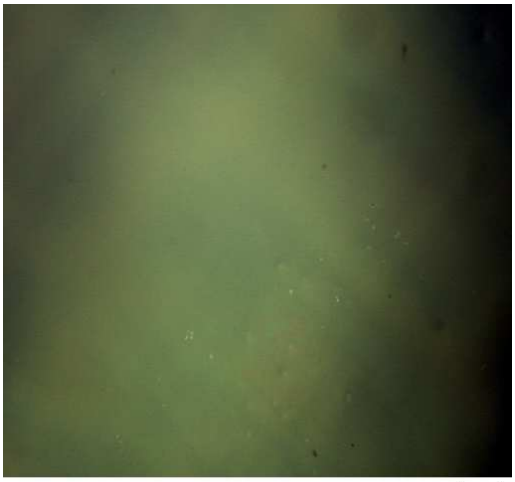

Figure 8-17 Active side of Used CTA Membrane exposed to hexane water mix

Cell 3

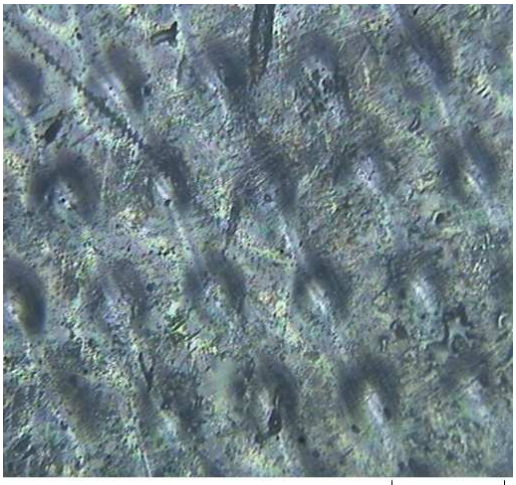

Figure 8-18 Active side of Used CTA Membrane exposed to diesel / water mix

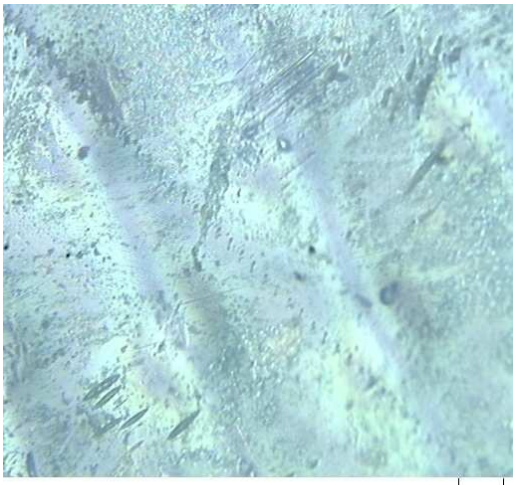

Figure 8-19 Active side of Used CTA Membrane exposed to diesel / water mix

Cell 4

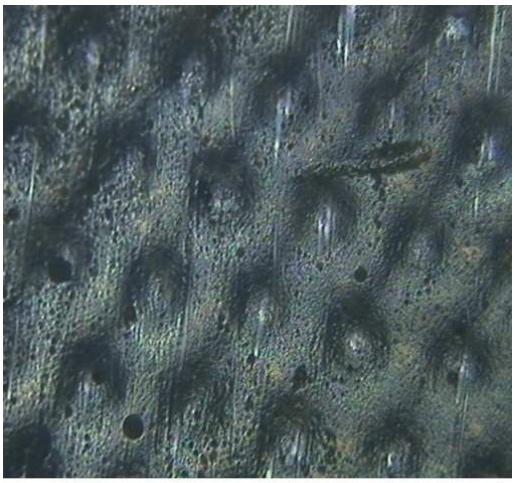

Figure 8-20 Active side of Used CTA Membrane exposed to diesel / water mix

Figure 8-21 Active side of Used CTA Membrane exposed to diesel / water mix

8.3 Scanning Electron Microscopy

The three types of membranes were examined under the microscope. The following is what was observed.

8.3.1 Initial Examination

Initial microscopical investigation utilised a Hitachi S4700 Scanning Electron Microscope. New membranes were examined under this microscope. The active surface of the SW 30 membrane revealed a distinct globular structure, see Figure 8-22.

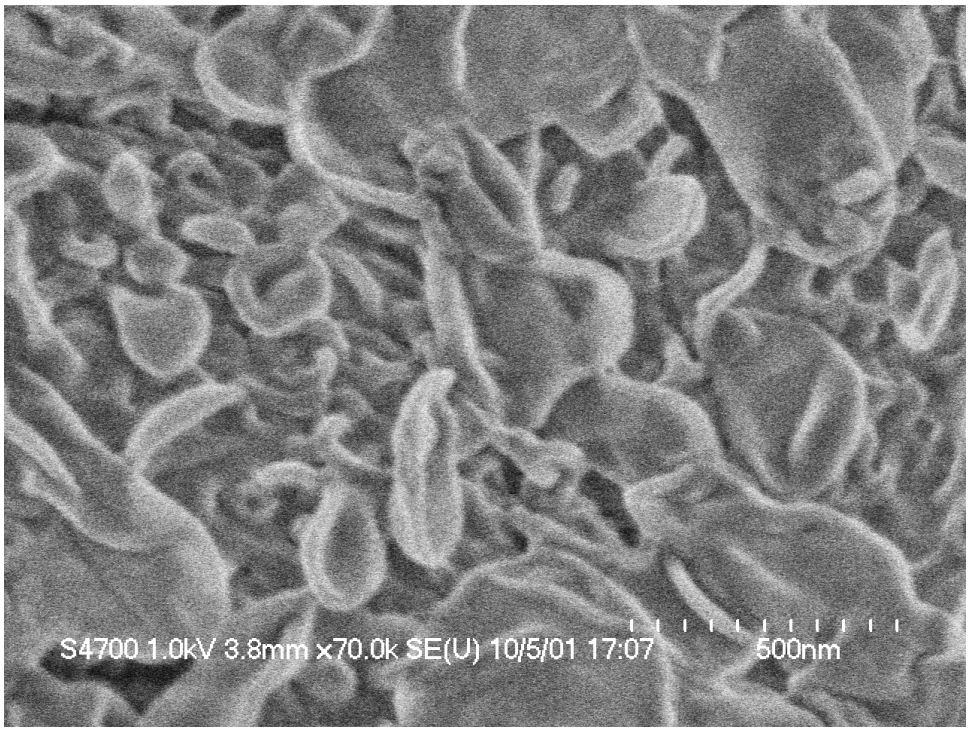

Figure 8-22 Active surface of SW 30 membrane at 70 000 magnification

The active surface of the CTA membrane, however was largely featureless Figure 8-23.

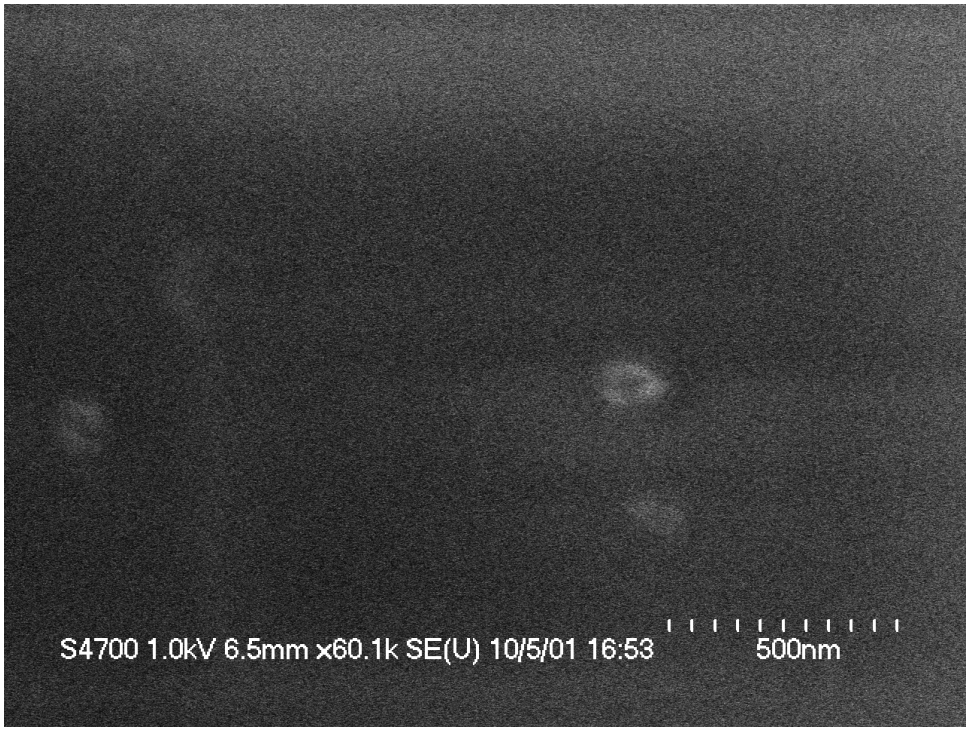

Figure 8-23 Active surface of CTA membrane at 60 000 magnification

Additional study of the membranes on this SEM was prevented by the microscope going out of service at the times relevant to this project. Consequently, further scanning electron microscopy was undertaken on a FEI Quanta 200F Environmental SEM and the output from the examination on this latter microscope is described in sections 8.3.2 and 8.3.3.

8.3.2 Cellulose Triacetate Membranes

The cellulose triacetate brackish water membrane proved to be very sensitive to the electron beam from the microscope. At low magnifications the membrane was not damaged but there were no surface feature that could be observed. At higher magnifications the electron beam created small pits on the surface of the membrane almost instantly. This meant that the surface of the membrane could not be observed at high magnifications.

8.3.3 Polyamide Membranes

The polyamide brackish water membrane (BW30) tolerated the electron beam much better than the CTA membrane. Unfortunately the polyamide membrane did not possess very distinguishable surface features. Only a few photographs were obtained. Figures 8-24 & 8-25 are an example, the rest are in the Appendix IV. Furthermore the polyester web backing material could not be separated from the back of the membrane shown in Figure 8-26. So the surface of the interlayer of the membrane could not be examined.

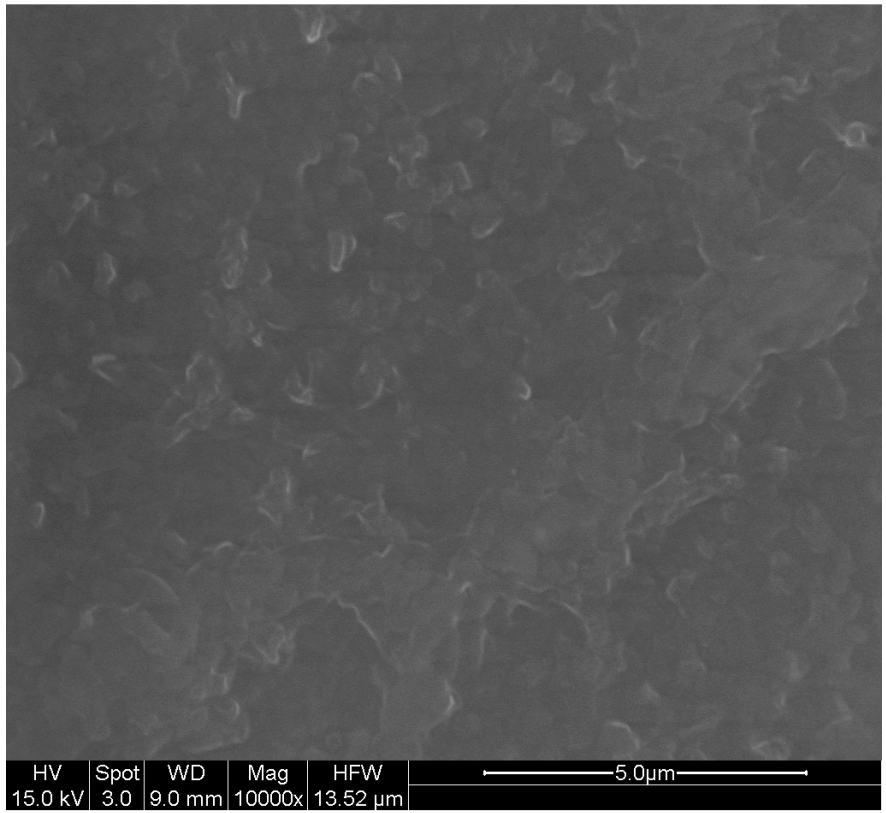

Figure 8-24 Active surface of BW 30 membrane (not exposed to hydrocarbons) at 10 000 magnification

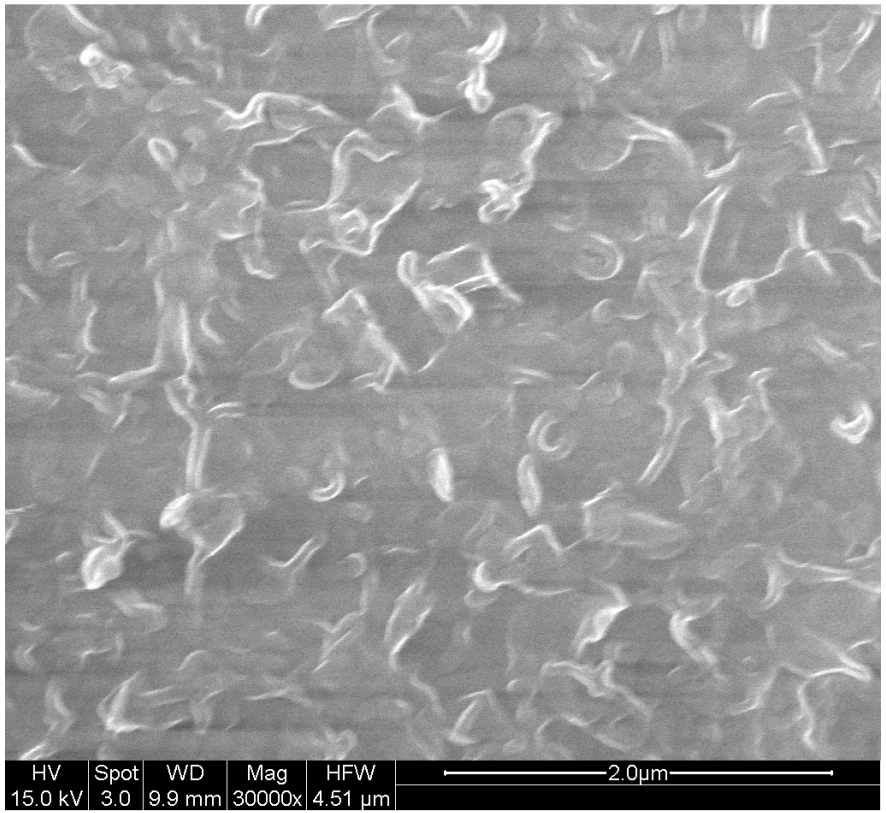

Figure 8-25 Active surface of BW 30 membrane (not exposed to hydrocarbons) at 30 000 magnification

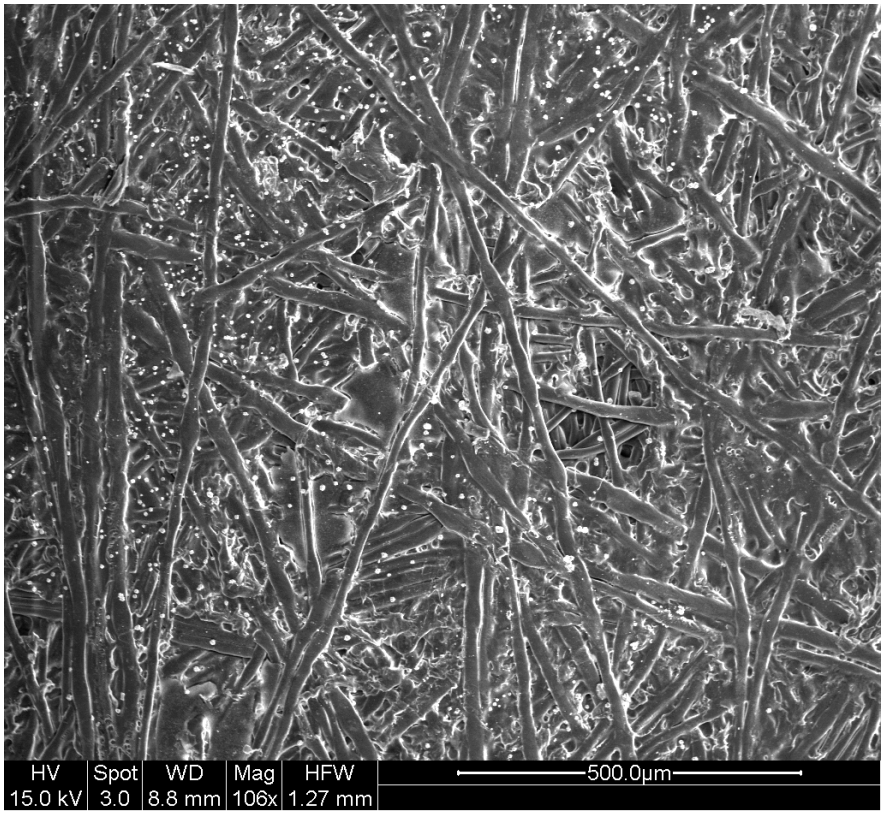

Figure 8-26 Backing support web of BW 30 membrane

The seawater polyamide membrane (SW 30) on the other hand provided much more interesting results. Photos of the active surface were taken at different magnifications. The membrane was successfully detached from the web-like backing support which is shown in Figure 8-2. It looks very much like the one used in the BW 30 membrane in Figure 8-26.

This allowed the back of the interlayer as well as the active surface of the membrane to be examined. Membrane samples were mostly examined in plan. The cross section of the membrane was also looked at but unfortunately due to the delicate nature of the membrane, cutting caused damage to the membrane. This obscured some details of the membrane structure (Figure 8-27 and 8-28). Thus all the following photographs Figures 8-29 to 8-42 are those resulting from the study of SW 30 membranes in plan.

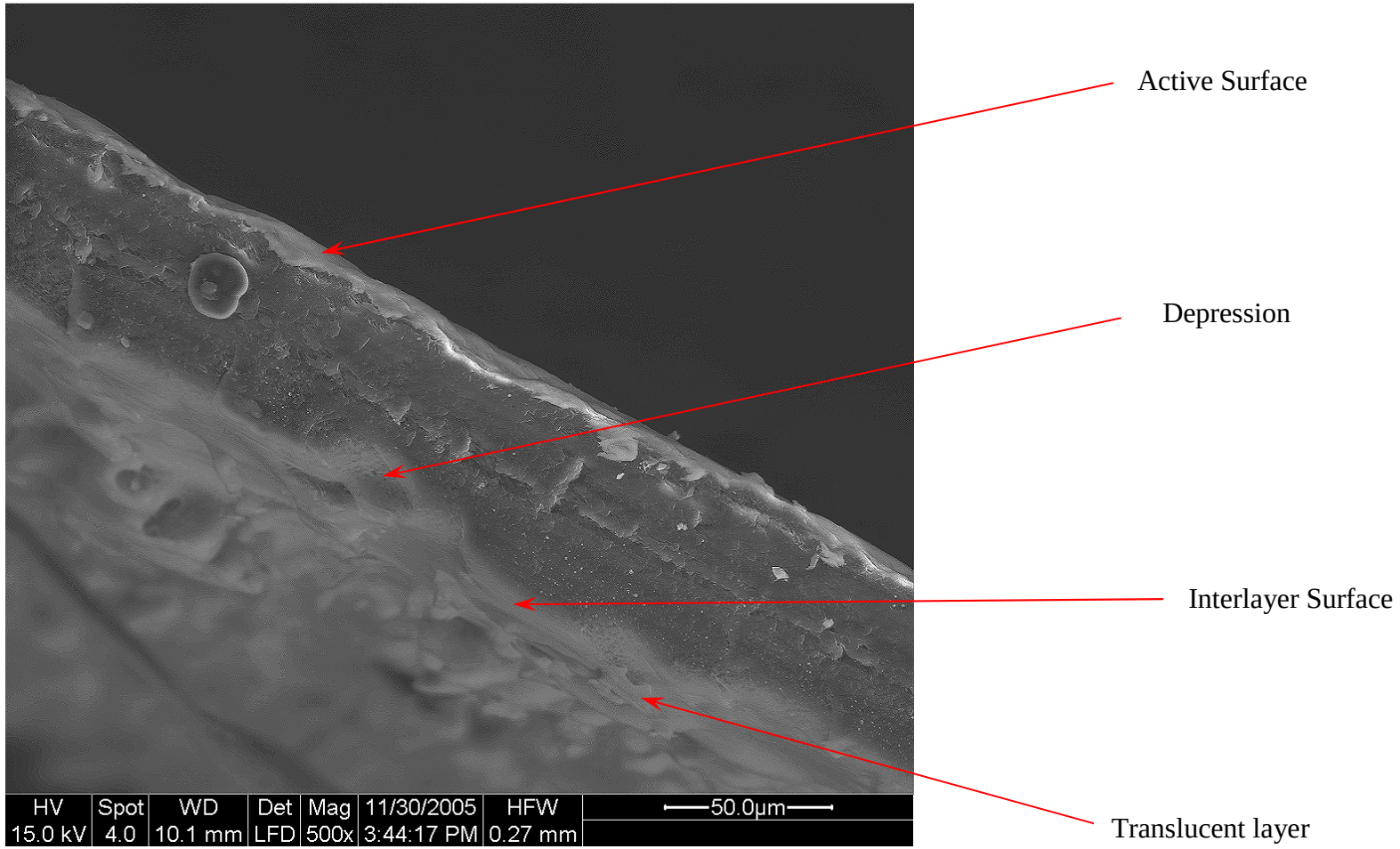

Figure 8-27 Cross Section of new SW 30 membrane at 500 magnification

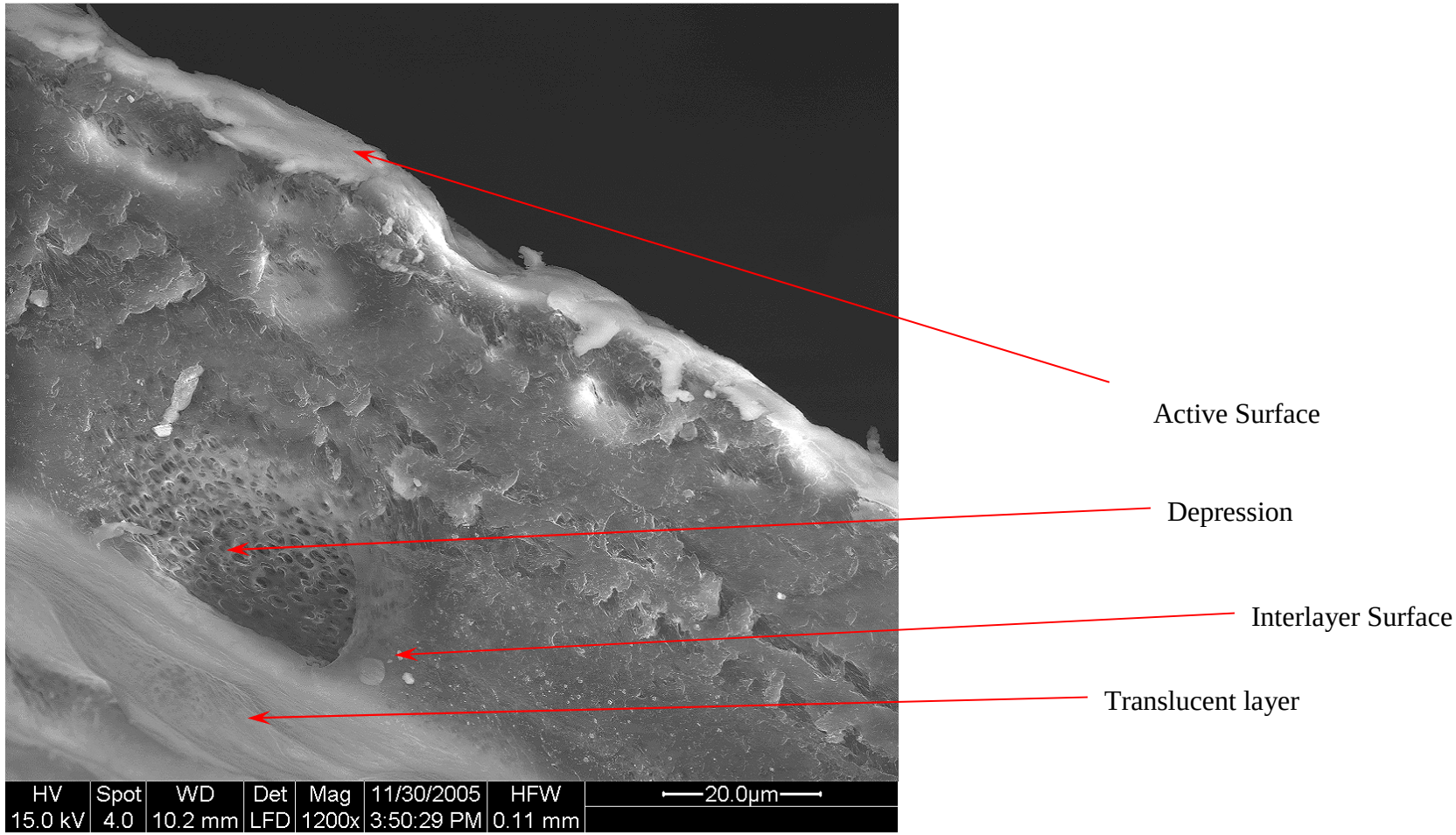

Figure 8-28 Cross Section of new SW 30 membrane at 1200 magnification

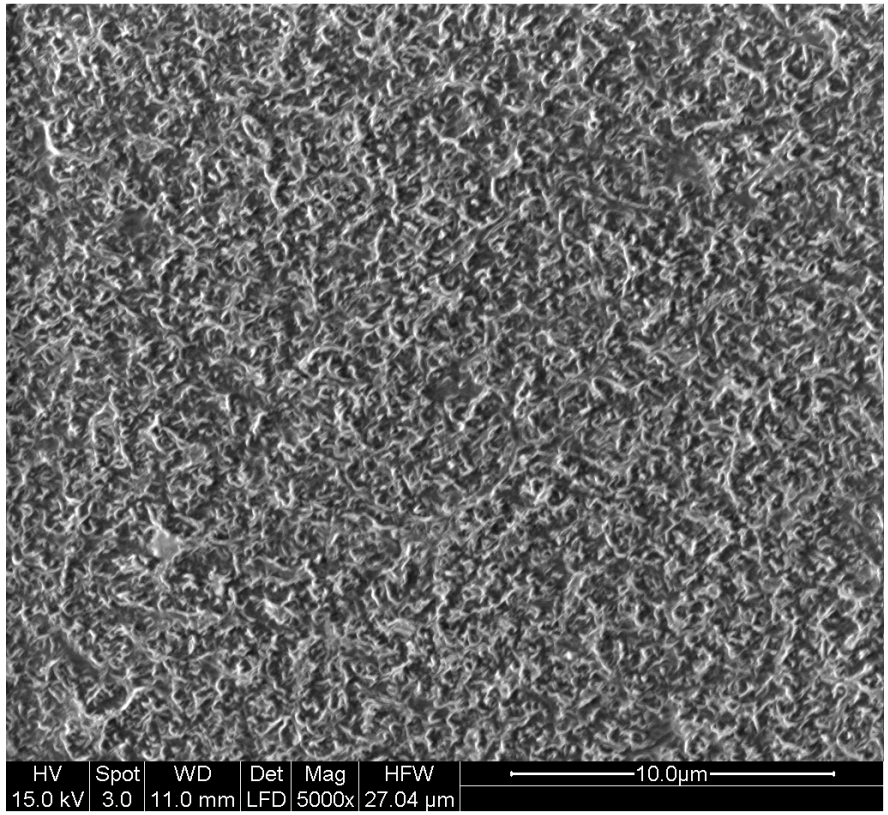

Figure 8-29 Active surface of new SW 30 membrane at 5 000 magnification

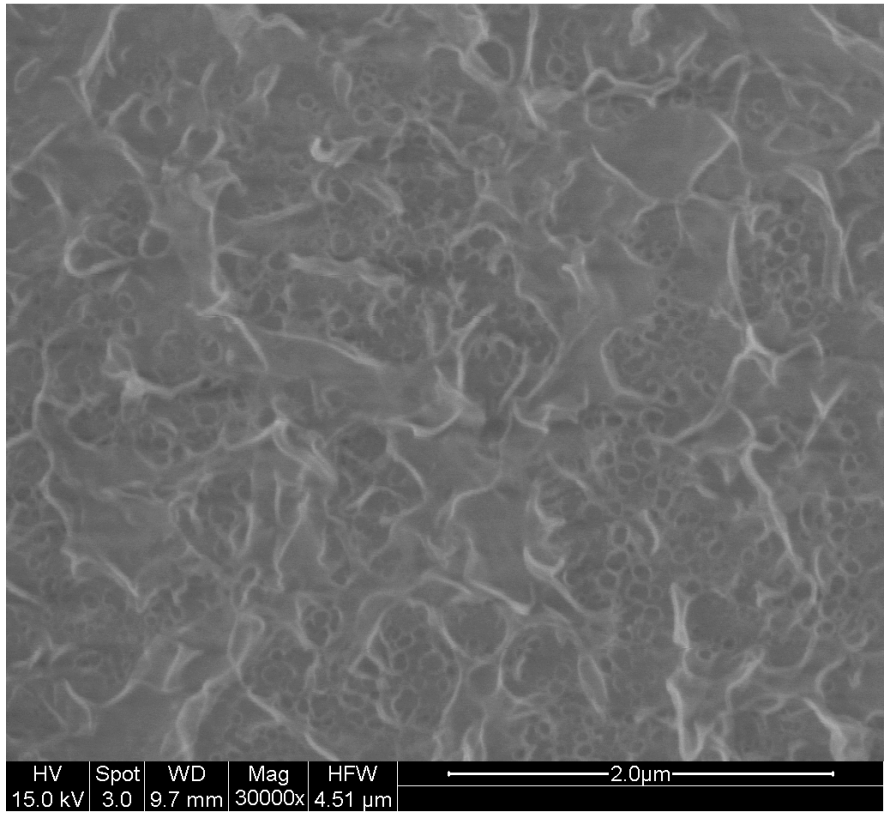

Figure 8-30 Active surface of SW 30 membrane at 30 000 magnification

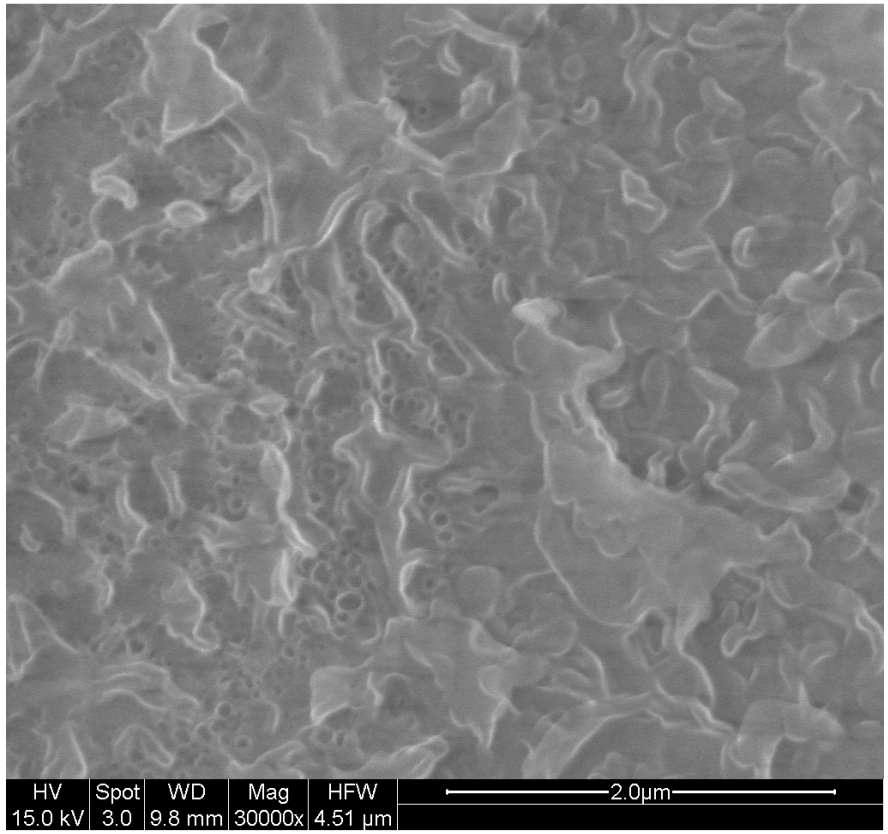

Figure 8-31 Active surface of SW 30 membrane at 30 000 magnification after exposure to Hexane

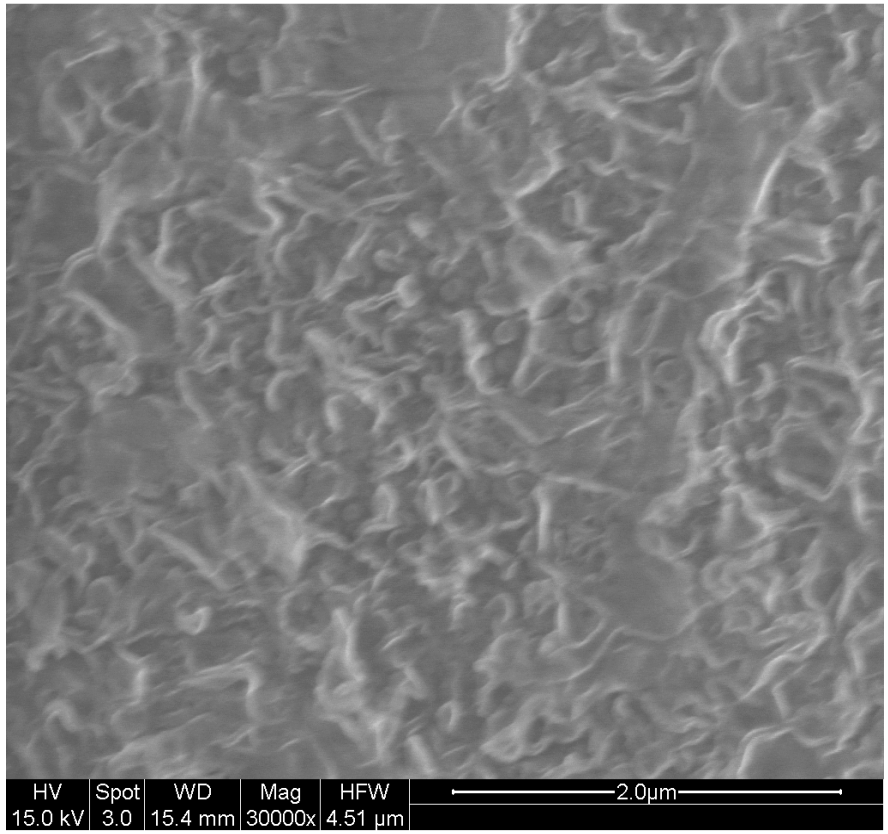

Figure 8-32 Active surface of SW 30 membrane at 30 000 magnification after exposure to Diesel

Figures 8-29 and 8-30 show the active surface of the SW 30 membrane which has not been exposed to any hydrocarbons. The structure of the surface is well defined, all the edges are sharp and are distinct.

In Figures 8-31 and 8-32 the active surface of the SW 30 membrane has been exposed to hydrocarbons, the one in Figure 8-31 to hexane and the one in Figure 8-32 to diesel. The change in surface structure of the membrane that has been exposed to hexane is not immediately apparent but when the Figures are closely compared the fouled membrane show a surface structure that is less sharp. The edges of that structure have lost some definition.

In Figure 8-32 the difference is even more apparent. All the surface details have started to merge and this gives the membrane a fuzzy appearance. These go to show that the membranes are actually susceptible to hydrocarbon fouling at a molecular level.

Figures 8-33 through 8-36 show the bottom surface of the interlayer of a new SW 30 membrane at different magnifications. It is immediately apparent that this material is much more porous than that used for the active surface. Detail of that structure can already be distinguished at much lower magnifications. The material looks honeycombed with pores. The surface of the membrane sample (Figures 8-33 and 8-34) has the largest pores, and when the focus of the microscope is changed the interior of the large pores (also visible in cross-section as depression in Figure 8-28) comprises (Figures 8-35 and 8-36) of a lattice-like structure composed of smaller pores.

Surface of interlayer

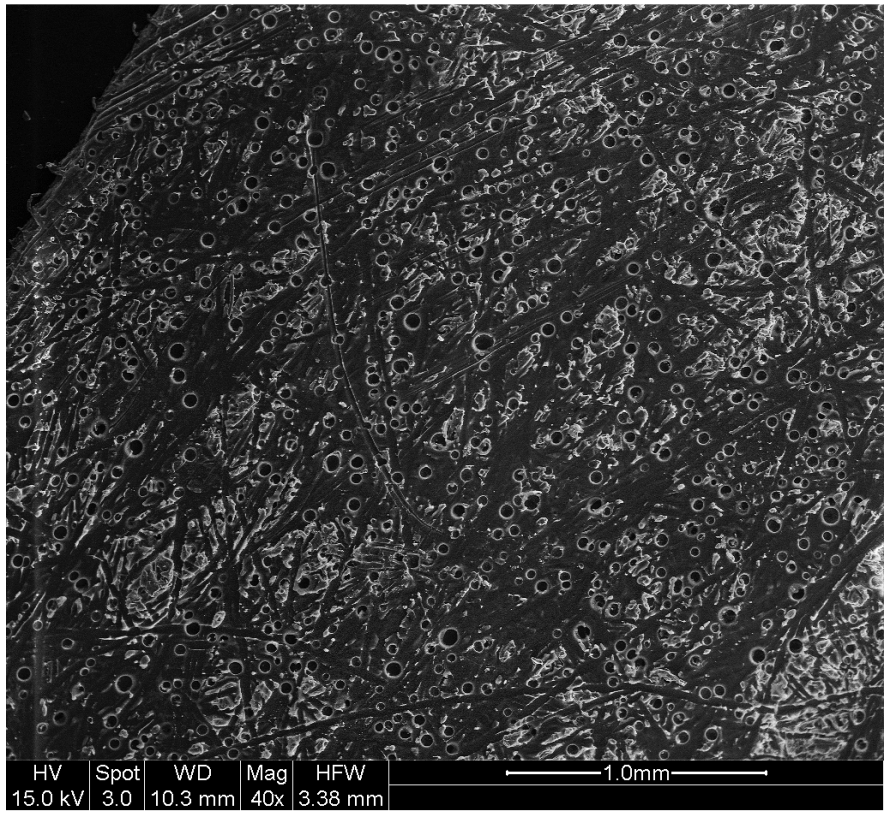

Figure 8-33 Surface of interlayer of new SW 30 membrane at 40 magnification

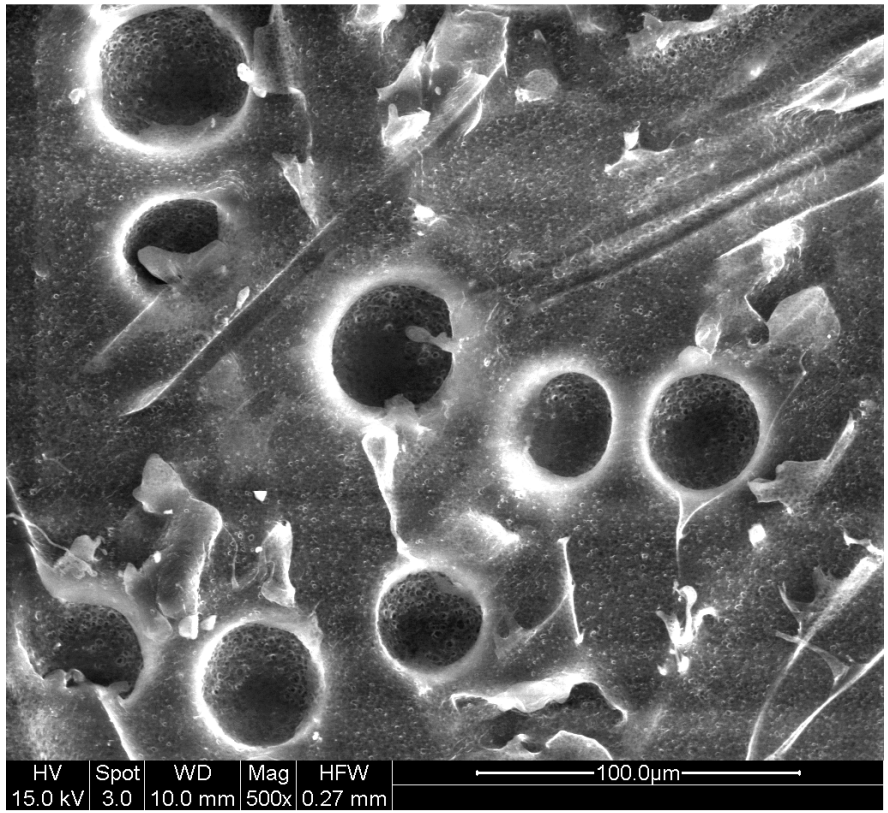

Figure 8-34 Surface of interlayer of new SW 30 membrane at 500 magnification

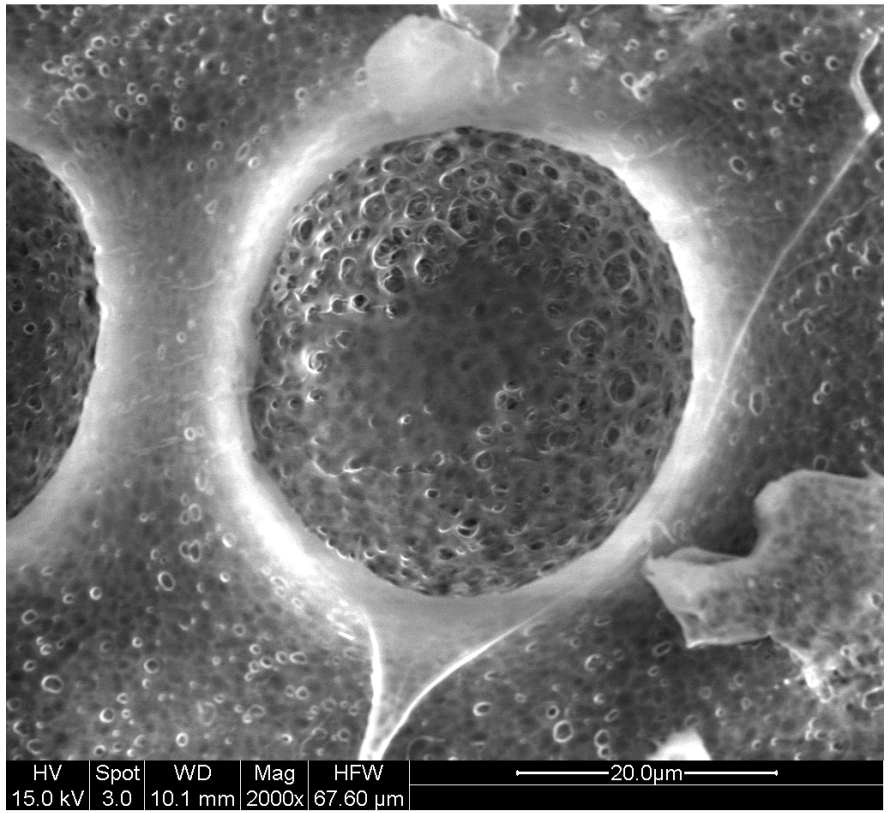

Figure 8-35 Surface of interlayer of new SW 30 membrane at 2000 magnification

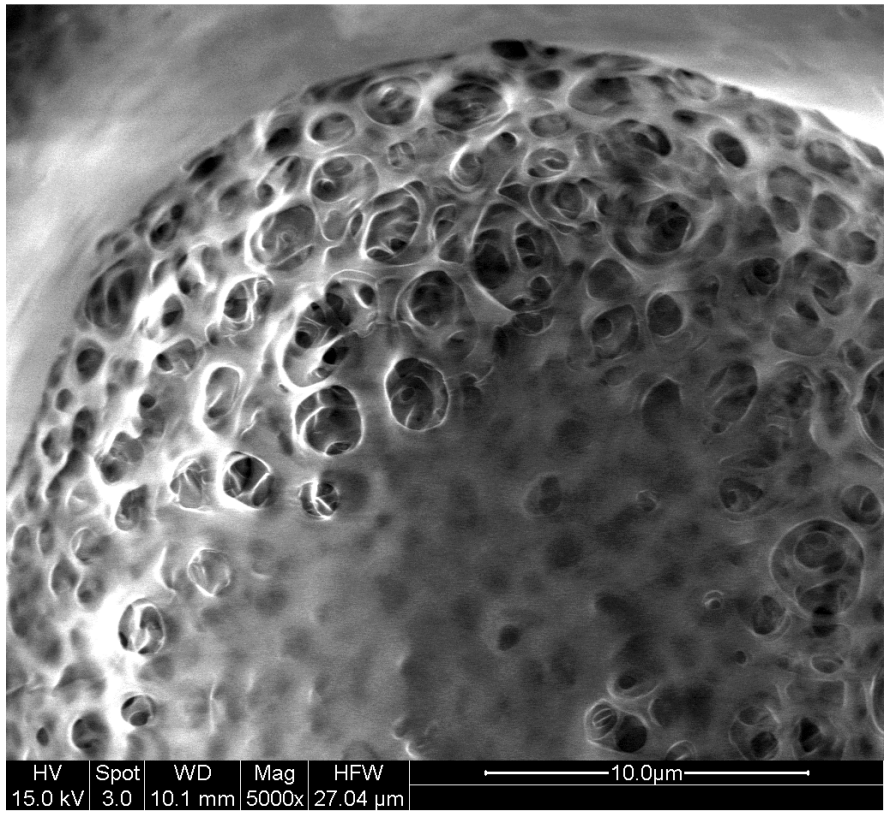

Figure 8-36 Surface of interlayer of new SW 30 membrane at 5000 magnification

Figures 8-37 to 8-42, show the bottom surface of the interlayer of the membrane after it has been exposed to hydrocarbons. Here, as opposed to the active layer, the difference between clean and fouled surface is much more visible. This can be most readily seen in the case of hexane by comparing Figure 8-34 to 8-37 and Figure 8-35 to 8-39, or in the case of diesel Figure 8-35 to 8-41 and Figure 8-36 to 8-42. Most of the honeycomb structure has been obliterated, leading to a massive reduction in the amount of space allowing the water from the active layer to pass. This obviously is very detrimental to the good running of the desalination process.

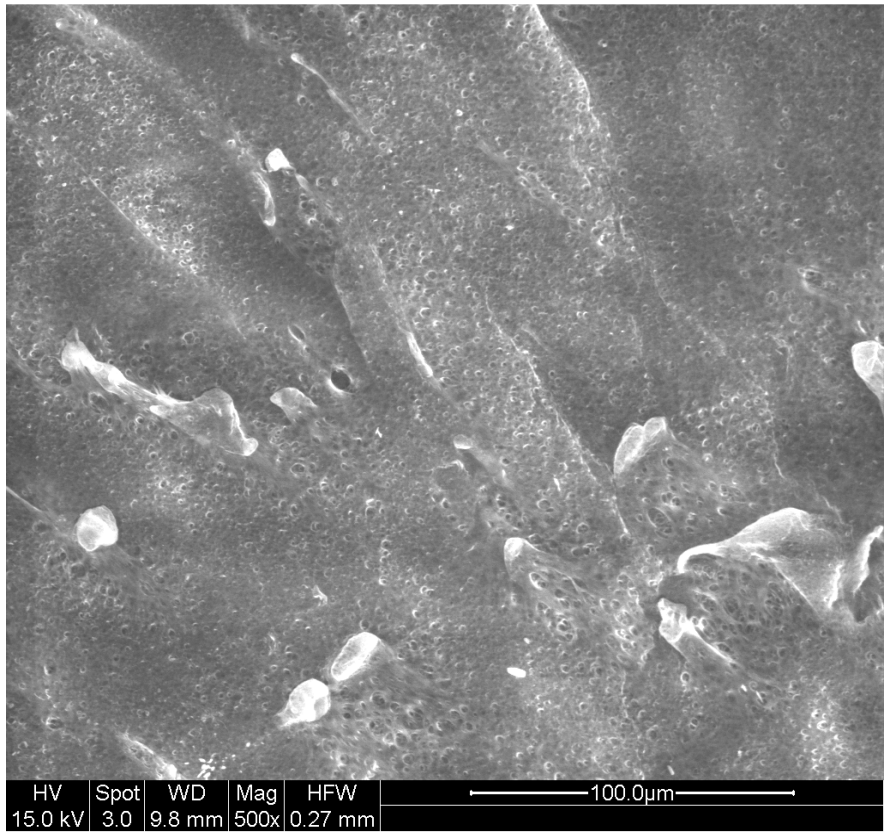

Figure 8-37 Surface of interlayer of SW 30 membrane exposed to Hexane at 500 magnification

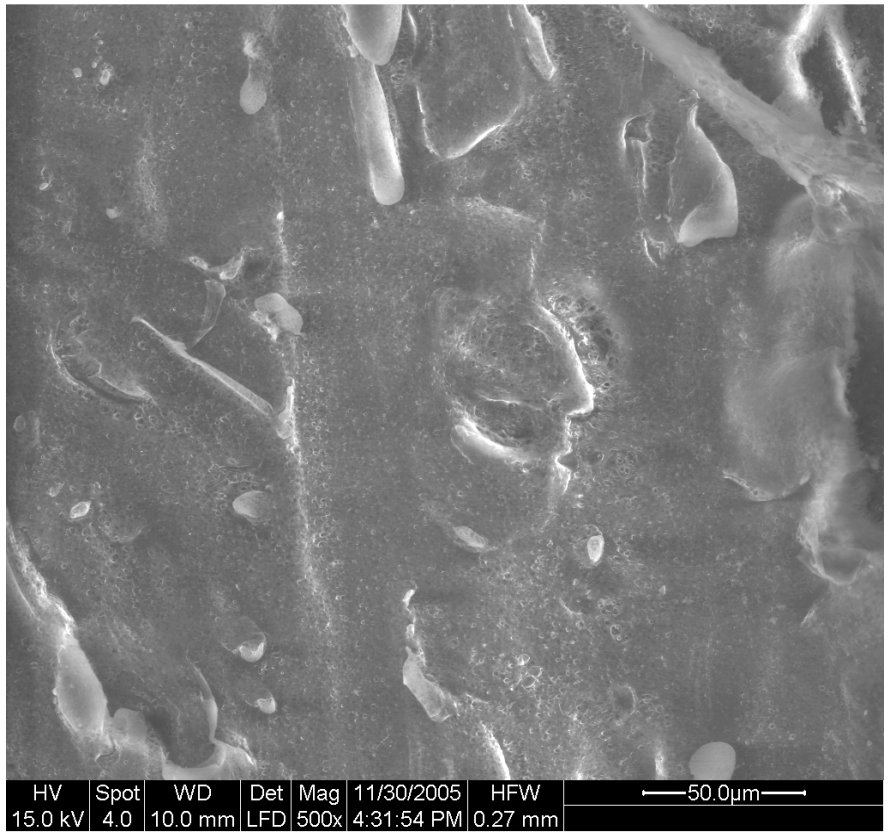

Figure 8-38 Surface of interlayer of SW 30 membrane exposed to Hexane at 500 magnification

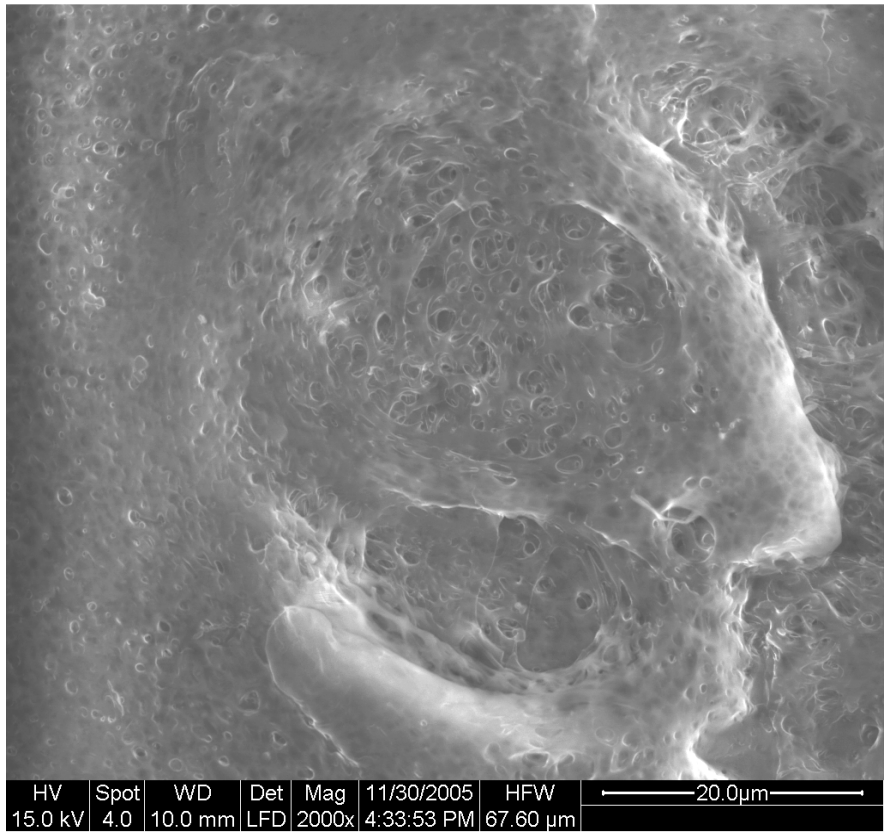

Figure 8-39 Surface of interlayer of SW 30 membrane exposed to Hexane at 2 000 magnification

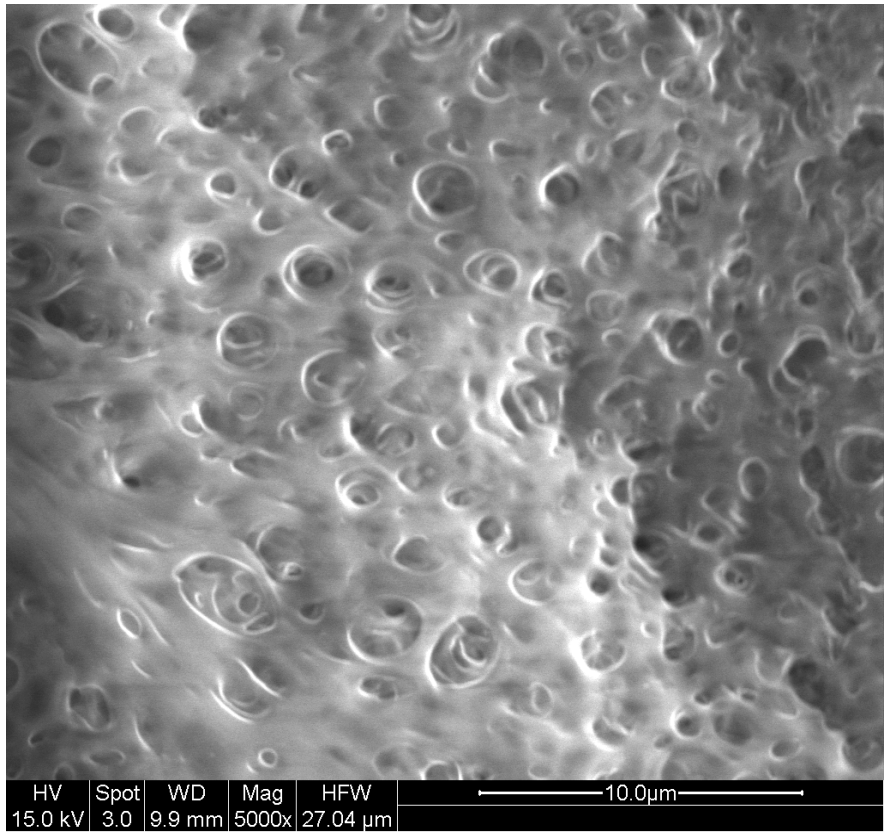

Figure 8-40 Surface of interlayer of SW 30 membrane exposed to Hexane at 5 000 magnification

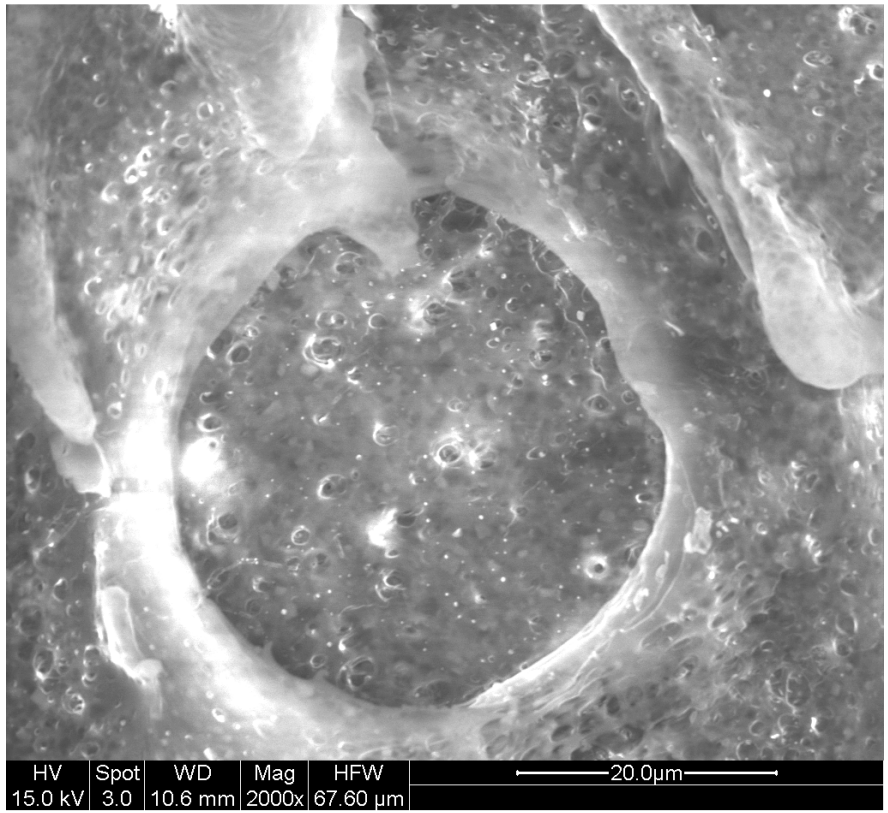

Figure 8-41 Surface of interlayer of SW 30 membrane exposed to Diesel at 2 000 magnification

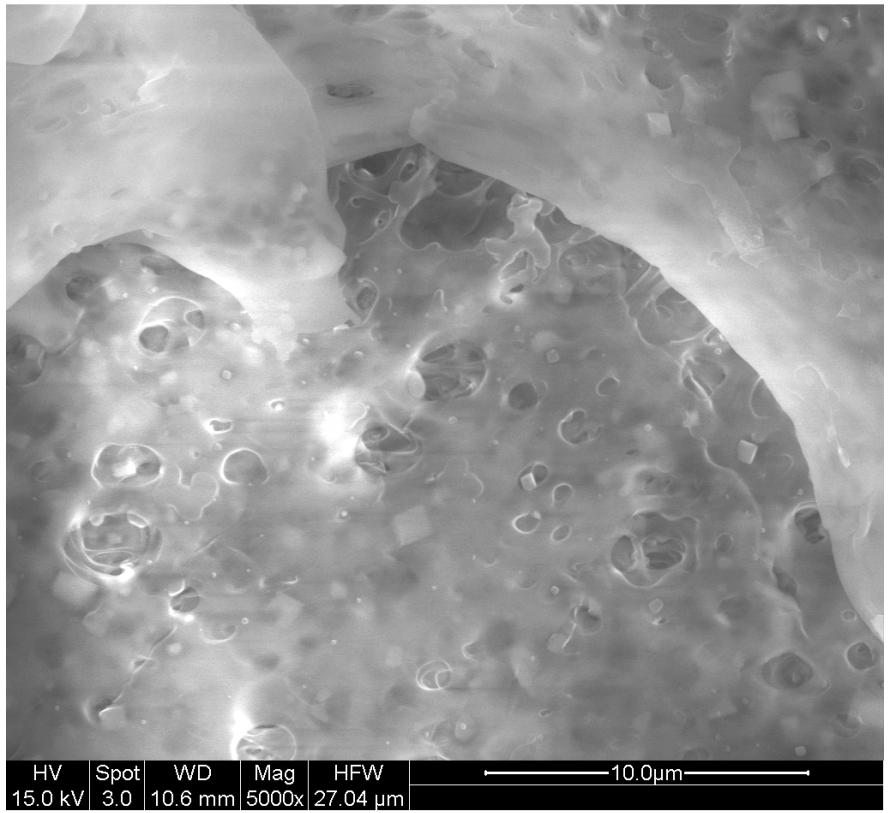

Figure 8-42 Surface of interlayer of SW 30 membrane exposed to Diesel at 5 000 magnification

CHAPTER 9 DISCUSSION

9.1 SW 30

9.1.1 Tests on Clean Seawater Membranes

Figures 9-1 and 9-2 summarise the scatter in percentage flux change and change in percentage salt passage for uncontaminated SW30 membranes from experiments SW/1 to SW/7 described in detail in Chapter 6.2. The range of the scatter is relatively small in both cases. This indicates that the results for the experiments involving this membrane should be mostly consistent throughout. The average percentage permeate flux change is about 5%, and the average change in percentage permeate flux is about 0.2. These changes are small compared to the equivalent ones measured on specimens that have been exposed to hydrocarbon (Figures 9-3 and 9-4) and discussed in the next section.

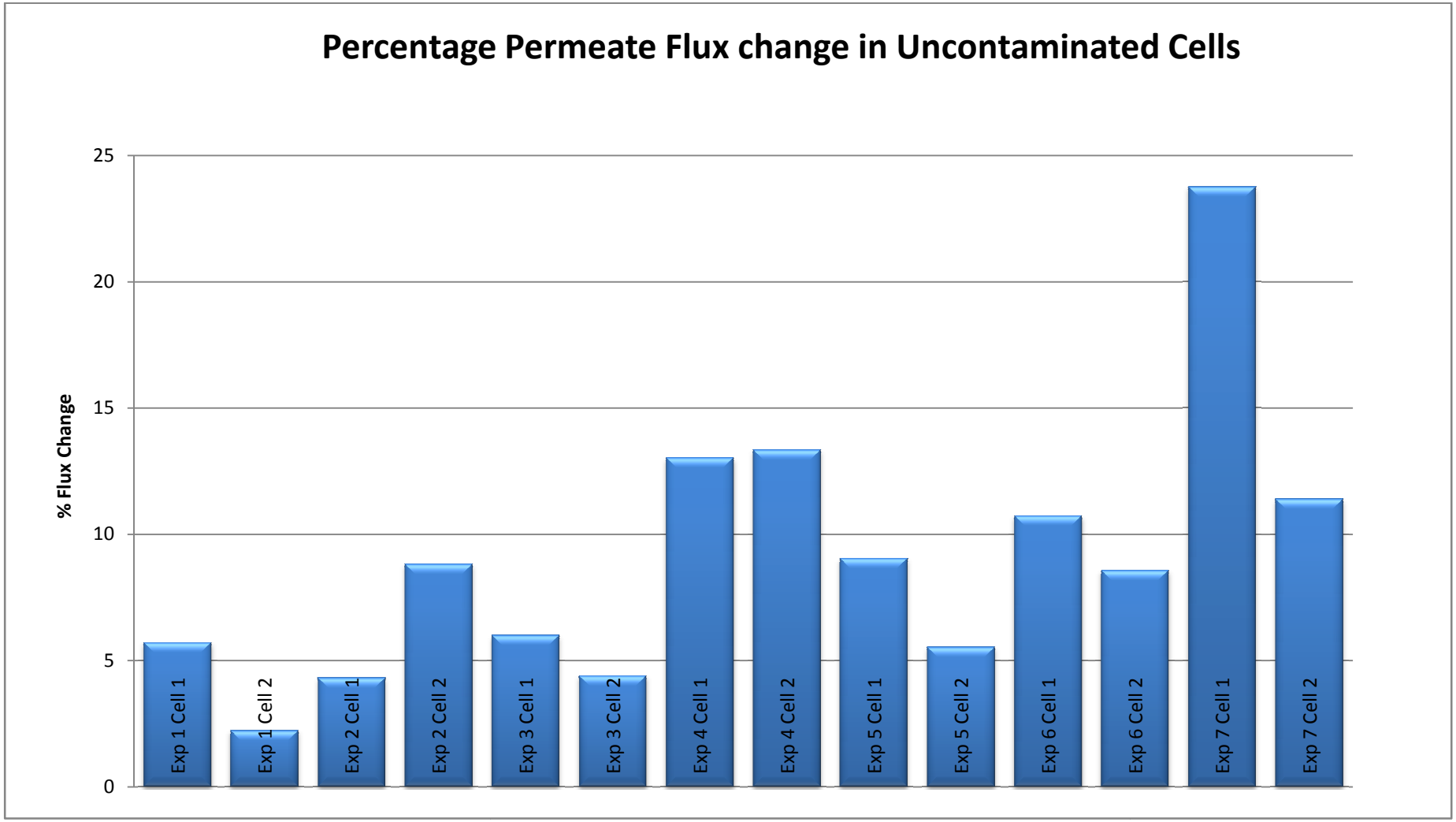

Figure 9-1 Percentage Flux Change for Uncontaminated SW30 Membranes

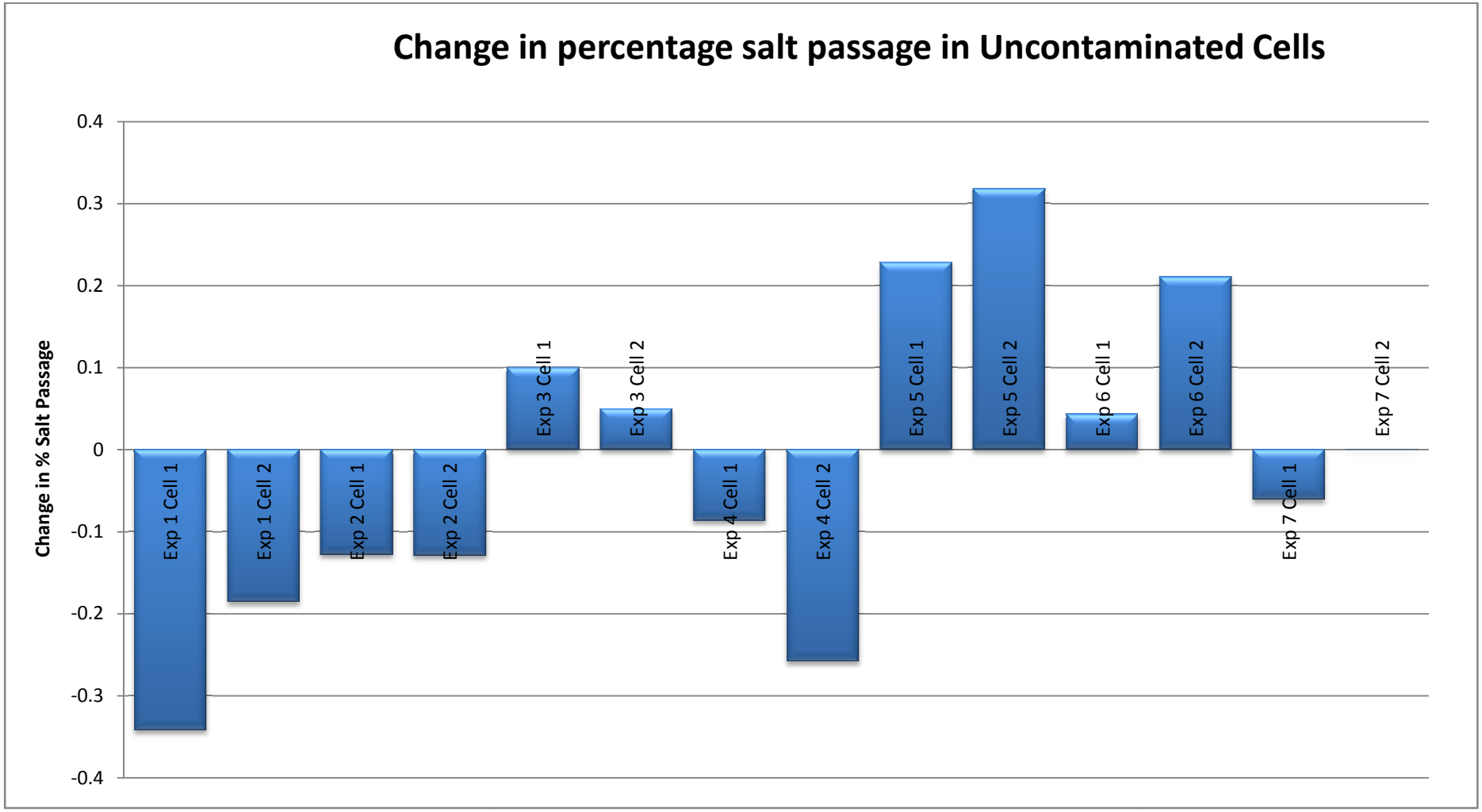

Figure 9-2 Change in Percentage Salt Passage for uncontaminated SW30 Membranes

9.1.2 Tests on Contaminated Seawater Membranes

Figures 9-3 and 9-4 present a summary of the reverse osmosis performances with respect to flux and salt passage of membranes exposed to the hydrocarbon containing fluids. These Figures, and those (Figures 8-26 to 8-42) obtained from the microscopy observations presented in Chapter 8, are used as basis for the following discussion.

When both sides of the membrane are exposed to hexane, whether in pure form or as an emulsion, it can be seen that the flux is reduced to zero. A similar situation pertains after exposure of both sides to pure diesel or diesel / water emulsion. As summarised in Table 5, these findings are in good agreement with relevant previous work in this laboratory [55]. These studies revealed that a very substantial reduction in water flux occurred when both sides of SW 30 membranes were exposed to hexane or diesel. Further confirmation of the potential effect of hydrocarbon fouling on membranes has been provided by a brief study [59] on Filmtec™ SR90 sulphate reducing membranes which also apparently utilize a polysulphone backing material.[60] This work [59] also revealed total blockage of the membrane when both sides had been exposed to a prior period in hexane but much less deterioration in properties when just the active surface was contaminated.

In the present study, additional experiments were undertaken in which only the active surface was exposed to hydrocarbons. A completely different situation arises when only the active side of the membrane is exposed to the above mentioned hydrocarbon contaminants. In the case of hexane / water emulsion an increase of about 12 – 22 % in flux was measured together with a small increase in the percentage salt passage. After exposure of the active side of the membrane to diesel / water emulsion the measured flux changes were rather similar to

those of the control tests and increases in percentage salt passage were observed but with a wider scatter than in the former tests.

Another study [61] has found that after exposure to bilge water containing hydrocarbons the permeate flux obtained from a SW 30 membrane fell by about 23%. In this study [61] the contaminated water was fed through the membrane under pressure (transmembrane pressure of 0.4 MPa {4 bar}) thereby possibly causing a small amount of hydrocarbons to pass through the active layer of the membrane. This would cause the interlayer to then be exposed to this tiny amount of hydrocarbon leading to an increasing fall in permeate flux the longer the experiment is carried out.

Microscopical examination was undertaken in an attempt to detect any structural changes on the membrane. Figures 8-22, 8-29 and 8-30 (Chapter 8) are photographs of the active surface of a membrane that has not been exposed to the hydrocarbon fluid and Figures 8-31 and 8-32 are those of membranes that have been exposed to hexane and diesel respectively. When compared to the photographs of uncontaminated membranes, Figures 8-31 and 8-32 show very little difference except for a slight coalescing of the ridges present on the surface. This agrees with the findings of the reverse osmosis experiments and demonstrates that the active surface of the SW 30 membrane undergoes only minor changes under the experimental conditions to which it has been subjected.

On the other hand, on a membrane sample which has had both sides exposed to hexane or diesel, examination of the bottom surface of the polysulphone interlayer revealed drastic changes in the structure. After exposure to pure hexane and diesel, the pores on the contaminated membrane have been either fused together or completely obliterated (Figures 8-37 to 8-42). This is in stark contrast to the open-pore structure of an

uncontaminated sample (Figures 8-33 to 8-36). This indicates that the more susceptible part of the membrane is the polysulfone interlayer.

The aqueous solution of hexane produce the opposite effect, that is an increase in flux which, at 20 - 40 %, is considerably greater than the flux changes 3 - 8%, (Figure 9-1) recorded in the control experiments. The percentage salt passage after exposure to the hexane / water solution, is seen to increase by 0.2 and 1.2 % in the two experiments as compared to measured changes, between -0.1 to +0.3 % in the control tests. It is clear that the low solubility of hexane in water (0.0013 g/100 ml at 20°C) [57] does not cause significant deterioration in the membrane properties; indeed it appears to produce an increase in water flux and a possible small increase in percentage salt passage.

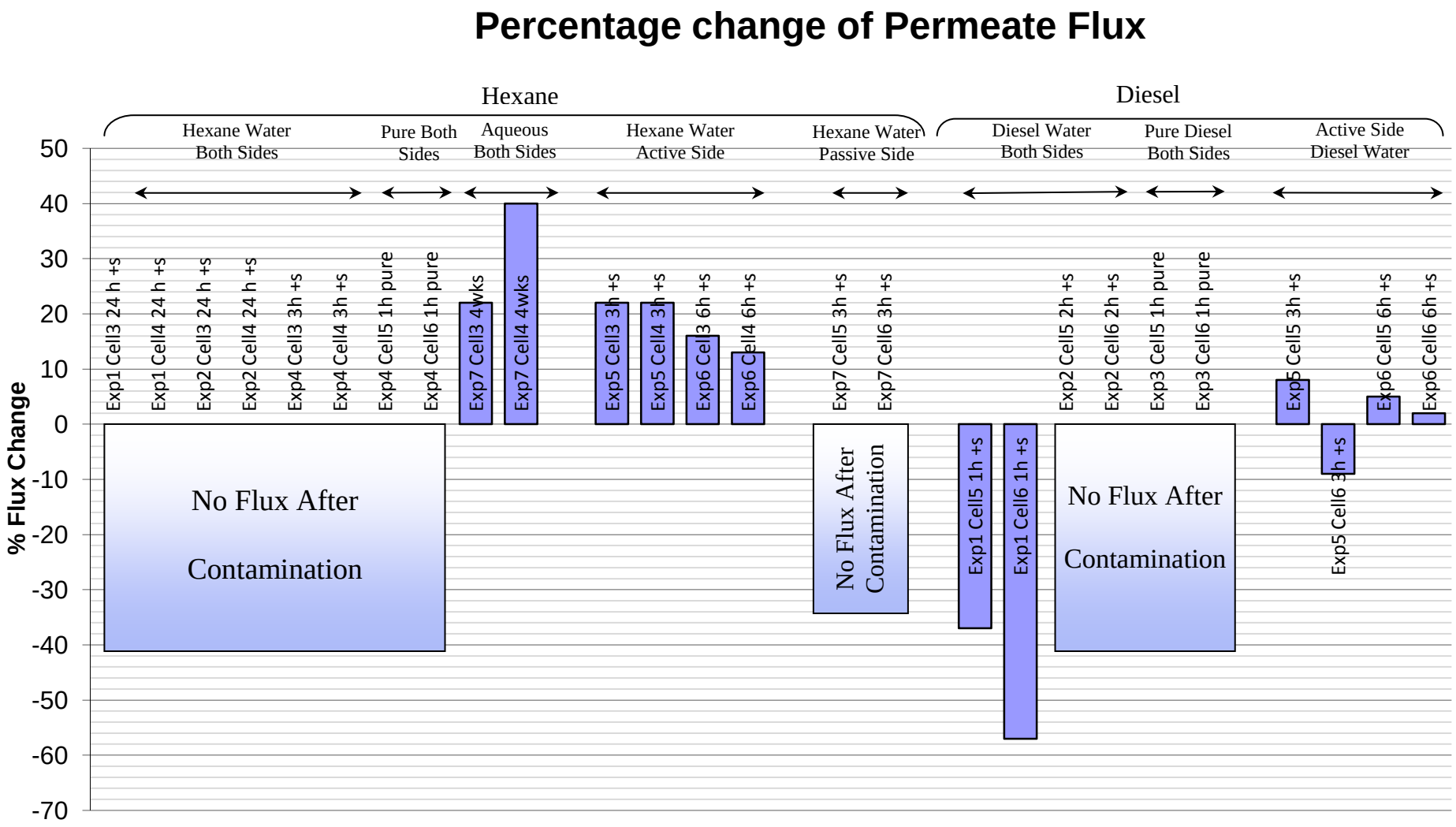

Figure 9-3 Percentage change in Permeate Flux for SW30 Membranes after Exposure to Hydrocarbons.

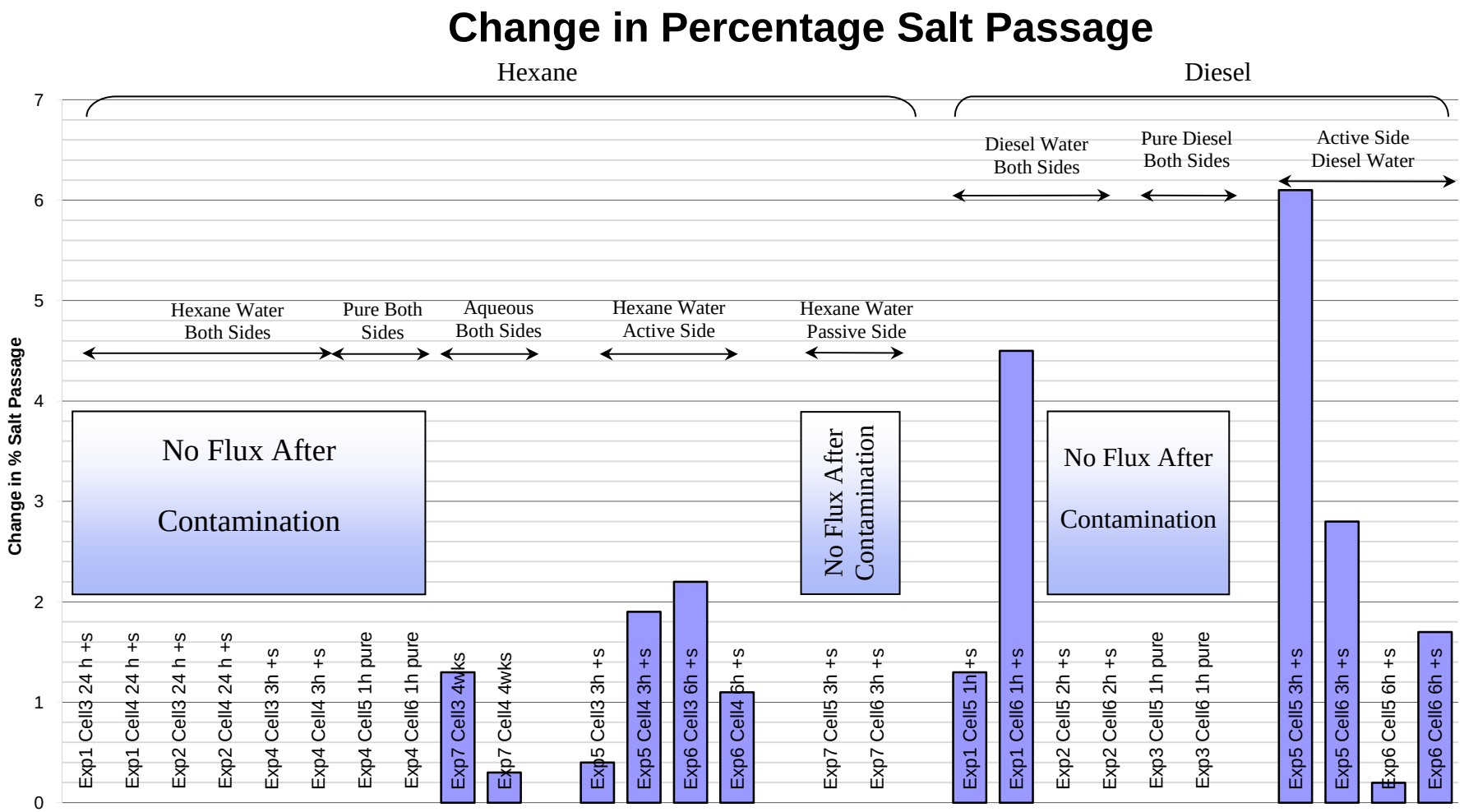

Figure 9-4 Change in Percentage Salt Passage for SW30 Membranes after exposure to Hydrocarbons

9.1.3 Comments on Mechanisms of Deterioration

The major observation was that exposure of the underlayer polysulphone of the SW 30 membrane to pure hexane, hexane / water emulsion and pure diesel render the membrane completely unusable in that the membrane was completely blocked with zero water flux.

Chemical resistance tables [62],[63] were consulted to find out if and how industrially produced polysulphone reacted to hexane and diesel. The tables indicated that polysulphone has a good chemical resistance to both hexane and diesel. This leads to the deduction that the polysulphone interlayer of the SW 30 membrane is not being significantly chemically affected but the change could be mainly physical. The exposure to the hydrocarbons could be causing the polysulphone to soften, then when the membrane is put back in the cell and exposed to pressure, the porous structure of the interlayer is compacted and the pores are blocked.

In this respect some authors [64] have postulated on the effect of hexane in causing swelling of polysulphone membranes.

Another instance of severe degradation of polysulphone has been reported, [65] but this time after contact with sodium hypochlorite, in which instance substantial effects on the polysulphone structure including chain scission were recorded.

Although the detailed characteristics of reverse osmosis membranes are difficult to identify due to commercial secrecy, apparently [66] many composite membranes utilise polysulphone as the support layer.

Replacing the polysulphone interlayer with a more resistant material would make the membrane more resistant to hydrocarbon fouling as a whole. Though in practice the backing surface would not be directly in contact with the hydrocarbon which would mostly be stopped by the membrane, some would still get though leading to an overall loss of H_2O flux.

As regards the much less-substantial effects of hydrocarbon contact with the polyamide active layer, it is likely that hydrocarbon-containing emulsions will form a film on the surface of the membrane and thereby interfere with the separation process. There may also be more direct effects of hydrocarbons on the membrane material and, in this respect, it is relevant to consider the two main models of separation in reverse osmosis, i.e. the pore model and the solution diffusion model.

If the second model is considered, a reasonable explanation for what is being observed would be that the hydrocarbons are causing structural modifications which have resulted in an increase in the diffusion rates of both H_2O molecules and the ionic solutes.

In relation to the pore model, the following suggestions can be presented:

The membrane ‘pores’ are loosened causing an increase in permeate flux and also an increase in percentage salt passage. This again points to physical damage to the membranes.

These results suggest that, even though the ‘pores’ are being loosened, only the ionic components of the feed was getting through. Given the extremely small thickness of the active layer and the exposure times to the hydrocarbon together with their high concentrations, it would appear that the active layer remains essentially impervious to hydrocarbon molecules even under the influence of a reverse osmosis plant operational pressure driving force.

Furthermore it should be noted that the membranes tested in this study were not exposed to the hydrocarbon under pressure. Consider the case where the hydrocarbon is present as a contaminant in the pressurised seawater feed to a membrane module. The result might be somewhat different and take longer to happen. It can be speculated, considering what has been observed, that the hydrocarbon will take some time to damage the active layer. This damage will be in the form of loosening the active surface structure allowing the hydrocarbon to pass through. When the hydrocarbon starts to permeate the active layer, it will be in direct contact with the sensitive substrate and damage it. In the module the feed will be under pressure, so instead of just fusing the substrate together it will obliterate its structure and undermine its strength causing it to start peeling off. These bits of substrate will then flow out with the product water further contaminating it. The reverse osmosis module uses a spiral bound configuration for efficiency, and this layout is particularly prone to blockage, so having loose bits of material floating in the module will be bound to cause blockages. After prolonged exposure the backing layer will fail completely and the active layer will not have a support anymore causing a total failure of the membrane module.

9.1.4 Relevance to Operation of Seawater Reverse Osmosis Plants

Although the cleaning of membranes, that have been fouled by organics, is feasible in some circumstances, this is less likely to be successful if the effects of such fouling are severe. For instance, a polyamide-membrane manufacturer [25] advised that cleaning of membranes that have been fouled by hydrocarbons may only be possible so long as the flux has not fallen by more than 15%.

Constant monitoring the intake of seawater will ensure that any hydrocarbon contamination of the feed is detected before it reaches the desalination plant. If it is only a minor contamination pre-treatment can take care of it. Special attention needs to be paid to the

location of and type of intake. This should encourage the inclusion of multiple intake points to be located apart from each other, or at least one backup intake to provide feed water to the plant in case of an emergency. This is particularly relevant in oil rich regions that heavily depend on seawater reverse osmosis as a source of fresh water. At least one of these countries [67] has setup an early warning system to detect and monitor its waters for the occurrence of an oil spill or the presence of oil slicks. Though the main concern should be an in depth analysis of the sites where the intake should be located. Analysis of the risks emanating from pollution and navigation is also relevant. The greatest risk of hydrocarbon spillage will come from either a shipwreck or the deliberate discharge of waste water from a ship. Therefore the ideal location for intakes would be in a region of the sea with constant water quality, no pollution and little or no navigation and where the general impact of the seawater intake will be minimal on the environment.

An obvious solution to this problem is to establish a robust pre-treatment of the feed water supply. The pre-treatment plant should have the ability to remove any hydrocarbon present in the water before it reaches the reverse osmosis plant. This will provide a safeguard for the membrane modules.

As this work has demonstrated, the main source of trouble arises with oil / water emulsion whilst salt water containing dissolved hydrocarbons, at least for short periods, is much less hazardous.

9.2 BW 30

Less attention was devoted in this work to the BW 30 membrane; for instance no tests involving diesel were undertaken.

The polyamide brackish water membrane, BW 30, reacted differently than SW 30 to exposure to hexane / water emulsion. During the test it was observed that there was an increase in the flux of the filtrate accompanied by a rise in the percentage salt passage. It is suspected that the hydrocarbon has had the effect of opening up the active layer of the membrane making it easier for the filtrate to go through. As this is a gradual process the deleterious effect on percentage salt passage was not immediately felt. Also it should be noted that said damage to the membrane structure may be permanent, cleaning the membrane may not restore the initial performance of the membrane.

These observations are different than those that were obtained in a previous study [55] summarised in table 5, where exposure of this membrane to hexane / water emulsion resulted in (non-catastrophic) decrease in water flux. This points to possible influences on the detailed hydrodynamic conditions on such fouling phenomenon.

Another important feature of this membrane is that there was no evidence of drastic damage to the polysulphone interlayer. The Dow/Filmtec literature implies that the interlayer backing material is the same (polysulphone) in both SW 30 and BW 30 “polyamide” membranes. It has been argued in the previous section that the damage to the polysulphone interlayer in SW 30 membranes is of a physical rather than chemical nature. It may therefore be postulated that the polysulphone interlayer in the BW 30 membrane is of a different physical structure (which is apparently more resistant to hydrocarbons) than on SW 30. This difference in design may be due to the fact that the BW 30 does not need to perform under the same higher pressures as the SW 30 membranes.

9.3 CTA

Results from the experiments on CTA membranes are summarised in Figures 9-5 to 9-10. There was wide scatter in the results- even in the control experiments; this scatter was much greater for water flux than for change in percentage salt passage. Despite this scatter, in fact there were some systematic trends in the change in percentage salt passage in that, a small overall increase in percentage salt passage can be seen particularly when the membrane was exposed to diesel; rather less evident after exposure to hexane.

The CTA membrane was examined under a light microscope and no major change could be observed between clean samples and those exposed to the hydrocarbon fluids. Use of the SEM proved inconclusive as the electron beam from the microscope altered the surface of the membrane.

Overall this CTA membrane is very resistant to fouling by hydrocarbon; even changing parameters like stirring during the membrane fouling did not have a profound effect on the results. It was also seen that the results remained the same when only the active surface was subjected to fouling. This indicates that the backing material of the membrane, which is the same chemically, is not affected by hydrocarbon fouling either.

From this study it can be deduced that the cellulose triacetate membrane is more resistant to the effects of the exposure to hydrocarbon.

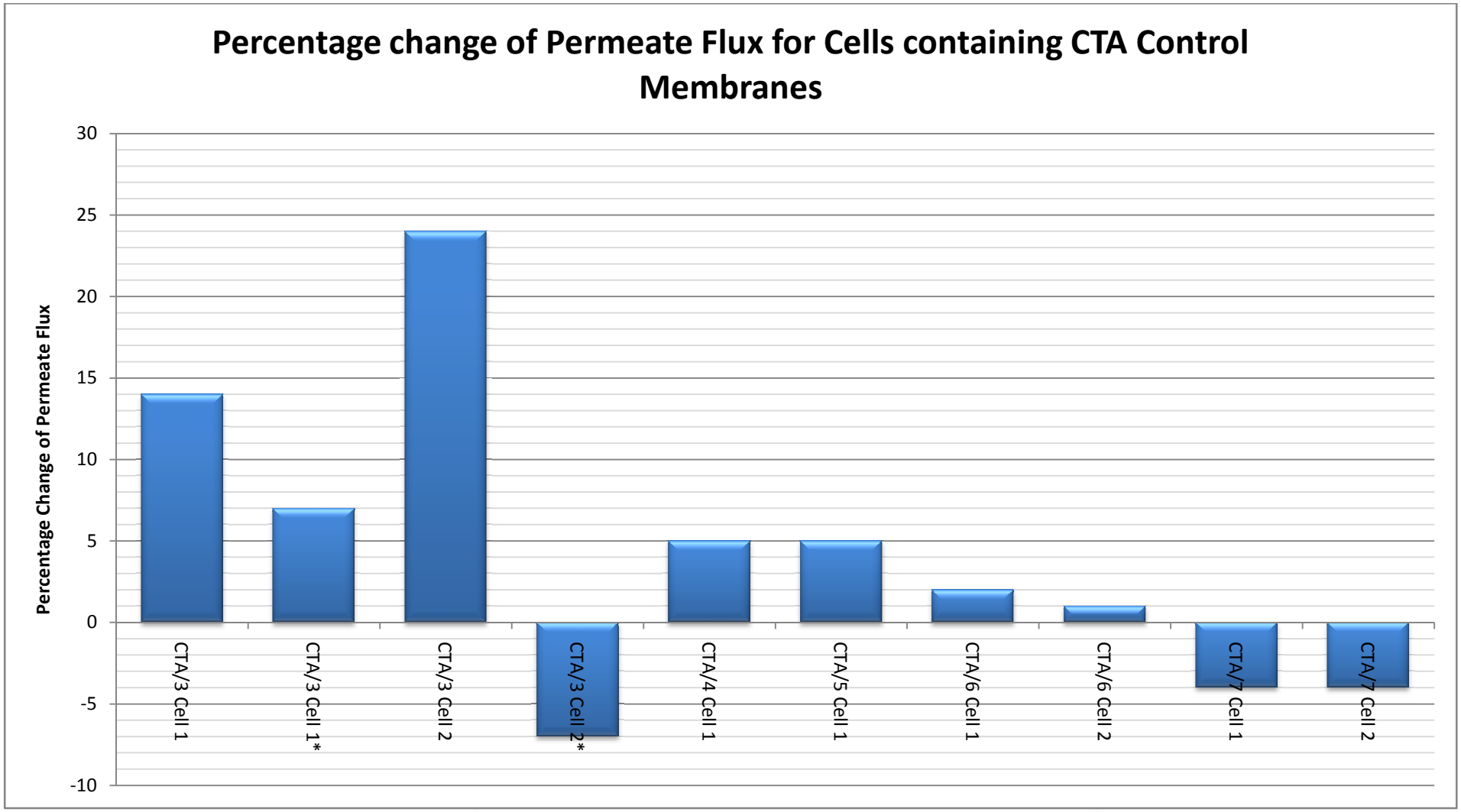

Figure 9-5 Percentage change of Permeate Flux for Cells containing CTA Control Membranes

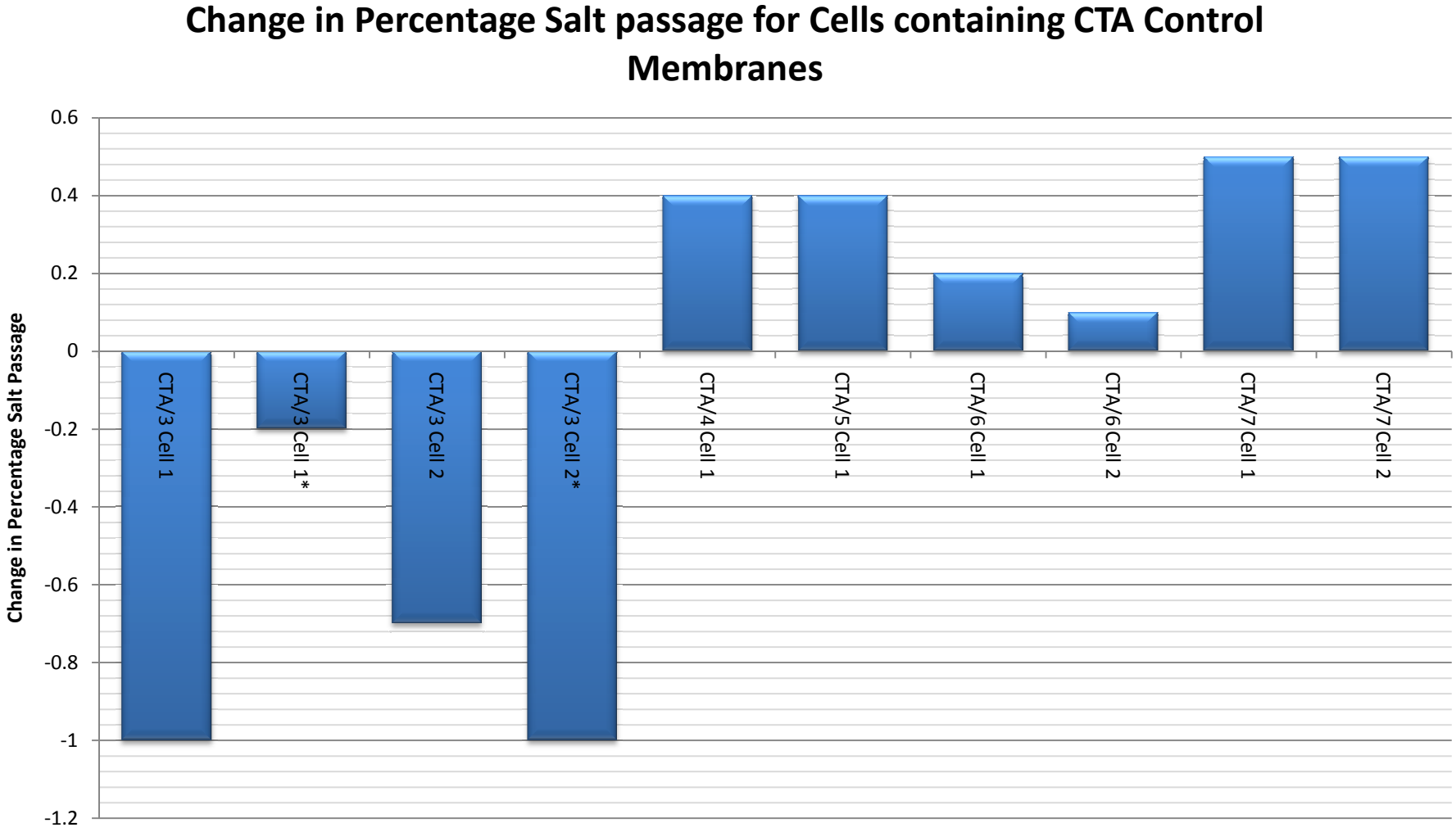

Figure 9-6 Change in Percentage Salt passage for Cells containing CTA Control Membranes

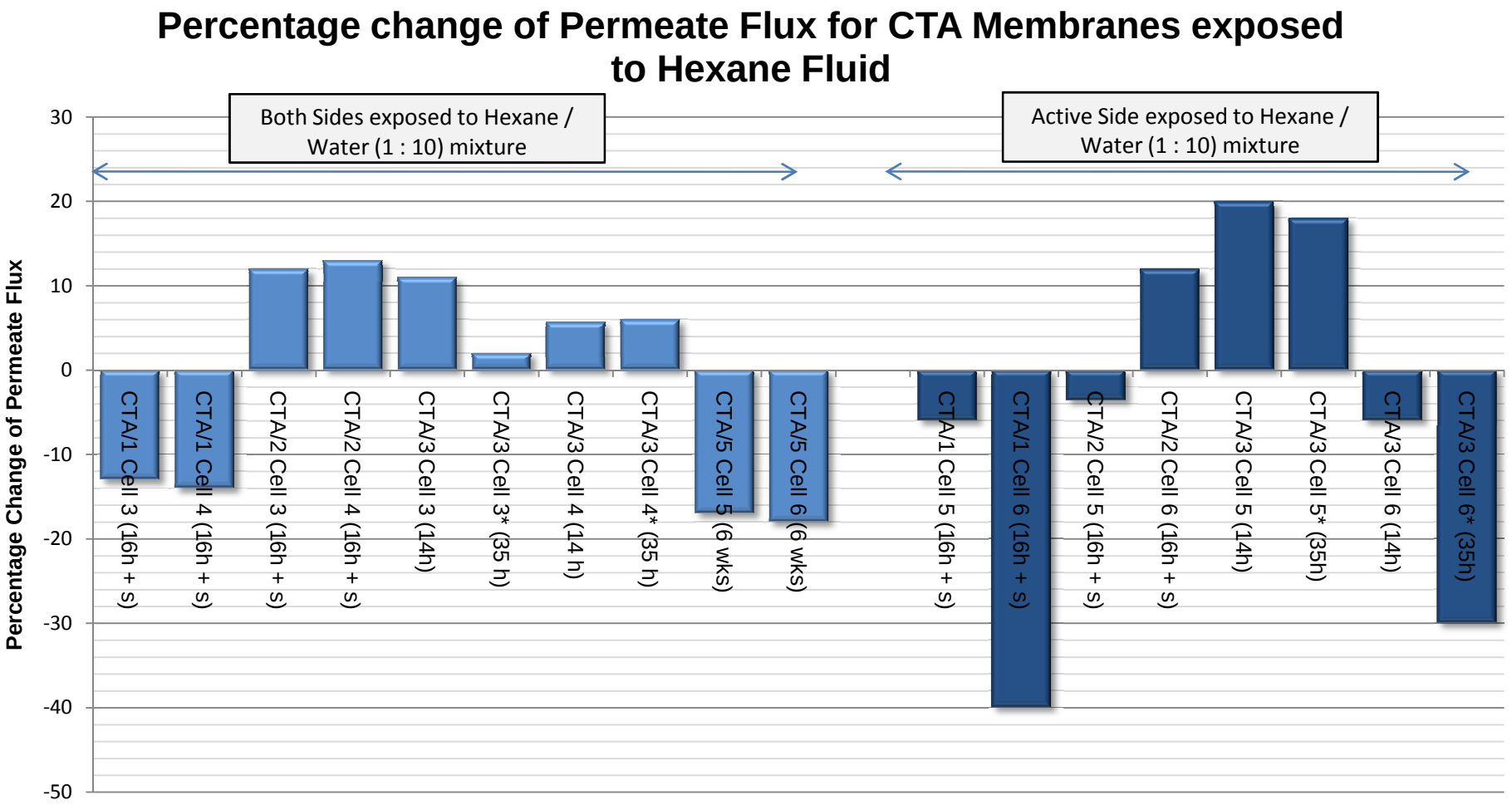

Figure 9-7 Percentage change of Permeate Flux for CTA Membranes exposed to Hexane Fluid

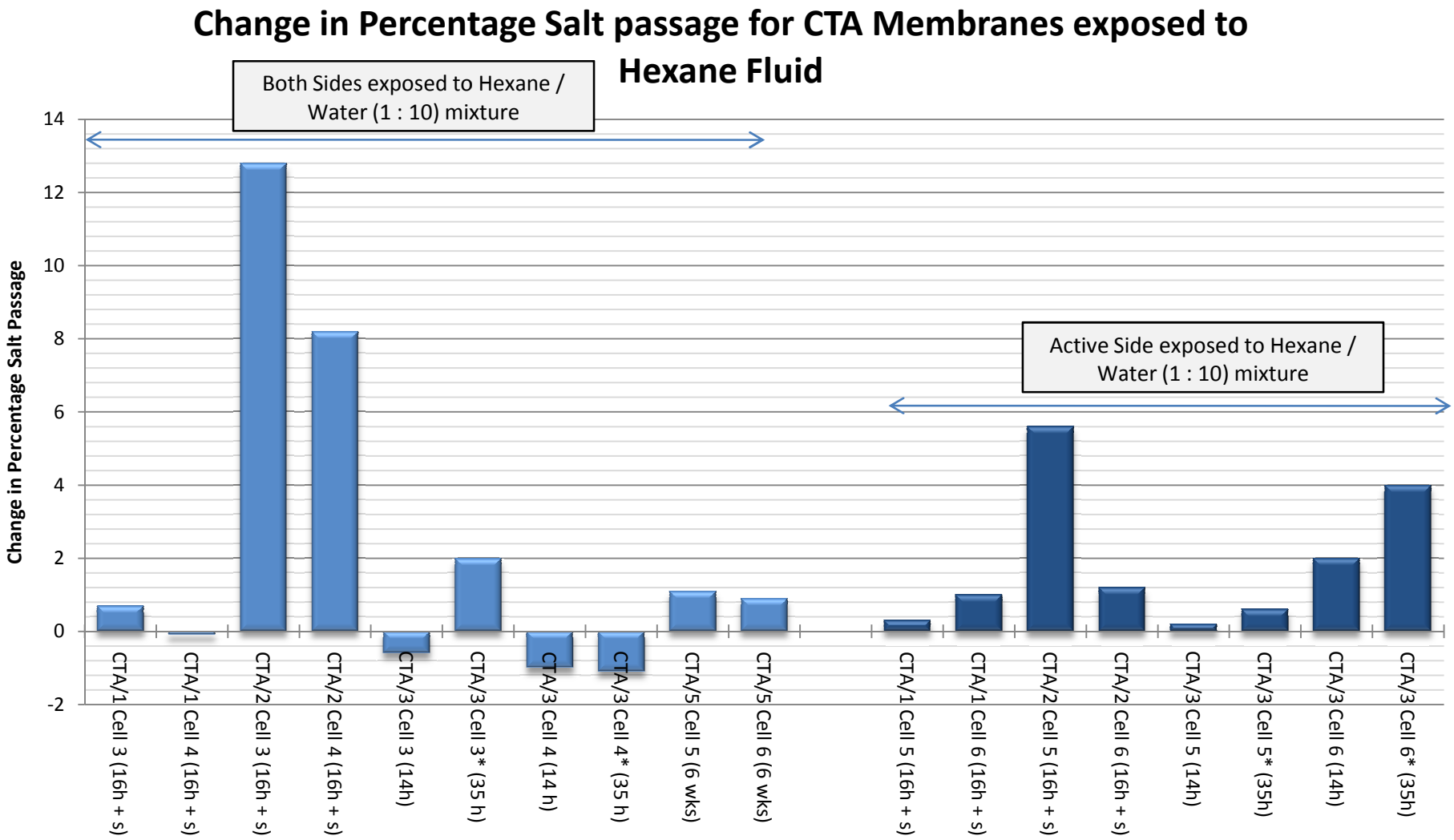

Figure 9-8 Change in Percentage Salt passage for CTA Membranes exposed to Hexane Fluid

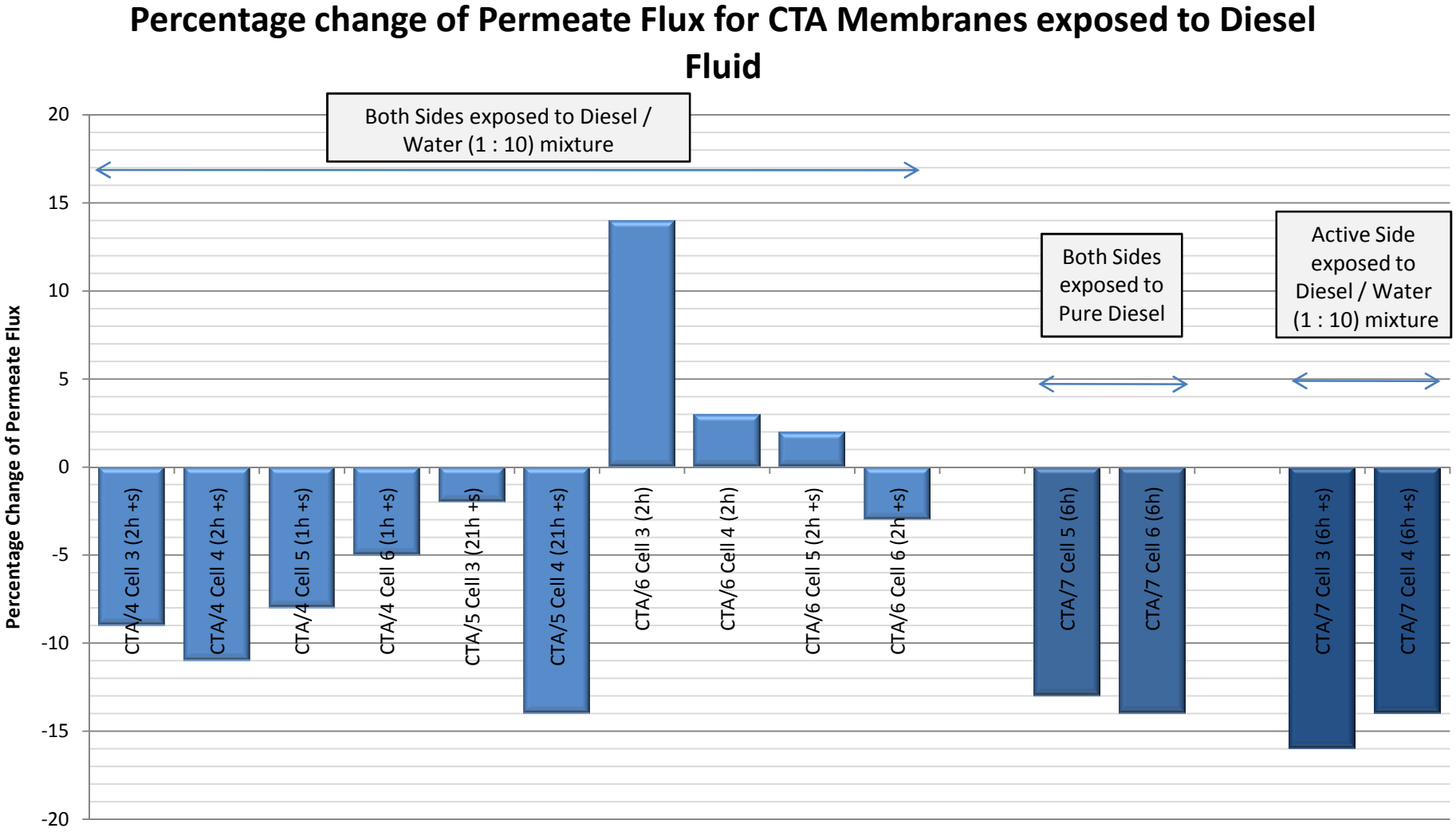

Figure 9-9 Percentage change of Permeate Flux for CTA Membranes exposed to Diesel Fluid

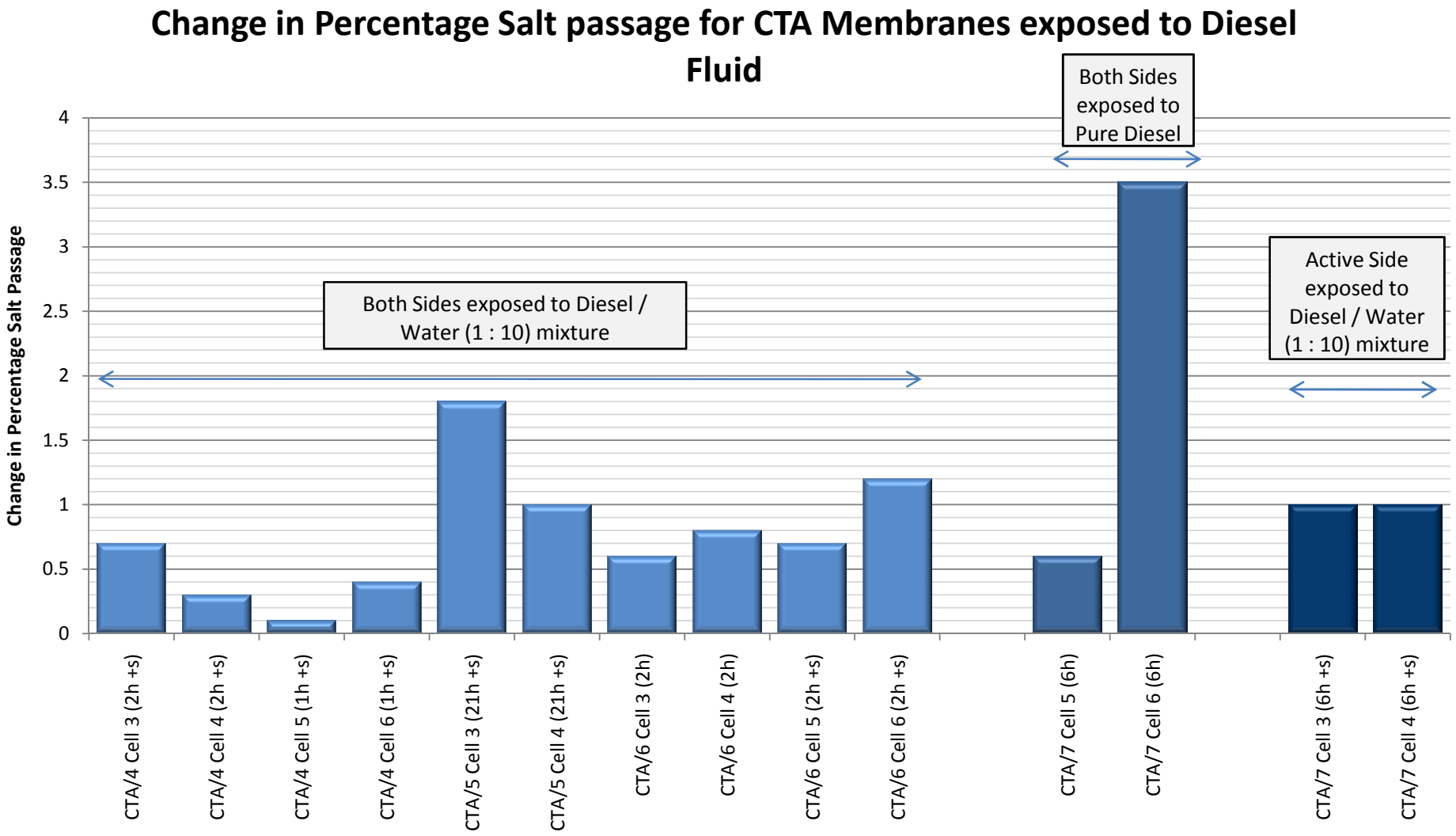

Figure 9-10 Change in Percentage Salt passage for CTA Membranes exposed to Diesel Fluid

CHAPTER 10 CONCLUSIONS

- The SW 30 polyamide membrane is particularly sensitive to exposure to hexane and diesel. Diesel is a more aggressive foulant as the damage happened faster. It was also observed that the failure of the membrane happened in the pure hydrocarbon.
  - The most harm was done to the polysulphone interlayer; it was observed microscopically that the pores of the above mentioned layer were fused together causing a complete blockage of the membrane.
  - The active polyamide layer of the SW 30 membrane was not as susceptible and prolonged exposure caused a relatively small increase in water flux and salt passage.
  - An aqueous solution of hexane in water was not found to be significantly damaging to the SW 30 membrane.

- The BW 30 polyamide membrane was more robust than the SW 30 membrane. The polysulphone interlayer did not fail when it was exposed to the water / hexane emulsion; a small increase in the percentage salt passage and a larger increase in permeated flux were observed.

- The cellulose triacetate membrane has shown the most resilience to hydrocarbon fouling, when exposed to both hexane and diesel contaminated brackish water. Furthermore, even when treated with the hydrocarbon in the pure state, the fall in performance of the membrane has been relatively small. The effects on percentage salt passage were about the same for all the fouling regimes i.e. an increase by an

average of 1.3 % throughout. The most damage, in terms of reduction of the permeate flux was seen when the membrane was exposed to the aqueous phase of hexane for a long period of time, an exposure of 6 weeks leading to a 17% reduction in flux. This leads to the conclusion that the fall in CTA membrane performance will be felt on the flux and prolonged exposure to dissolved hydrocarbons in the feed water may result in a significant reduction in performance of the plant.

10.1 Suggestions for Further Work

1.) The rig that was used to conduct the experiments can be modified to find out more about the effect of fouling on the membranes. This can be achieved by directly pumping contaminated feed water to the desalination cells. This will need the addition of two more cells. They can be added in parallel to cells 5 and 6. The hydrocarbons fluid can then be constantly injected in the feed stream at point A in Figure 10-1 making sure that the exact proportion of hydrocarbon coming in contact with the membrane can be recorded; this would also ensure that there is no loss of hydrocarbon by evaporation. The performance of the membrane can then be monitored for a number of hours. For this to be practical the flowrate of the feed must be much lower than that of the rest of the cells. This can be achieved by using smaller tubes and smaller cells. This is because the rejected feed cannot be re-circulated as it would contaminate the rest of the rig as it will be almost impossible to completely remove all the hydrocarbon that might be still present. Furthermore as this experiment will take a long time, a much larger holding tank for that feed will be required. This method of contamination will give a more precise indication as to how long it would take for observable, if any, effects to start taking place.

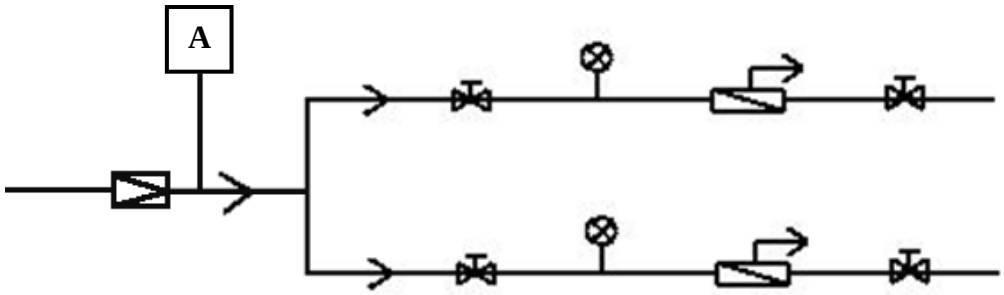

Figure 10-1 Additional branch for the rig.

This part of the rig setup will be separate from the rest making sure that there is no accidental contamination of the rest of the rig and remove the need for cleaning the whole rig before a new run.

2.) Further investigation of the different fouling behaviour of BW 30 and SW 30 polysulphone backing material can be undertaken with the help of microscopy.
This can be achieved by developing an easier method of examining the different layers of the membrane using the scanning electron microscope (SEM).
Atomic force microscopy (AFM) can also be employed to improve the understanding of the surface characteristic of the membrane before and after it has been exposed to the hydrocarbons.

3.) An oil pollution incident might lead to the seawater containing dissolved hydrocarbons for a prolonged period after the “clean-up” of the major contamination. Thus experiments to simulate the long-term (many weeks) exposure of the membranes to aqueous solution of hydrocarbon in seawater would be useful.

APPENDIX I

Graphs for experiments on SW 30 membranes

Experiment SW/2

Cells 1 & 2 no exposure to hydrocarbon (Control)

Cells 3 & 4 --> 24 hours exposure in a hexane / water mixture (1:10) with stirring and both sides of the membrane exposed. (i.e. replication of experiment 1)

Cells 5 & 6 --> 2 hours exposure in a Diesel / water mixture (1:10) with stirring and both sides of the membrane exposed.

Experiment SW/3

Cells 1 & 2 no exposure to hydrocarbon (Control)

Cells 5 & 6 --> 1 hour exposure to Pure Diesel without stirring and both sides of the membrane exposed.

Experiment SW/4

Cells 1 & 2 no exposure to hydrocarbon (Control)

Cells 3 & 4 --> 3 hours exposure to a hexane water mixture (1:10) with stirring both sides of the membrane exposed with stirring

Cells 5 & 6 --> 1 hour exposure to Pure hexane without stirring both sides of the membrane exposed.

EXP SW/2

Cells 1 & 2 no exposure to hydrocarbon (Control)

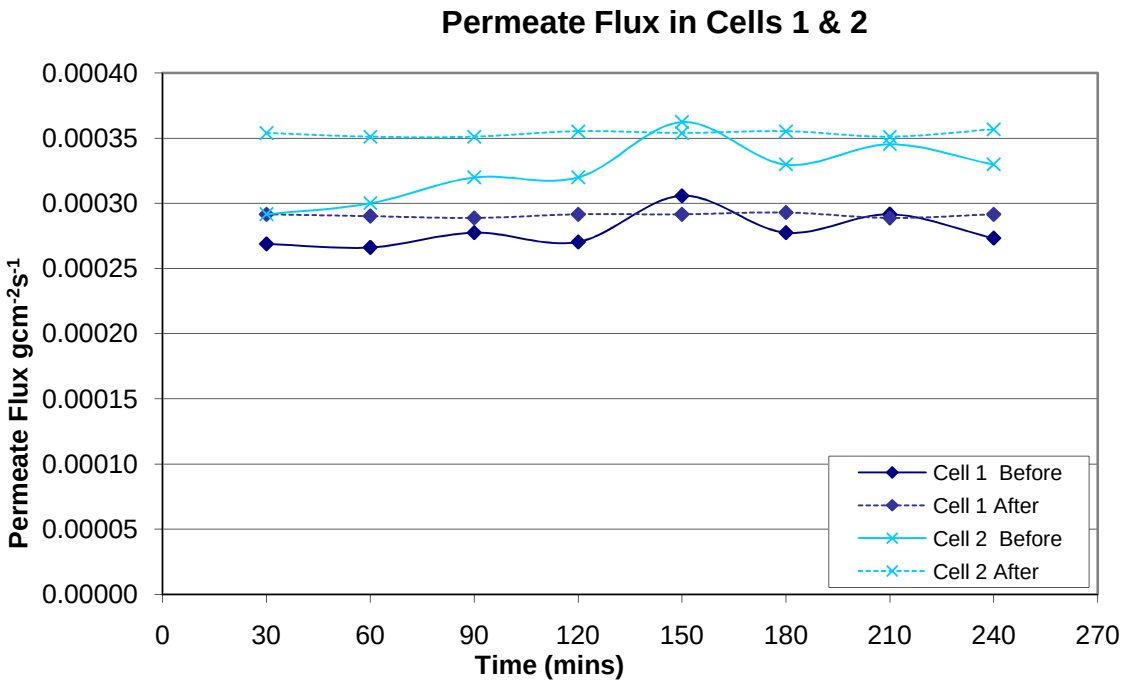

Figure I-1 Permeate Flux in Cells 1 & 2 of Exp. SW/2

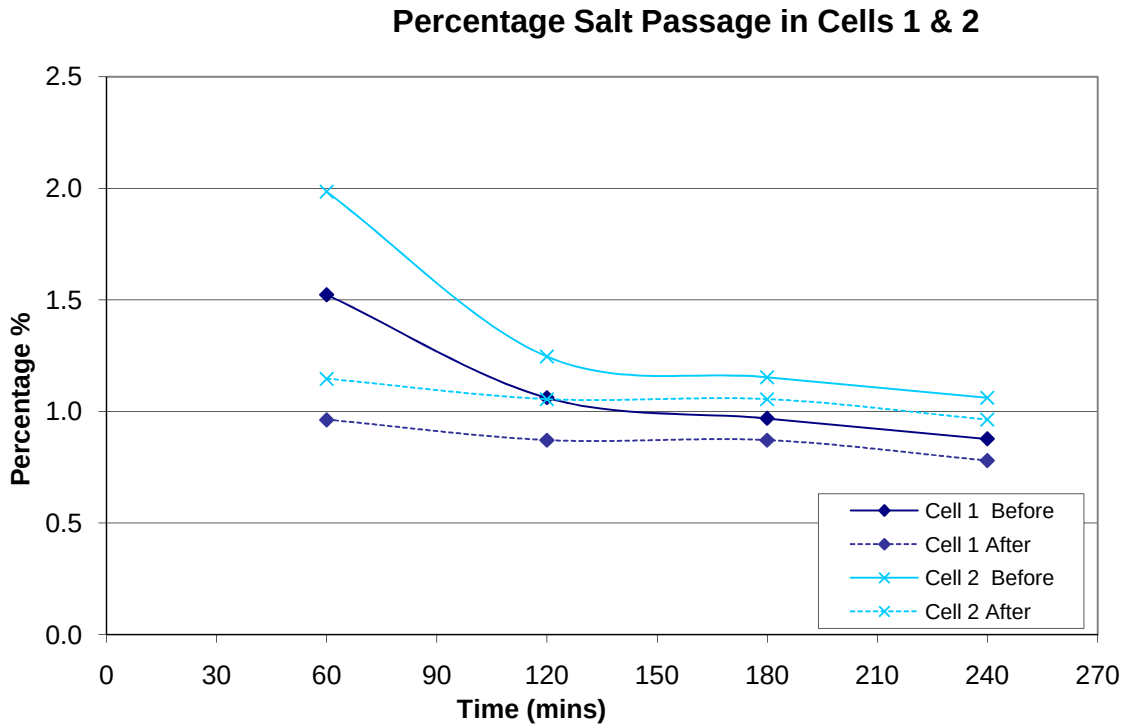

Figure I-2 Percentage Salt Passage in Cells 1 & 2 of Exp. SW/2

Cells 3 & 4 --> 24 hours exposure in a hexane / water mixture (1:10) with stirring and both sides of the membrane exposed. (i.e. replication of experiment 1)

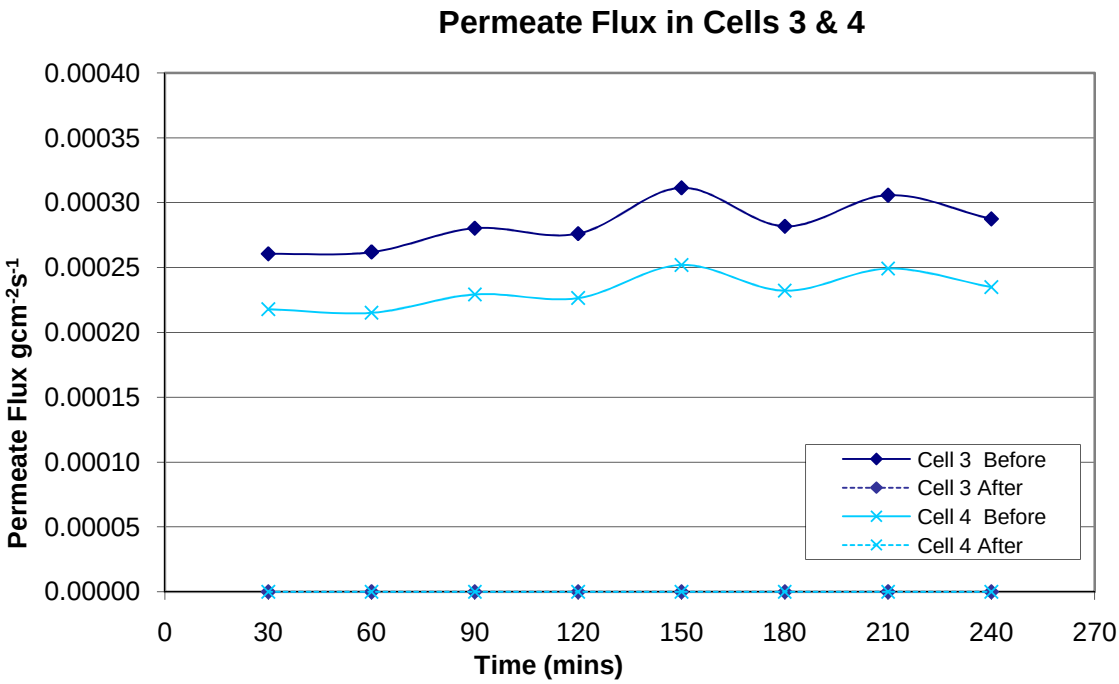

Figure I-3 Permeate Flux in Cells 3 & 4 of Exp. SW/2

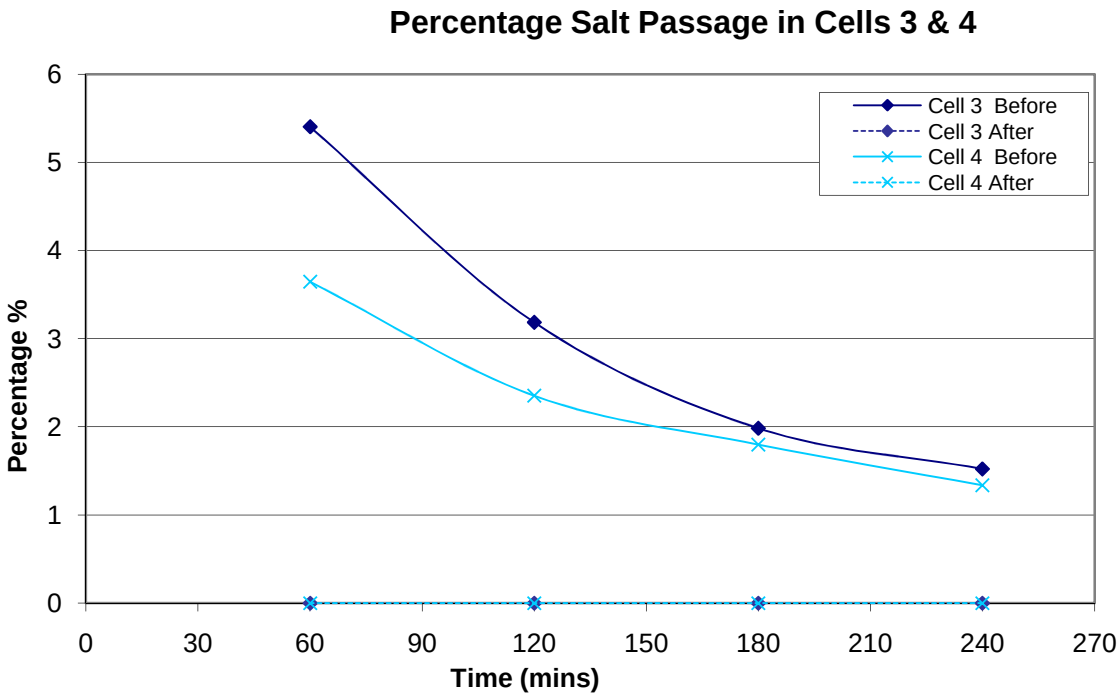

Figure I-4 Percentage Salt Passage in Cells 3 & 4 of Exp. SW/2

Cells 5 & 6 --> 2 hours exposure in a Diesel / water mixture (1:10) with stirring and both sides of the membrane exposed.

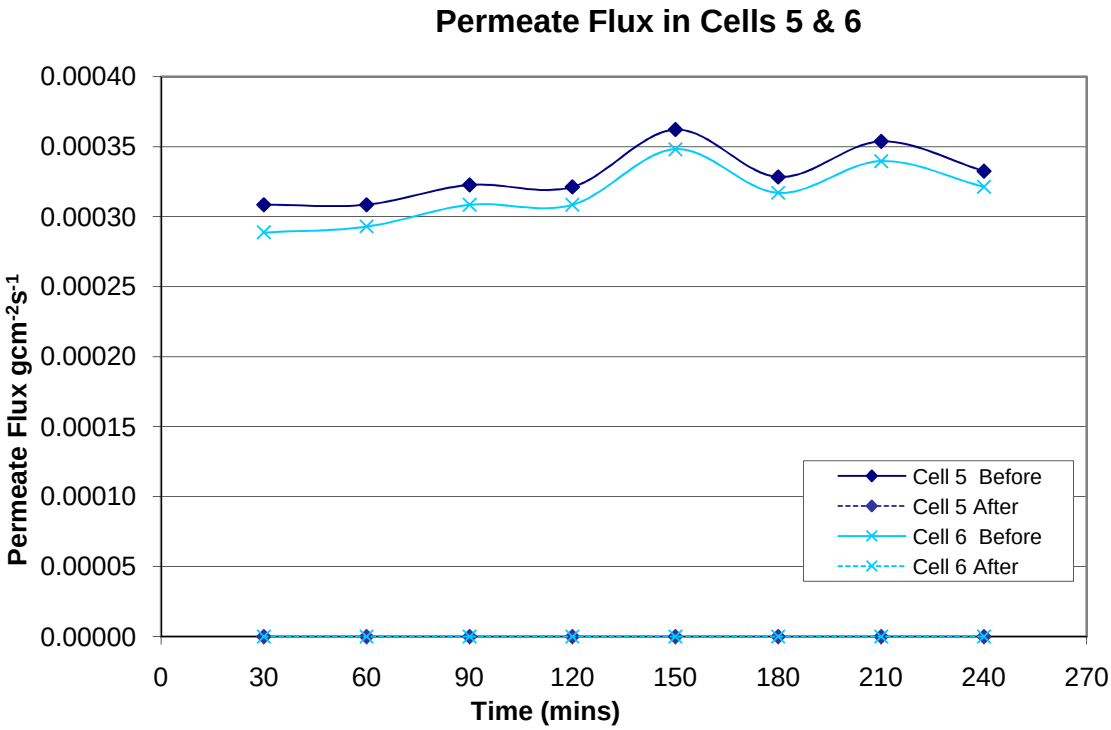

Figure I-5 Permeate Flux in Cells 5 & 6 of Exp. SW/2

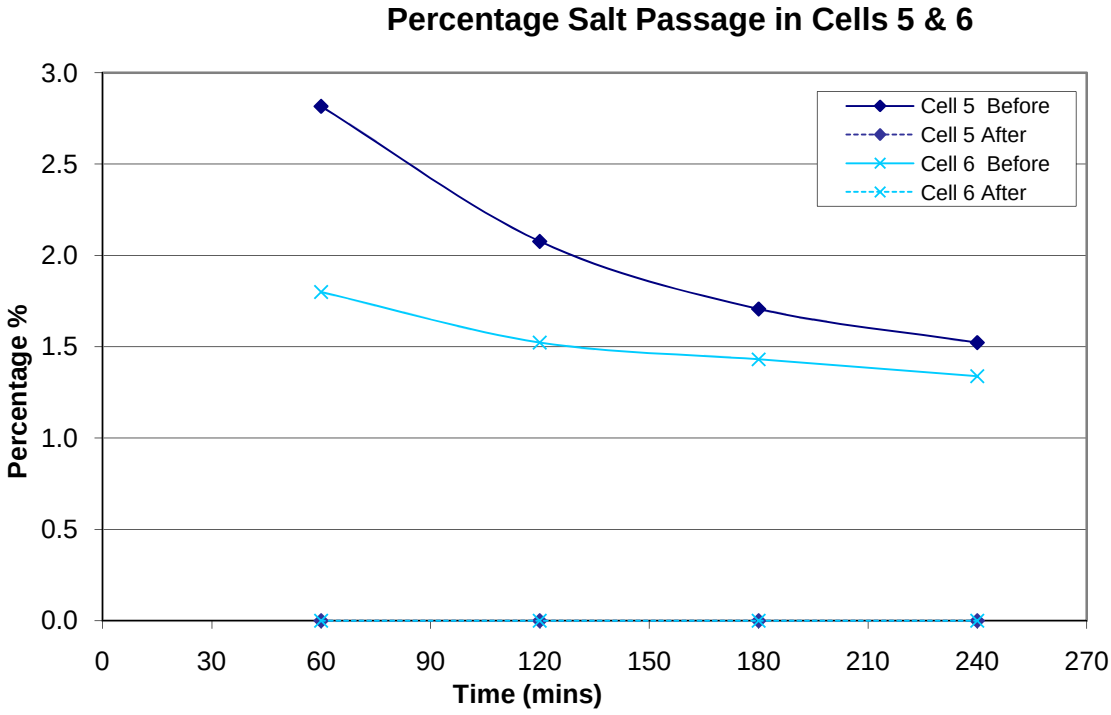

Figure I-6 Percentage Salt Passage in Cells 5 & 6 of Exp. SW/2

EXP SW/3

Cells 1 & 2 no exposure to hydrocarbon (Control)

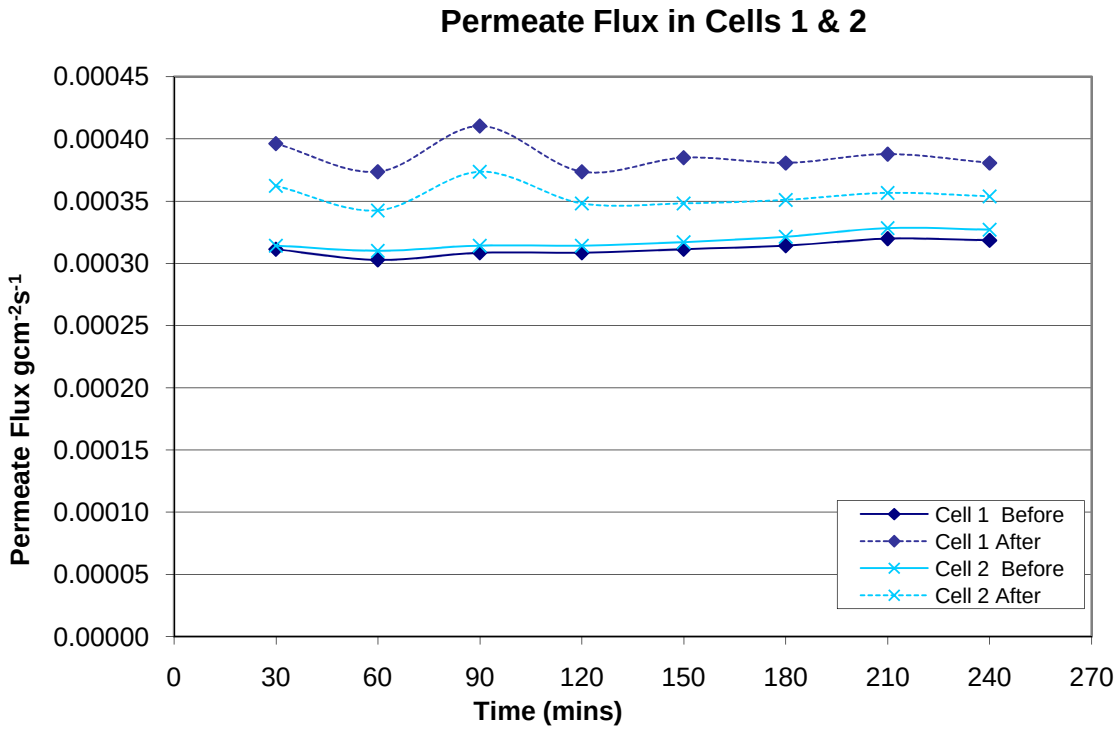

Figure I-7 Permeate Flux in Cells 1 & 2 of Exp. SW/3

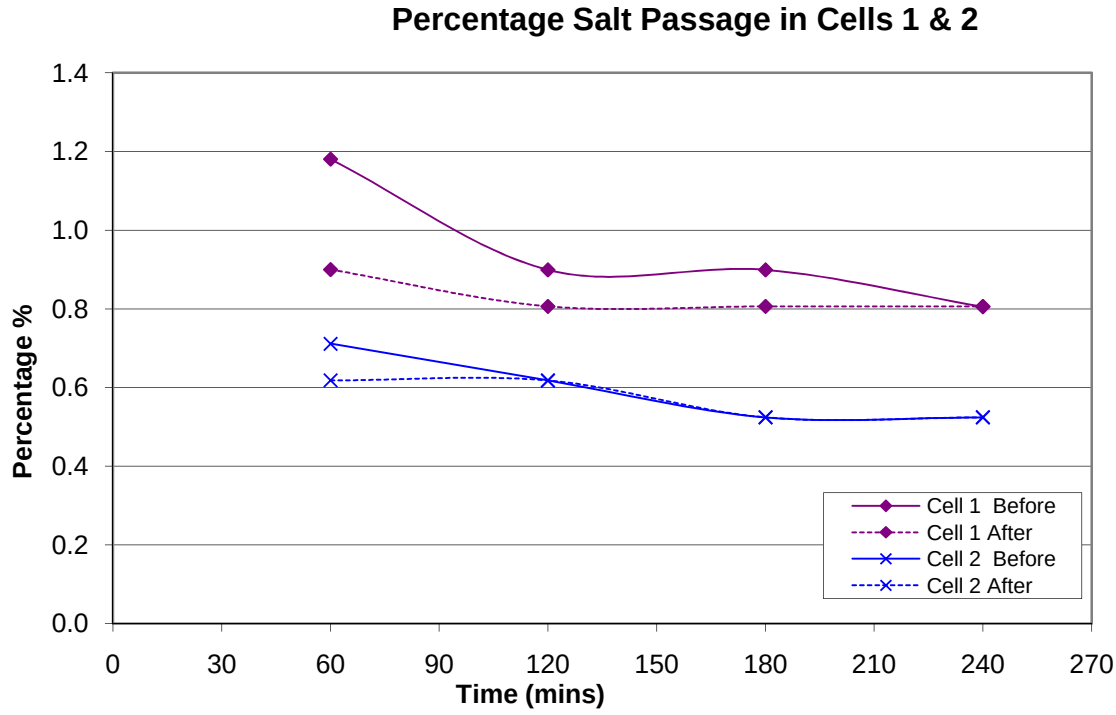

Figure I-8 Percentage Salt Passage in Cells 1 & 2 of Exp. SW/3

Cells 5 & 6 --> 1 hour exposure to Pure Diesel without stirring and both sides of the membrane exposed

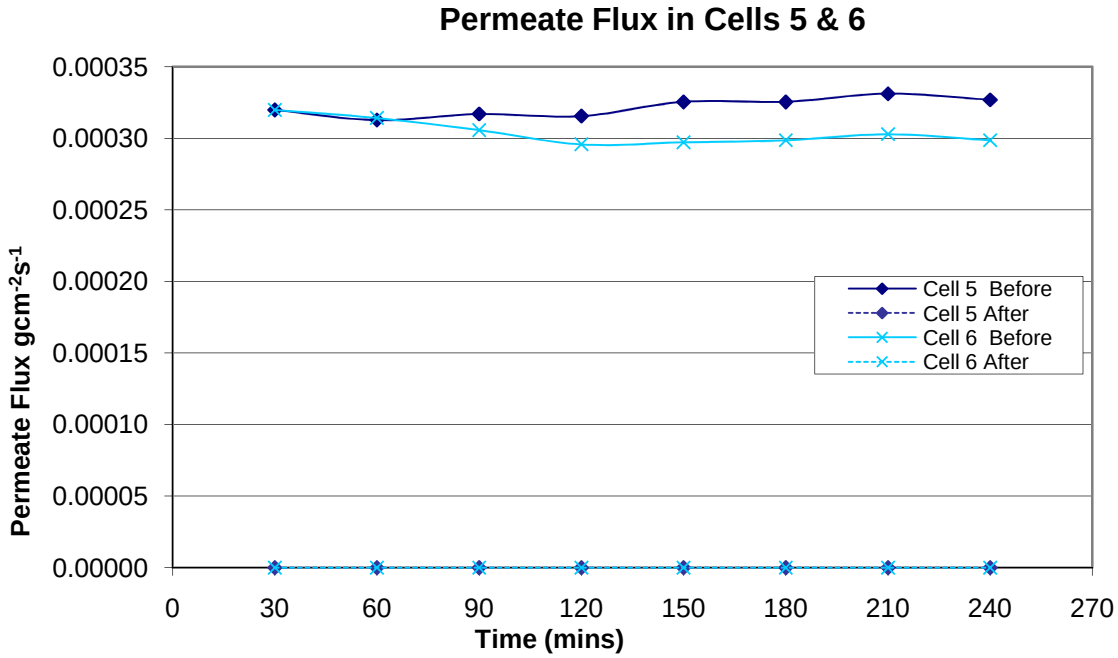

Figure I-9 Permeate Flux in Cells 5 & 6 of Exp. SW/3

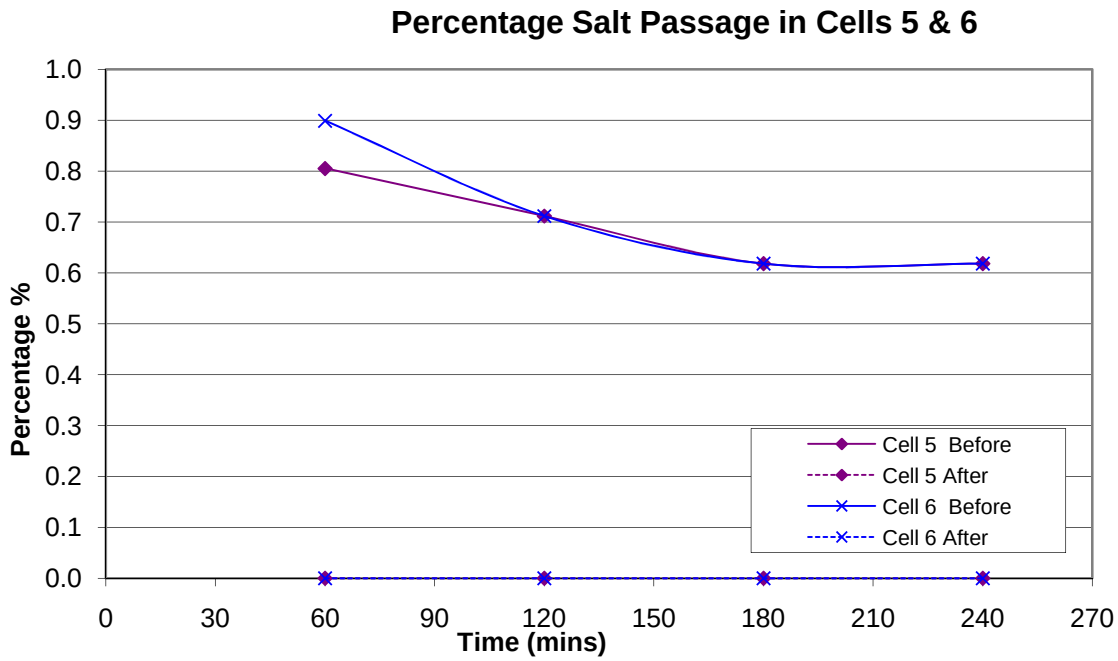

Figure I-10 Percentage Salt Passage in Cells 5 & 6 of Exp. SW/3

EXP SW/4

Cells 1 & 2 no exposure to hydrocarbon (Control)

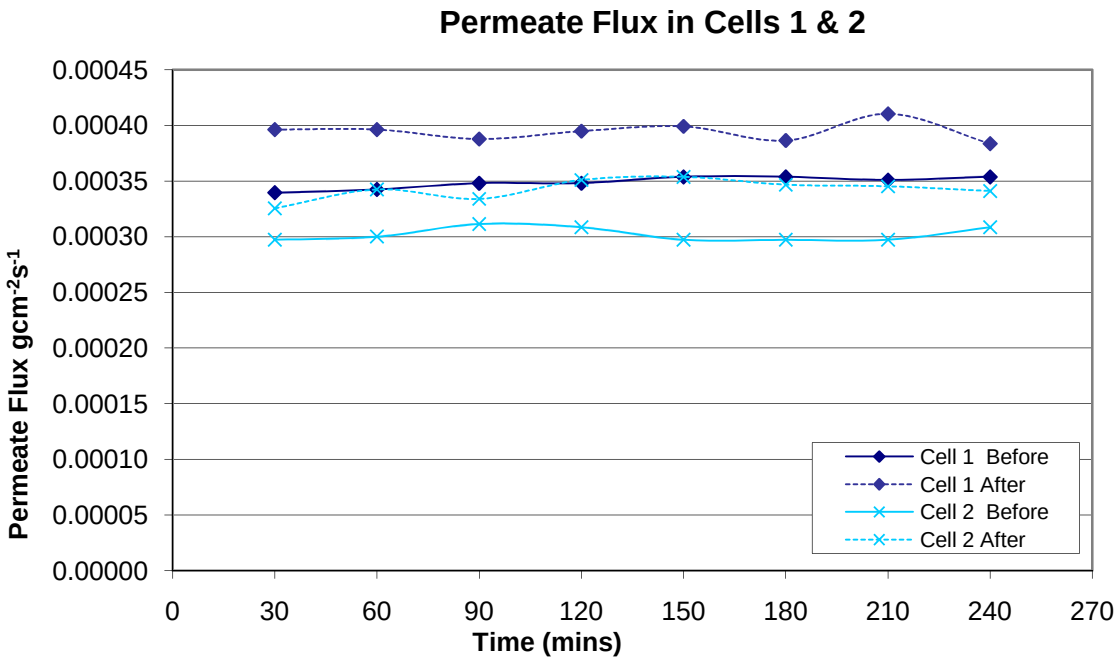

Figure I-11 Permeate Flux in Cells 1 & 2 of Exp. SW/4

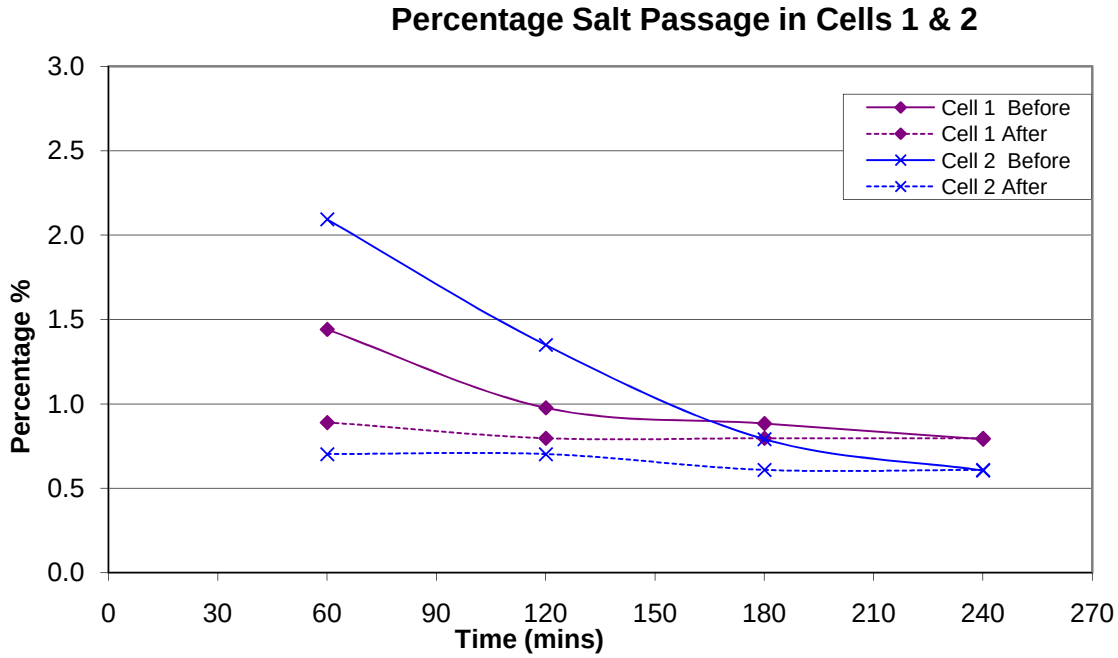

Figure I-12 Percentage Salt Passage in Cells 1 & 2 of Exp. SW/4

Cells 3 & 4 --> 3 hours exposure to a hexane water mixture (1:10) with stirring both sides of the membrane exposed with stirring

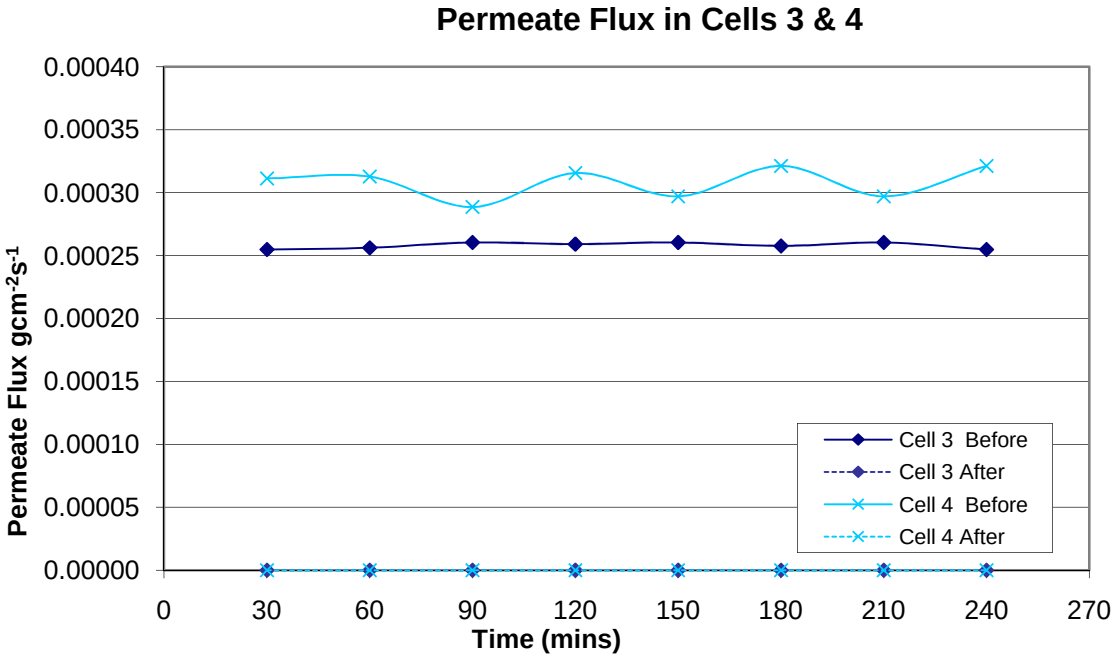

Figure I-13 Permeate Flux in Cells 3 & 4 of Exp. SW/4

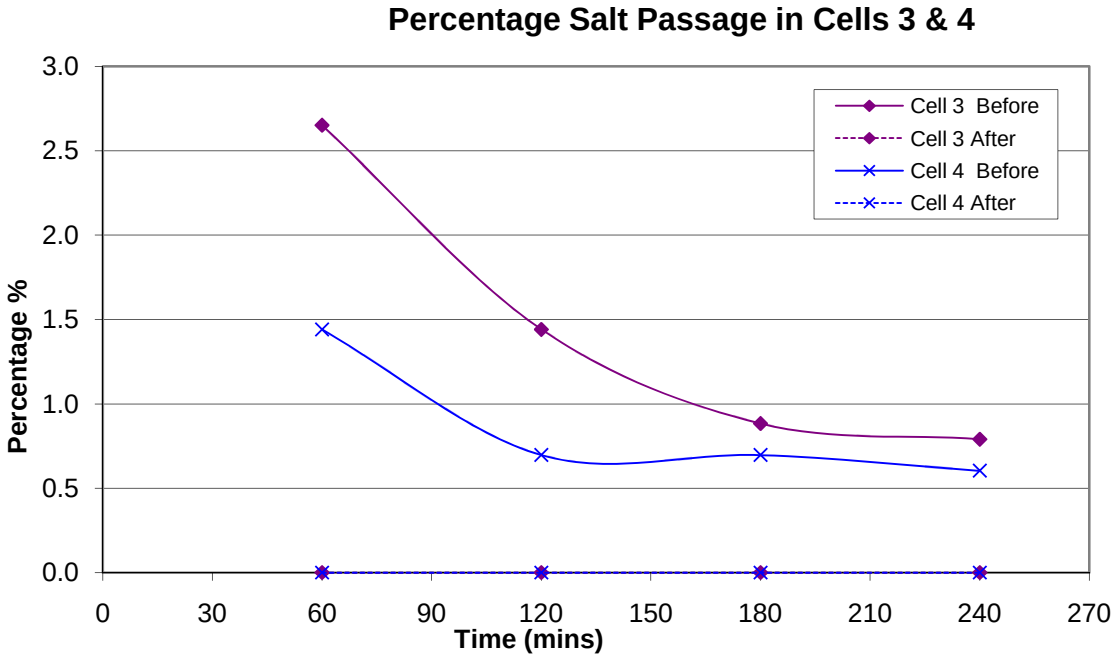

Figure I-14 Percentage Salt Passage in Cells 3 & 4 of Exp. SW/4

Cells 5 & 6 --> 1 hour exposure to Pure hexane without stirring both sides of the membrane exposed

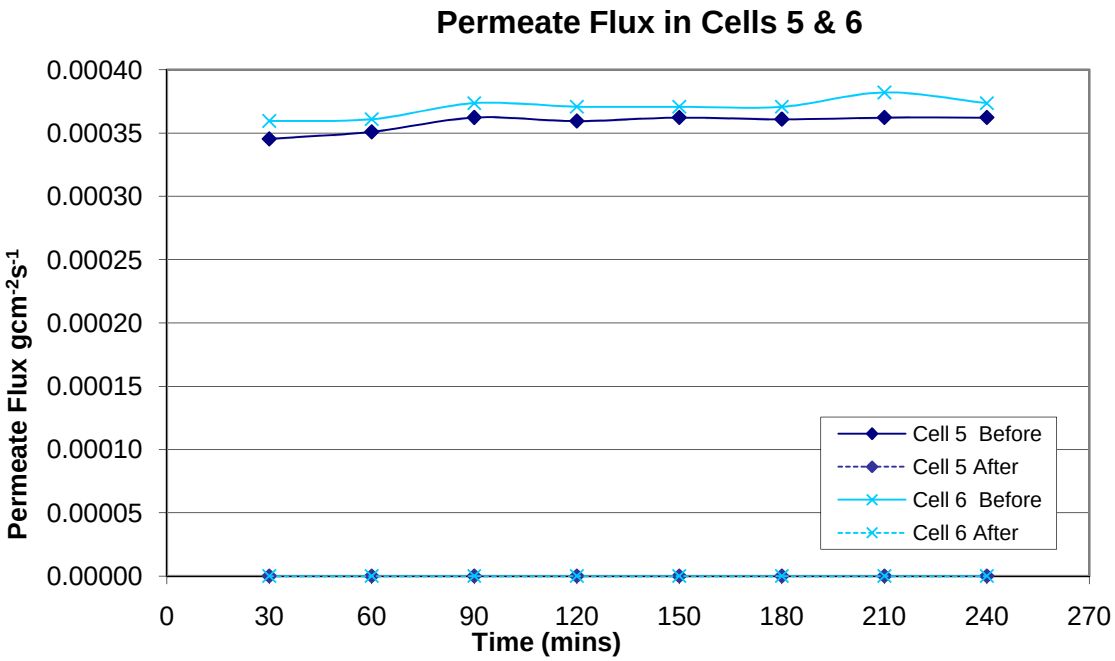

Figure I-15 Permeate Flux in Cells 5 & 6 of Exp. SW/4

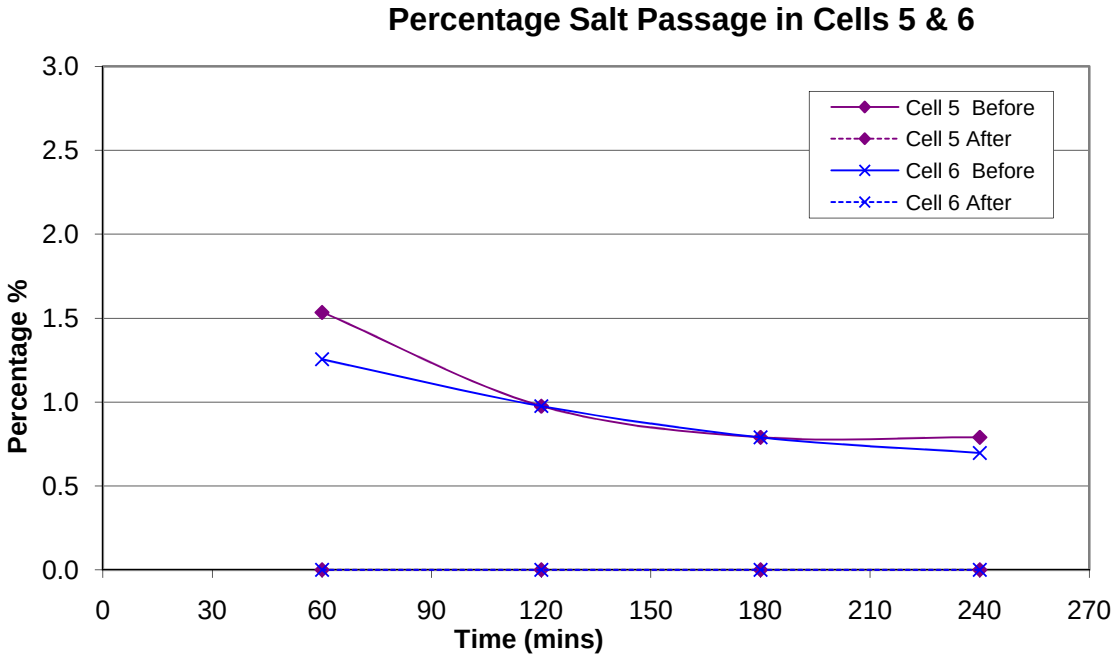

Figure I-16 Percentage Salt Passage in Cells 5 & 6 of Exp. SW/4

APPENDIX II

Graphs for experiments on BW 30 membranes

Experiment BW/3

In the next set of experiments all membranes were initially exposed for 14 hours

The membranes were divided as follows.

Cells 1 & 2 --> Dipped in a sample of tank solution

Cells 3 & 4 --> Kept in container with tank solution and hexane 10 : 1 proportion with stirring. Both sides of the membranes are being contaminated.

Cells 5 & 6 --> Kept in container with tank solution and hexane 10 : 1 proportion with stirring. Only the active sides of the membranes are being contaminated.

The membranes were dipped for a further 21 hours

The additional 21 hours of fouling was done to make the effects of fouling more visible.

Explanations of the Legend

Clean – Initial Run for Cell 2.
After –Run after Treatment
2nd XP – Run after additional 21 hours Treatment.

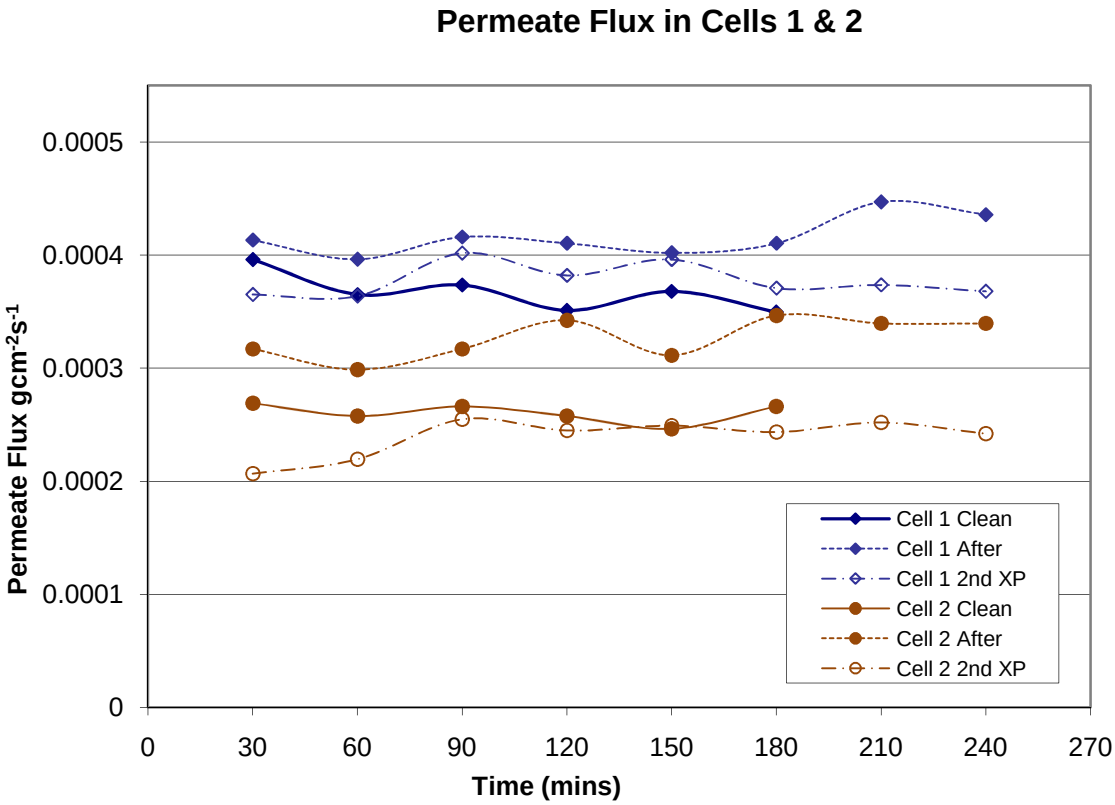

Figure II-1 Permeate Flux in Cells 1 & 2 of Exp. BW/3

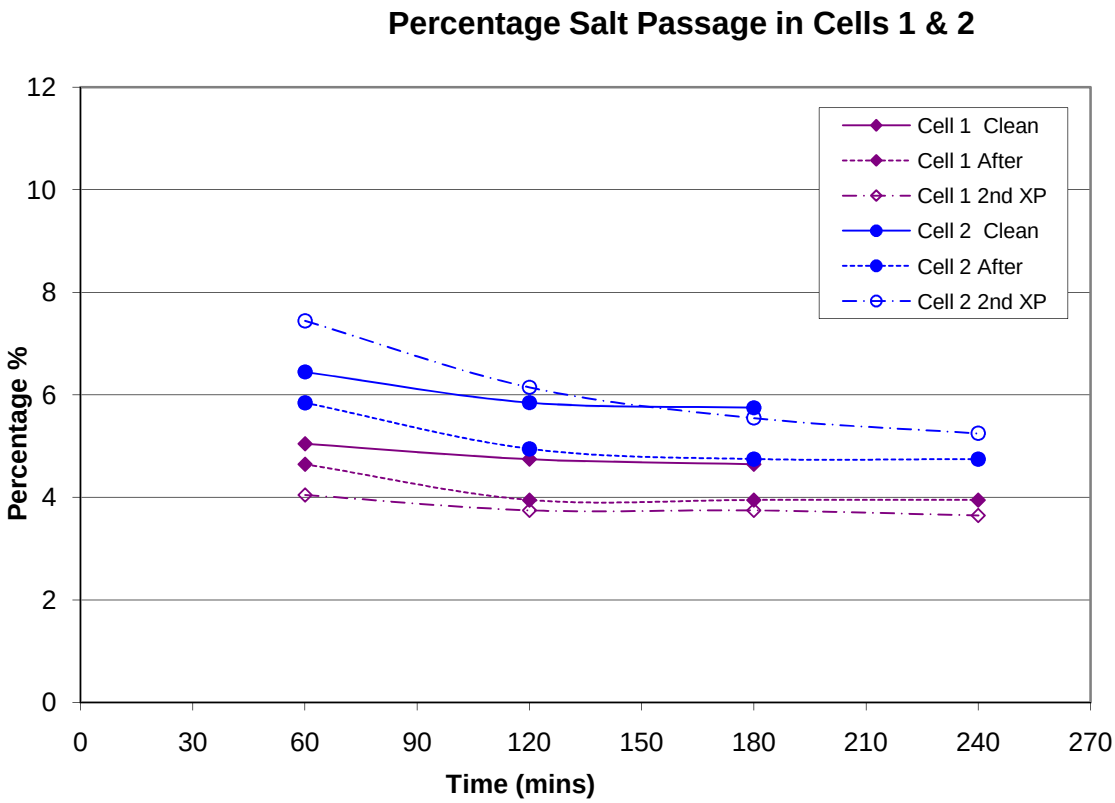

Figure II-2 Percentage Salt Passage in Cells 1 & 2 of Exp. BW/3

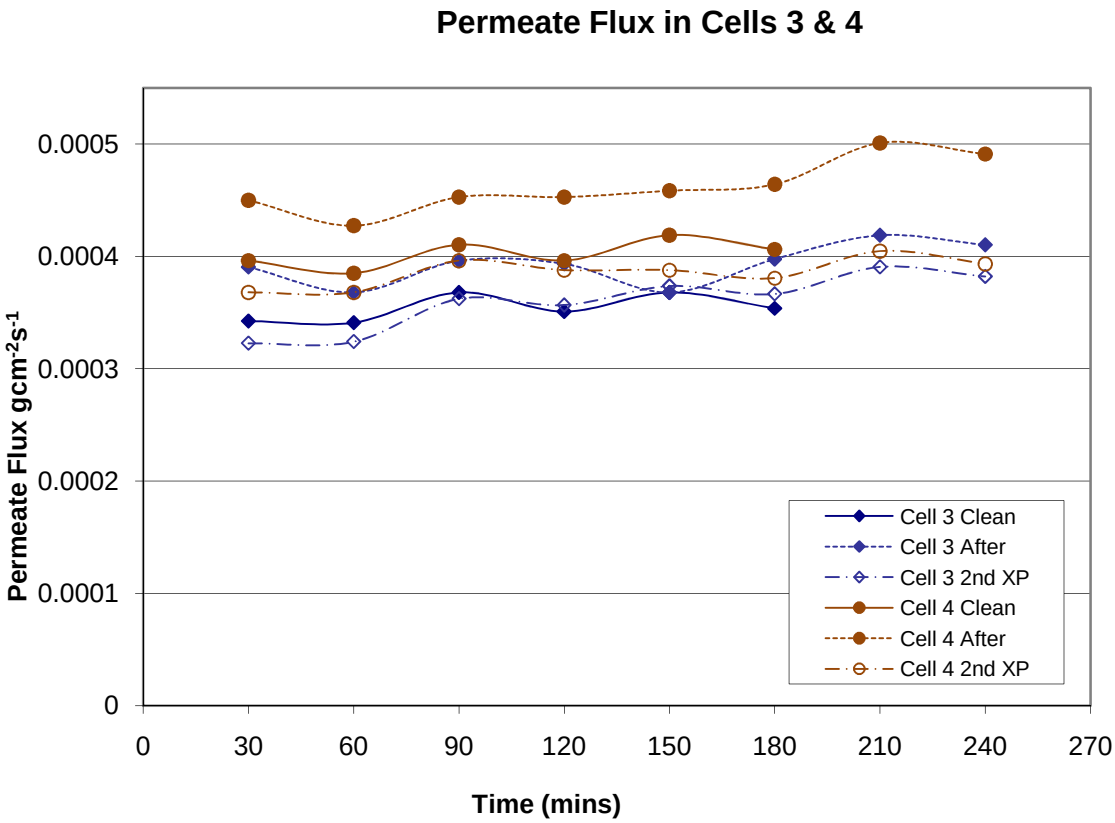

Figure II-3 Permeate Flux in Cells 3 & 4 of Exp. BW/3

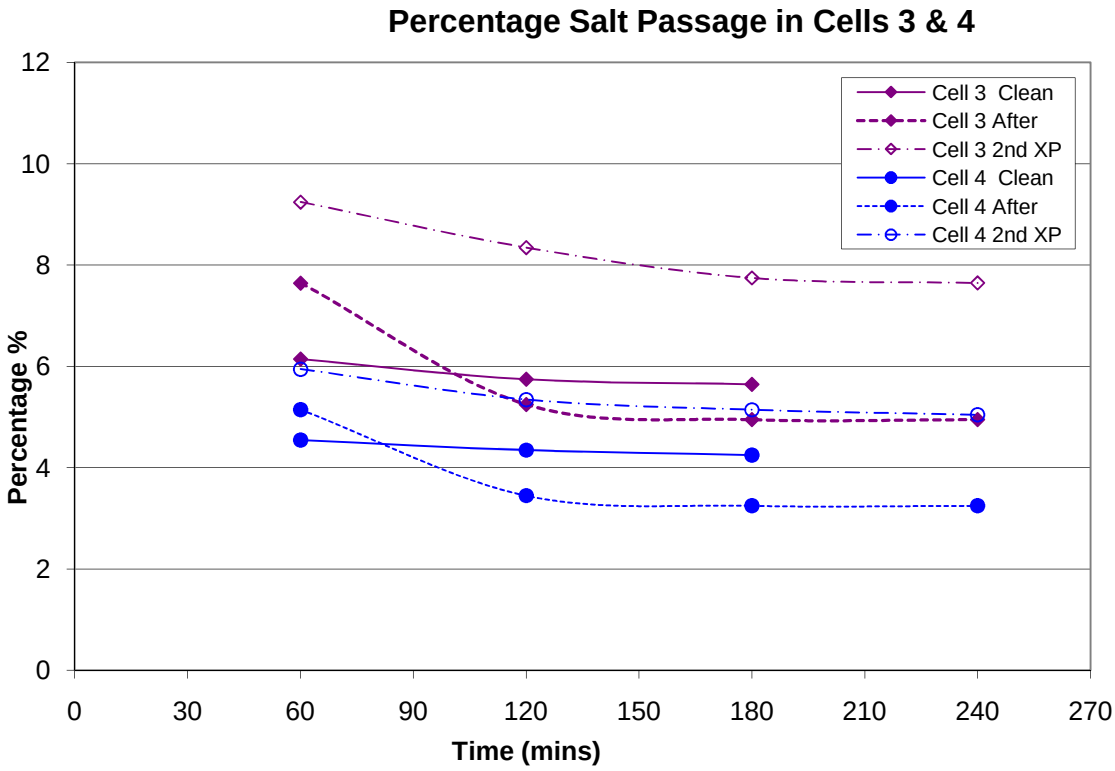

Figure II-4 Percentage Salt Passage in Cells 3 & 4 of Exp. BW/3

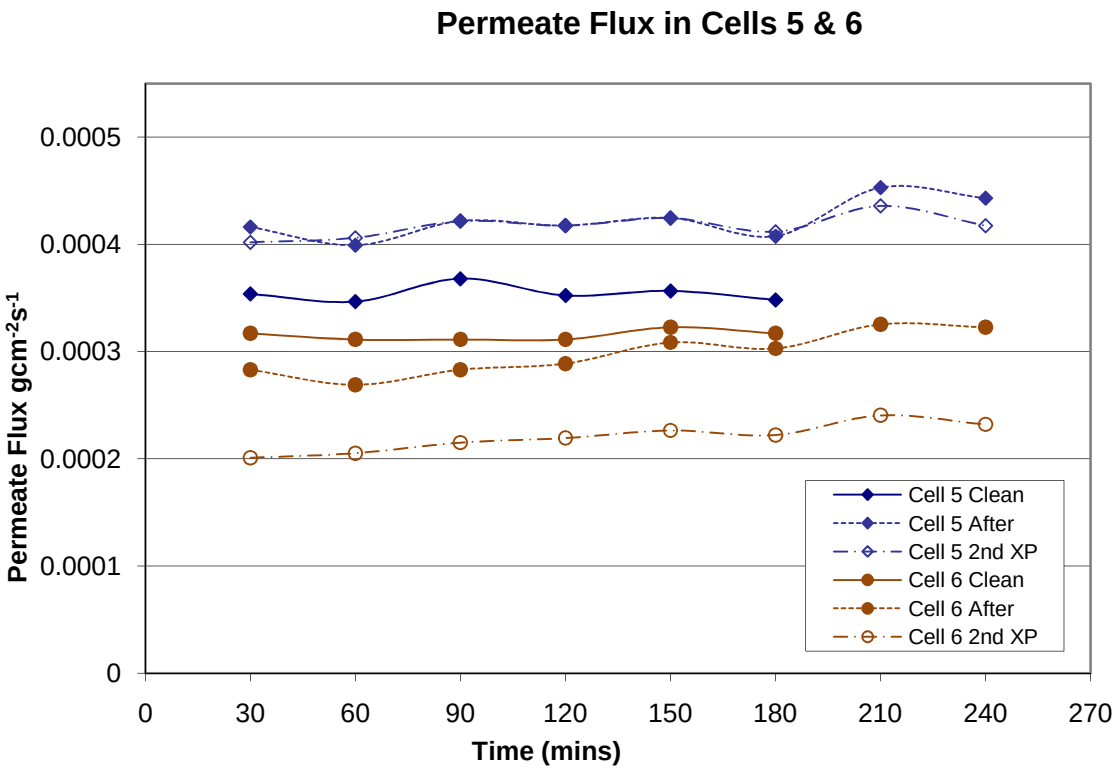

Figure II-5 Permeate Flux in Cells 5 & 6 of Exp. BW/3

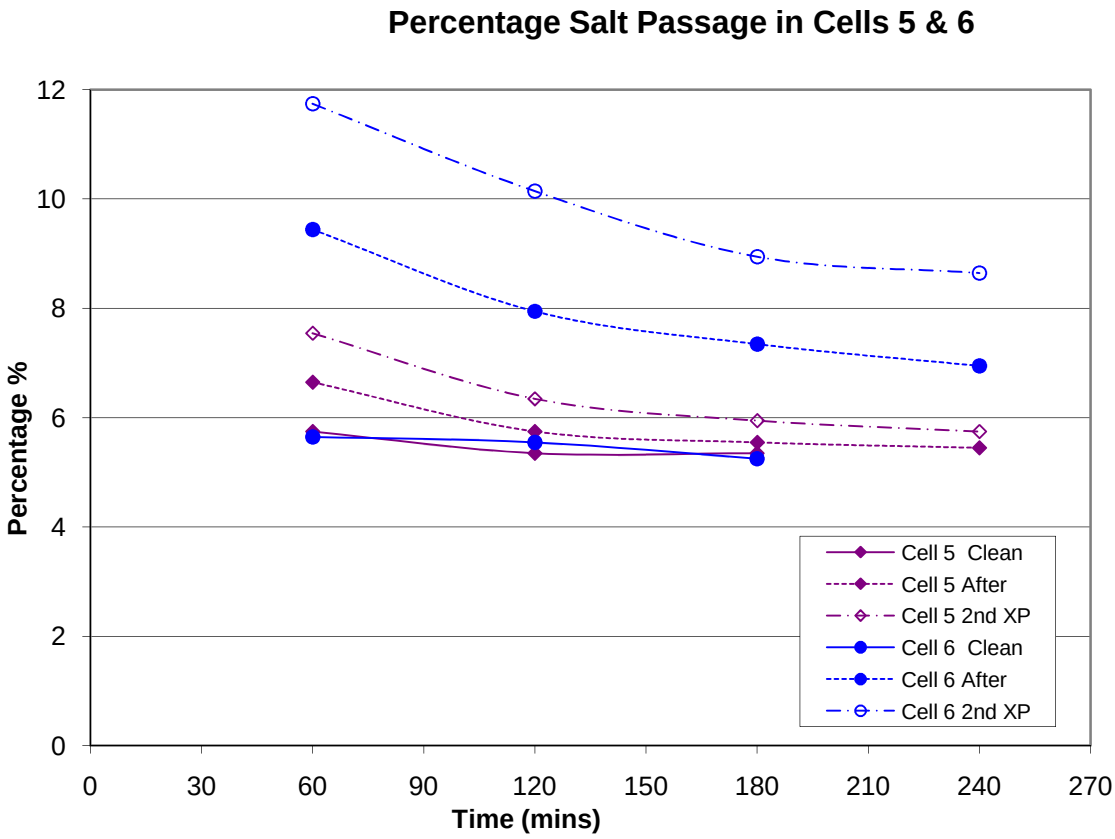

Figure II-6 Percentage Salt Passage in Cells 5 & 6 of Exp. BW/3

APPENDIX III

Graphs for experiments on CTA membranes

Experiment CTA/1

Cells 3&4 Both sides of the membrane were exposed to a 1:10 hexane / water mixture for 16 hours with stirring

Cells 5&6 The active side was exposed to a 1:10 hexane / water mixture for 16 hours with stirring.

Experiment CTA/2

Cells 3&4 Both sides of the membrane were exposed to a 1:10 hexane / water mixture for 16 hours with stirring

Cells 5&6 The active side was exposed to a 1:10 hexane / water mixture for 16 hours with stirring

Experiment CTA/3

Cells 1&2 Control

Cells 3&4 Both sides of the membrane were exposed to a 1:10 hexane / water mixture with stirring for a first interval of 14 hours then a further one of 21 hours

Cells 5&6 The active side was exposed to a 1:10 hexane / water mixture with stirring for a first interval of 14 hours then a further one of 21 hours.

Explanations of the Legend

Clean – Initial Run with clean membrane.

After – Run after Treatment.

2nd XP – Run after additional 21 hours Treatment.

Experiment CTA/4

Cell 1 Control

Cell 2 Empty

Cells 3&4 Both sides of the membrane were exposed to a 1:10 diesel / water mixture for 2 hours with stirring

Cells 5&6 Both sides of the membrane were exposed to a 1:10 diesel / water mixture for 1 hour with stirring.

Experiment CTA/5

Cell 1 Control

Cell 2 Empty

Cells 3&4 Both sides of the membrane were exposed to a 1:10 diesel / water mixture for 21 hours with stirring

Cells 5&6 The membranes were left in the aqueous phase of a 1:10 hexane / water solution for 6 weeks without stirring.

Experiment CTA/7

Cells 1&2 Control

Cells 3&4 Active surface of the membrane was exposed to a 1:10 diesel / water mixture for 6 hours with stirring

Cells 5&6 Both sides of the membrane were exposed to pure diesel for 6 hours with stirring.

EXP CTA/1

Cells 3-6

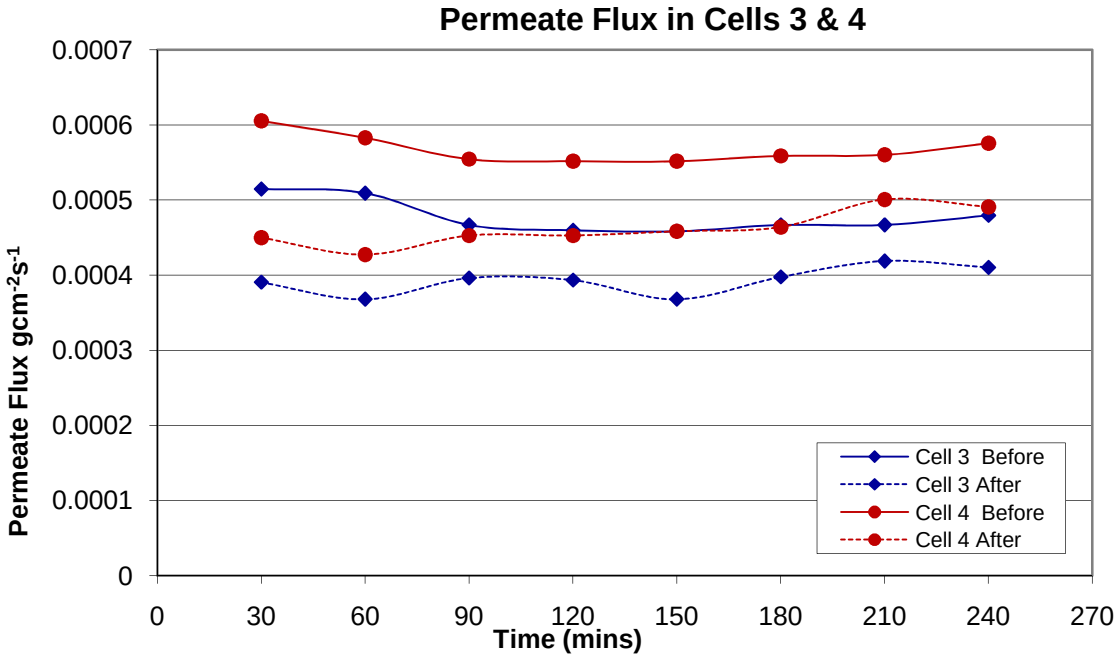

Figure III-1 Permeate Flux in Cells 3 & 4 of Exp. CTA/1

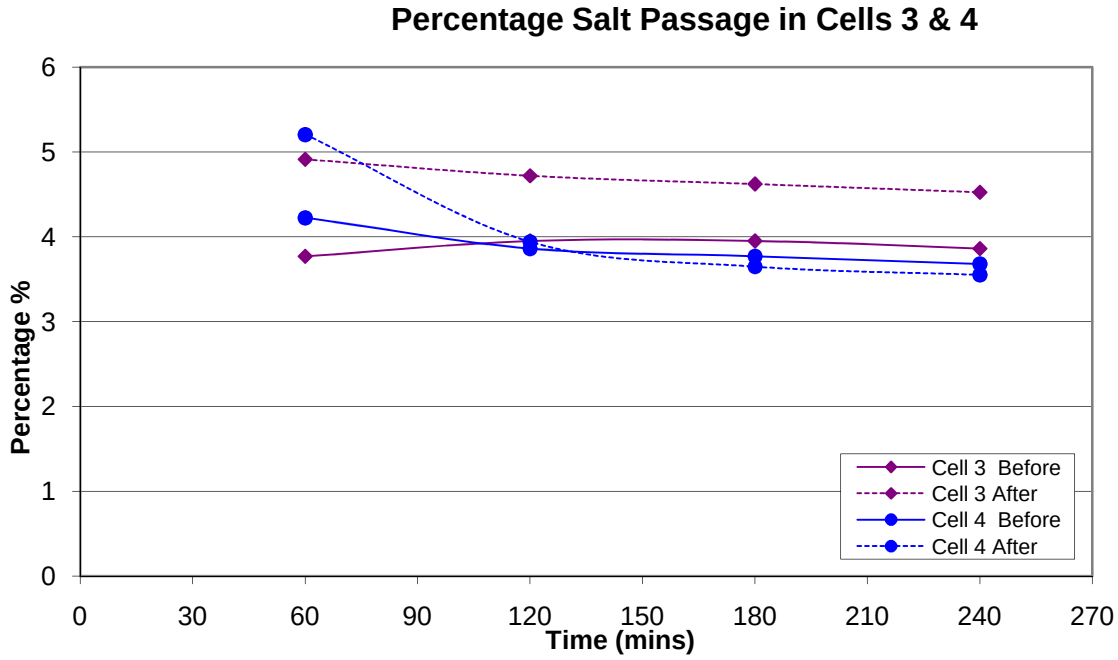

Figure III-2 Percentage Salt Passage in Cells 3 & 4 of Exp. CTA/1

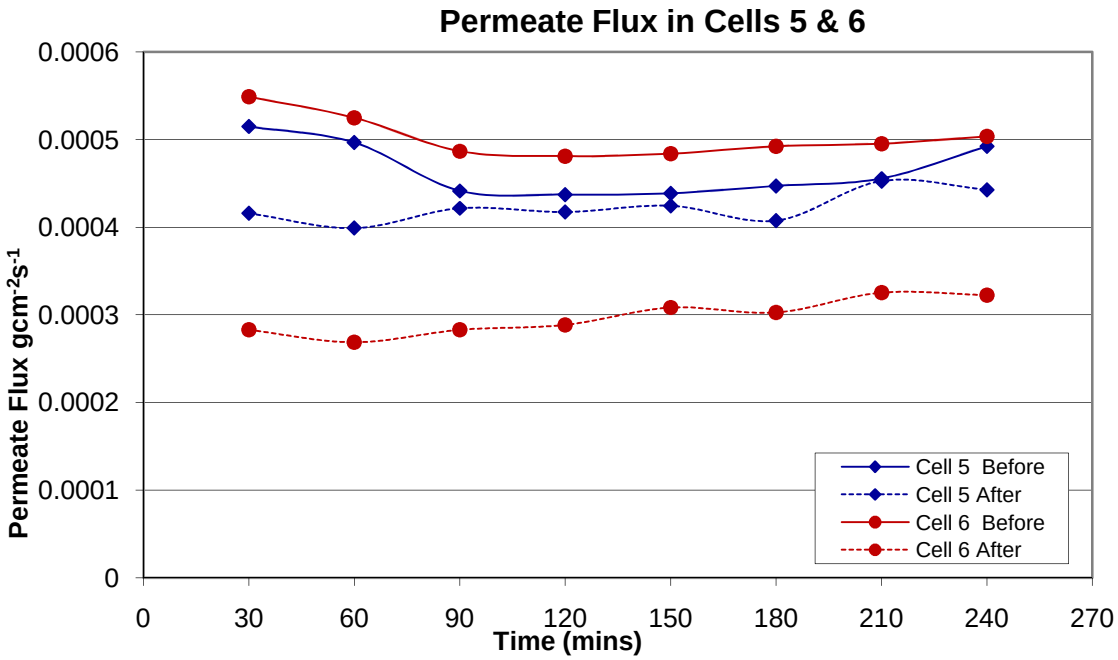

Figure III-3 Permeate Flux in Cells 5 & 6 of Exp. CTA/1

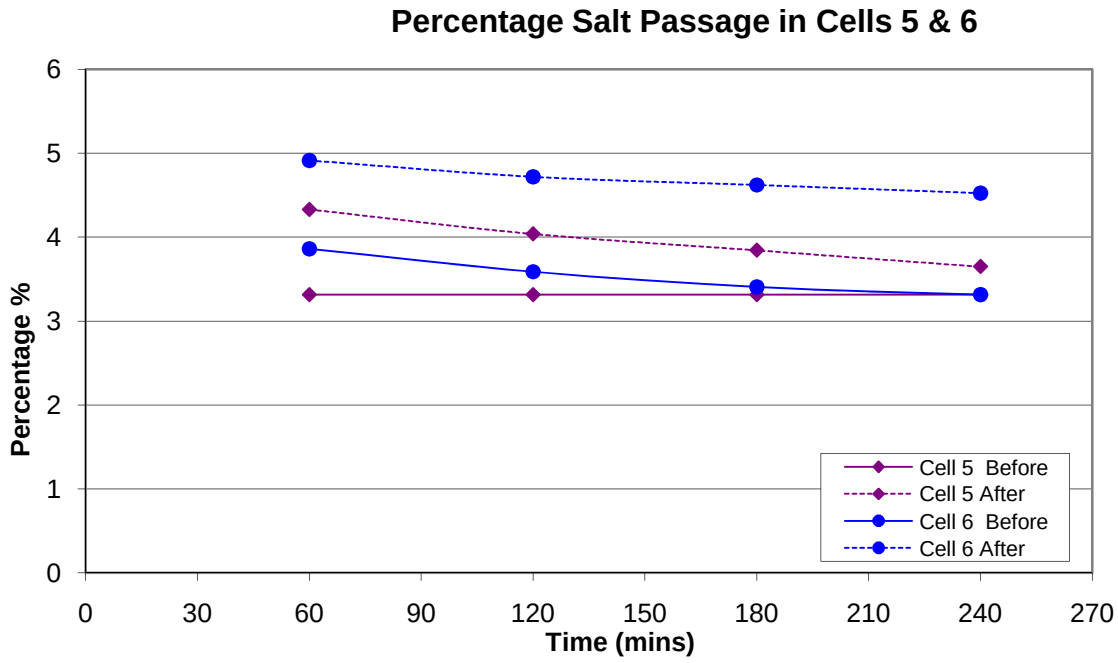

Figure III-4 Percentage Salt Passage in Cells 5 & 6 of Exp. CTA/1

EXP CTA/2

Cells 3-6

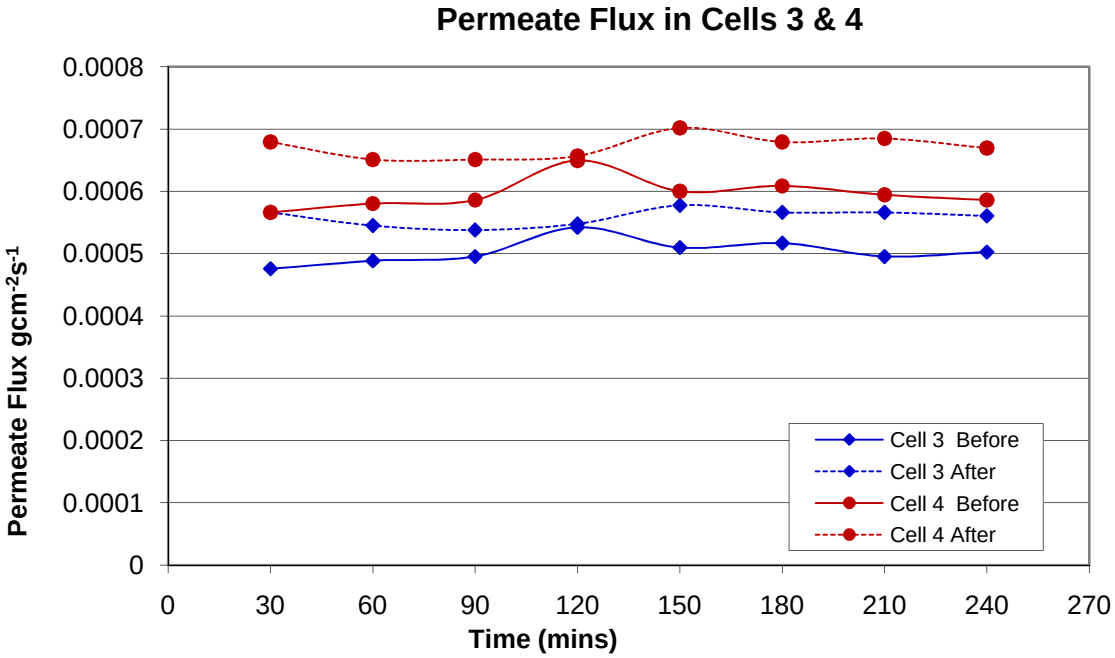

Figure III-5 Permeate Flux in Cells 3 & 4 of Exp. CTA/2

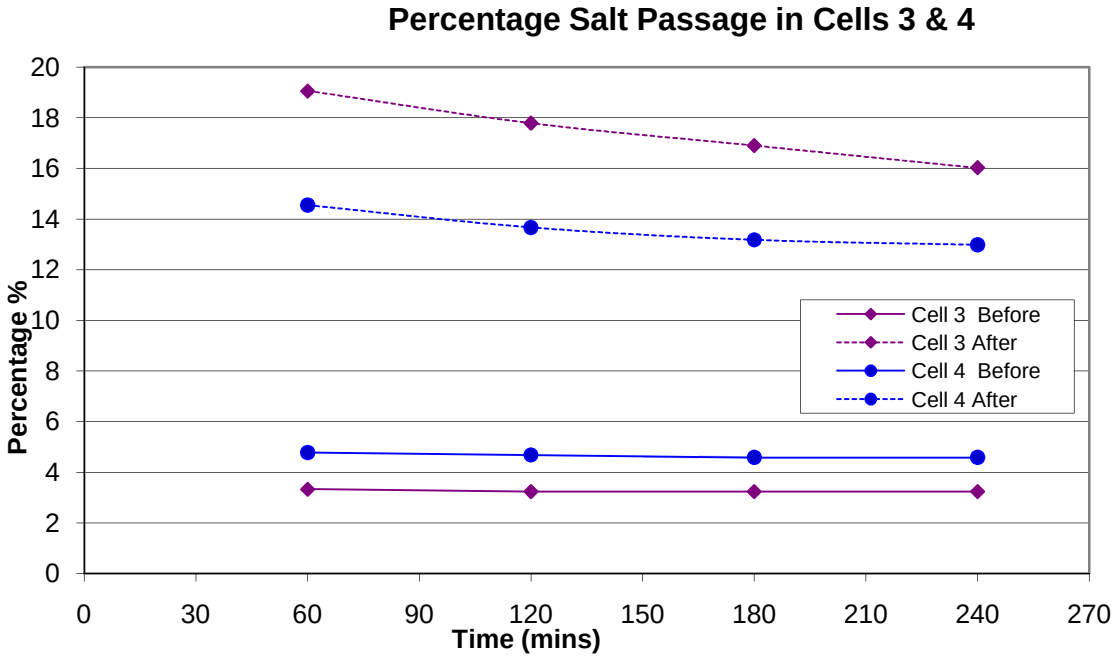

Figure III-6 Percentage Salt Passage in Cells 3 & 4 of Exp. CTA/2

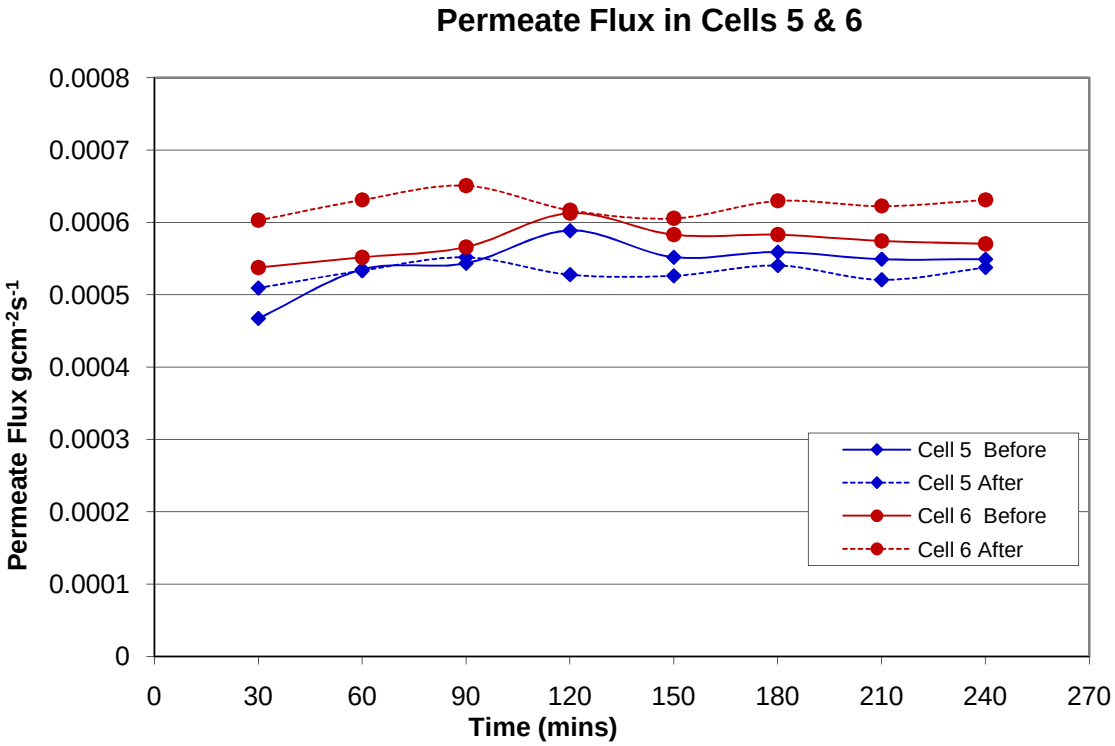

Figure III-7 Permeate Flux in Cells 5 & 6 of Exp. CTA/2

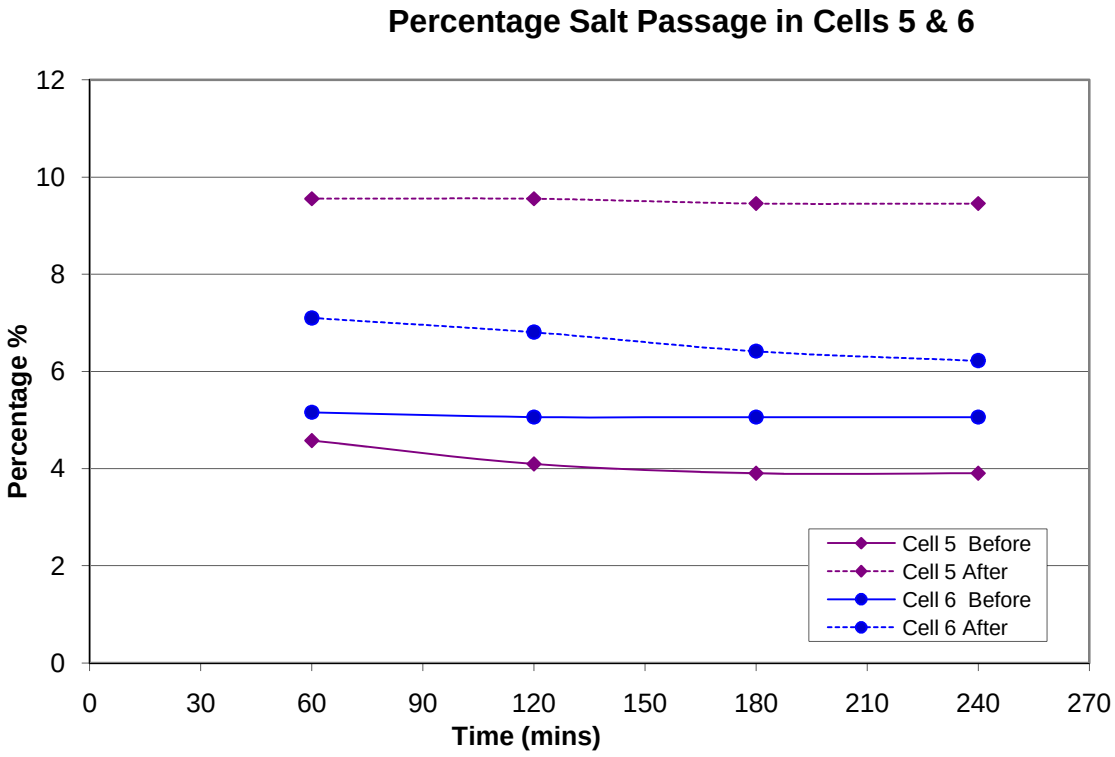

Figure III-8 Percentage Salt Passage in Cells 5 & 6 of Exp. CTA/2

EXP CTA/3

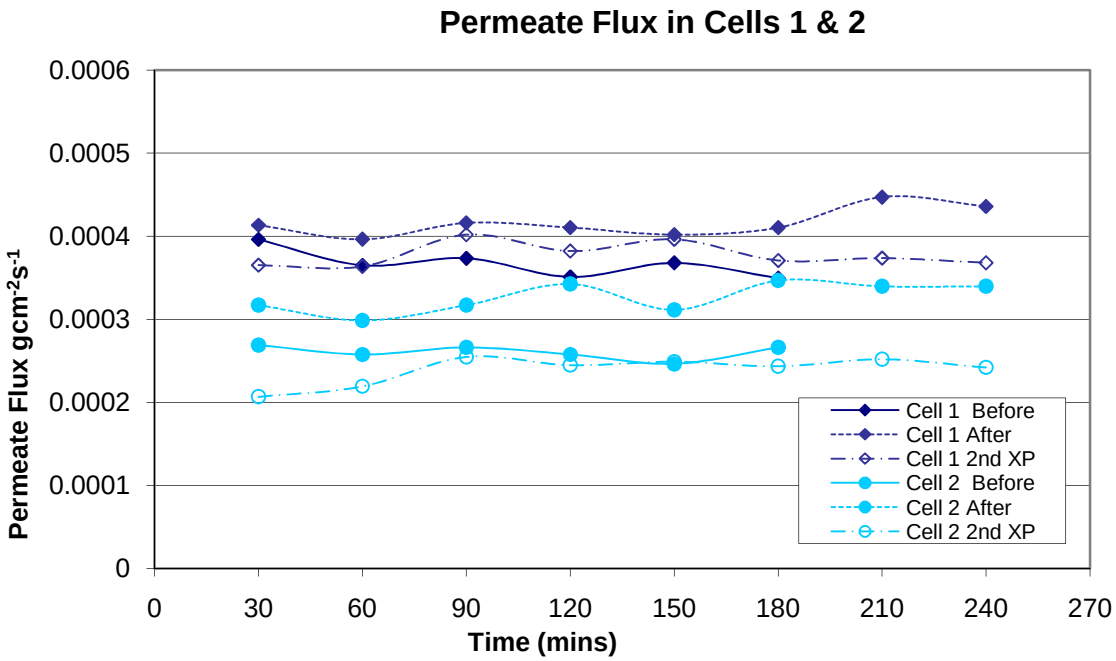

Figure III-9 Permeate Flux in Cells 1 & 2 of Exp. CTA/3

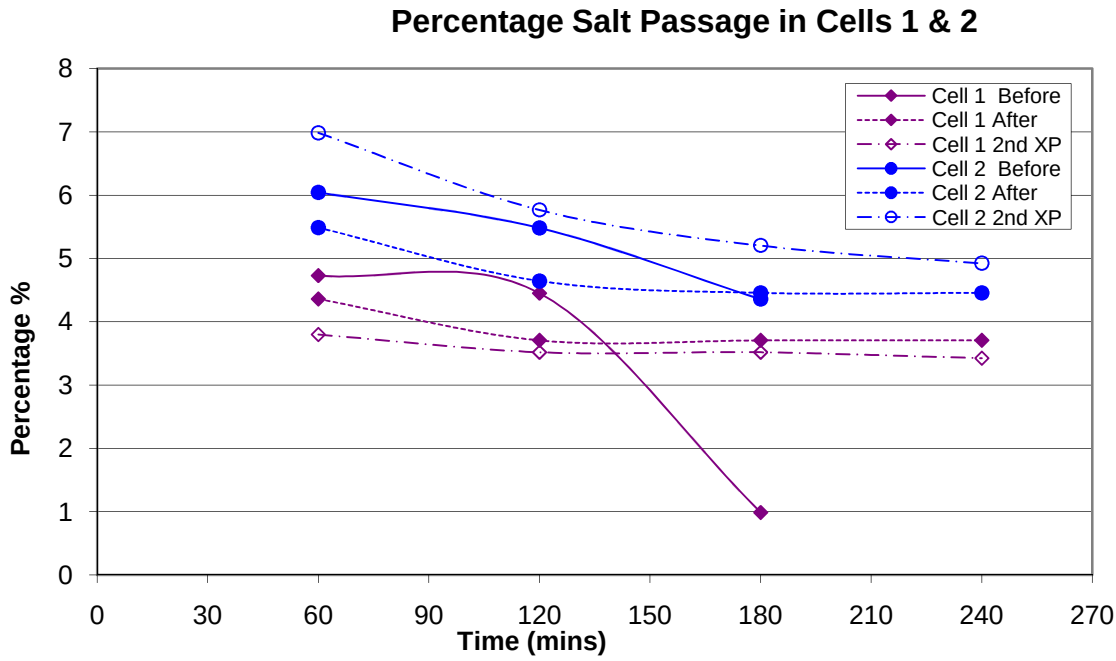

Figure III-10 Percentage Salt Passage in Cells 1 & 2 of Exp. CTA/3

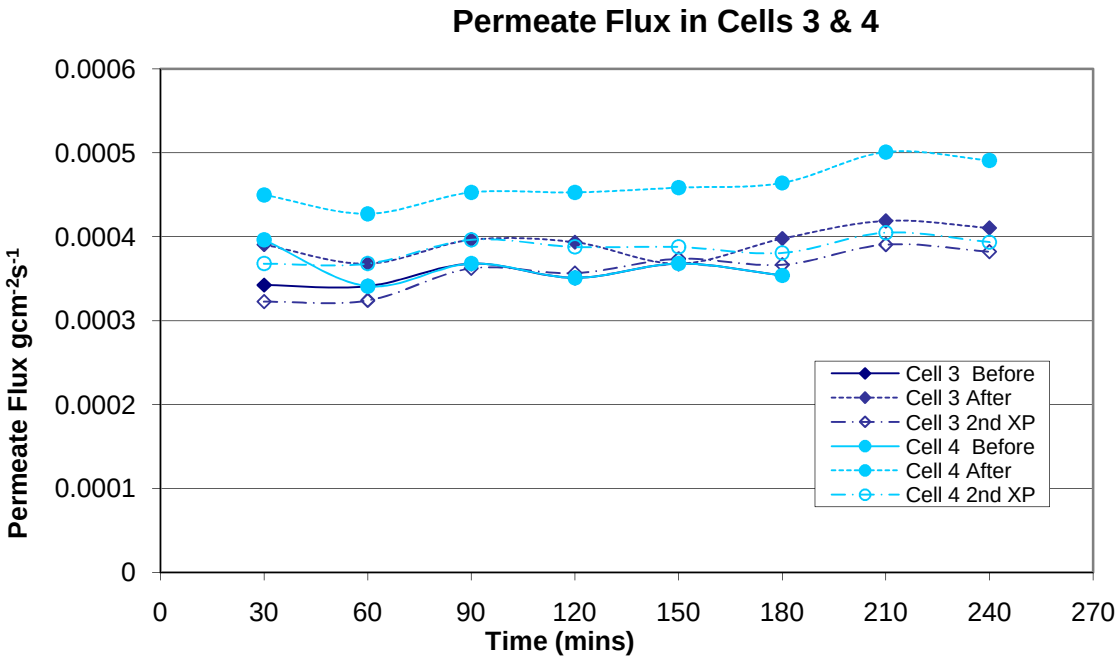

Figure III-11 Permeate Flux in Cells 3 & 4 of Exp. CTA/3

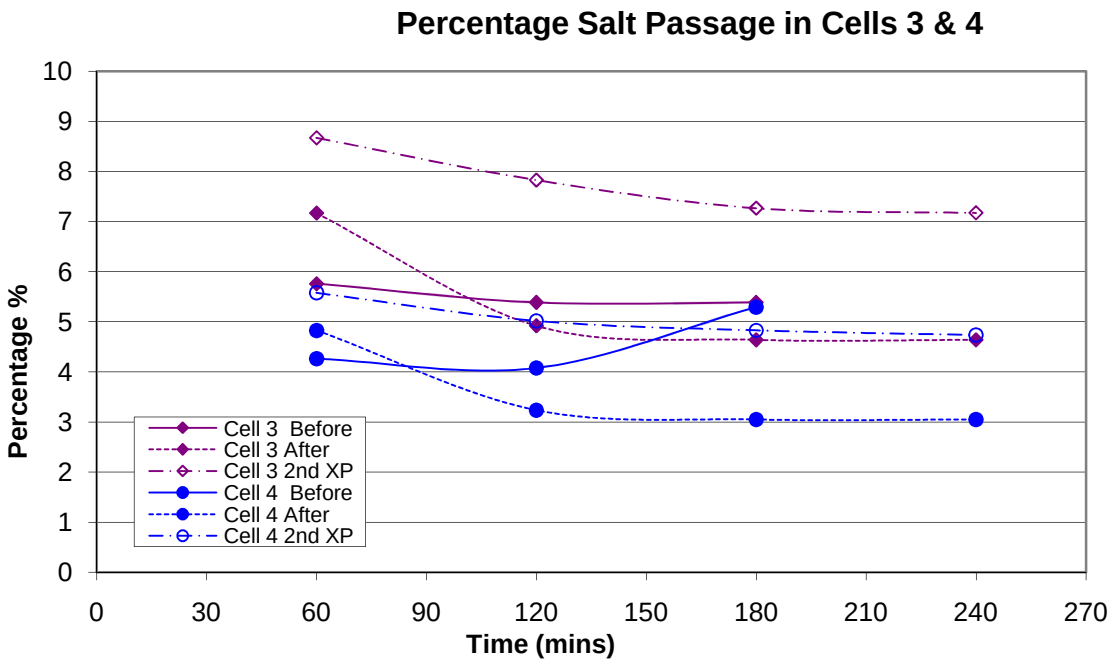

Figure III-12 Percentage Salt Passage in Cells 3 & 4 of Exp. CTA/3

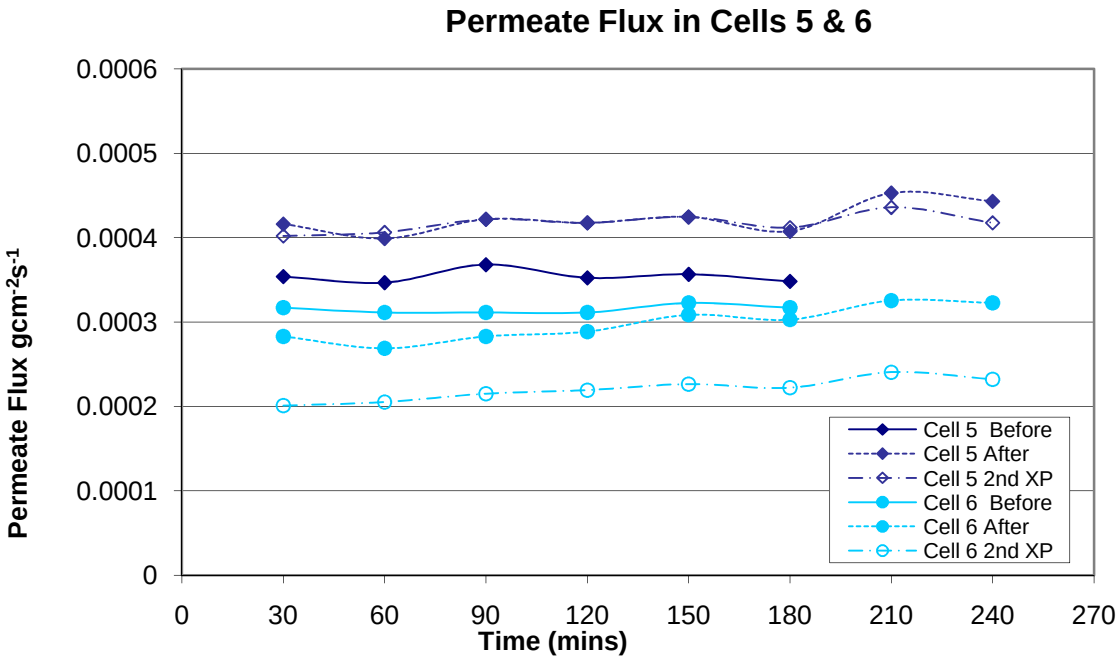

Figure III-13 Permeate Flux in Cells 5 & 6 of Exp. CTA/3

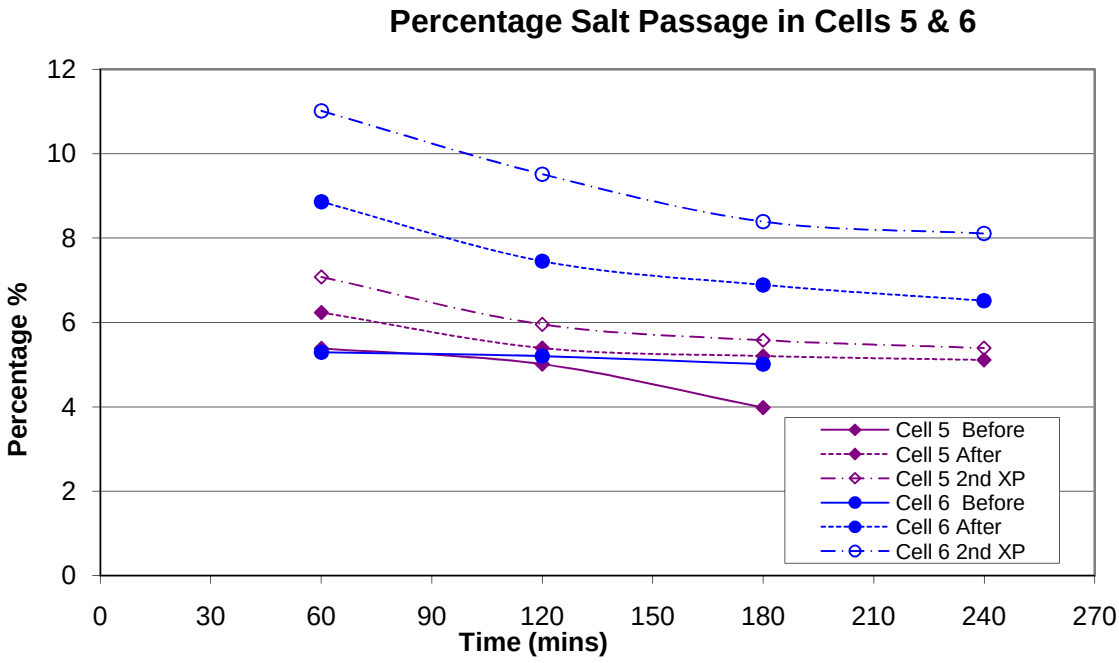

Figure III-14 Percentage Salt Passage in Cells 5 & 6 of Exp. CTA/3

EXP CTA/4

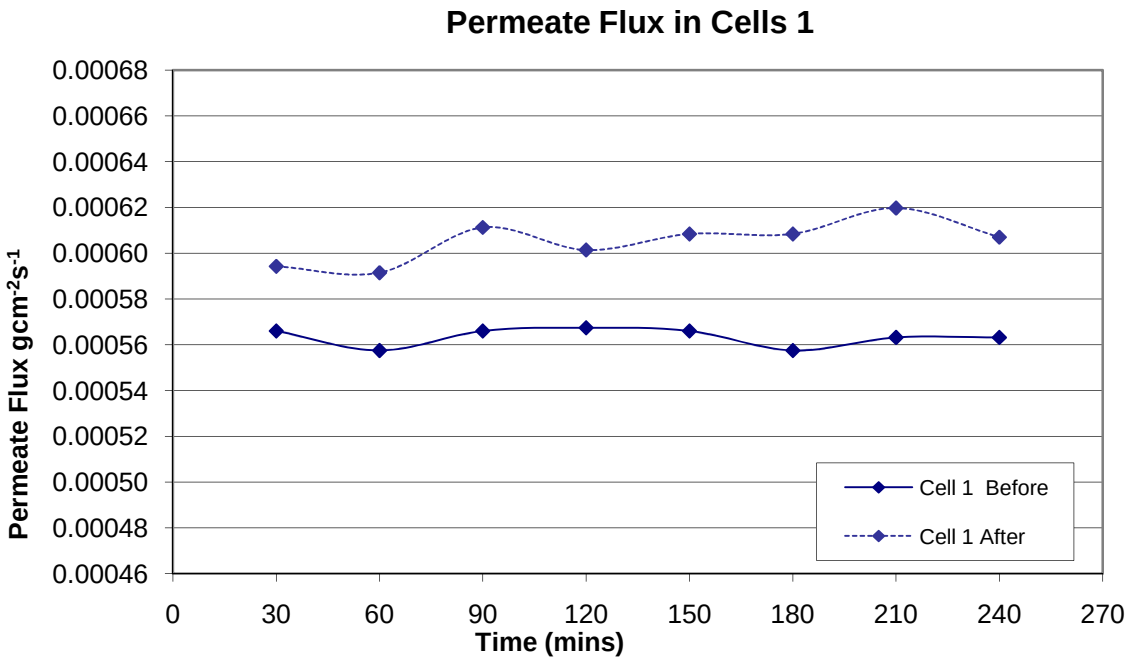

Figure III-15 Permeate Flux in Cells 1 of Exp. CTA/4

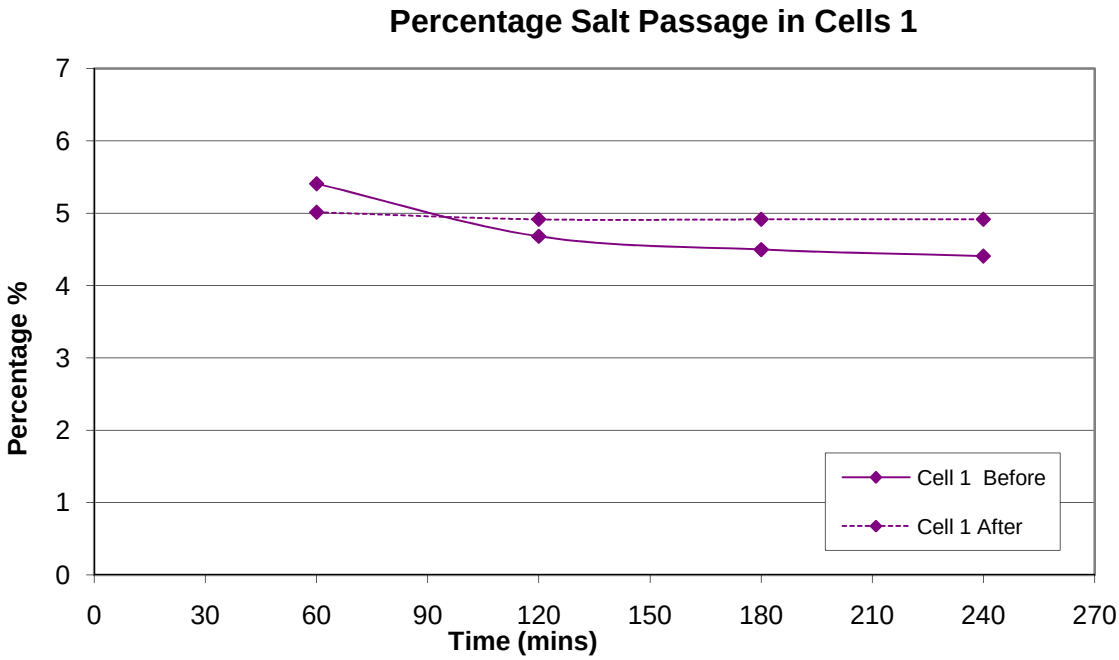

Figure III-16 Percentage Salt Passage in Cells 1 of Exp. CTA/4

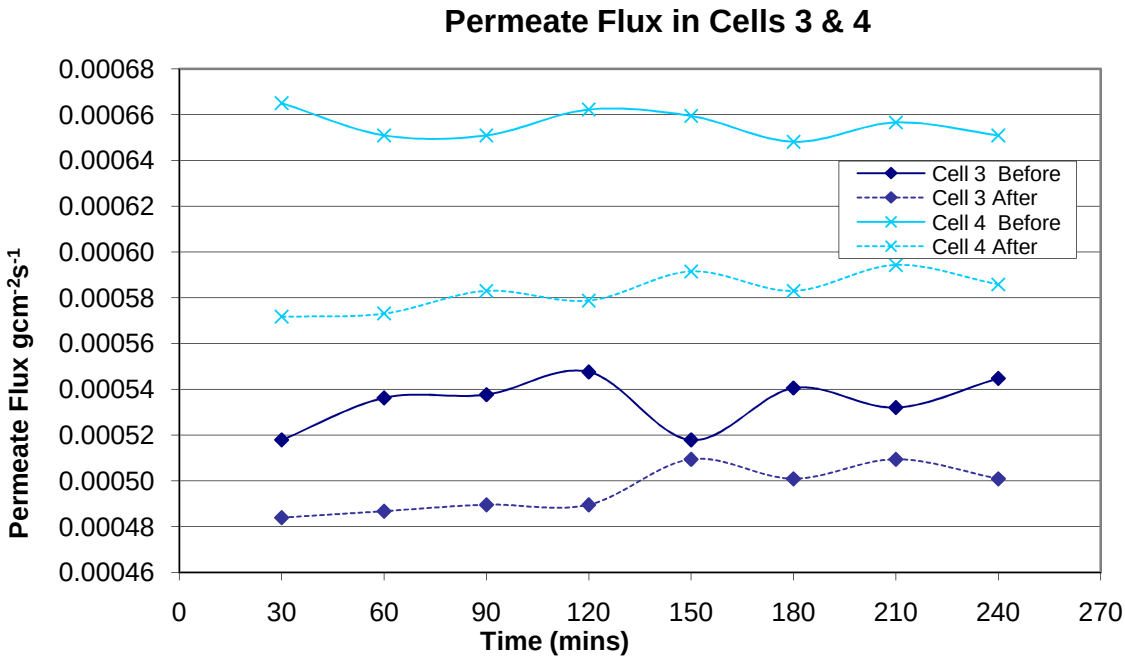

Figure III-17 Permeate Flux in Cells 3 & 4 of Exp. CTA/4

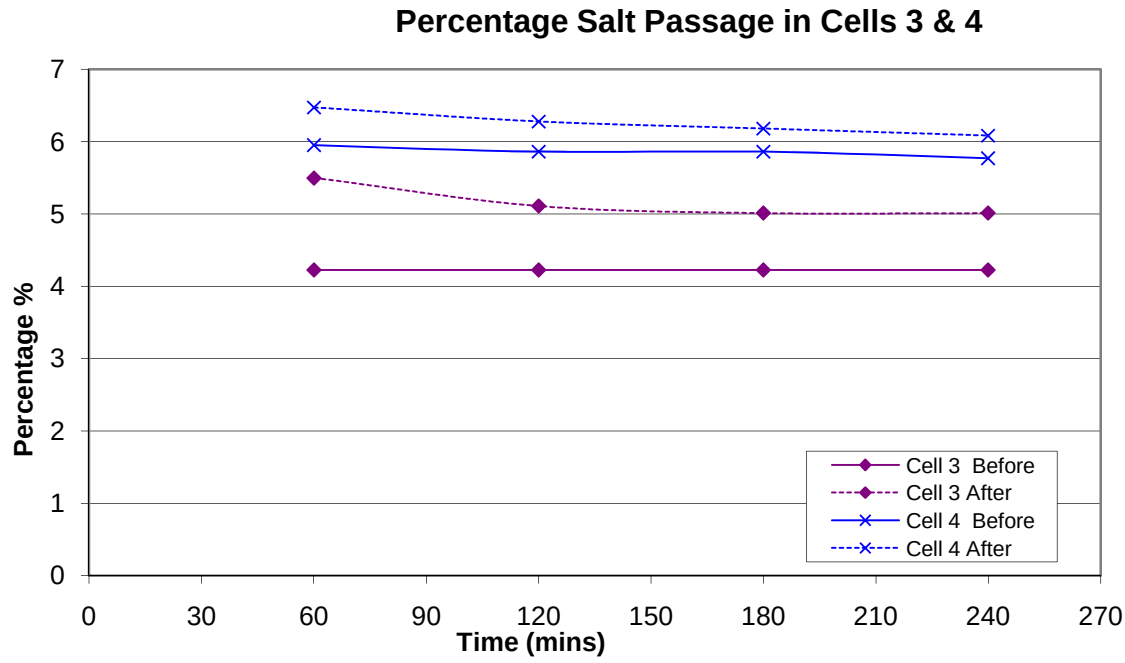

Figure III-18 Percentage Salt Passage in Cells 3 & 4 of Exp. CTA/4

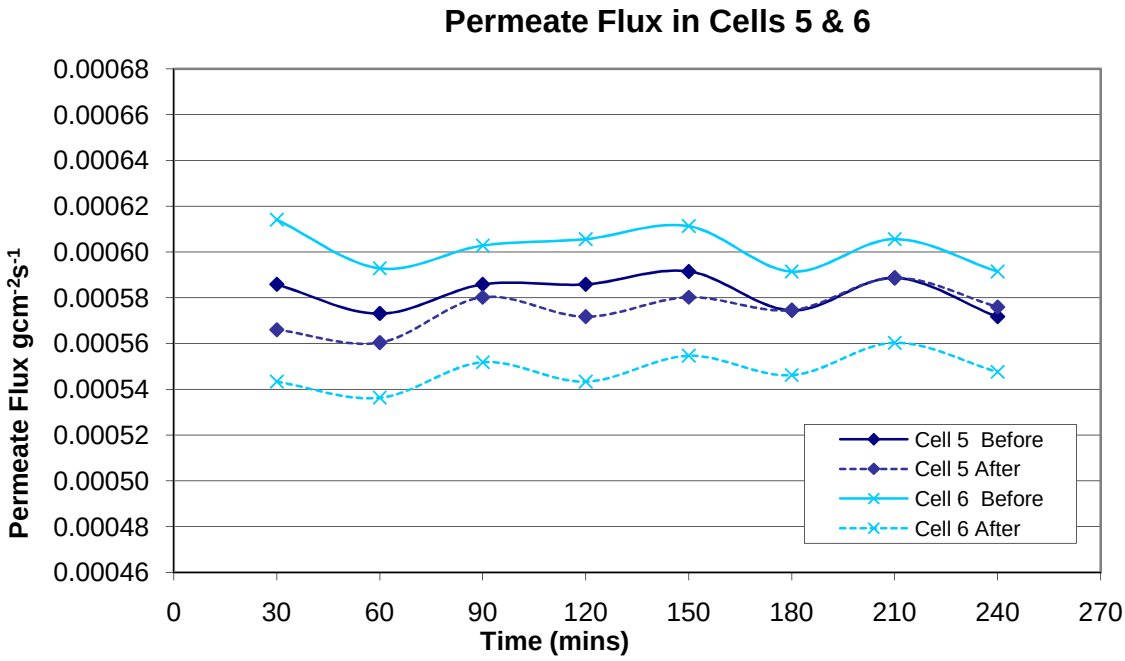

Figure III-19 Permeate Flux in Cells 5 & 6 of Exp. CTA/4

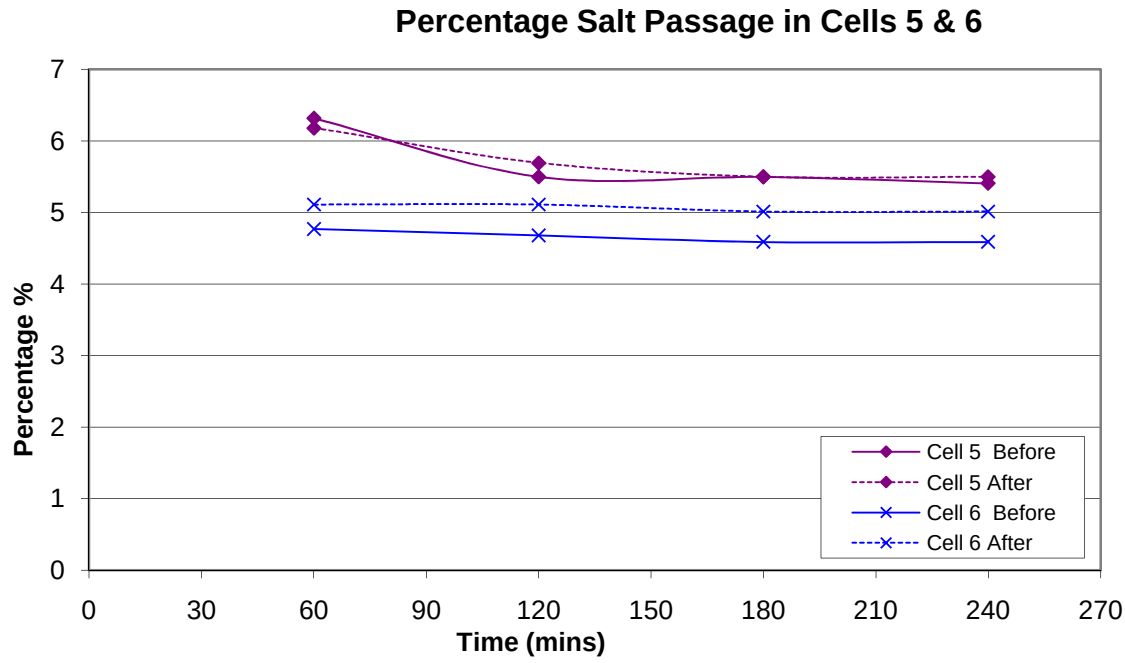

Figure III-20 Percentage Salt Passage in Cells 5 & 6 of Exp. CTA/4

EXP CTA/5

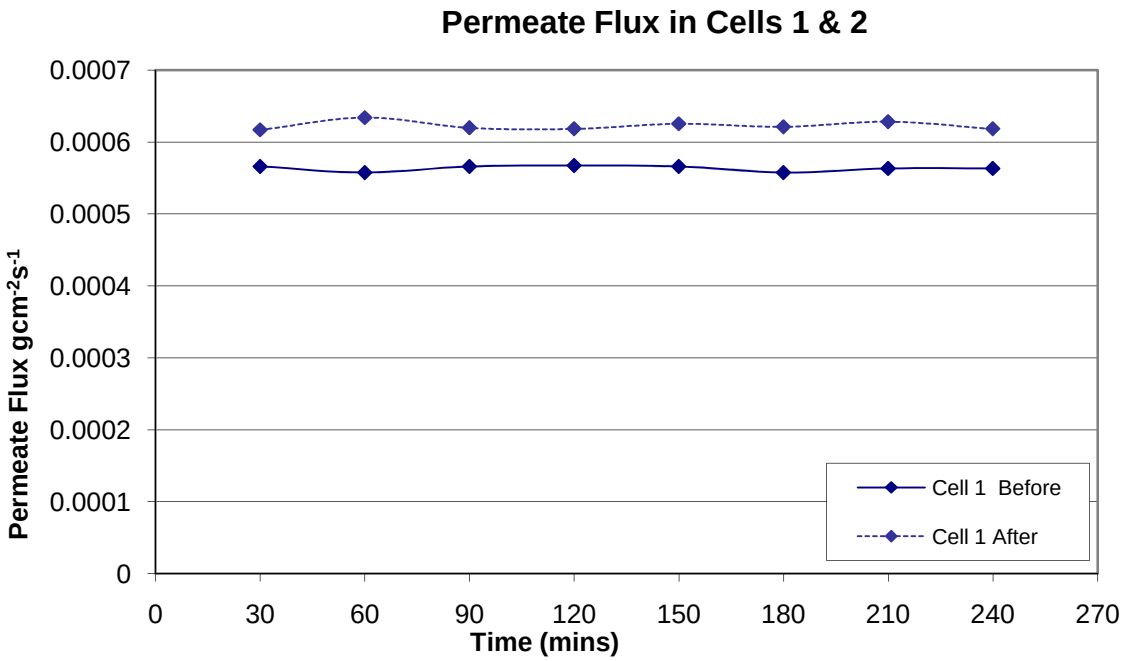

Figure III-21 Permeate Flux in Cells 1 & 2 of Exp. CTA/5

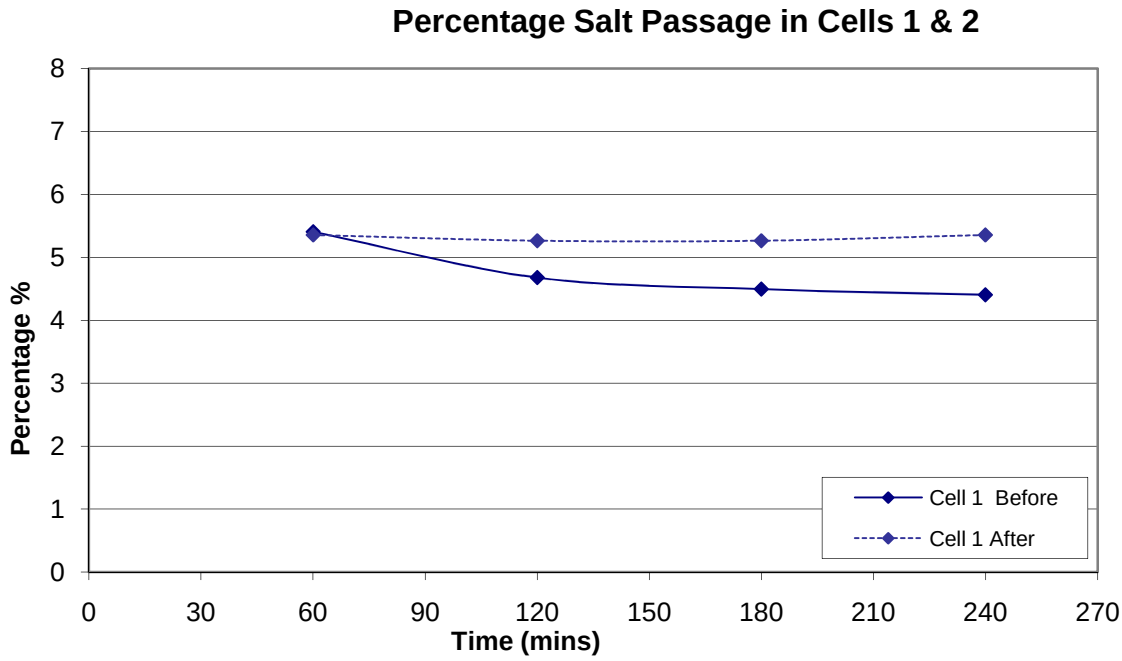

Figure III-22 Percentage Salt Passage in Cells 1 & 2 of Exp. CTA/5

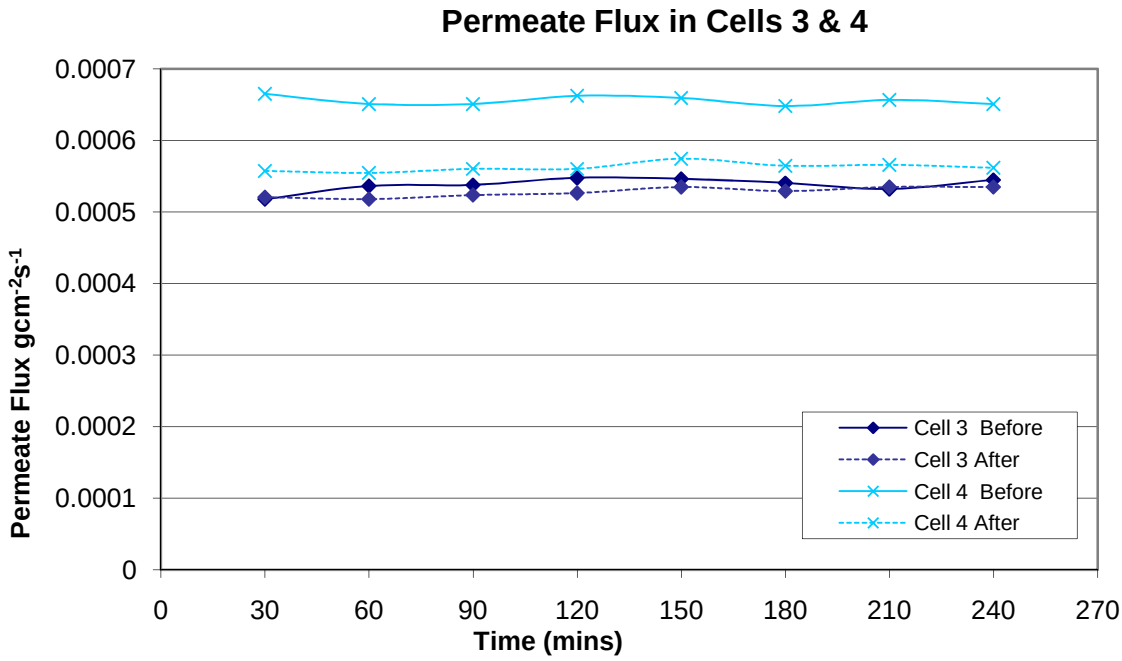

Figure III-23 Permeate Flux in Cells 3 & 4 of Exp. CTA/5

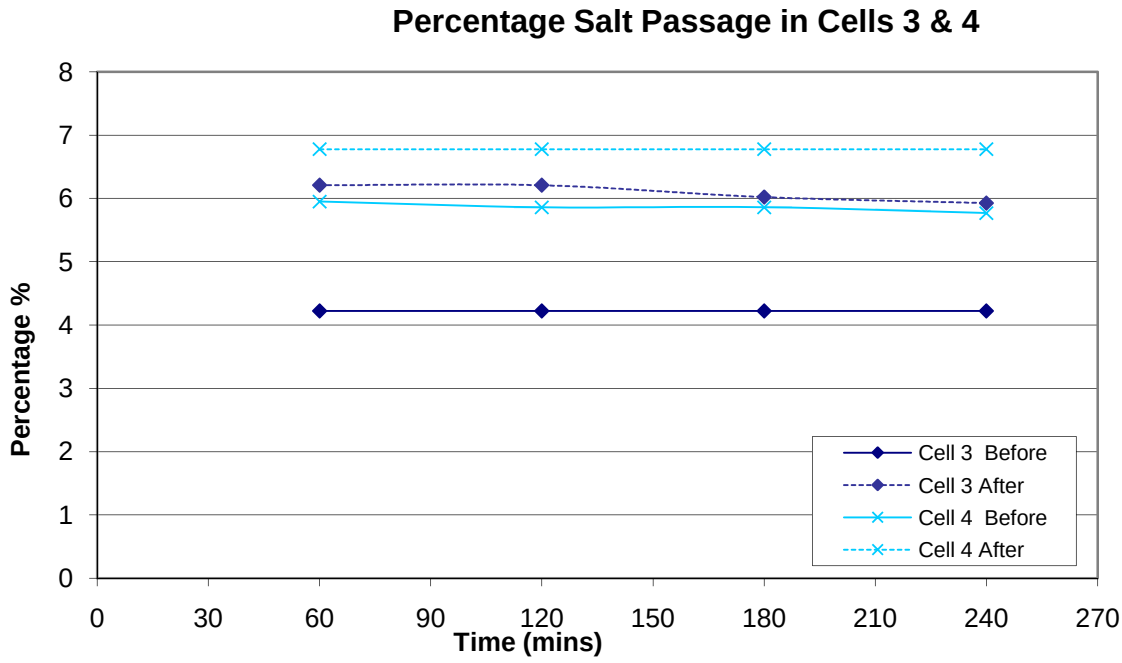

Figure III-24 Percentage Salt Passage in Cells 3 & 4 of Exp. CTA/5

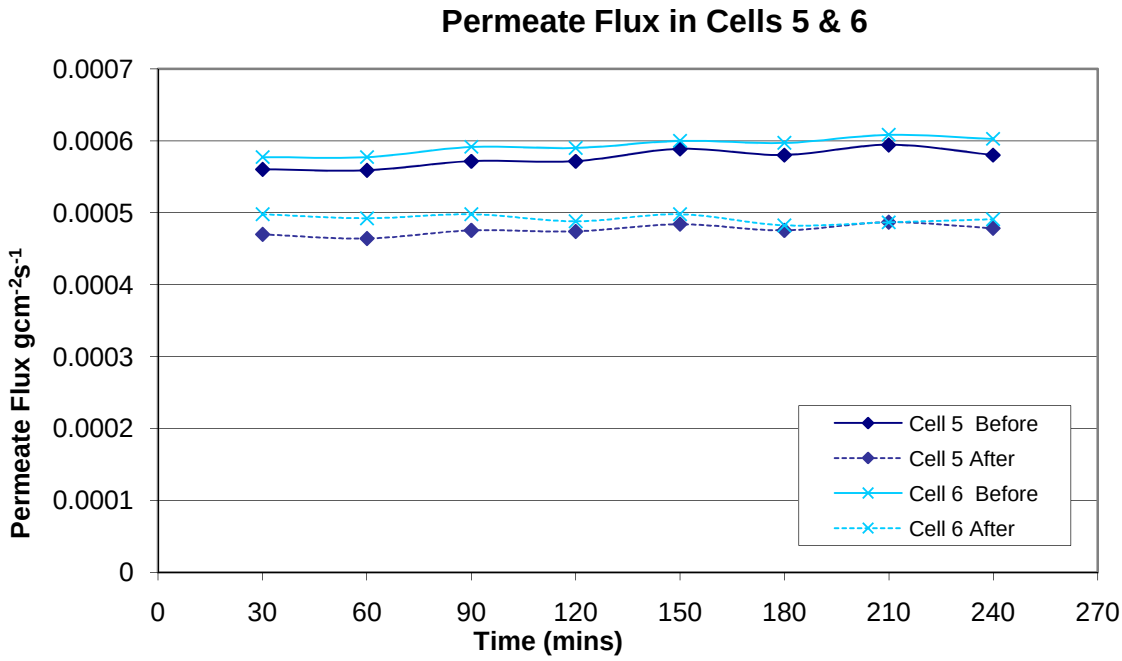

Figure III-25 Permeate Flux in Cells 5 & 6 of Exp. CTA/5

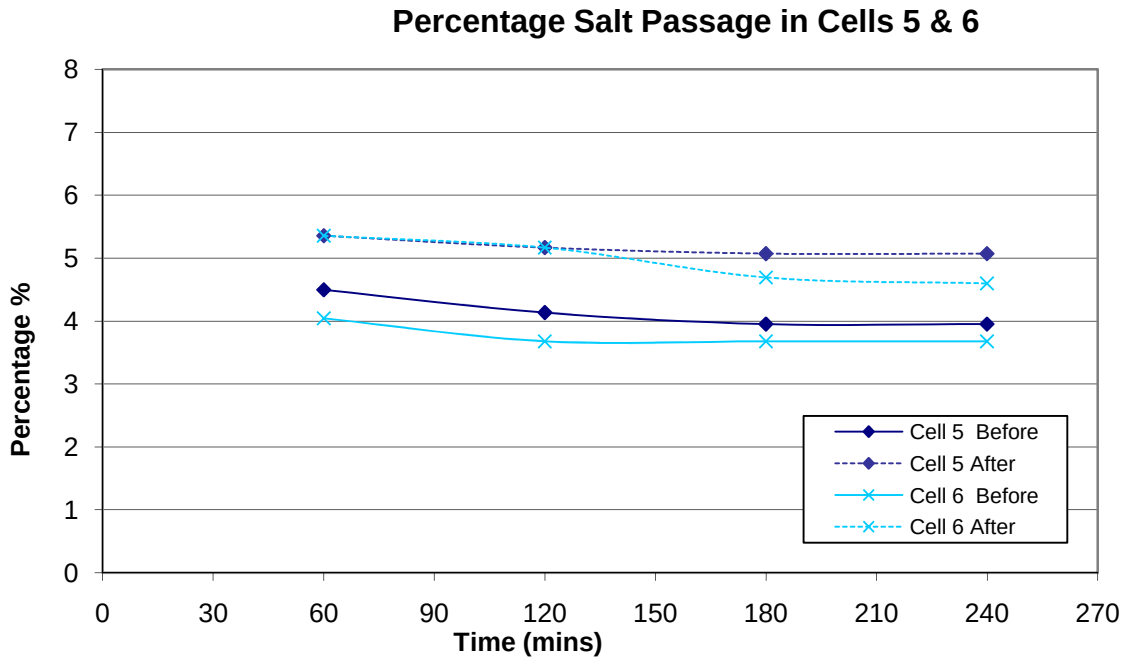

Figure III-26 Percentage Salt Passage in Cells 5 & 6 of Exp. CTA/5

EXP CTA/7

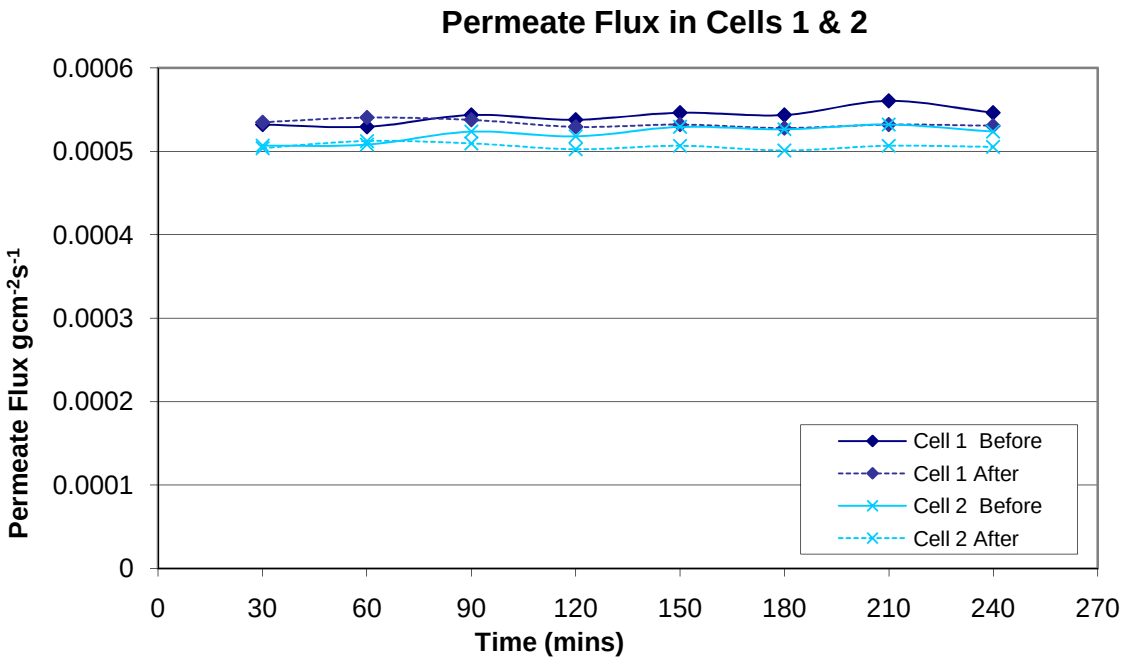

Figure III-27 Permeate Flux in Cells 1 & 2 of Exp. CTA/7

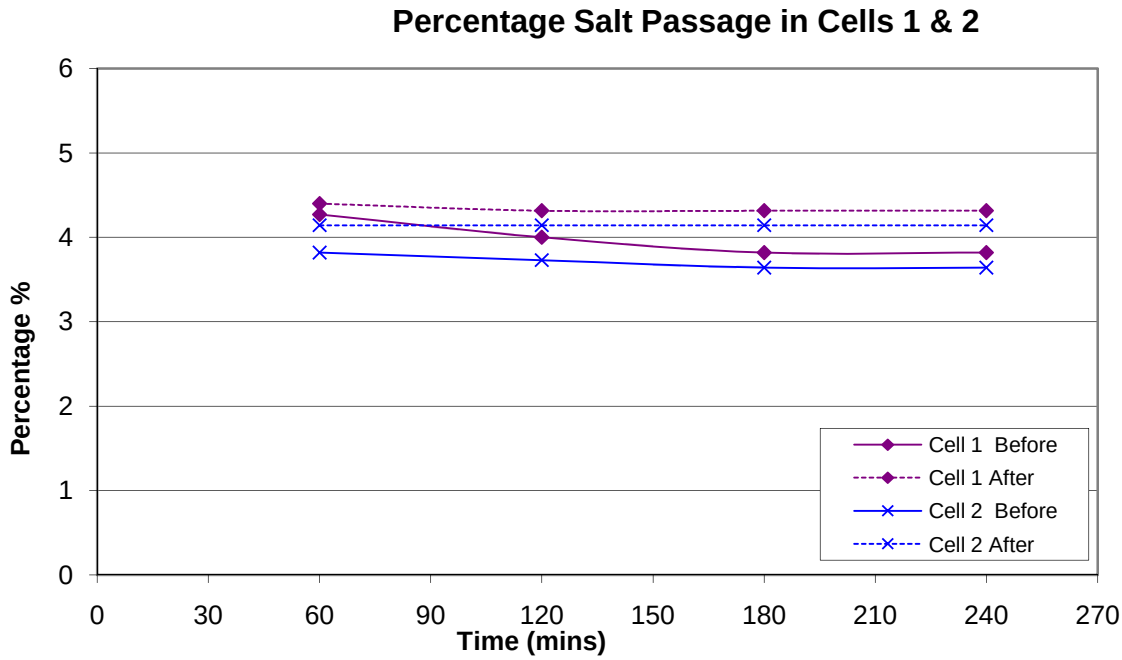

Figure III-28 Percentage Salt Passage in Cells 1 & 2 of Exp. CTA/7

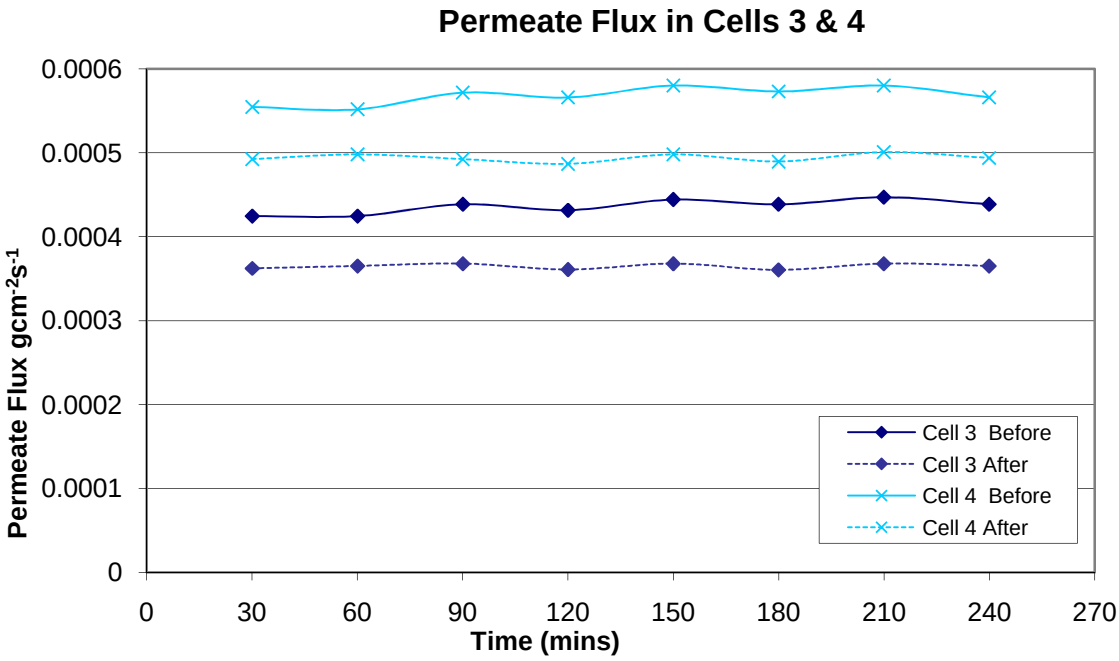

Figure III-29 Permeate Flux in Cells 3 & 4 of Exp. CTA/7

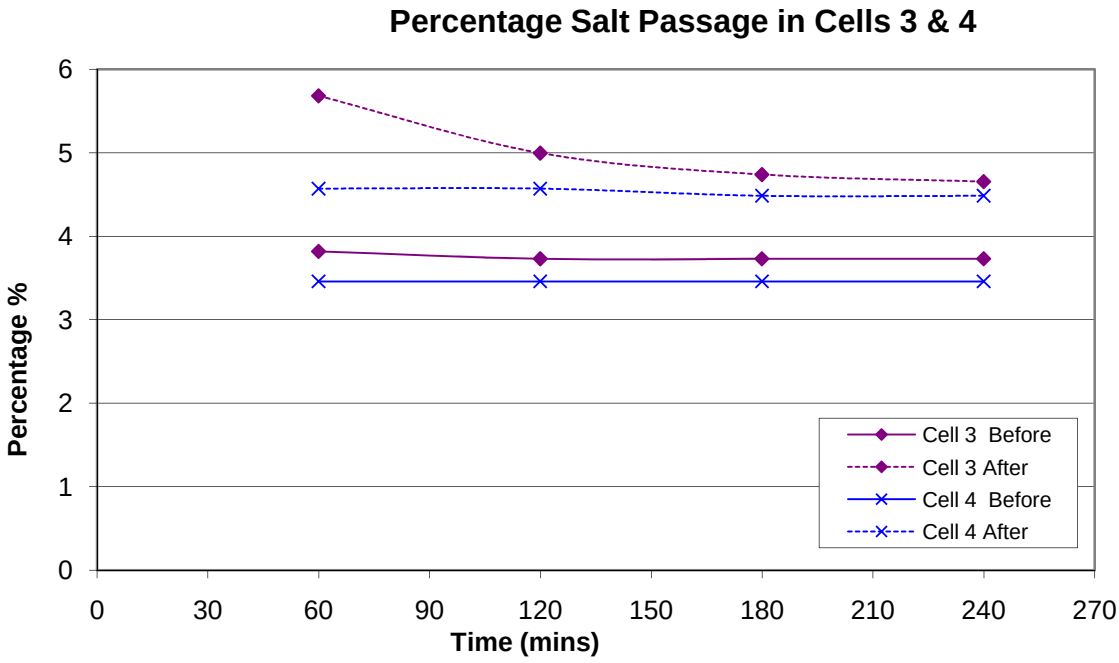

Figure III-30 Percentage Salt Passage in Cells 3 & 4 of Exp. CTA/7

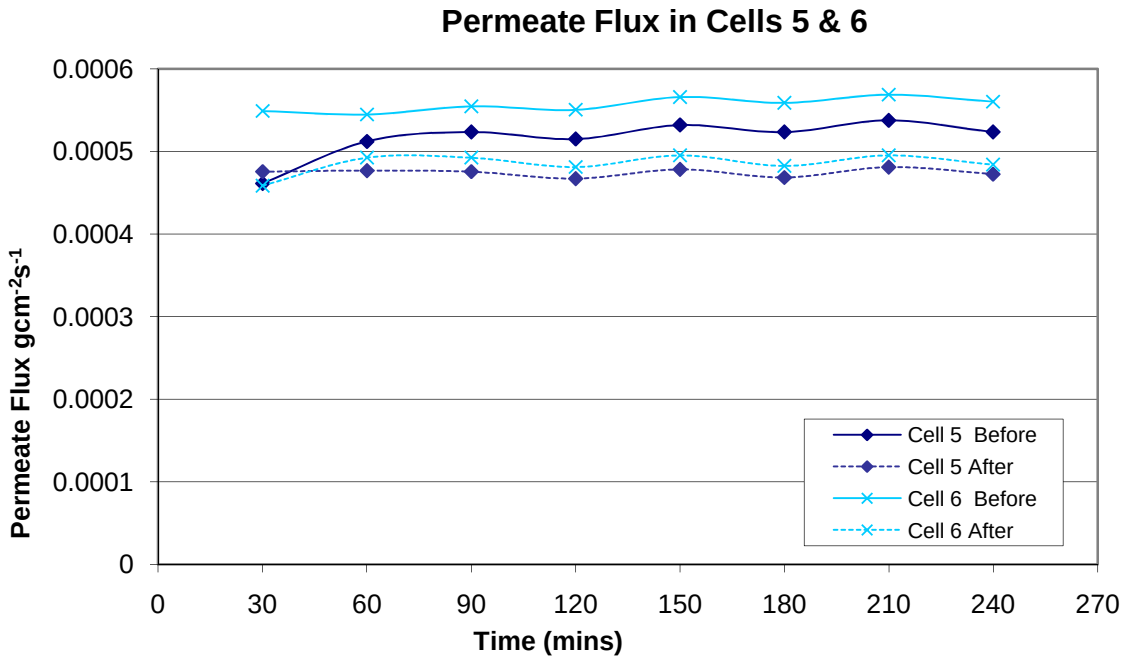

Figure III-31 Permeate Flux in Cells 5 & 6 of Exp. CTA/7

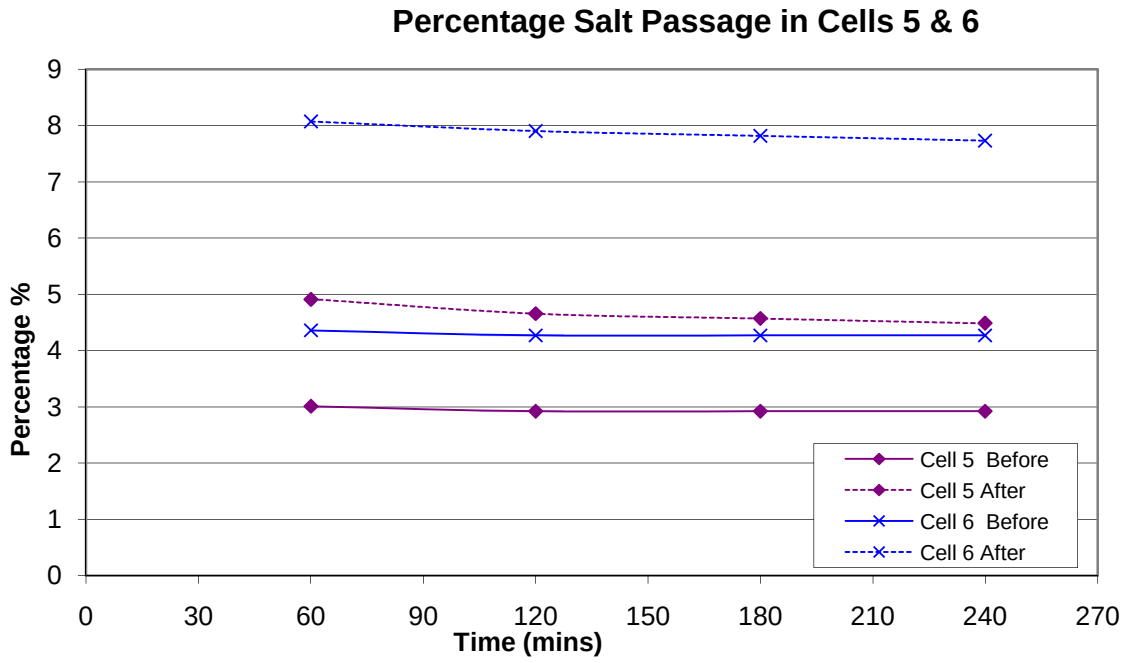

Figure III-32 Percentage Salt Passage in Cells 5 & 6 of Exp. CTA/7

APPENDIX IV

Microscopy

SCANNING ELECTRON MICROSCOPY

Hitachi S4700

Figure IV-1 Hitachi S4700 Scanning Electron Microscope

The Hitachi S-4700 FE-SEM is a cold field emission high resolution scanning electron microscope. This SEM permits ultra high resolution imaging of thin films and semi-conductor materials on exceptionally clean specimens. It is also suitable for polymeric materials. The S-4700 is conFigured to detect secondary and backscattered electrons as well as characteristic X-rays. The system is fully automated and is operated via easy-to-use menu driven software.

SW 30

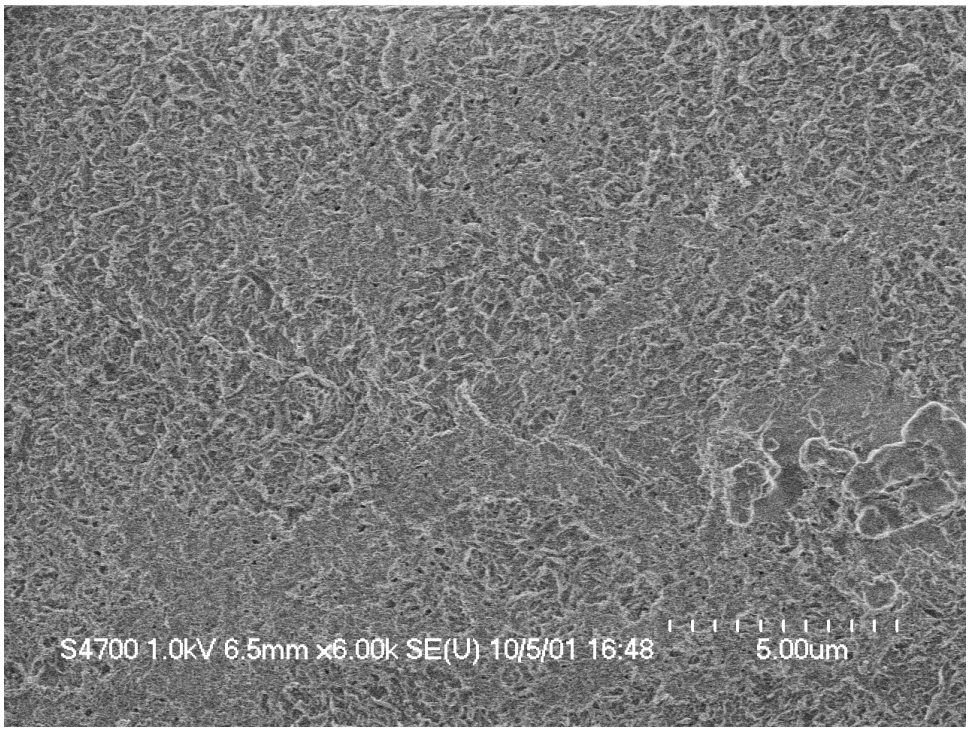

Figure IV-2 Active surface of SW 30 membrane at 6 000 magnification

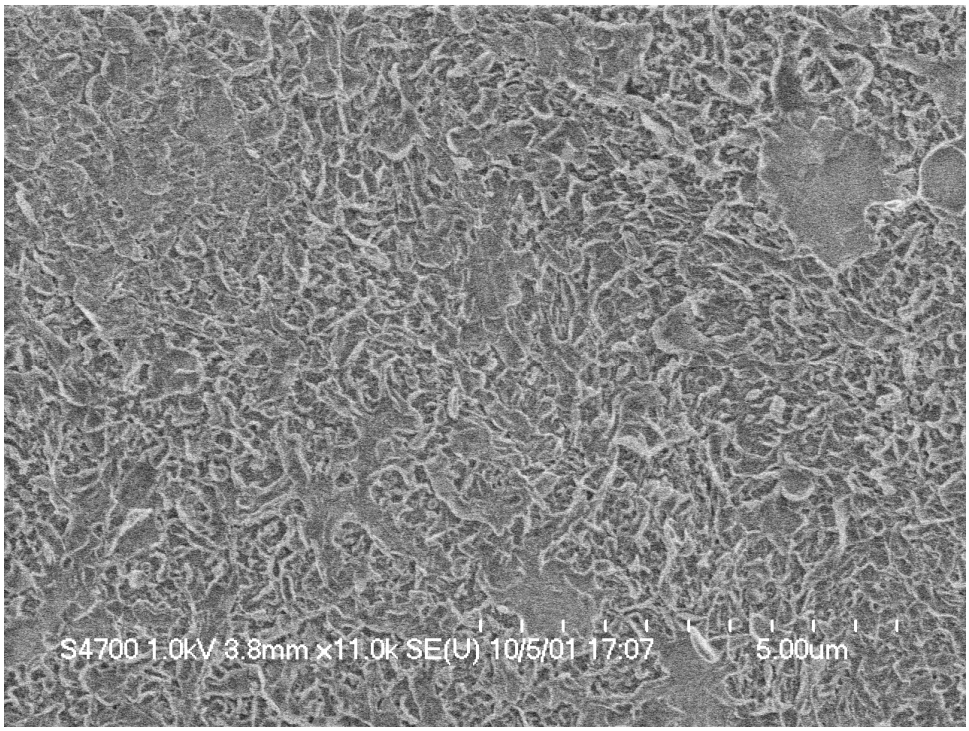

Figure IV-3 Active surface of SW 30 membrane at 11 000 magnification

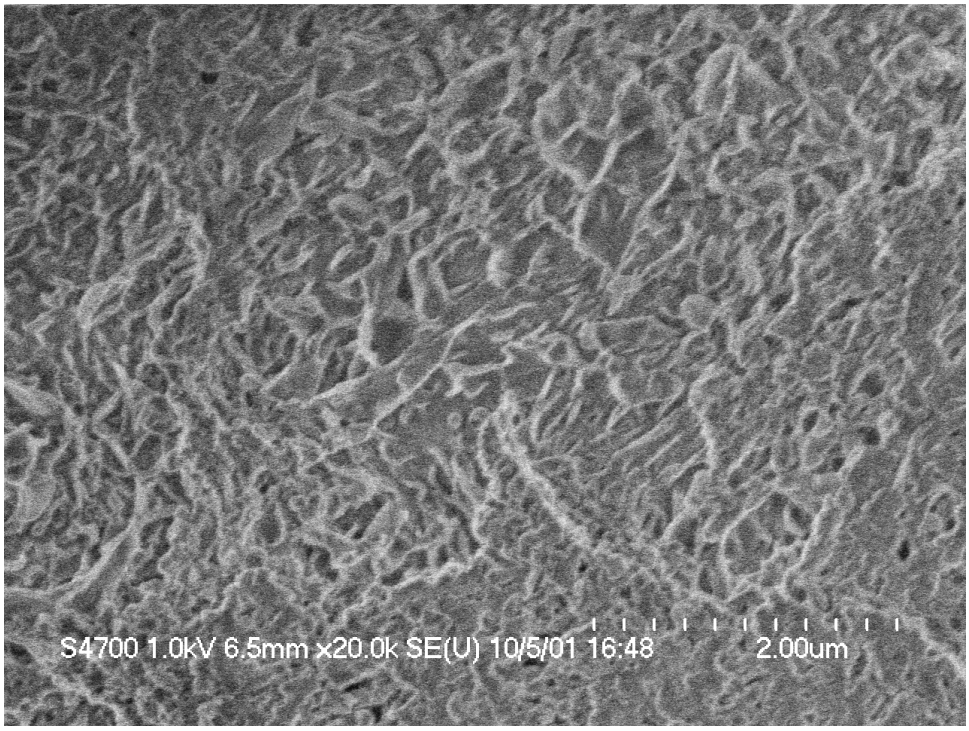

Figure IV-4 Active surface of SW 30 membrane at 20 000 magnification

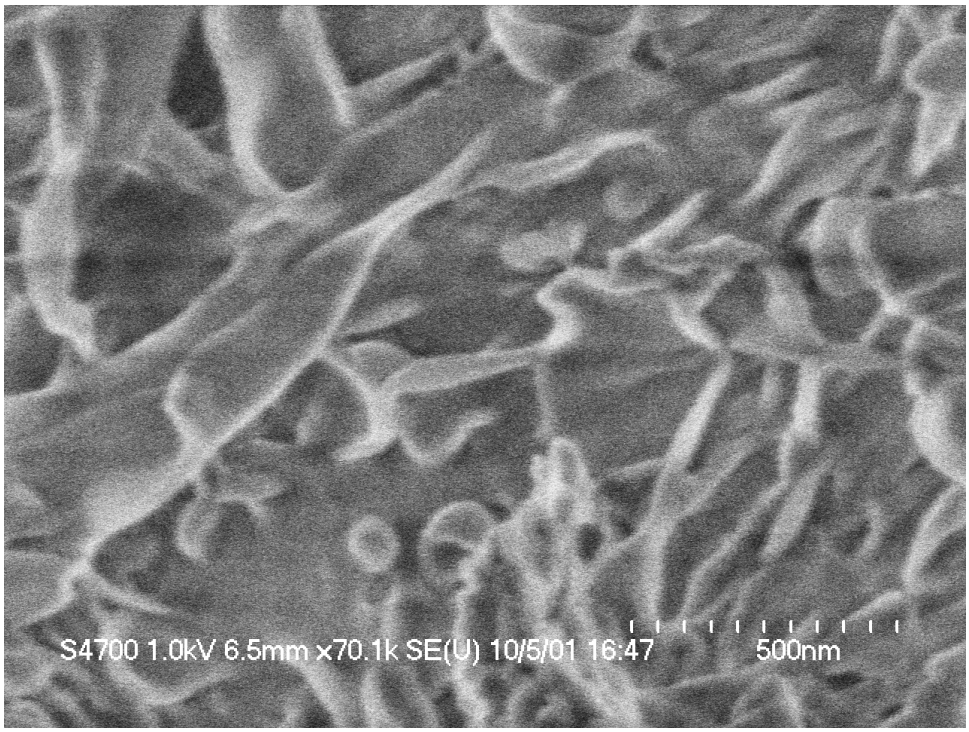

Figure IV-5 Active surface of SW 30 membrane at 70 000 magnification

CTA

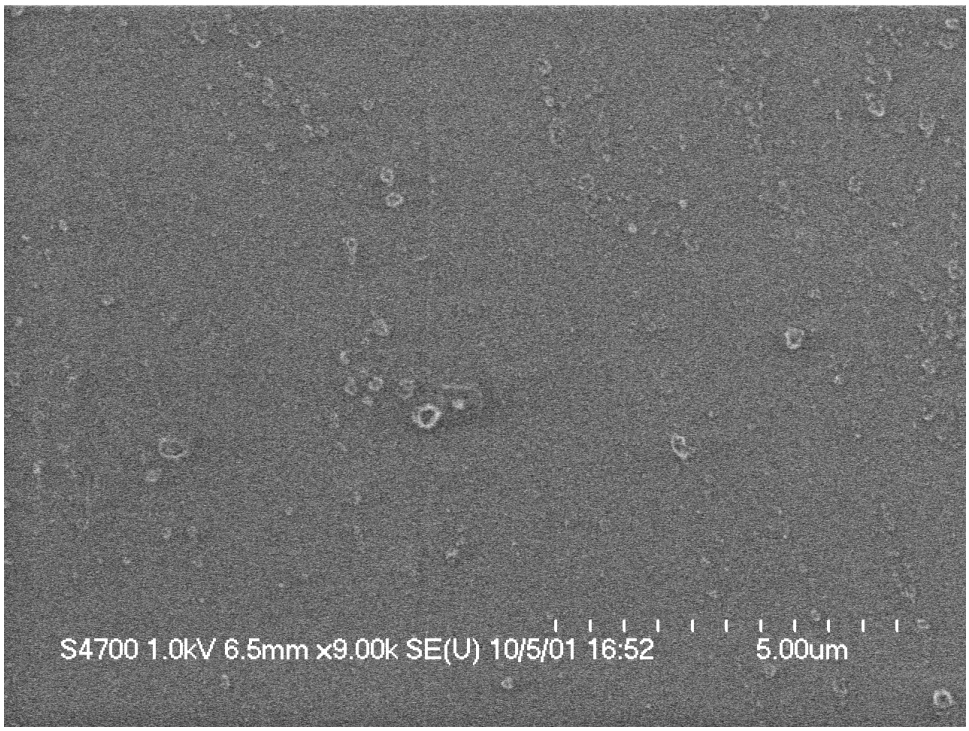

Figure IV-6 Active surface of CTA membrane at 9 000 magnification

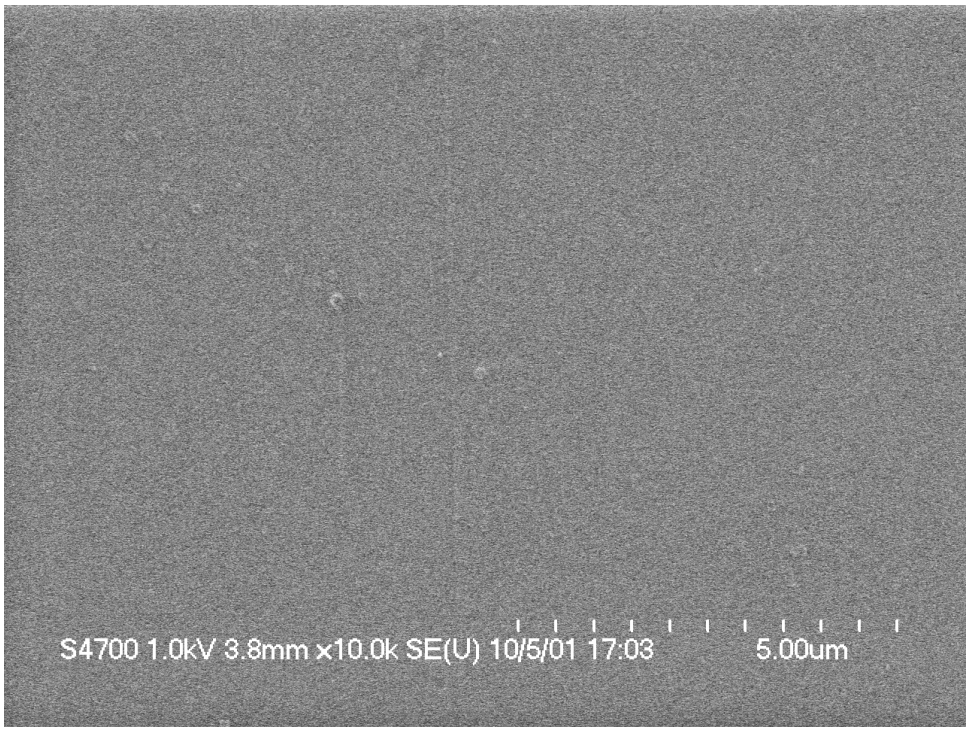

Figure IV-7 Active surface of CTA membrane at 10 000 magnification

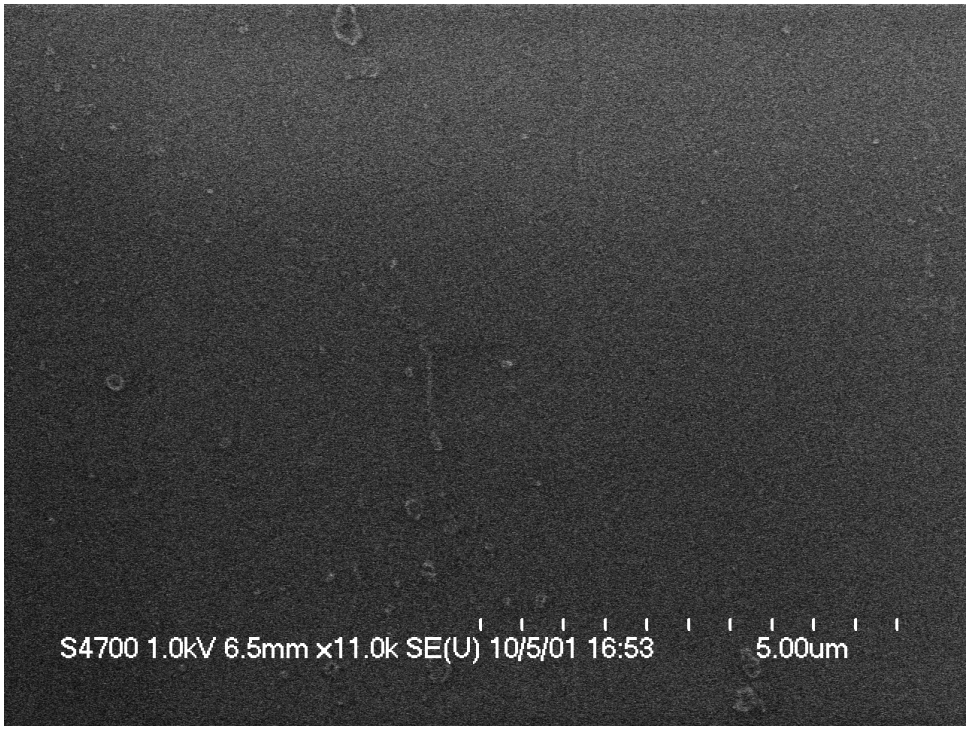

Figure IV-8 Active surface of CTA membrane at 11 000 magnification

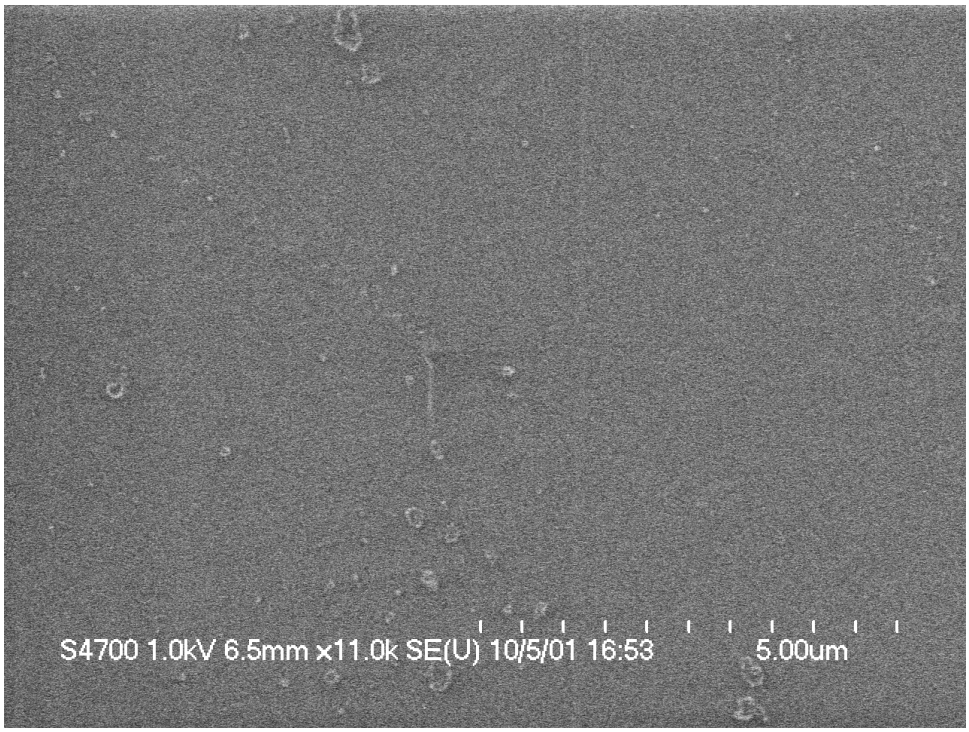

Figure IV-9 Active surface of CTA membrane at 11 000 magnification

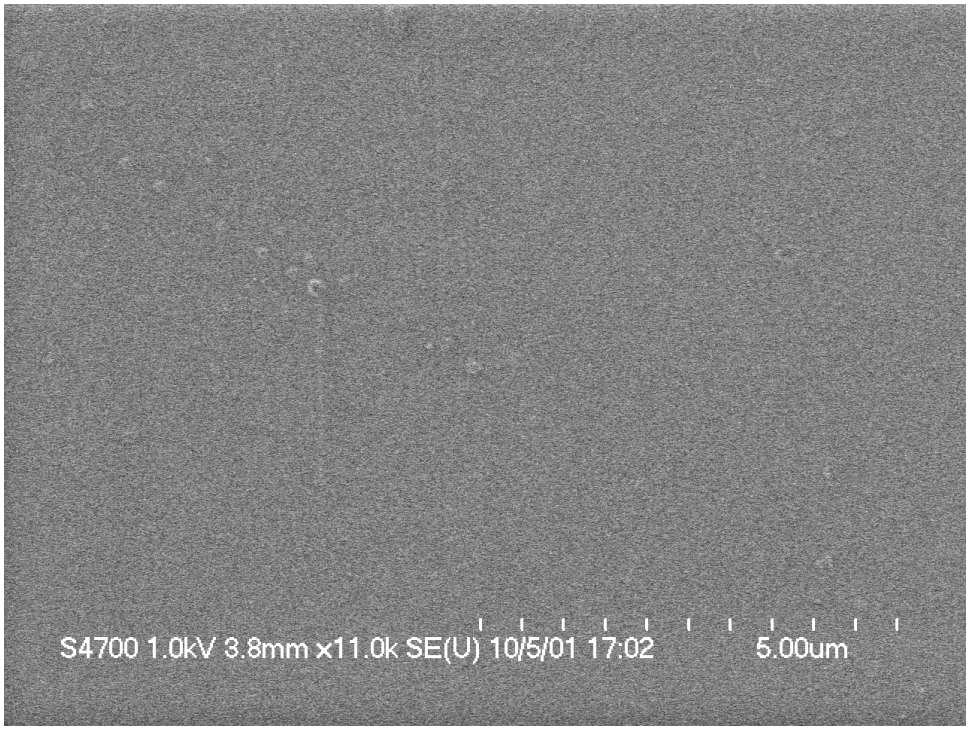

Figure IV-10 Active surface of CTA membrane at 11 000 magnification

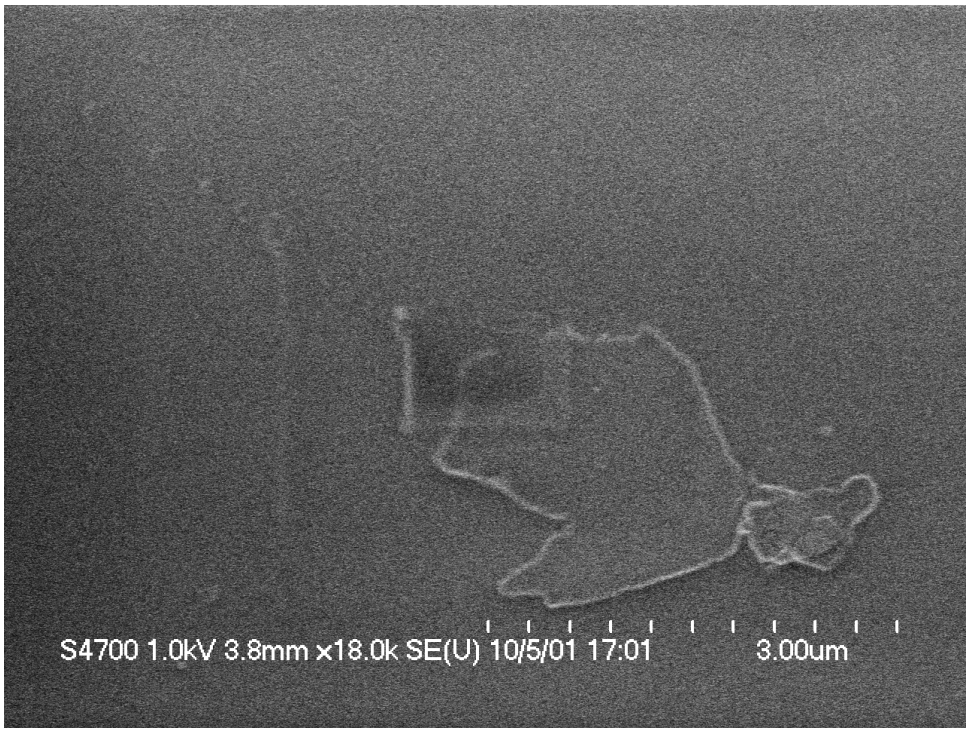

Figure IV-11 Active surface of CTA membrane at 18 000 magnification

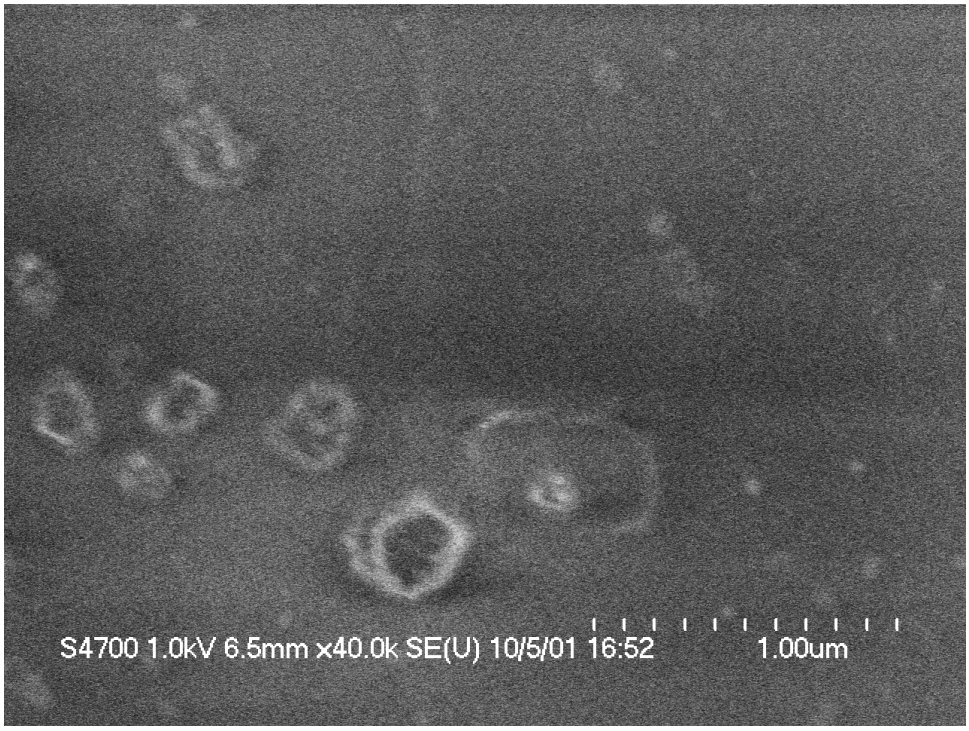

Figure IV-12 Active surface of CTA membrane at 40 000 magnification

FEI Quanta 200F Environmental SEM

Installed in 2004, this state of the art instrument is one of the most sophisticated and versatile electron microscopes in UK geoscience.

Figure IV-13 FEI Quanta 200F

Modes of operation

The Quanta has a Schottky field-emission source gun and three modes of imaging and analysis:

- High vacuum for characterisation of conductive samples,
- Low vacuum (<200 Pa), for analysis of non-conductive samples,
- Environmental mode (<4000 Pa) for studying wet organic or inorganic materials.

ACTIVE LAYER OF SW 30 MEMBRANE

Clean

Figure IV-14 Active surface of SW 30 membrane at 500 magnification

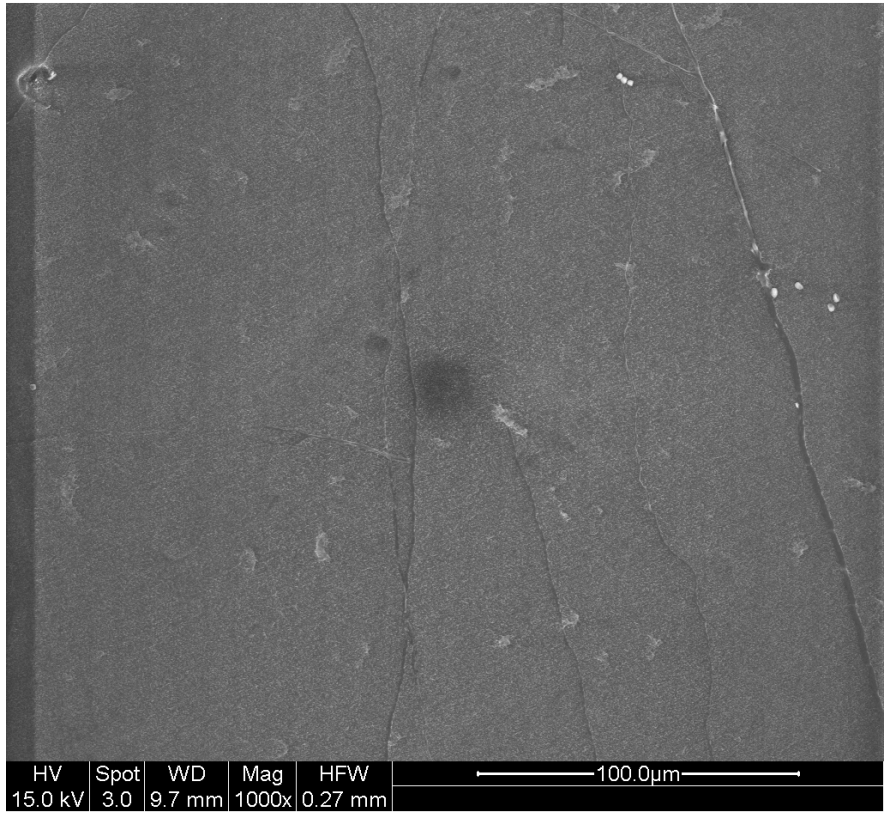

Figure IV-15 Active surface of SW 30 membrane at 1 000 magnification

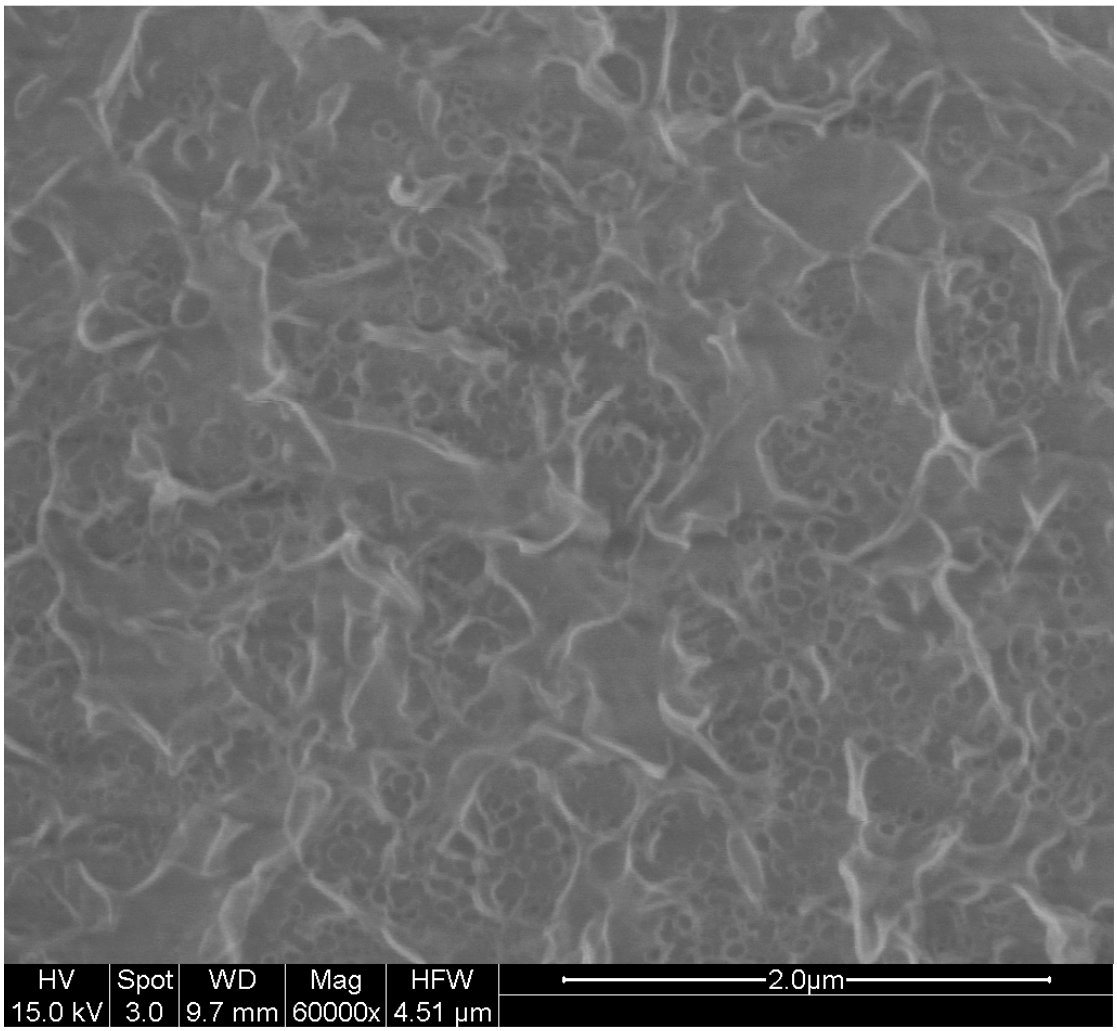

Figure IV-16 Active surface of SW 30 membrane at 60 000 magnification

Hexane

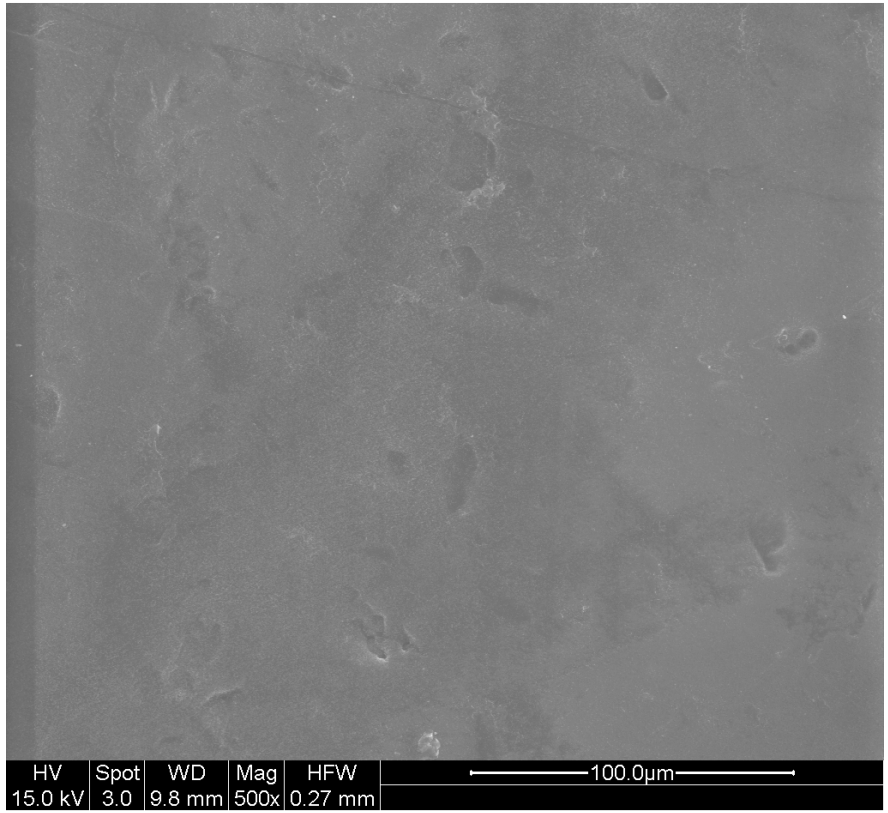

Figure IV-17 Active surface of SW 30 membrane at 500 magnification after exposure to Pure Hexane

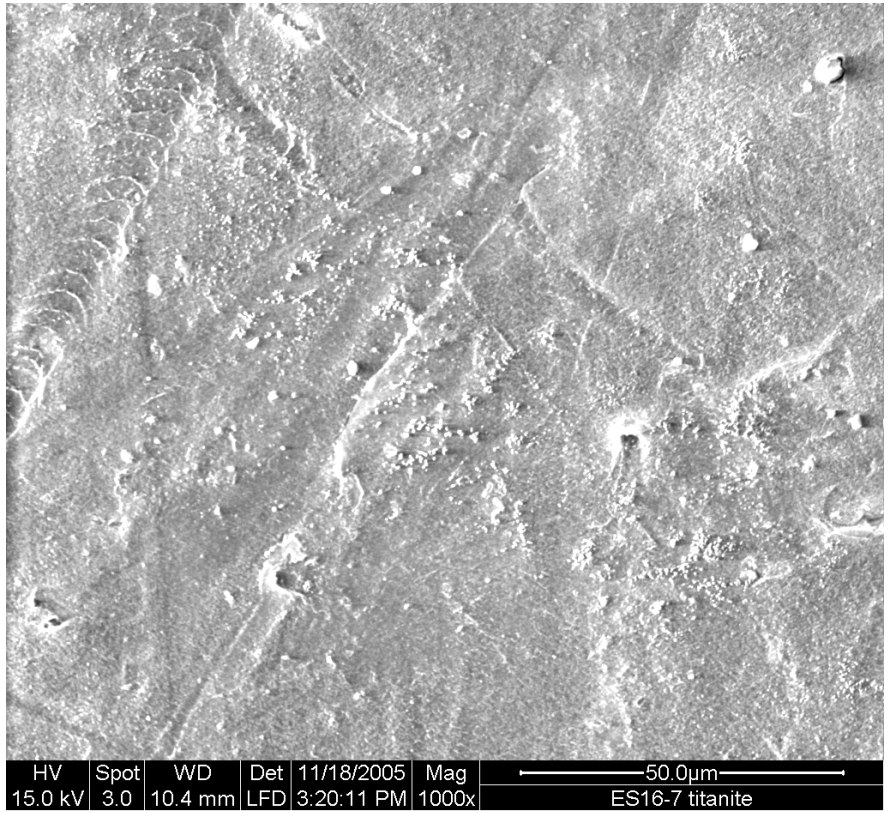

Figure IV-18 Active surface of SW 30 membrane at 1 000 magnification after exposure to Pure Hexane

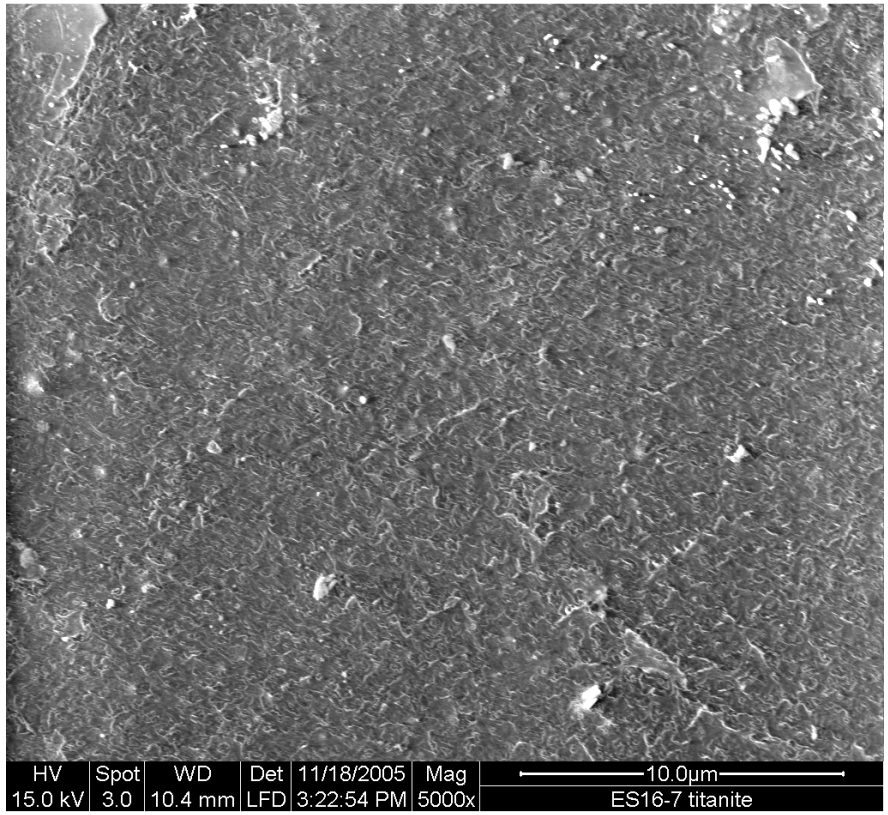

Figure IV-19 Active surface of SW 30 membrane at 5 000 magnification after exposure to Pure Hexane

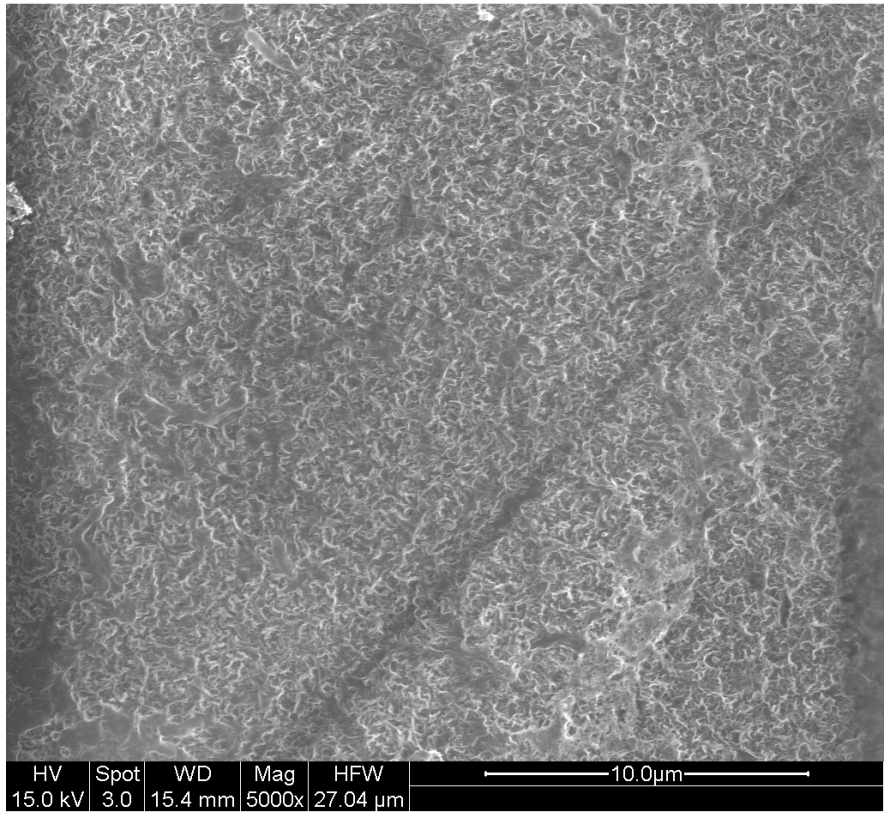

Figure IV-20 Active surface of SW 30 membrane at 5 000 magnification after exposure to Pure Hexane

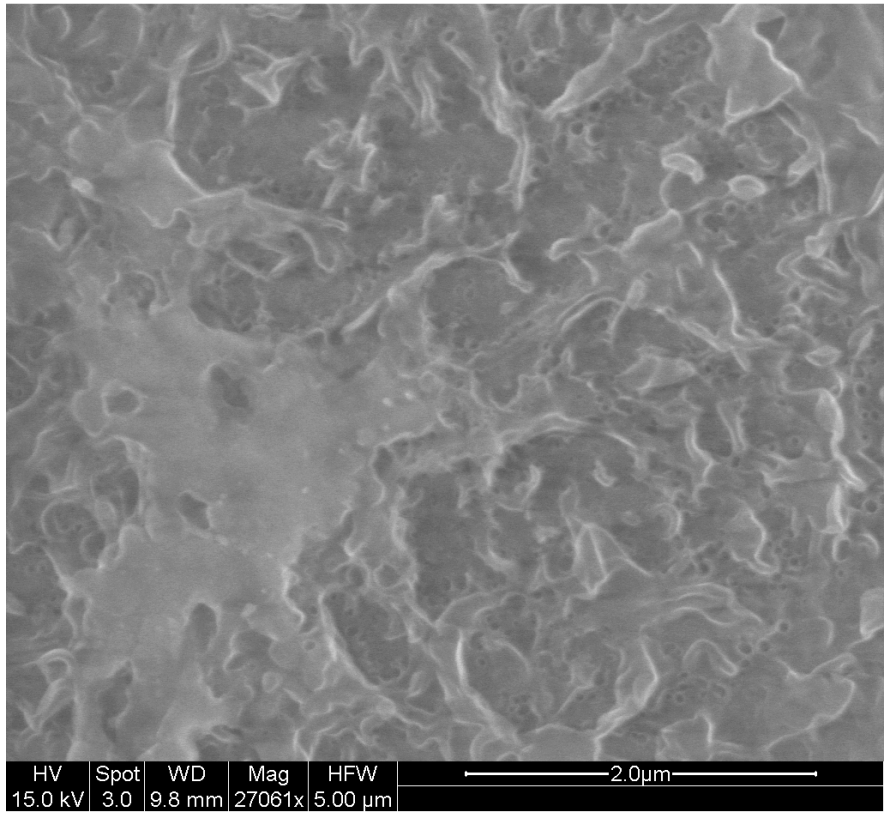

Figure IV-21 Active surface of SW 30 membrane at 27 000 magnification after exposure to Pure Hexane

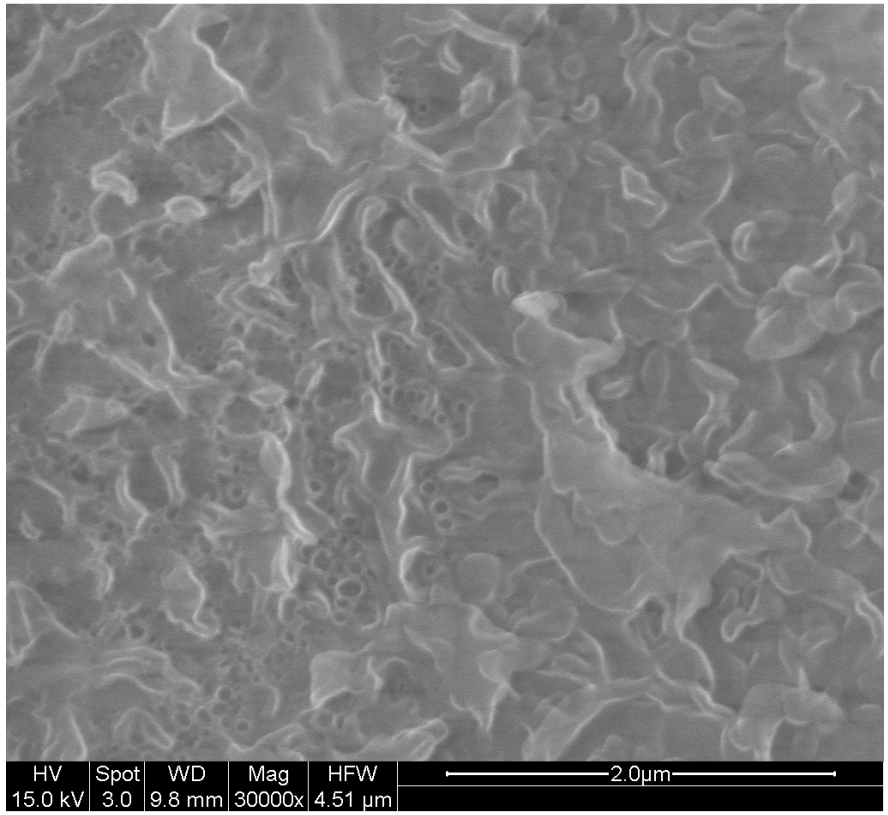

Figure IV-22 Active surface of SW 30 membrane at 30 000 magnification after exposure to Pure Hexane

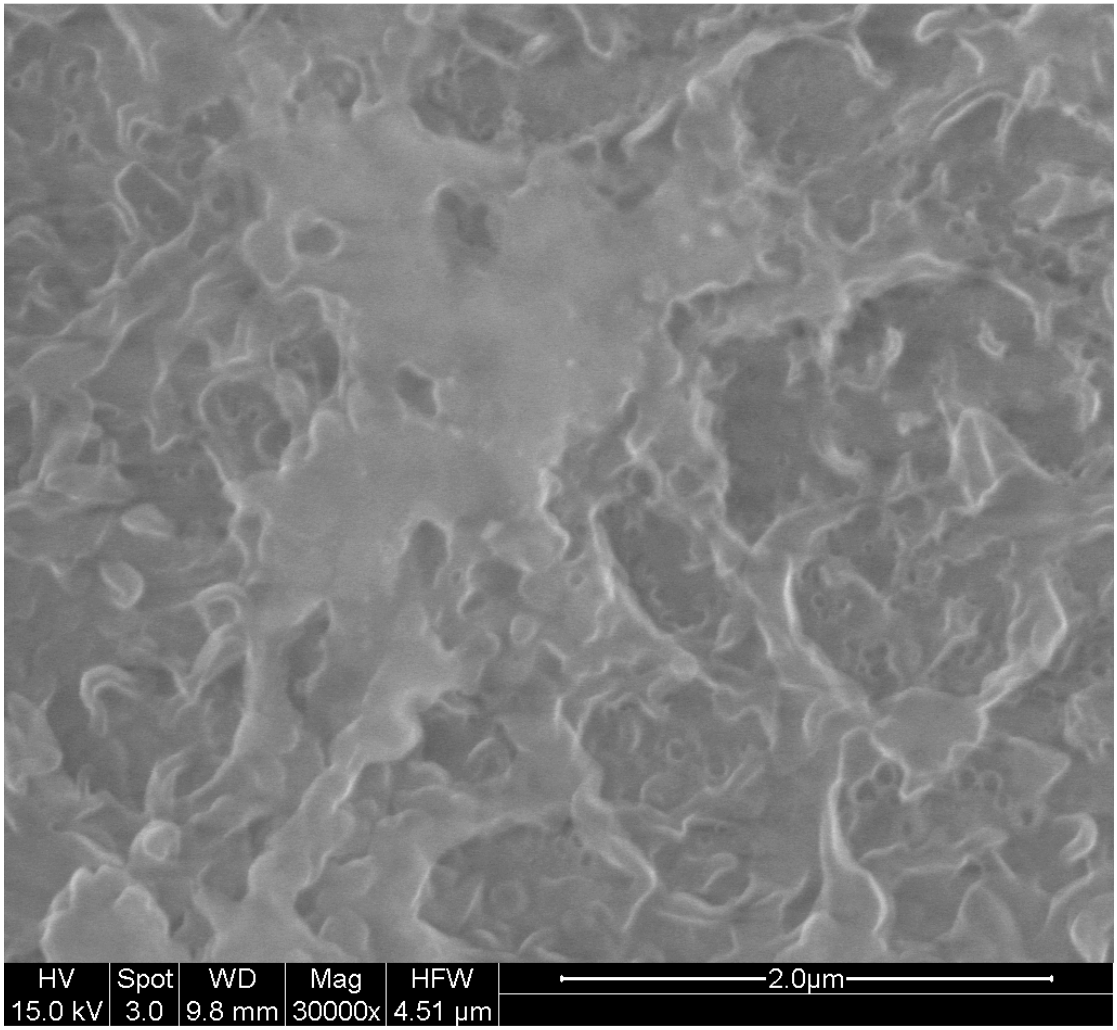

Figure IV-23 Active surface of SW 30 membrane at 30 000 magnification after exposure to Pure Hexane

Diesel

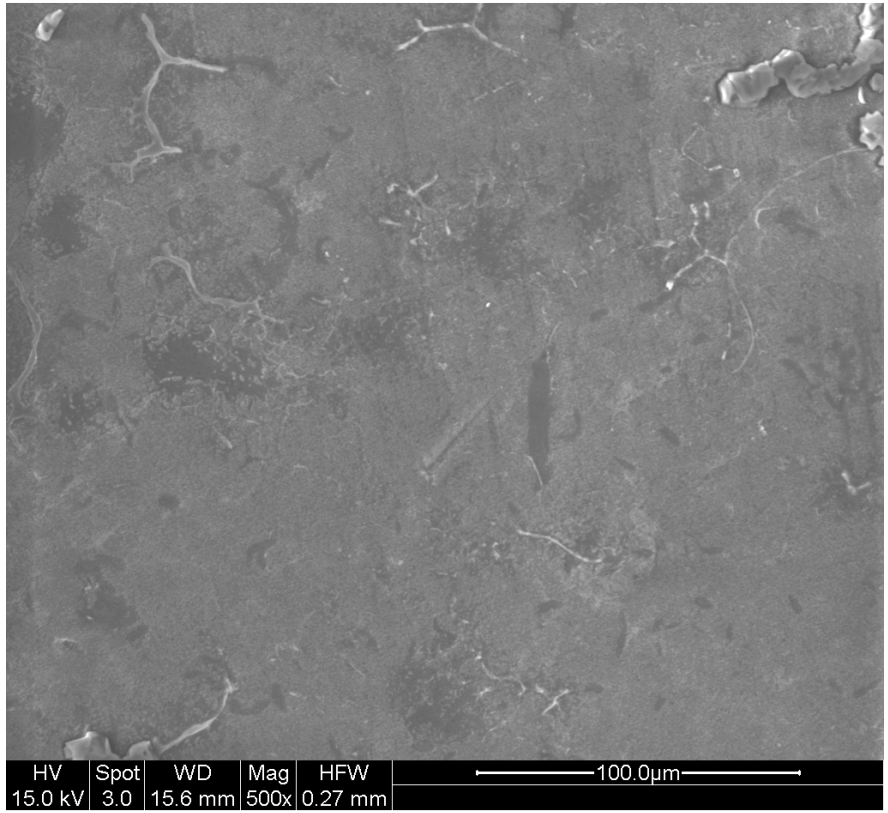

Figure IV-24 Active surface of SW 30 membrane at 500 magnification after exposure to Pure Diesel

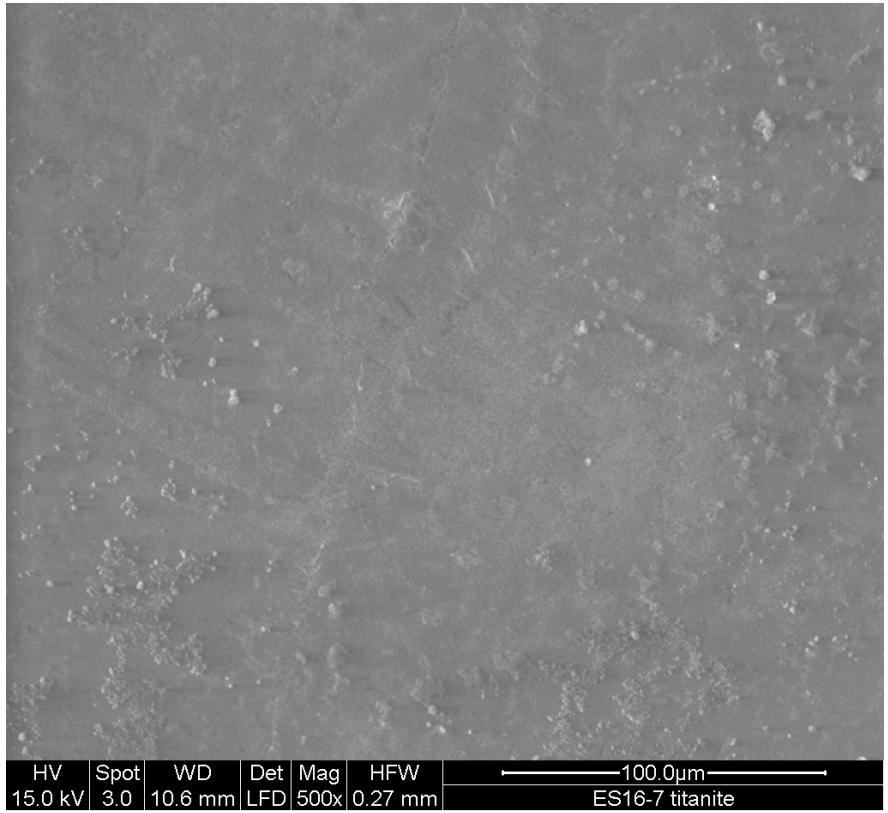

Figure IV-25 Active surface of SW 30 membrane at 500 magnification after exposure to Pure Diesel

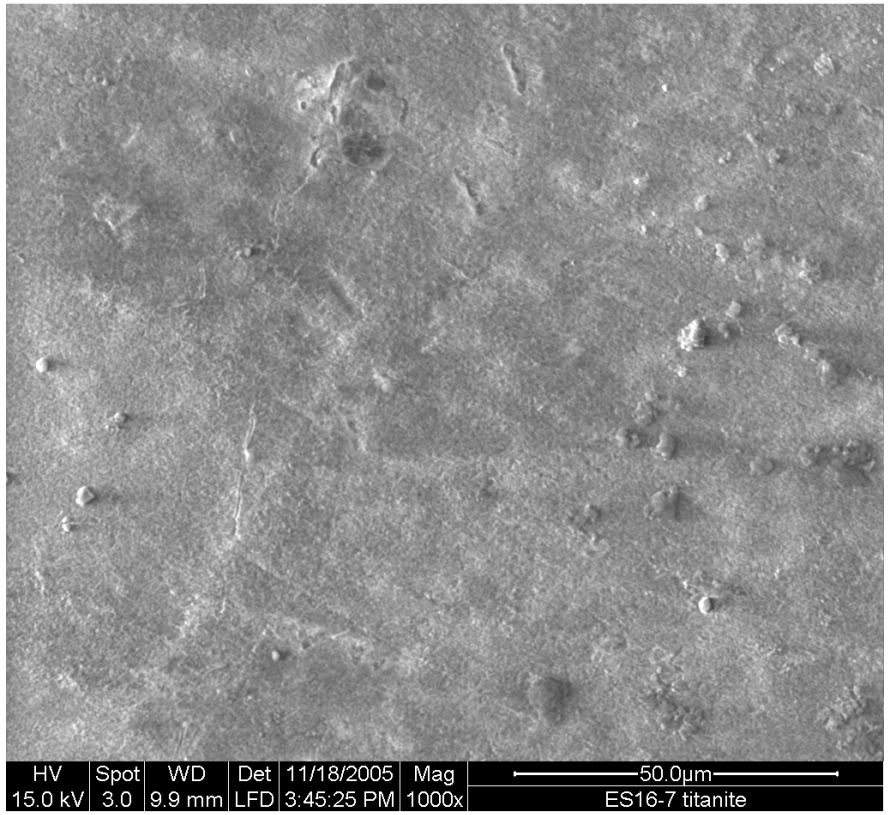

Figure IV-26 Active surface of SW 30 membrane at 1 000 magnification after exposure to Pure Diesel

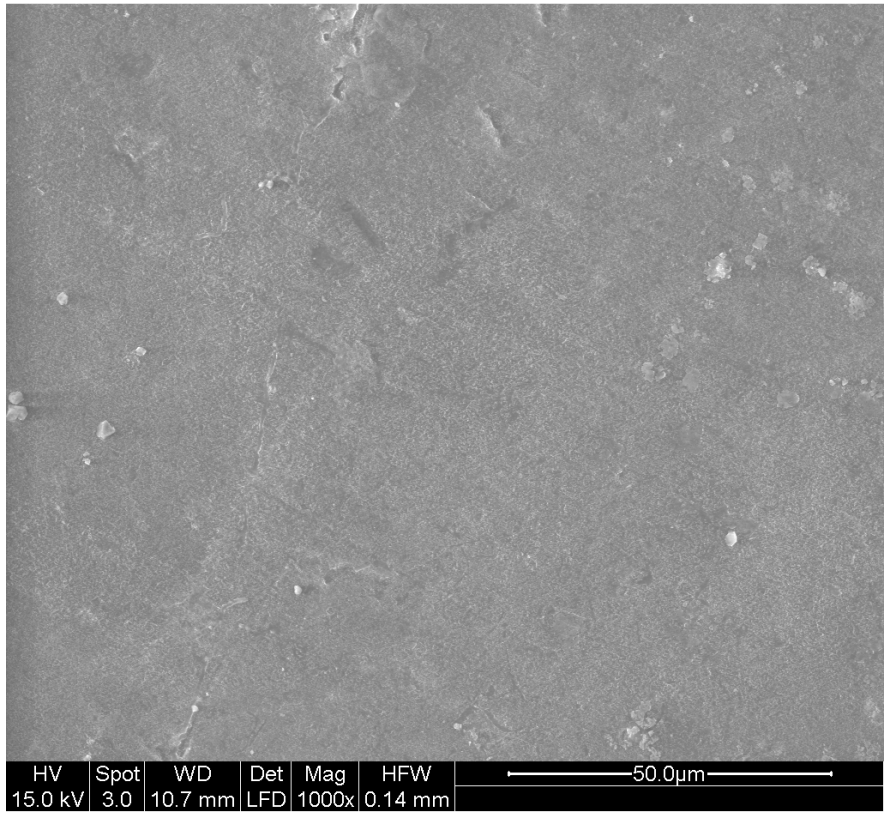

Figure IV-27 Active surface of SW 30 membrane at 1 000 magnification after exposure to Pure Diesel

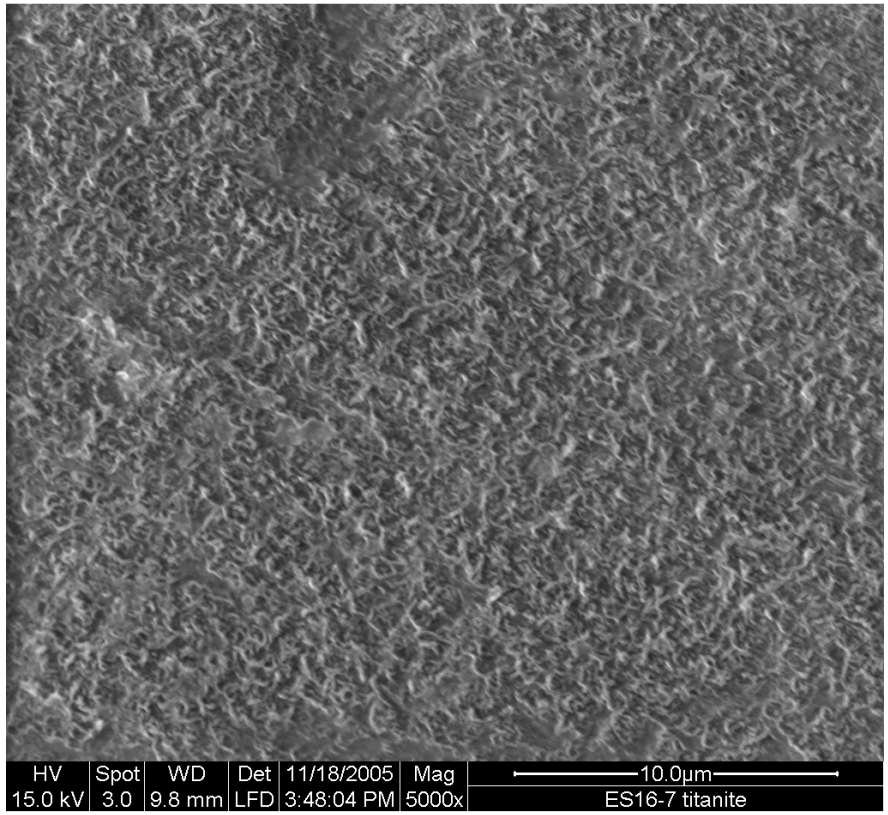

Figure IV-28 Active surface of SW 30 membrane at 5 000 magnification after exposure to Pure Diesel

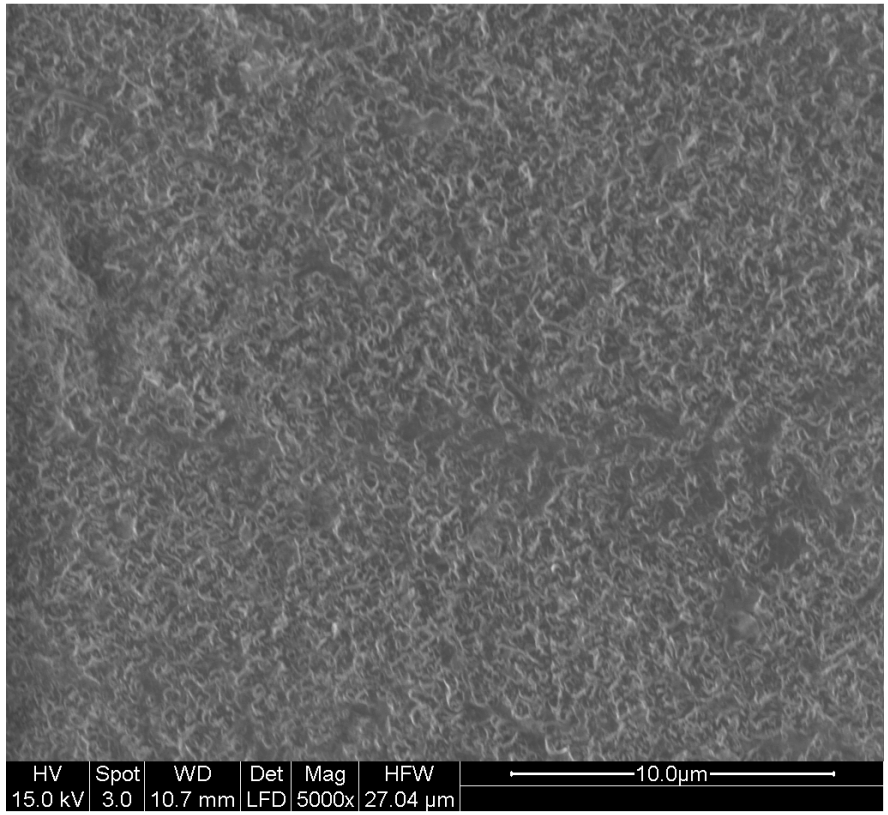

Figure IV-29 Active surface of SW 30 membrane at 5 000 magnification after exposure to Pure Diesel

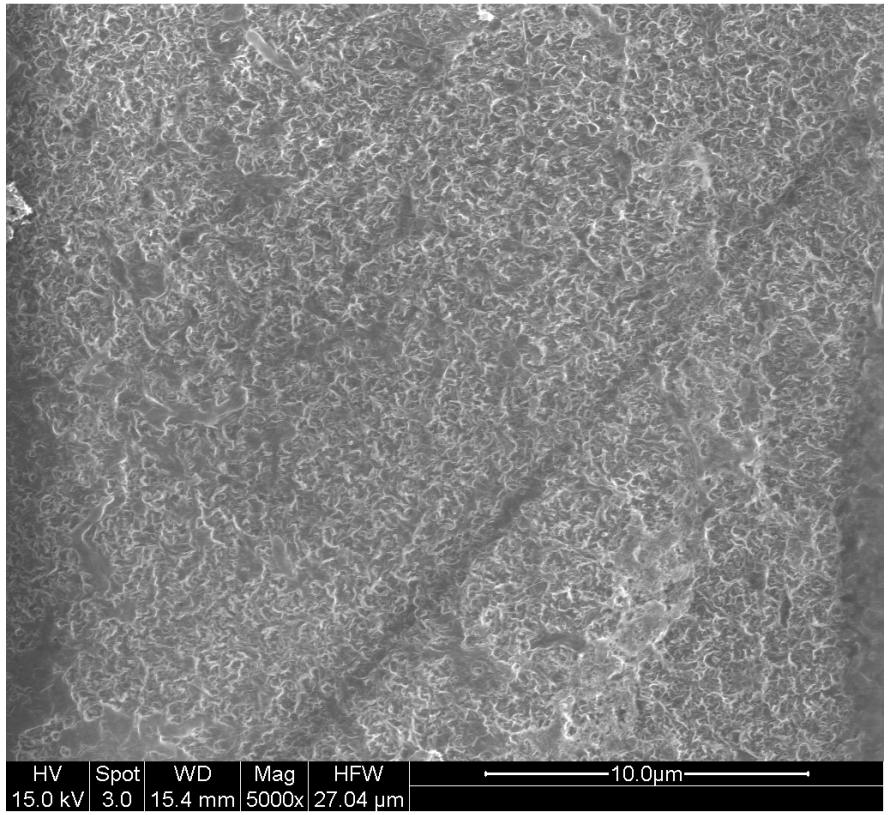

Figure IV-30 Active surface of SW 30 membrane at 5 000 magnification after exposure to Pure Diesel

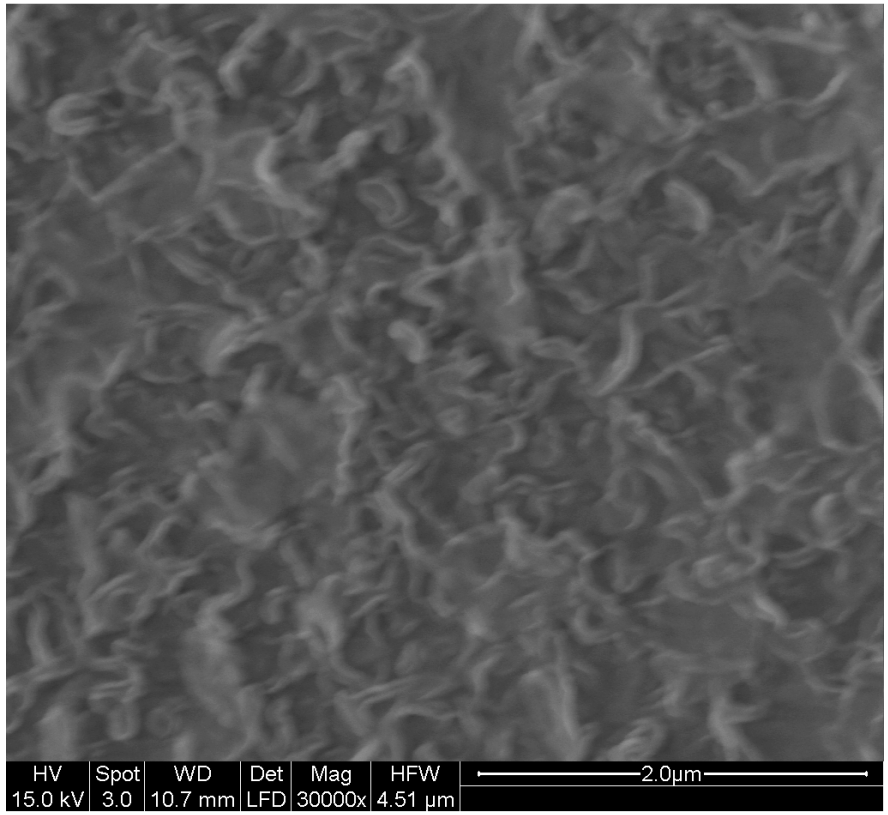

Figure IV-31 Active surface of SW 30 membrane at 30 000 magnification after exposure to Pure Diesel

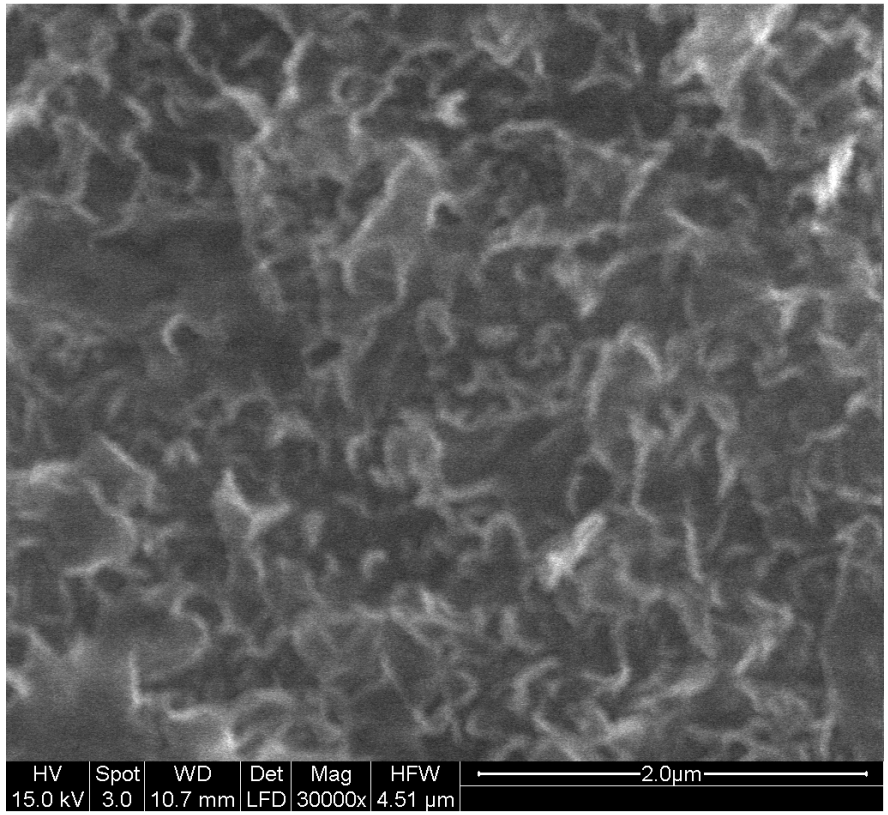

Figure IV-32 Active surface of SW 30 membrane at 30 000 magnification after exposure to Pure Diesel

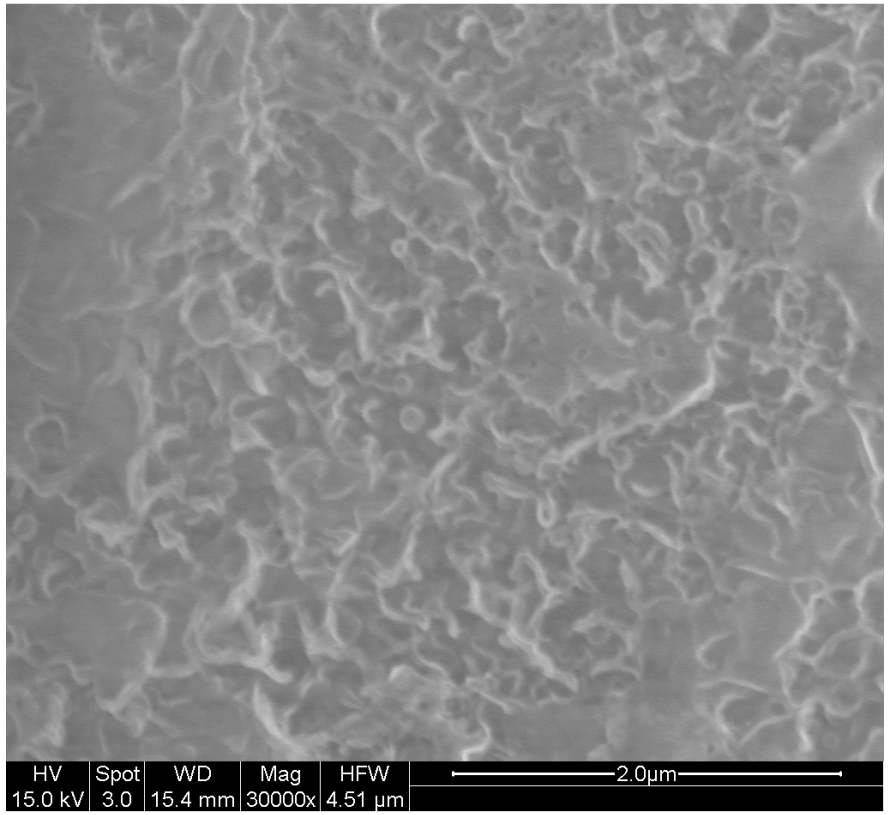

Figure IV-33 Active surface of SW 30 membrane at 30 000 magnification after exposure to Pure Diesel

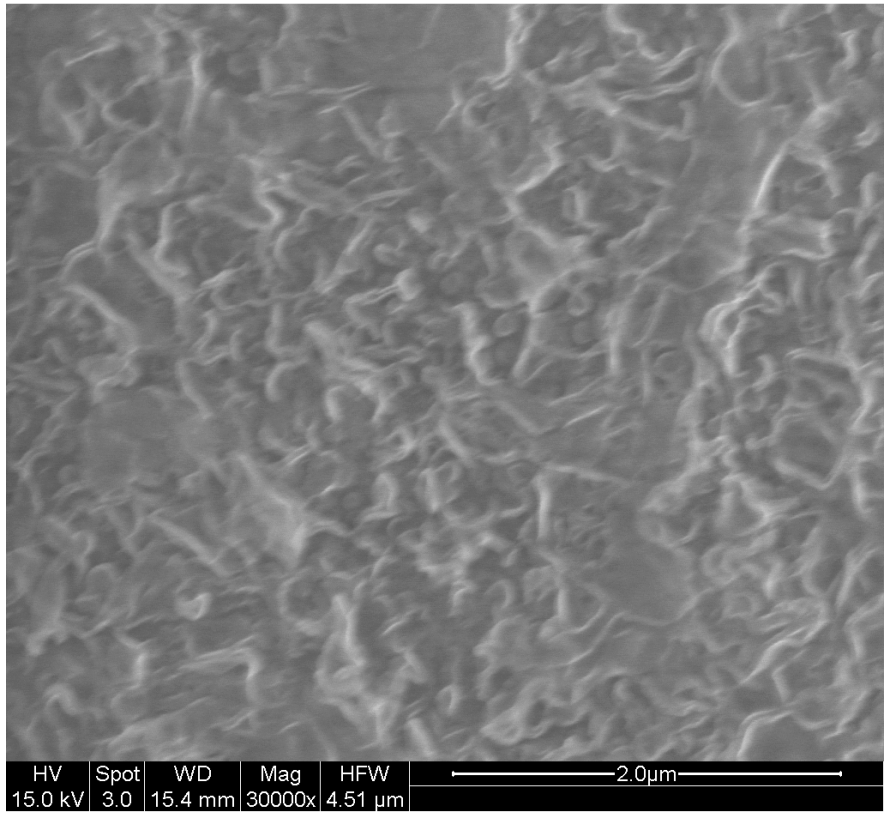

Figure IV-34 Active surface of SW 30 membrane at 30 000 magnification after exposure to Pure Diesel

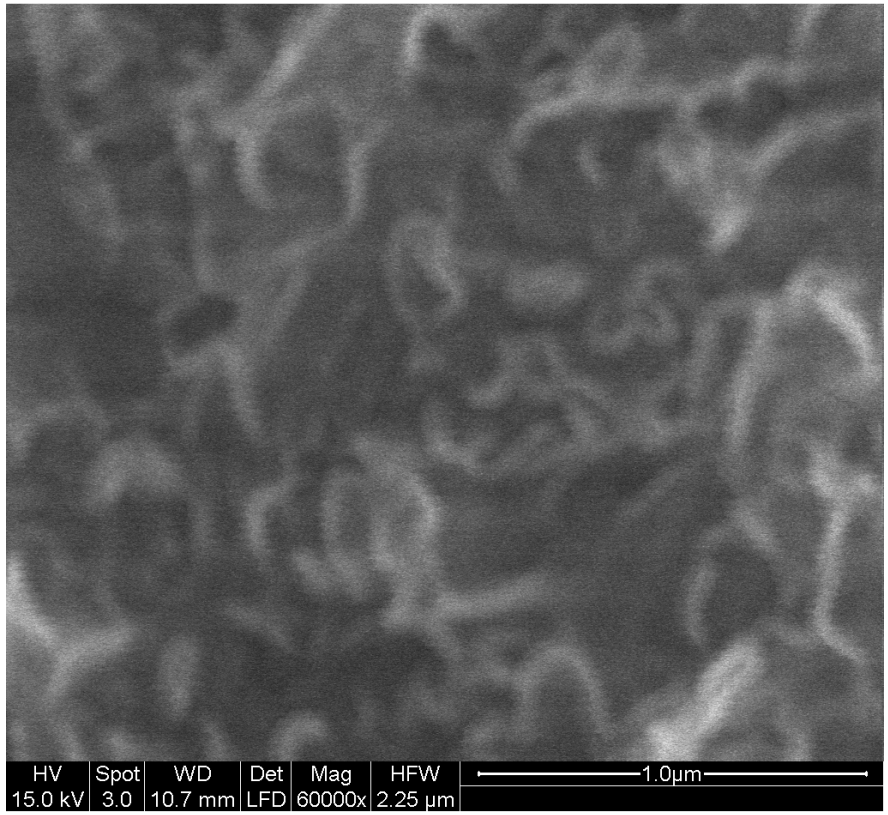

Figure IV-35 Active surface of SW 30 membrane at 30 000 magnification after exposure to Pure Diesel

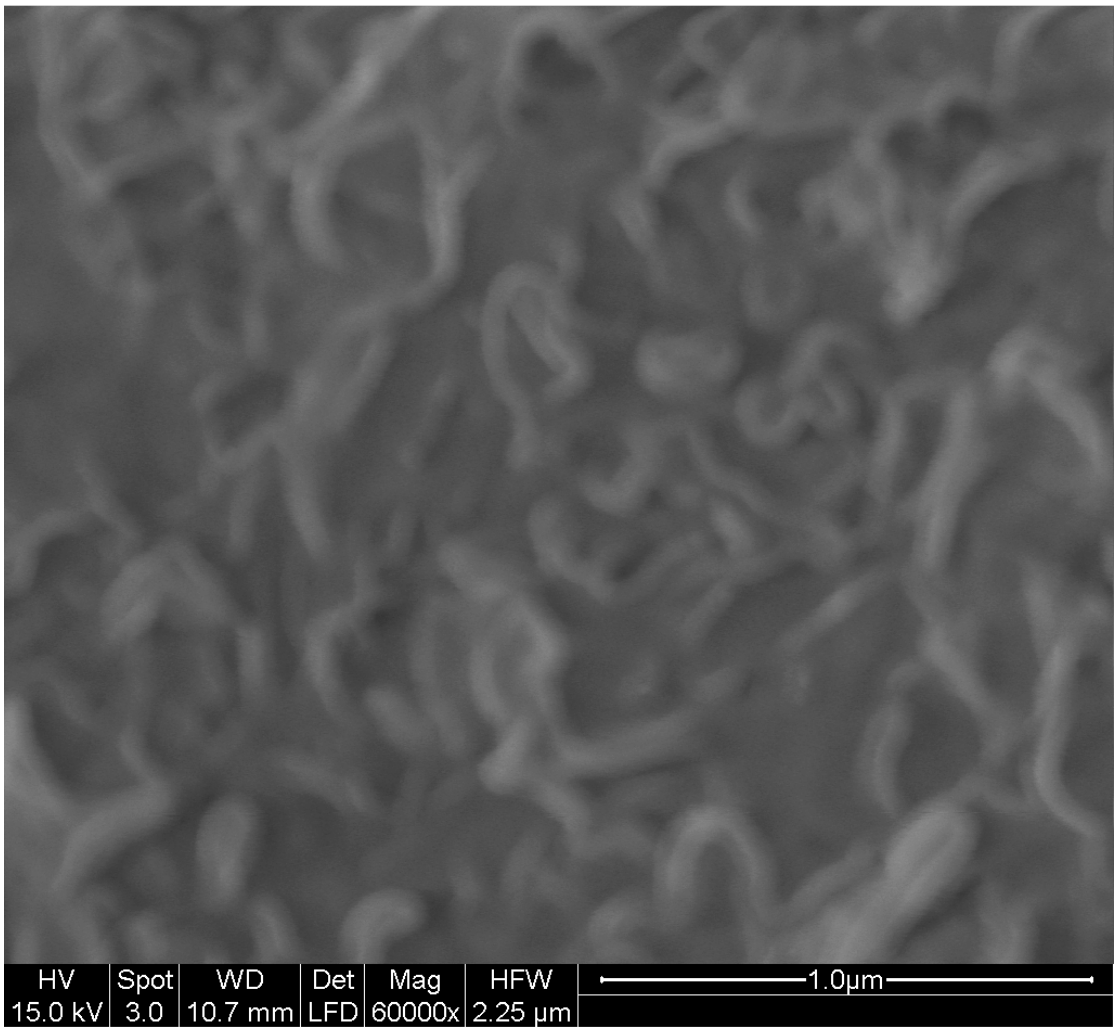

Figure IV-36 Active surface of SW 30 membrane at 60 000 magnification after exposure to Pure Diesel

POLYSULPHONE INTERLAYER OF SW 30 MEMBRANE

Clean

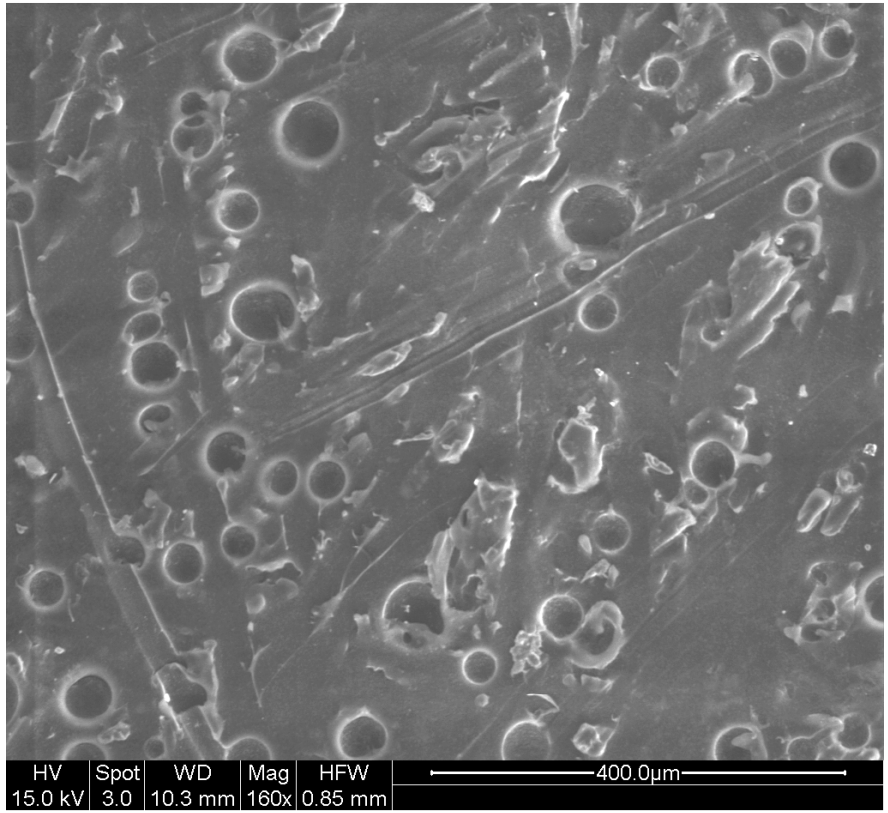

Figure IV-37 Surface of interlayer of New SW 30 membrane at 160 magnification

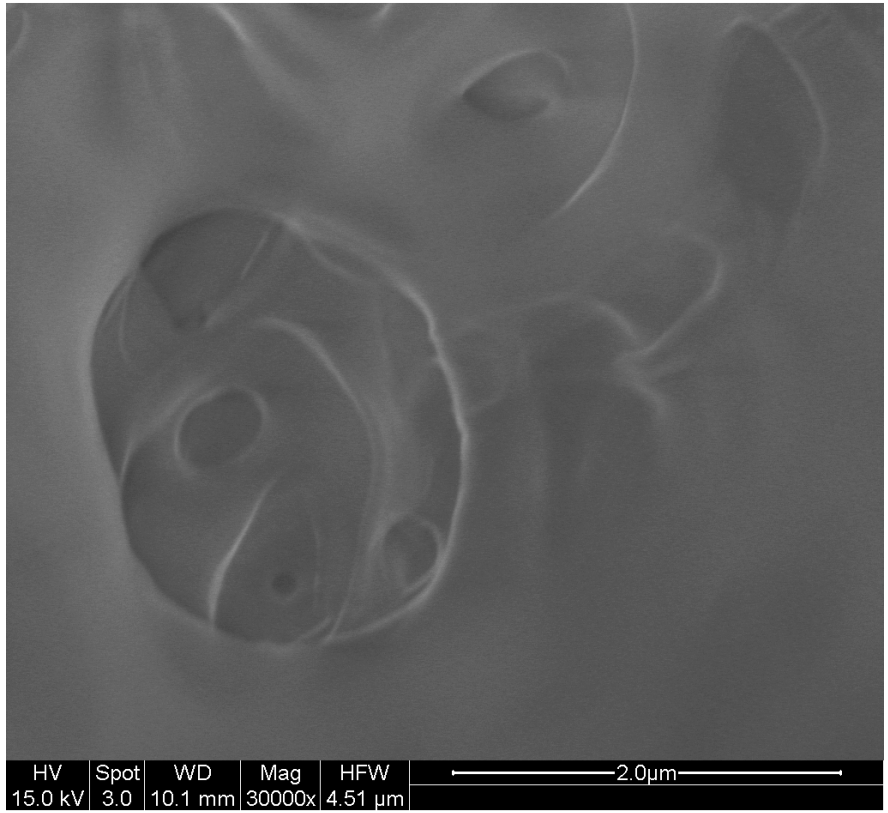

Figure IV-38 Surface of interlayer of New SW 30 membrane exposed to Hexane at 30 000 magnification

Hexane

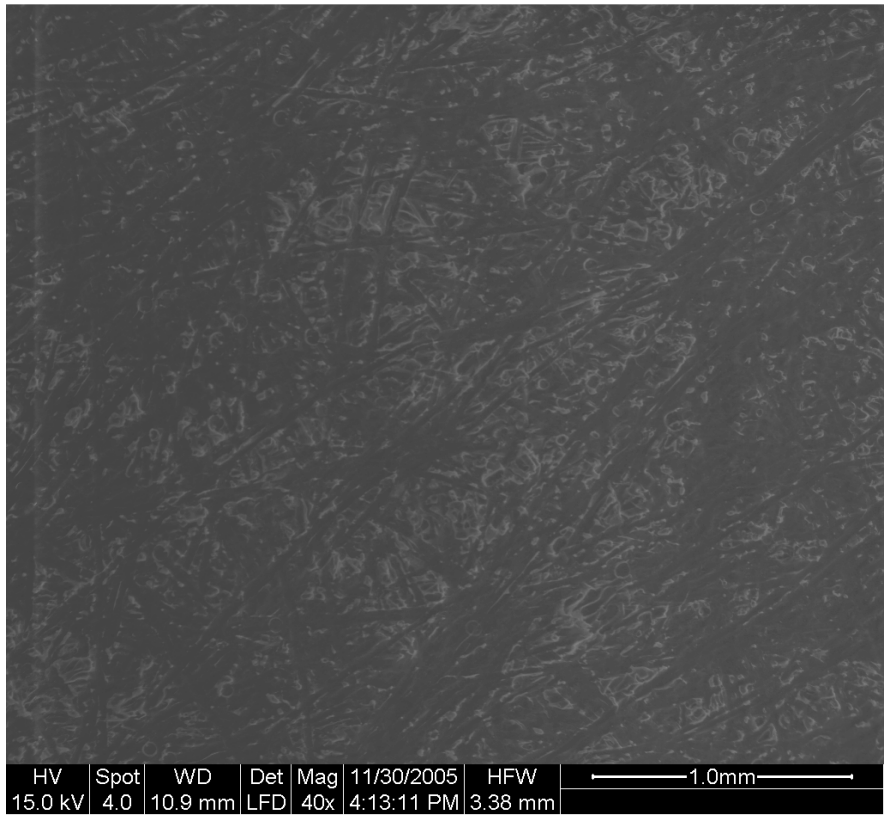

Figure IV-39 Surface of interlayer of SW 30 membrane exposed to Hexane at 40 magnification

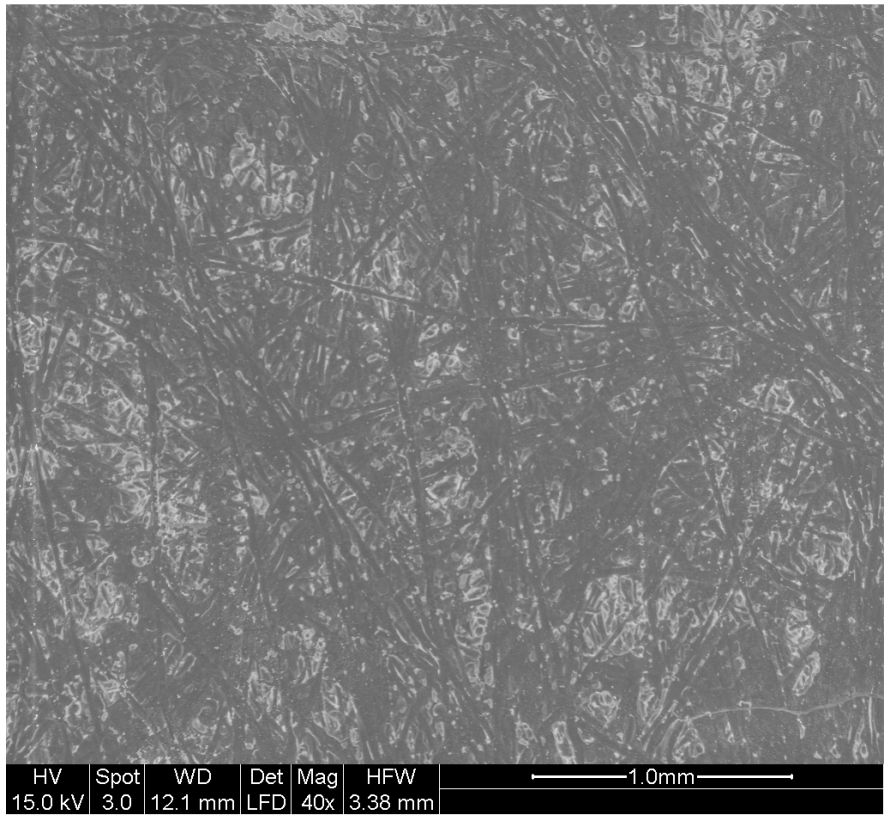

Figure IV-40 Surface of interlayer of SW 30 membrane exposed to Hexane at 40 magnification

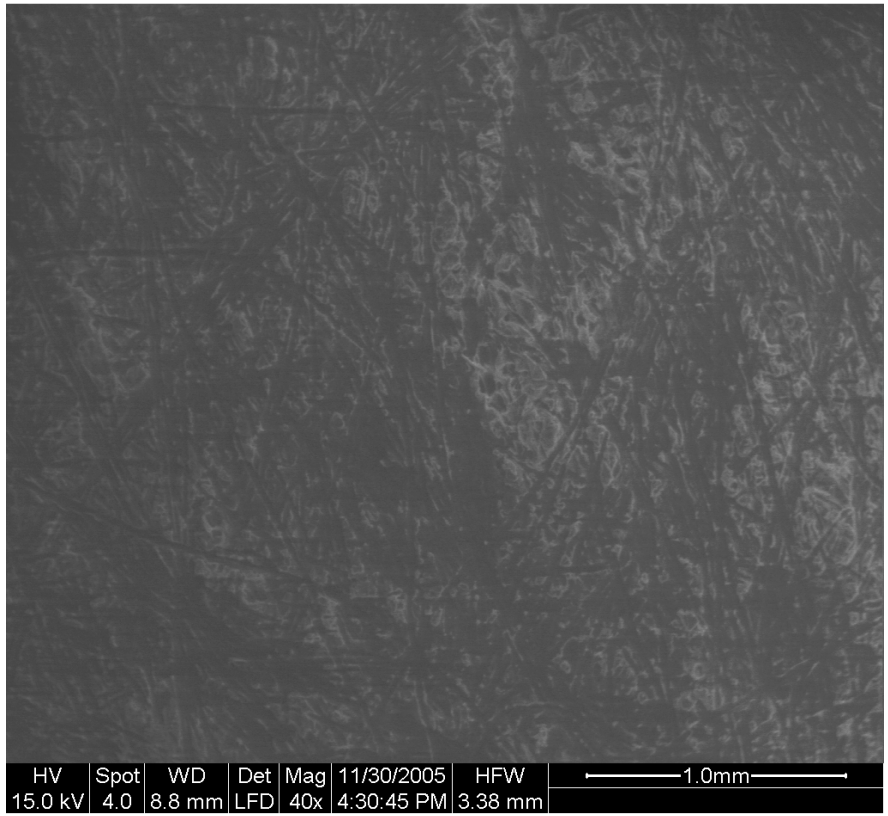

Figure IV-41 Surface of interlayer of SW 30 membrane exposed to Hexane at 40 magnification

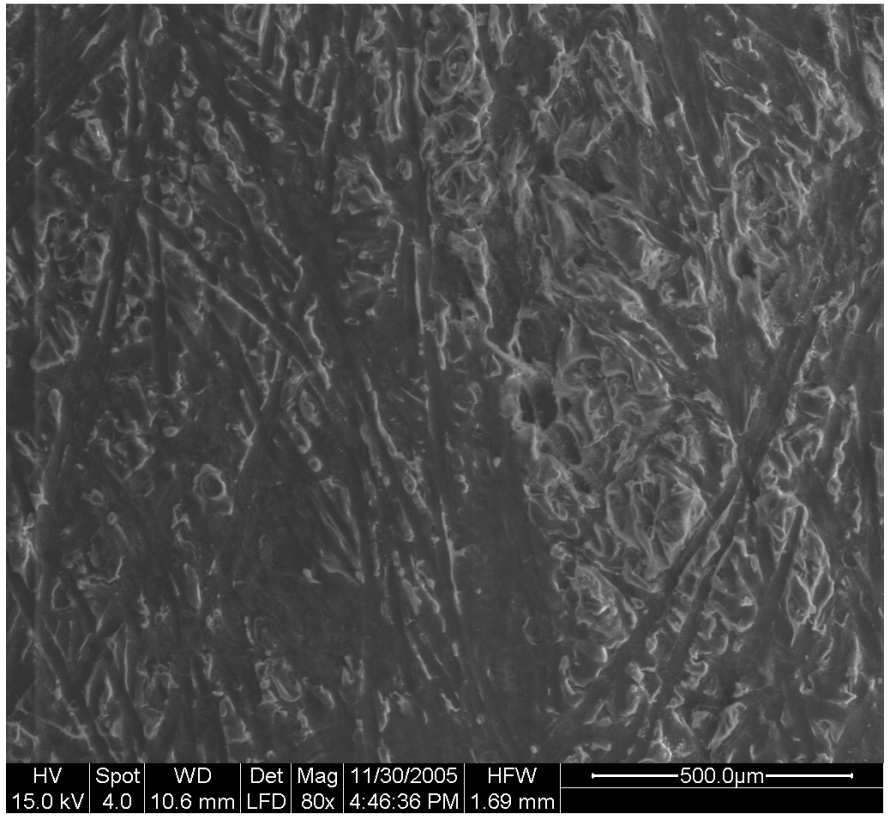

Figure IV-42 Surface of interlayer of SW 30 membrane exposed to Hexane at 80 magnification

Figure IV-43 Surface of interlayer of SW 30 membrane exposed to Hexane at 500 magnification

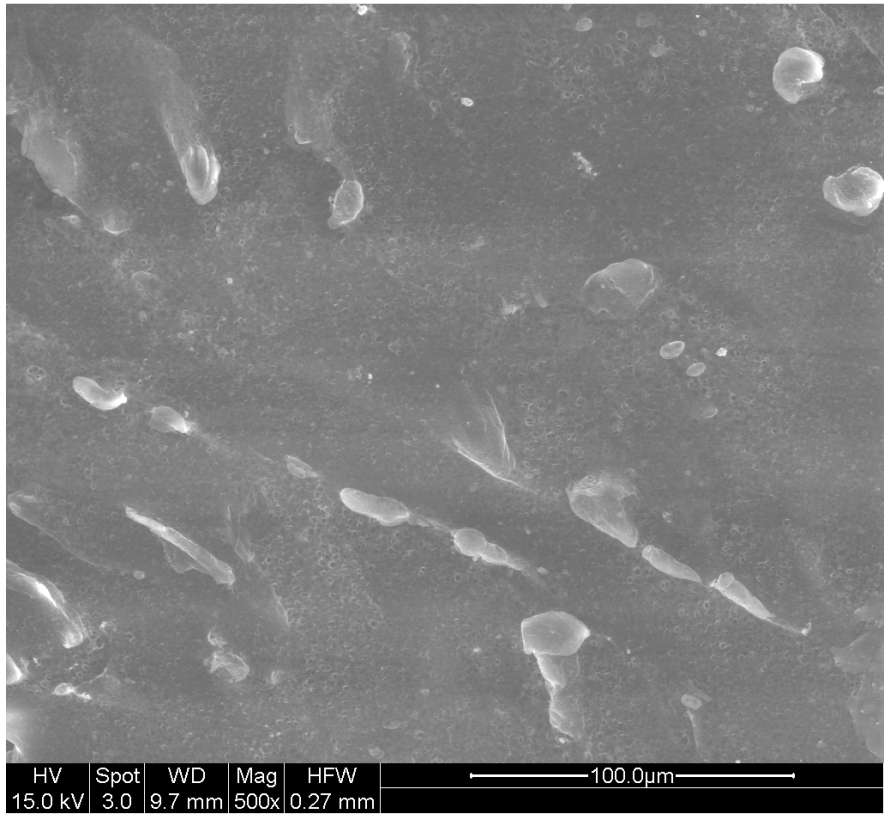

Figure IV-44 Surface of interlayer of SW 30 membrane exposed to Hexane at 500 magnification

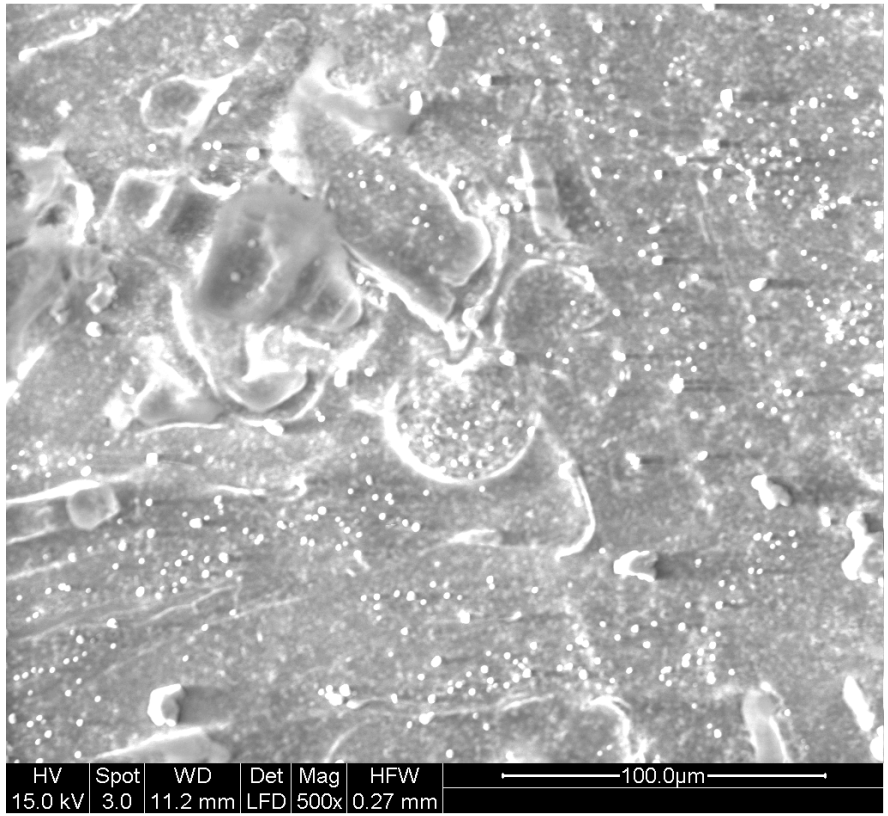

Figure IV-45 Surface of interlayer of SW 30 membrane exposed to Hexane at 500 magnification

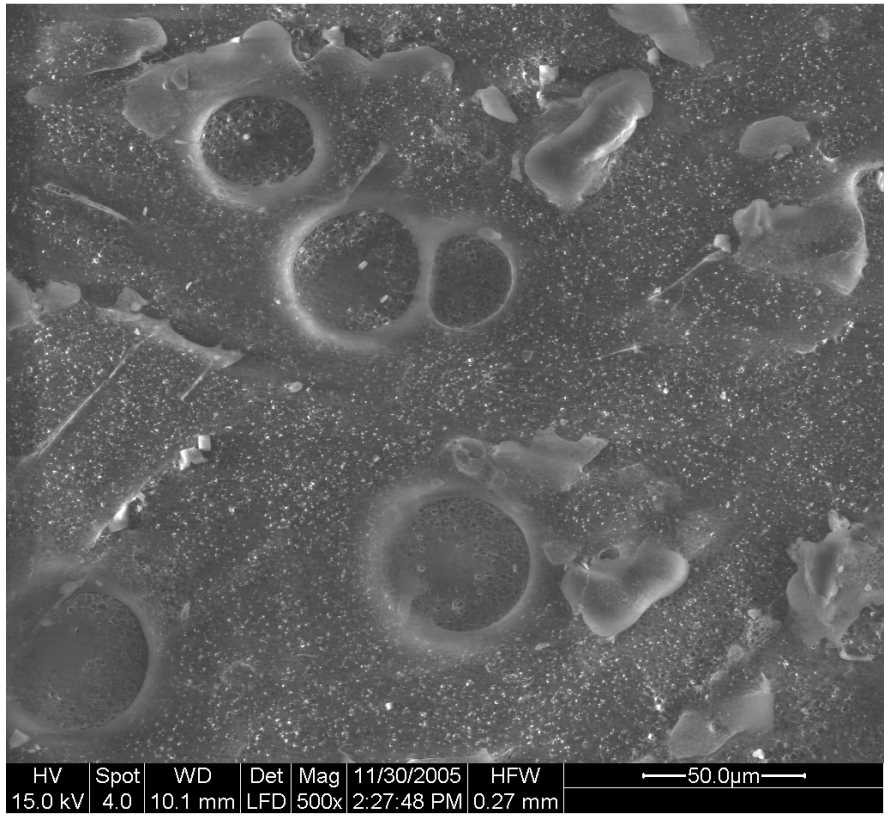

Figure IV-46 Surface of interlayer of SW 30 membrane exposed to Hexane at 500 magnification

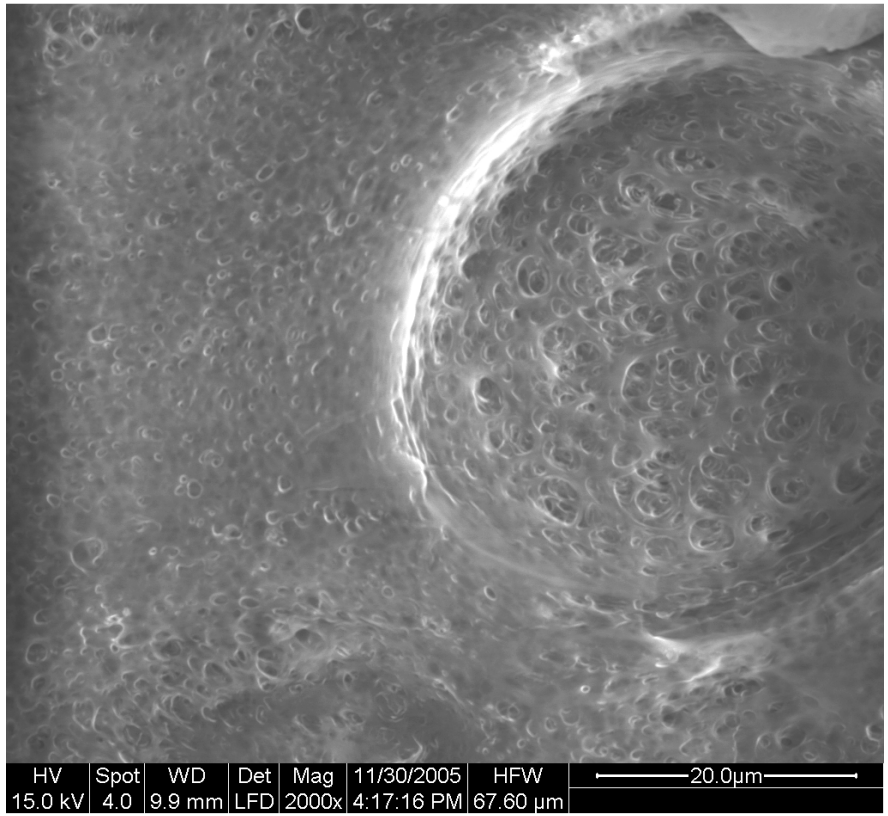

Figure IV-47 Surface of interlayer of SW 30 membrane exposed to Hexane at 2 000 magnification

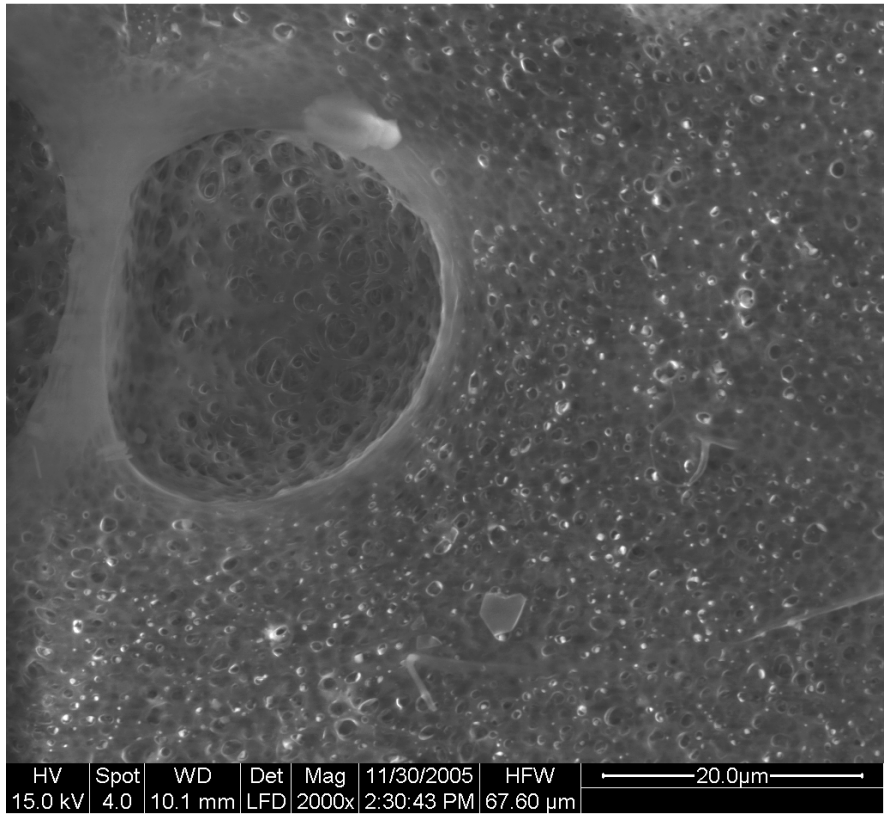

Figure IV-48 Surface of interlayer of SW 30 membrane exposed to Hexane at 2 000 magnification

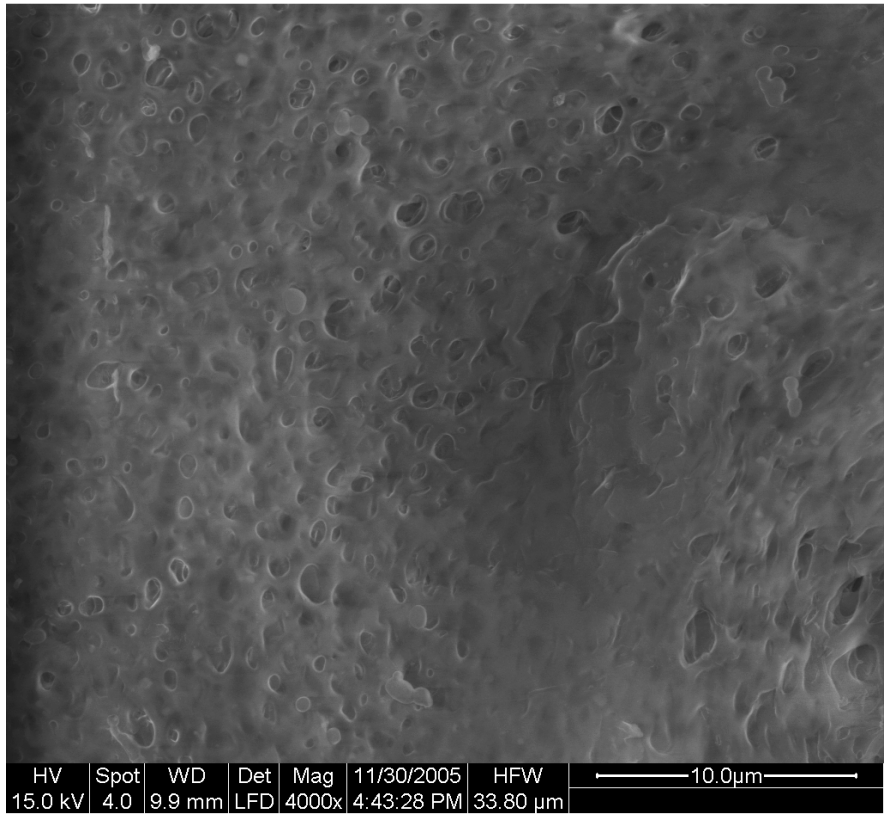

Figure IV-49 Surface of interlayer of SW 30 membrane exposed to Hexane at 4 000 magnification

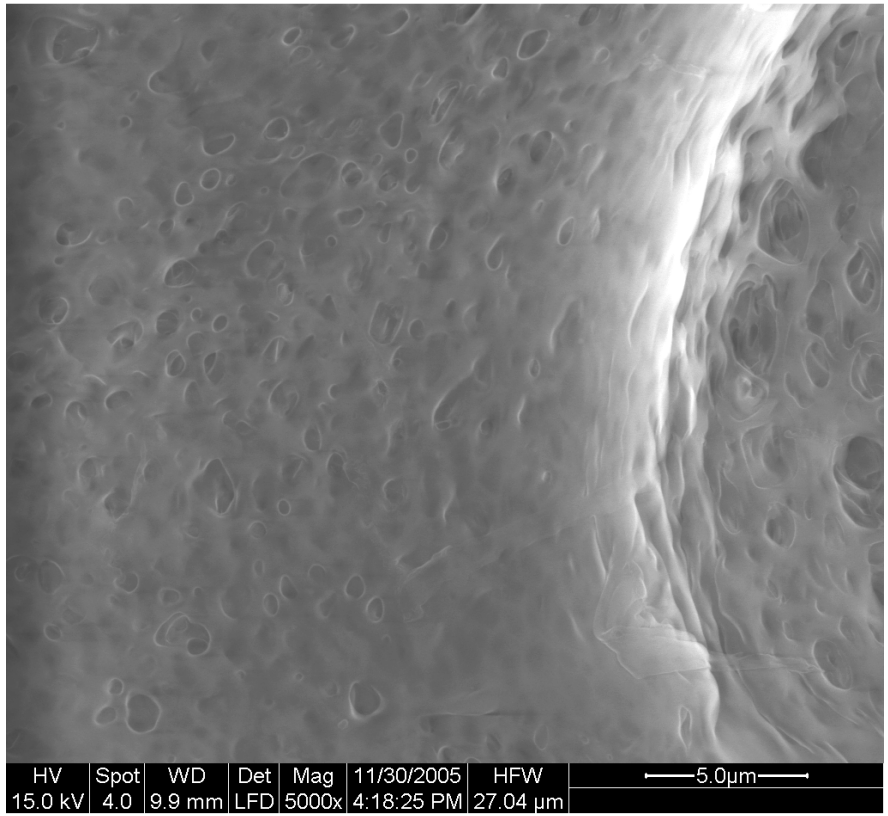

Figure IV-50 Surface of interlayer of SW 30 membrane exposed to Hexane at 5 000 magnification

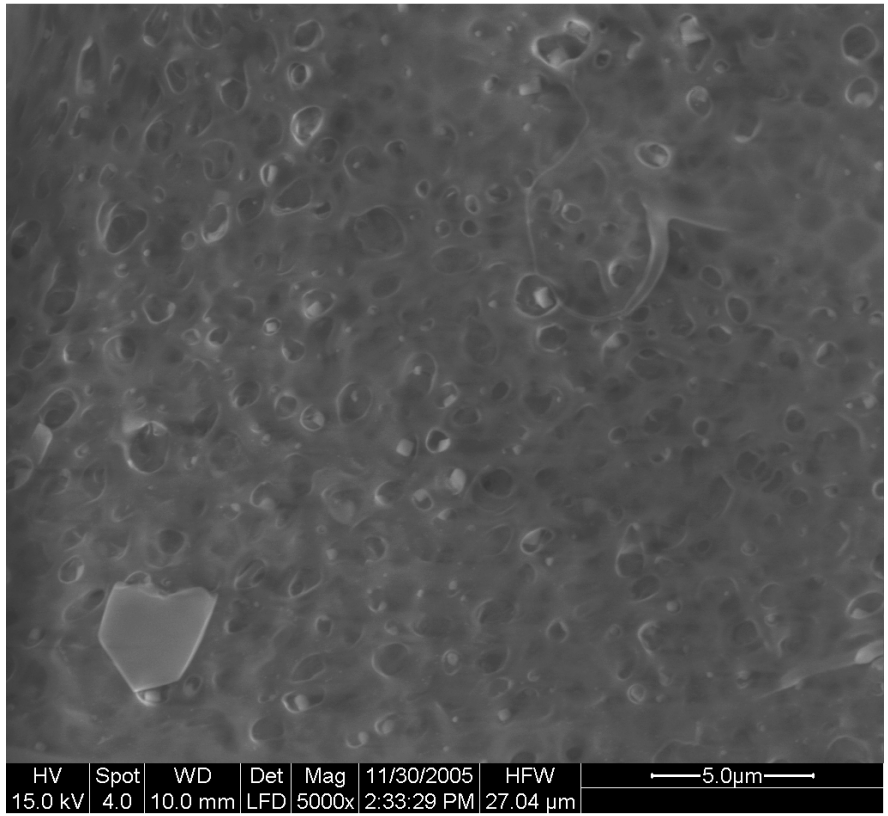

Figure IV-51 Surface of interlayer of SW 30 membrane exposed to Hexane at 5 000 magnification

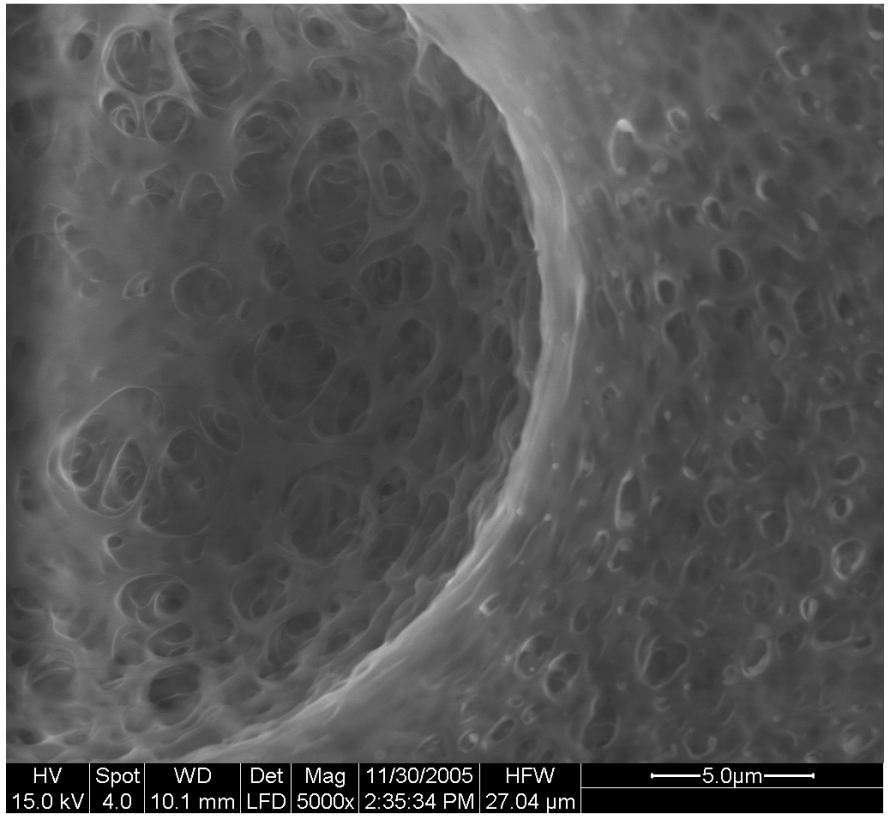

Figure IV-52 Surface of interlayer of SW 30 membrane exposed to Hexane at 5 000 magnification

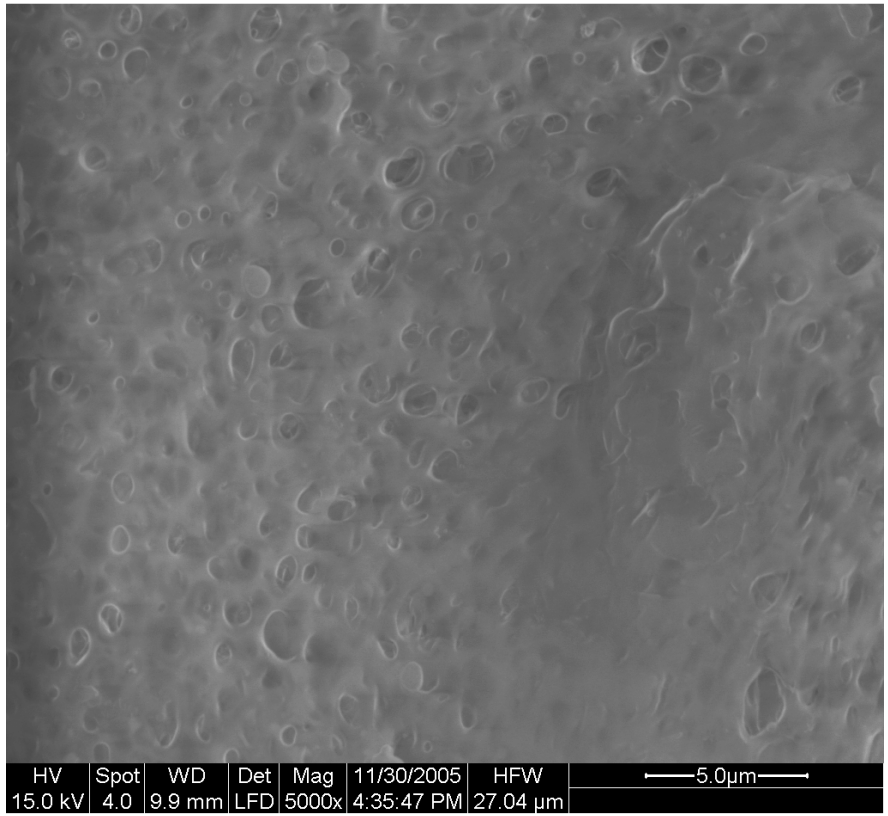

Figure IV-53 Surface of interlayer of SW 30 membrane exposed to Hexane at 5 000 magnification

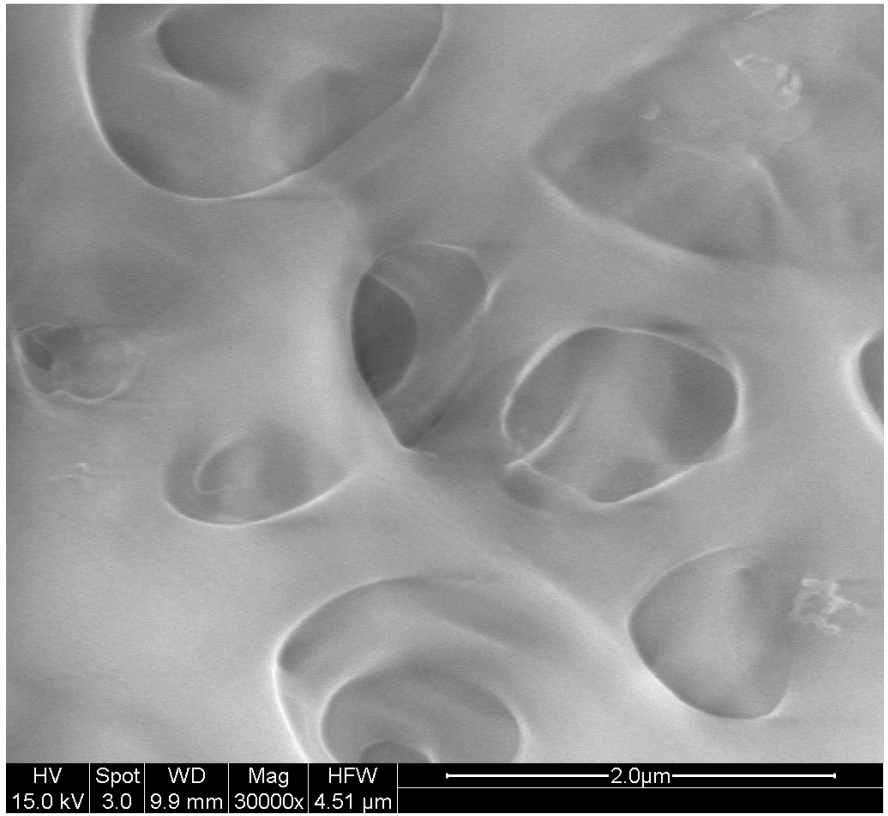

Figure IV-54 Surface of interlayer of SW 30 membrane exposed to Hexane at 30 000 magnification

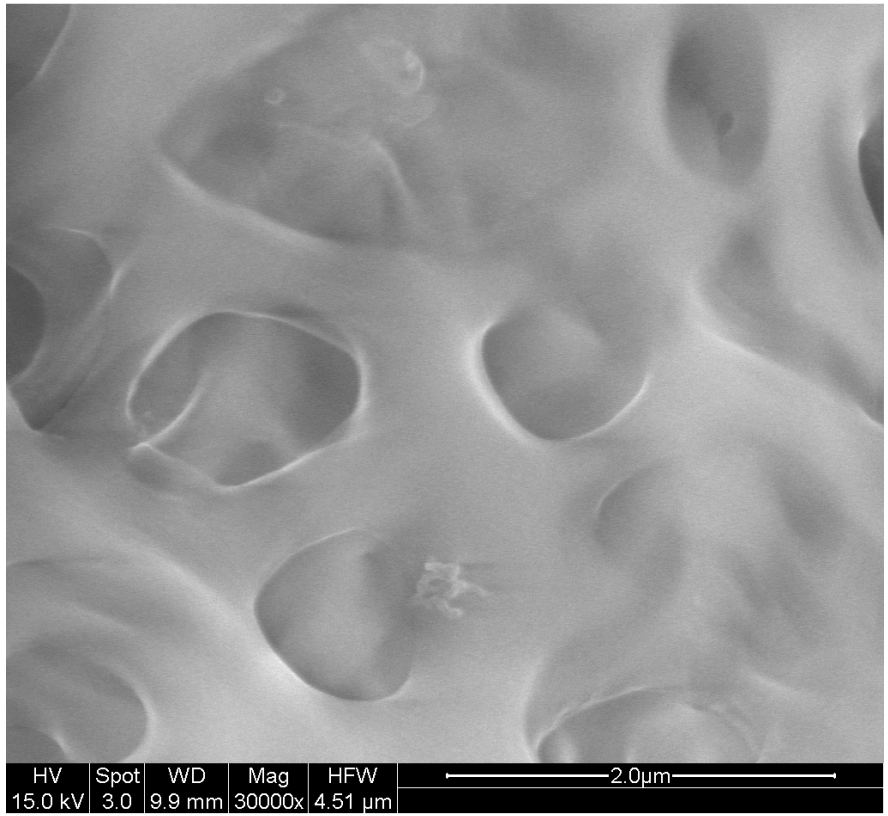

Figure IV-55 Surface of interlayer of SW 30 membrane exposed to Hexane at 30 000 magnification

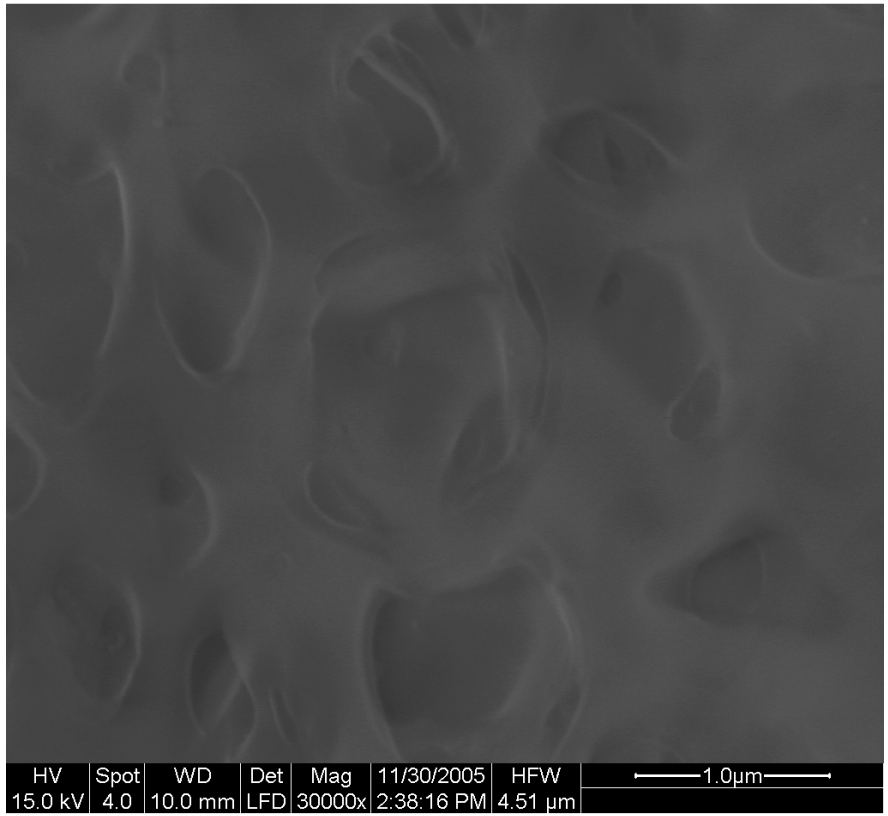

Figure IV-56 Surface of interlayer of SW 30 membrane exposed to Hexane at 30 000 magnification

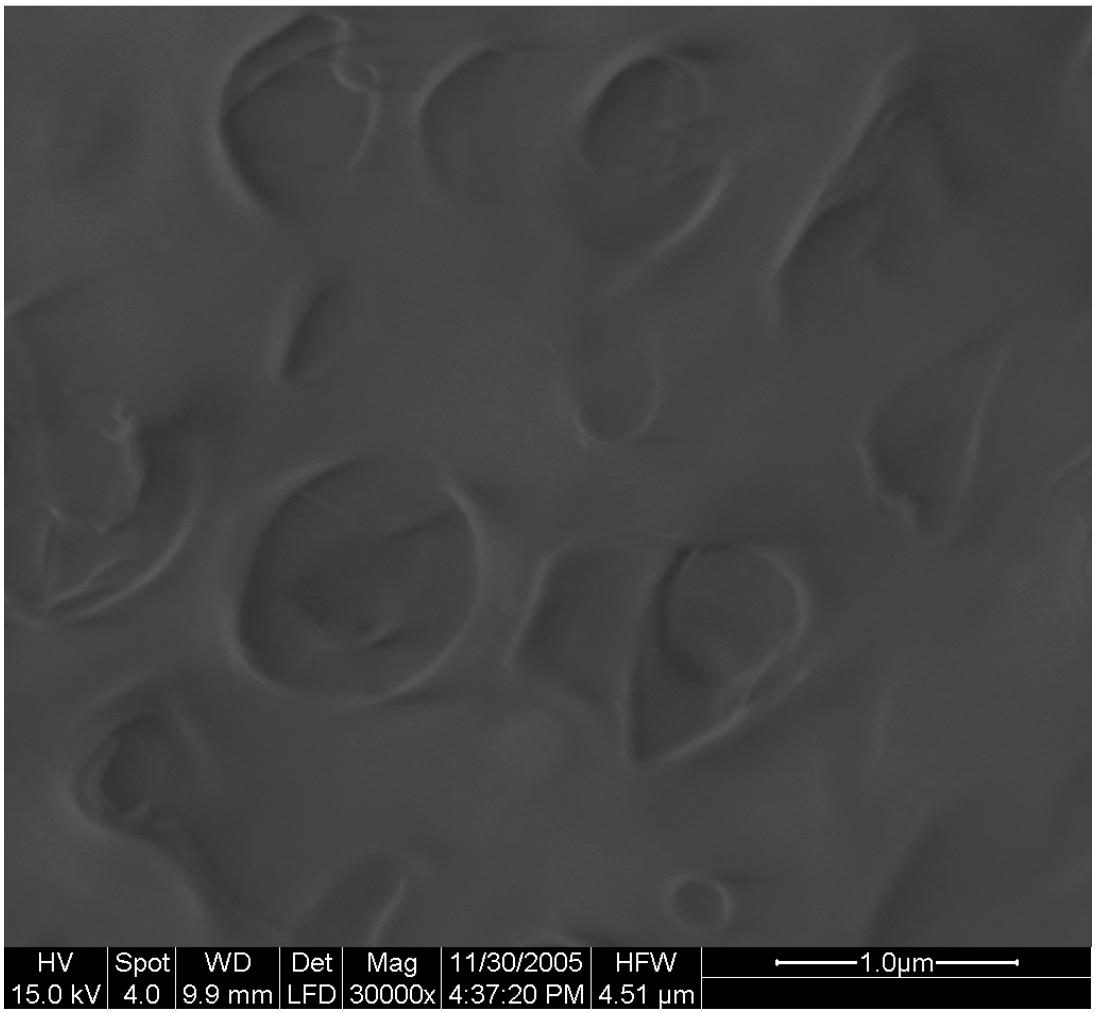

Figure IV-57 Surface of interlayer of SW 30 membrane exposed to Hexane at 30 000 magnification

Diesel

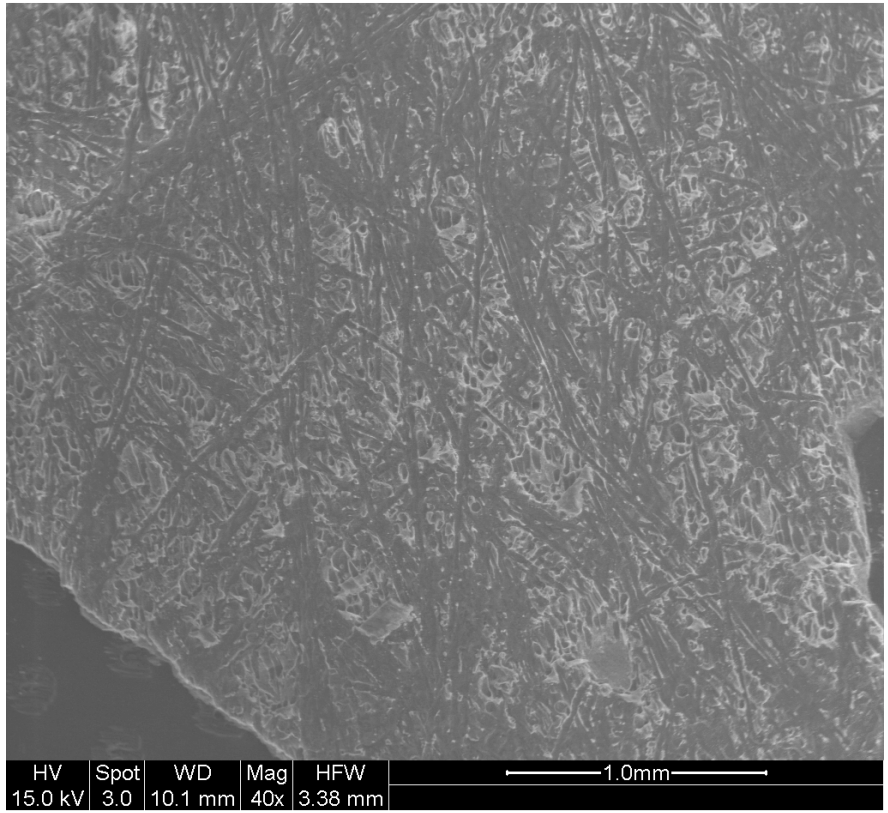

Figure IV-58 Surface of interlayer of SW 30 membrane exposed to Diesel at 40 magnification

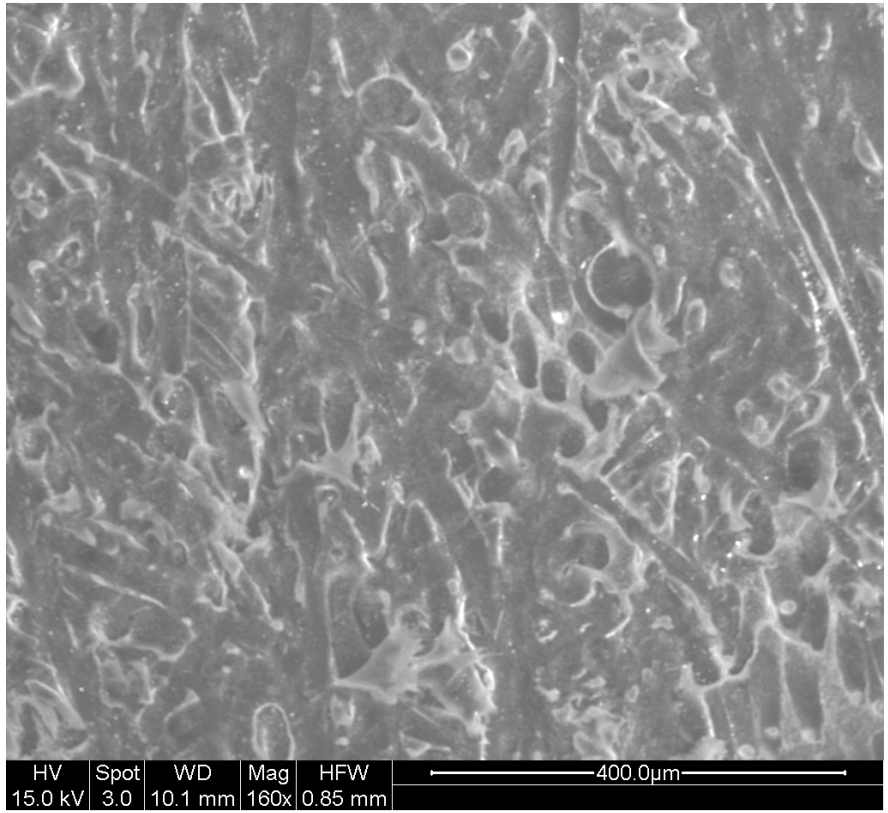

Figure IV-59 Surface of interlayer of SW 30 membrane exposed to Diesel at 160 magnification

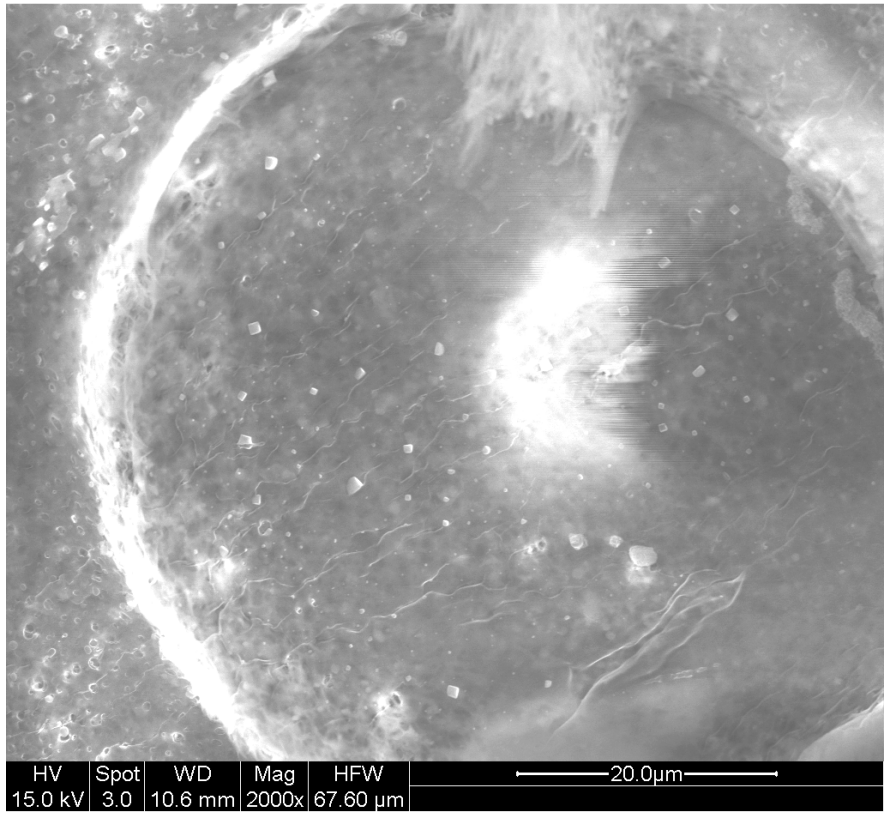

Figure IV-60 Surface of interlayer of SW 30 membrane exposed to Diesel at 2 000 magnification

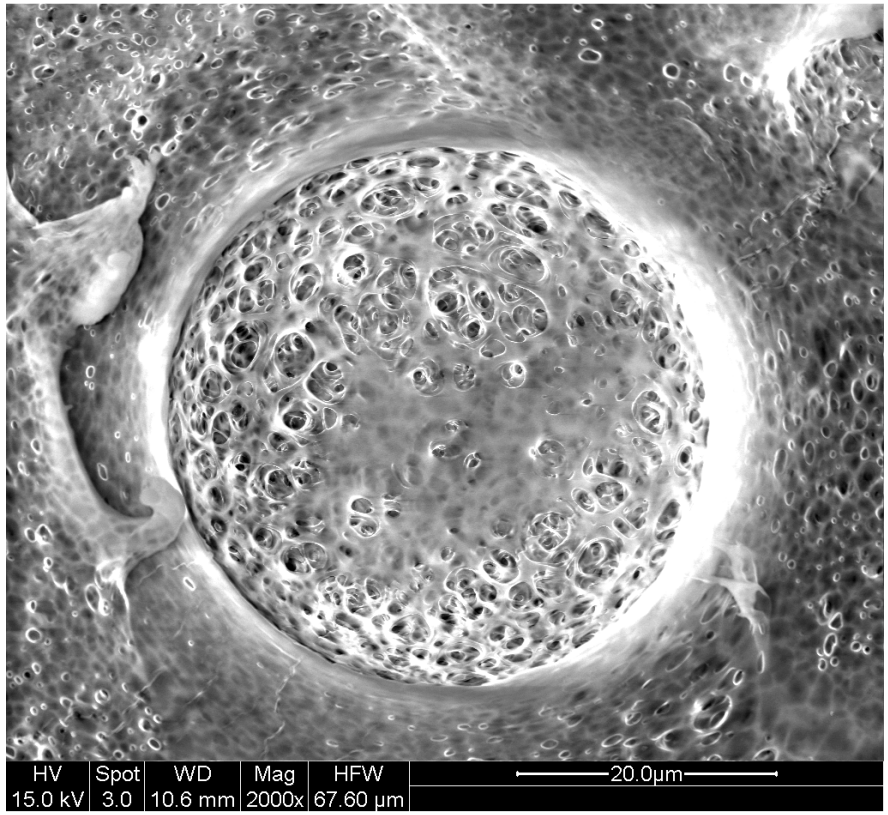

Figure IV-61 Surface of interlayer of SW 30 membrane exposed to Diesel at 2 000 magnification

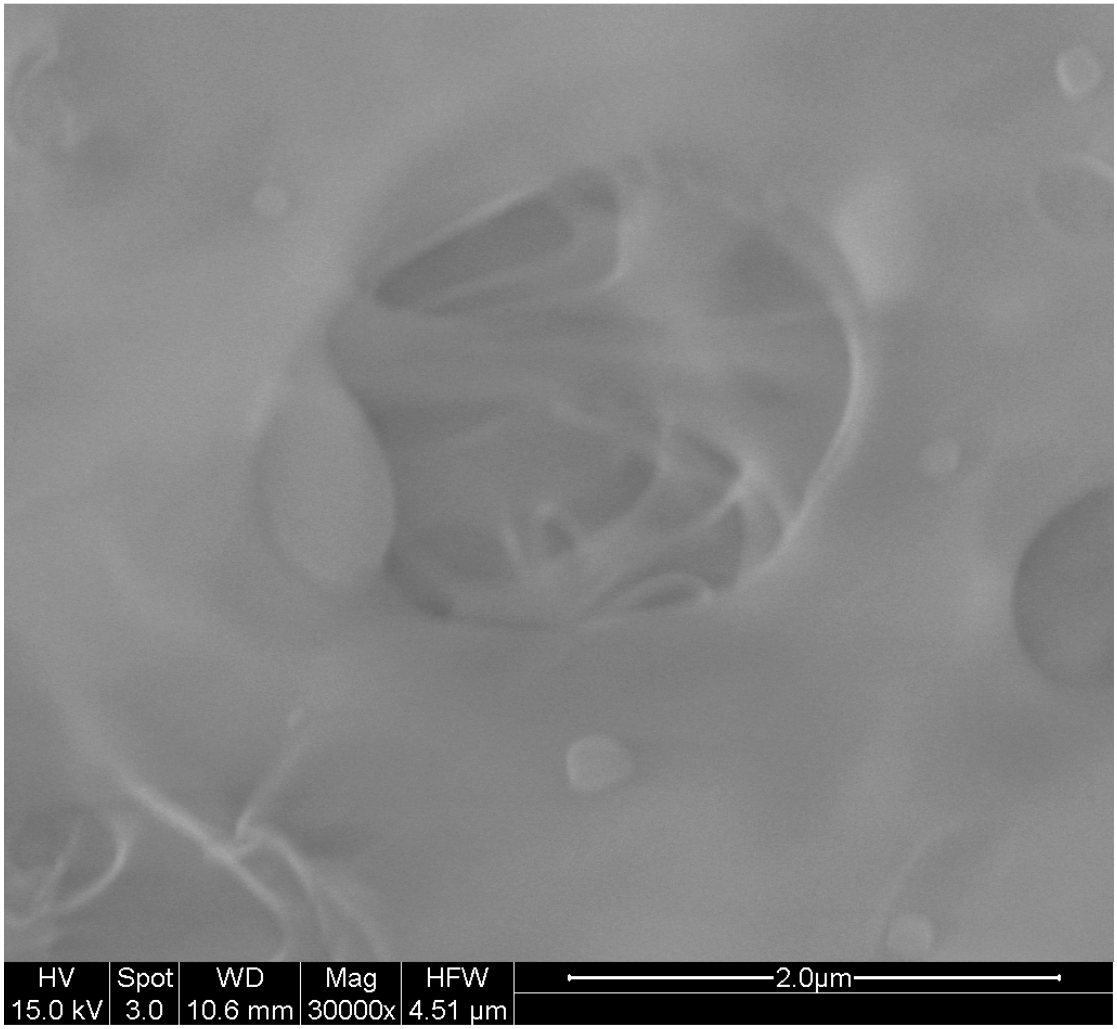

Figure IV-62 Surface of interlayer of SW 30 membrane exposed to Diesel at 30 000 magnification

CROSS-SECTION OF SW 30 MEMBRANE

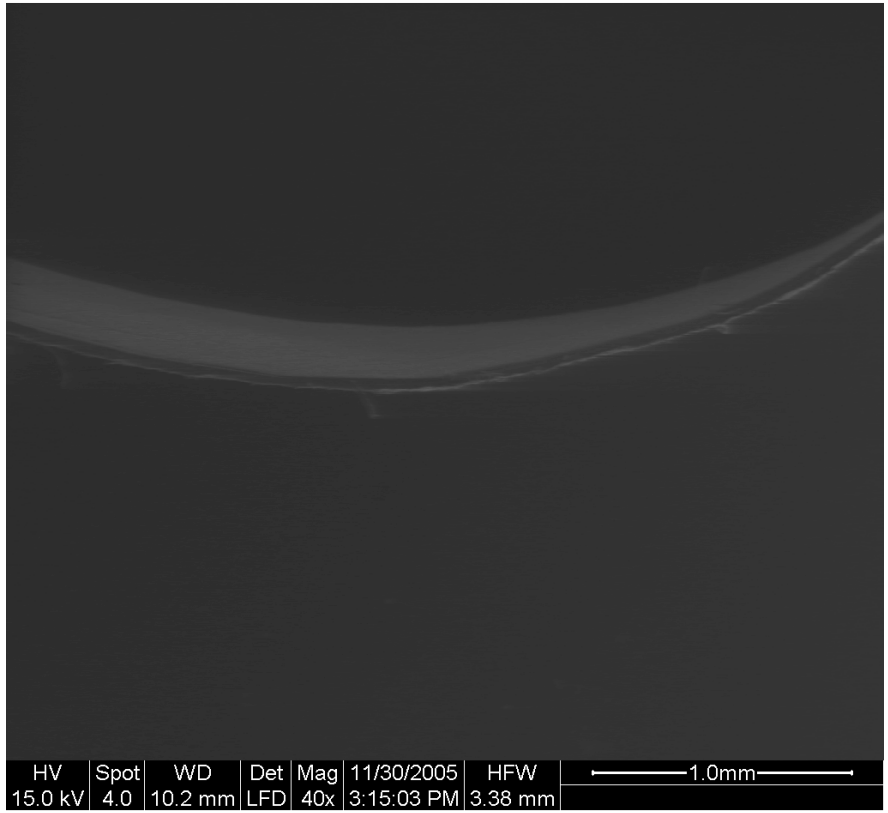

Figure IV-63 Cross Section of New SW 30 membrane at 40 magnification

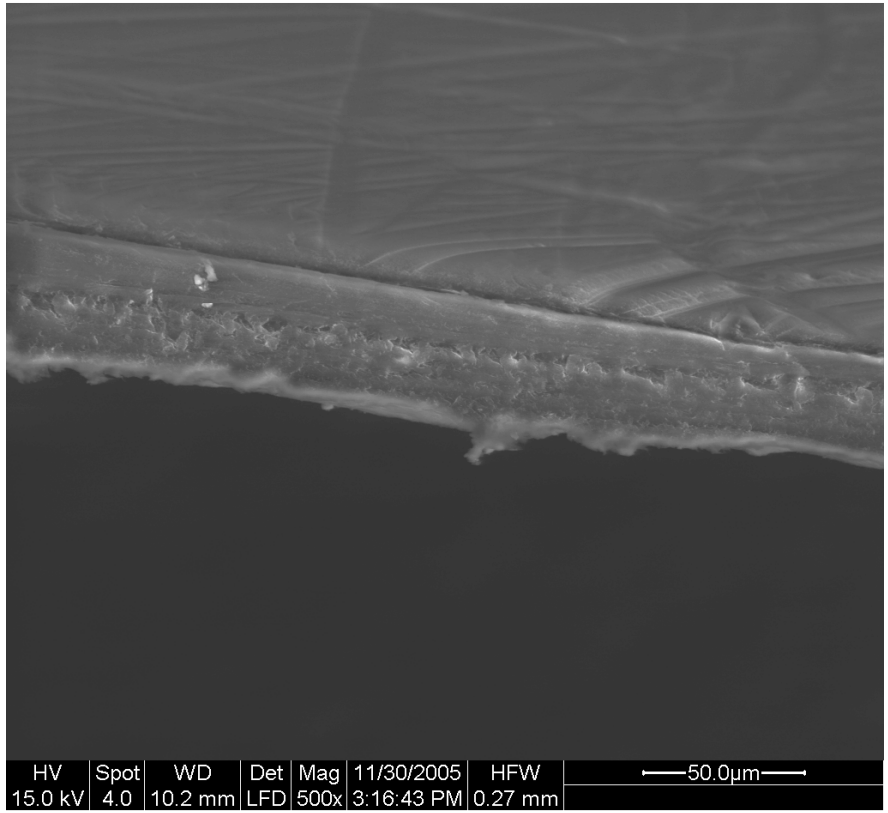

Figure IV-64 Cross Section of New SW 30 membrane at 500 magnification

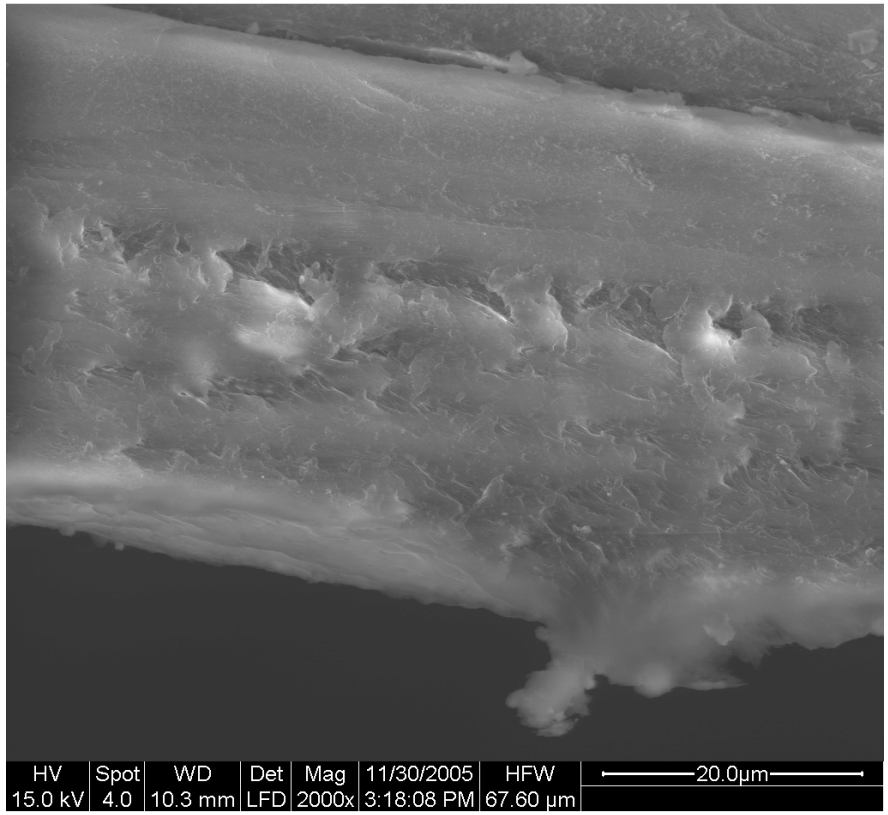

Figure IV-65 Cross Section of New SW 30 membrane at 2 000 magnification

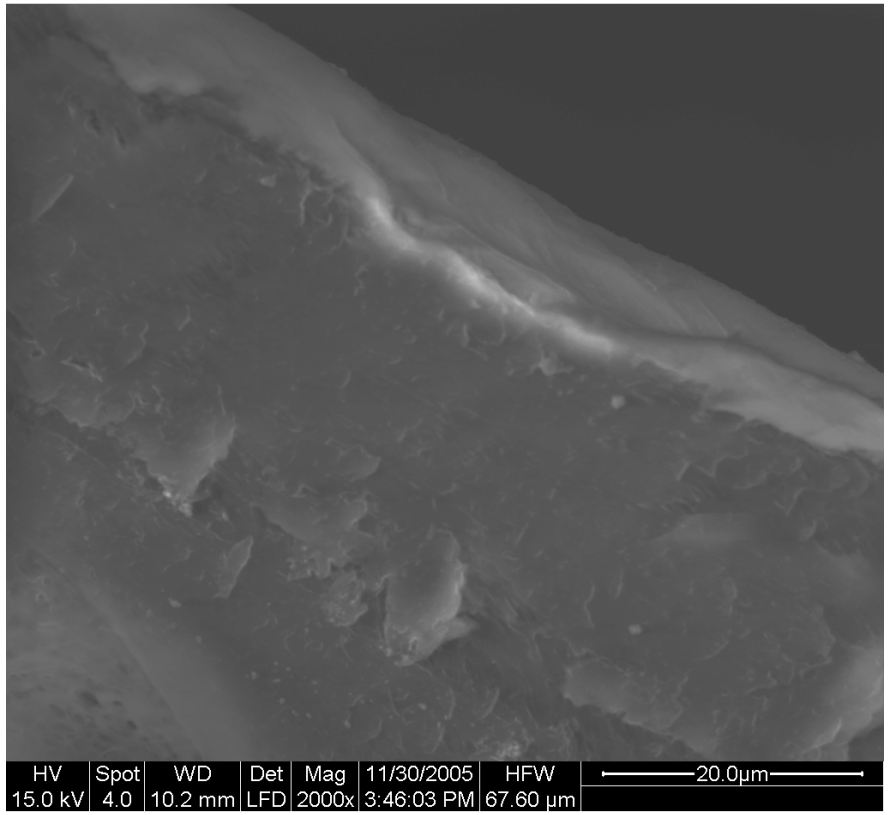

Figure IV-66 Cross Section of New SW 30 membrane at 2 000 magnification

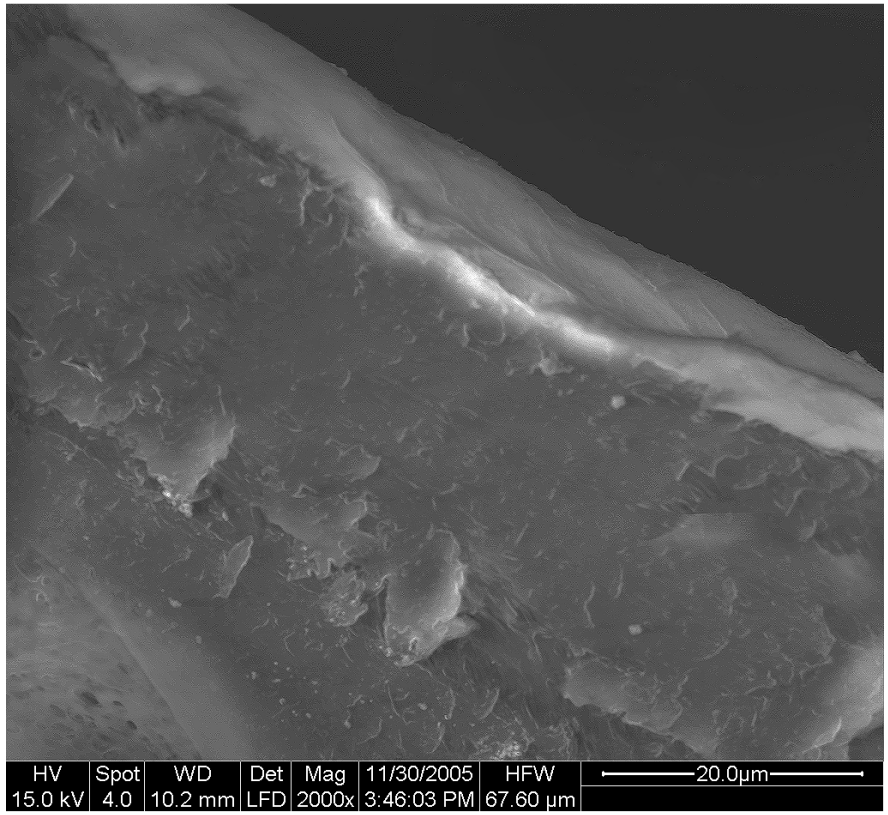

Figure IV-67 Cross Section of New SW 30 membrane at 2 000 magnification

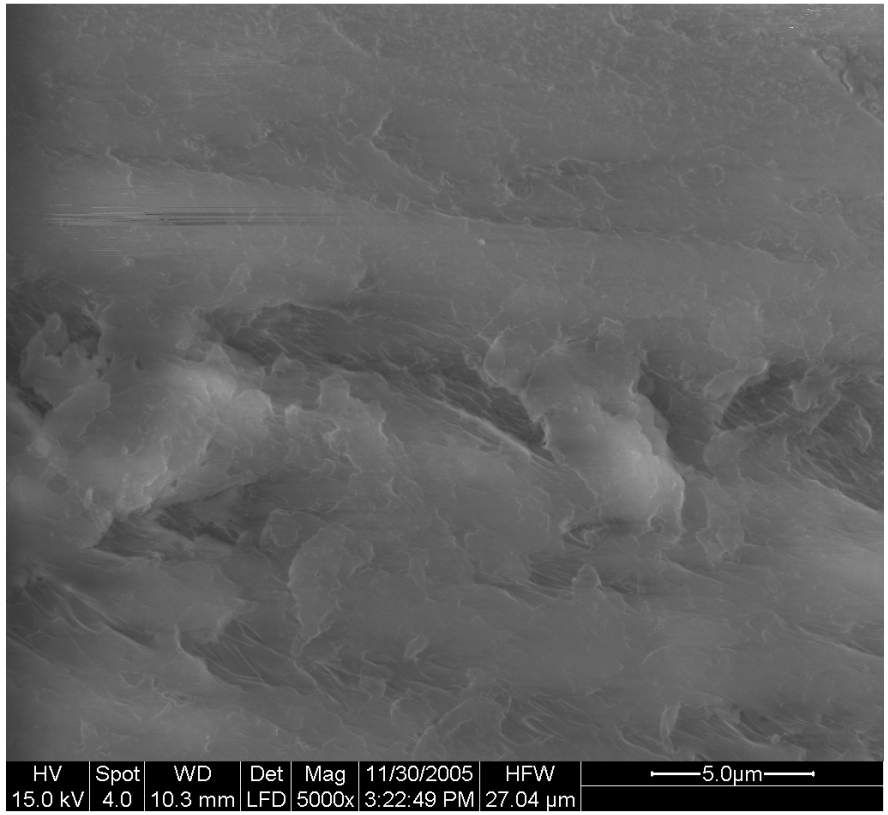

Figure IV-68 Cross Section of New SW 30 membrane at 5 000 magnification

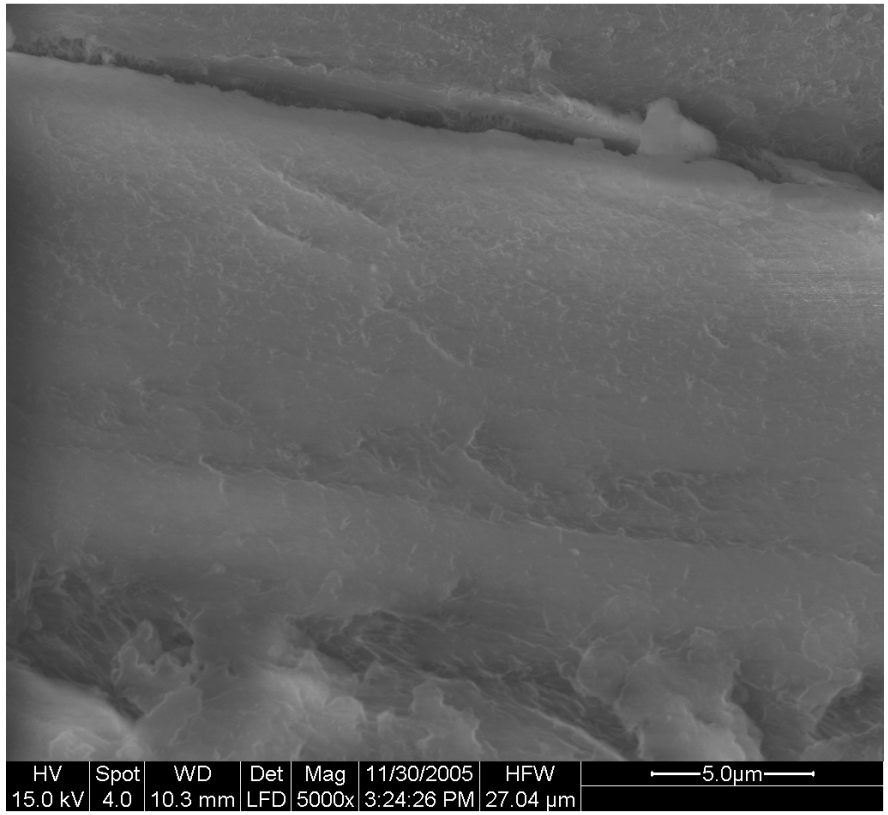

Figure IV-69 Cross Section of New SW 30 membrane at 5 000 magnification

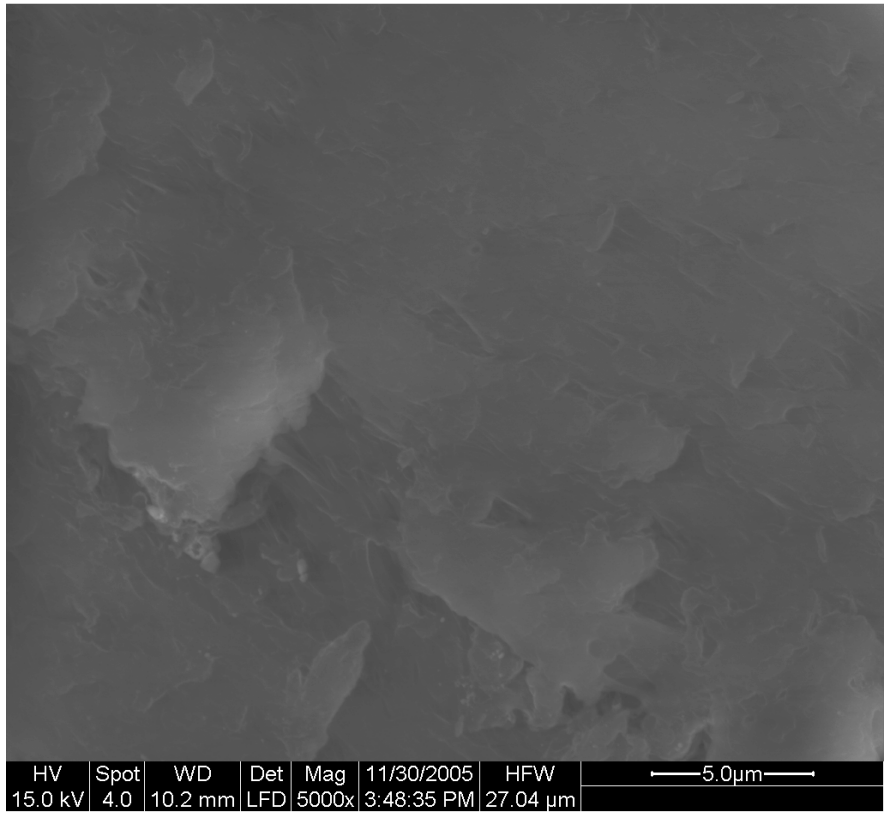

Figure IV-70 Cross Section of New SW 30 membrane at 5 000 magnification

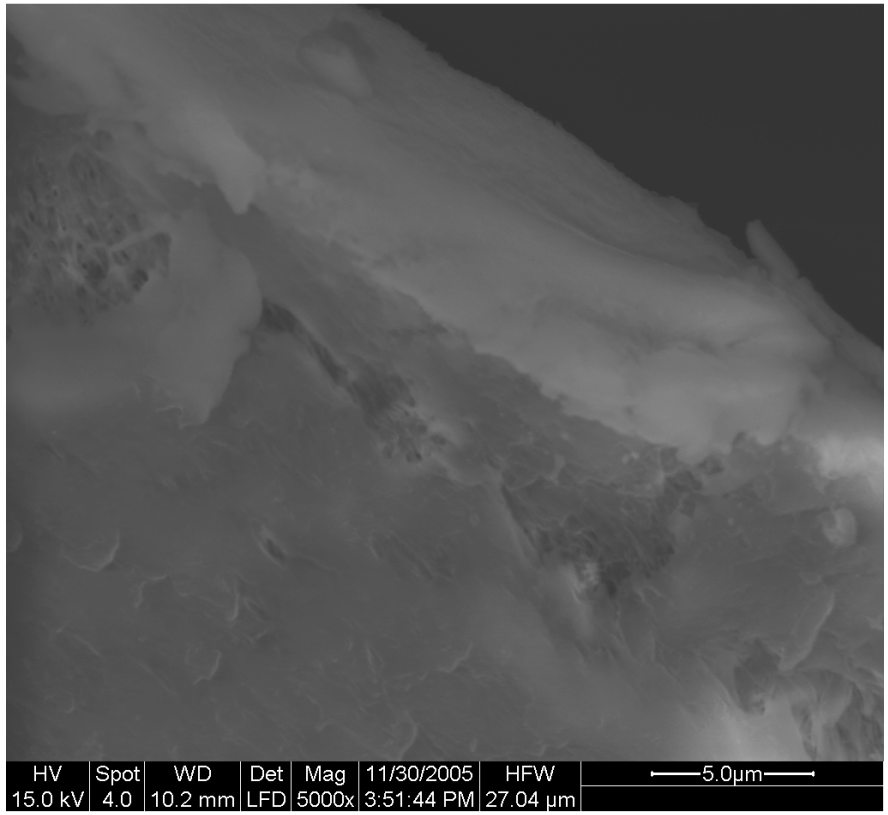

Figure IV-71 Cross Section of New SW 30 membrane at 5 000 magnification

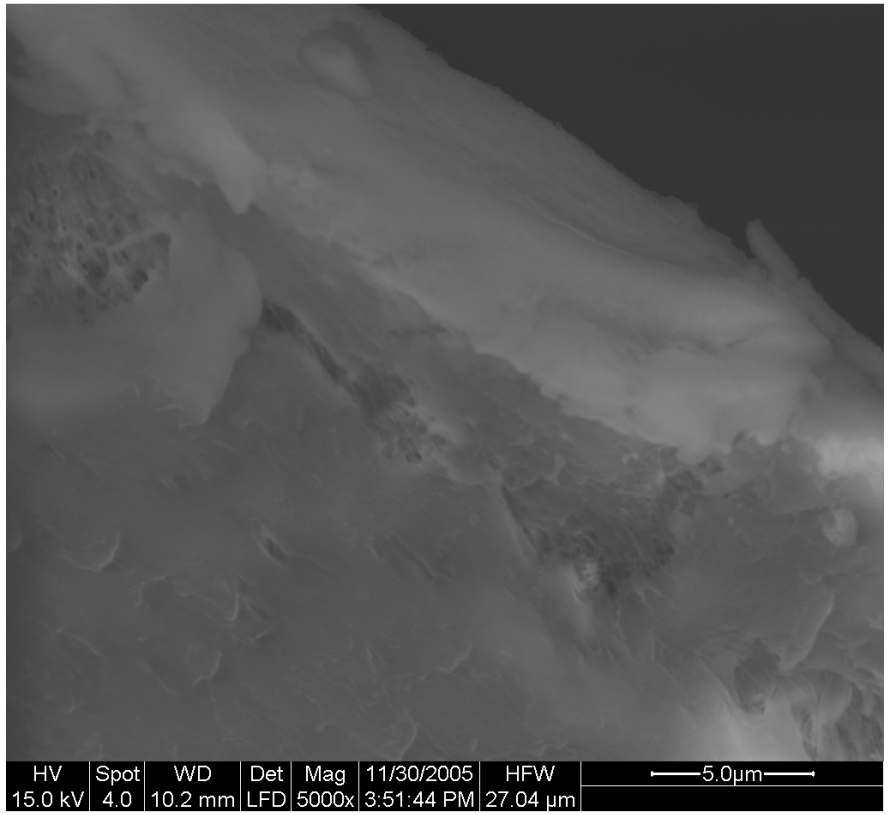

Figure IV-72 Cross Section of New SW 30 membrane at 5 000 magnification

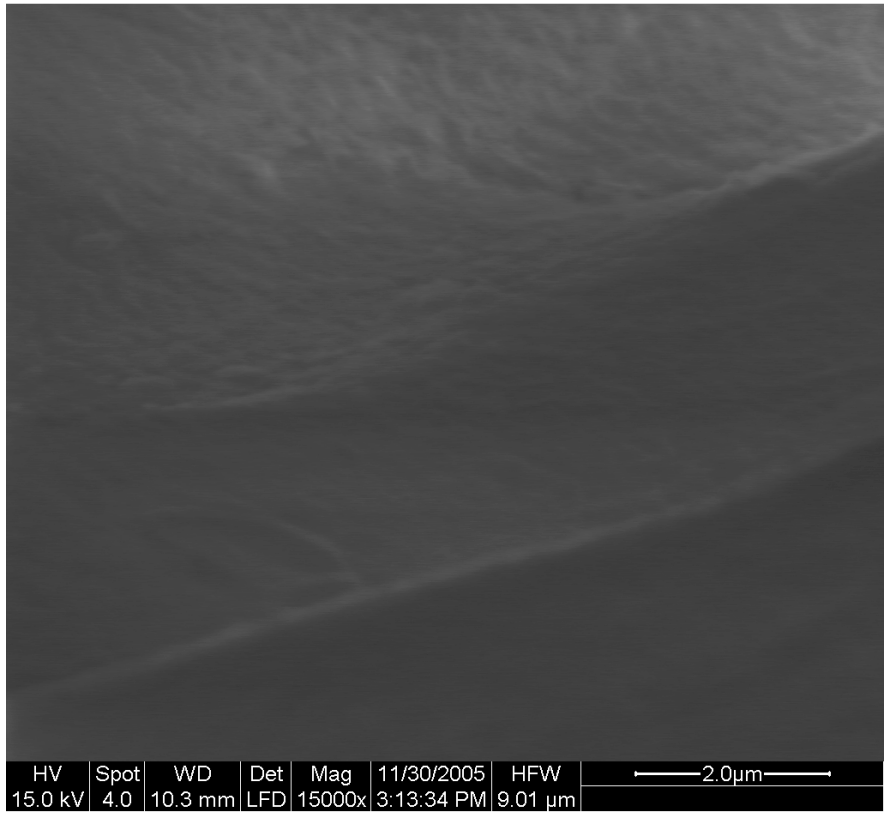

Figure IV-73 Cross Section of New SW 30 membrane at 15 000 magnification

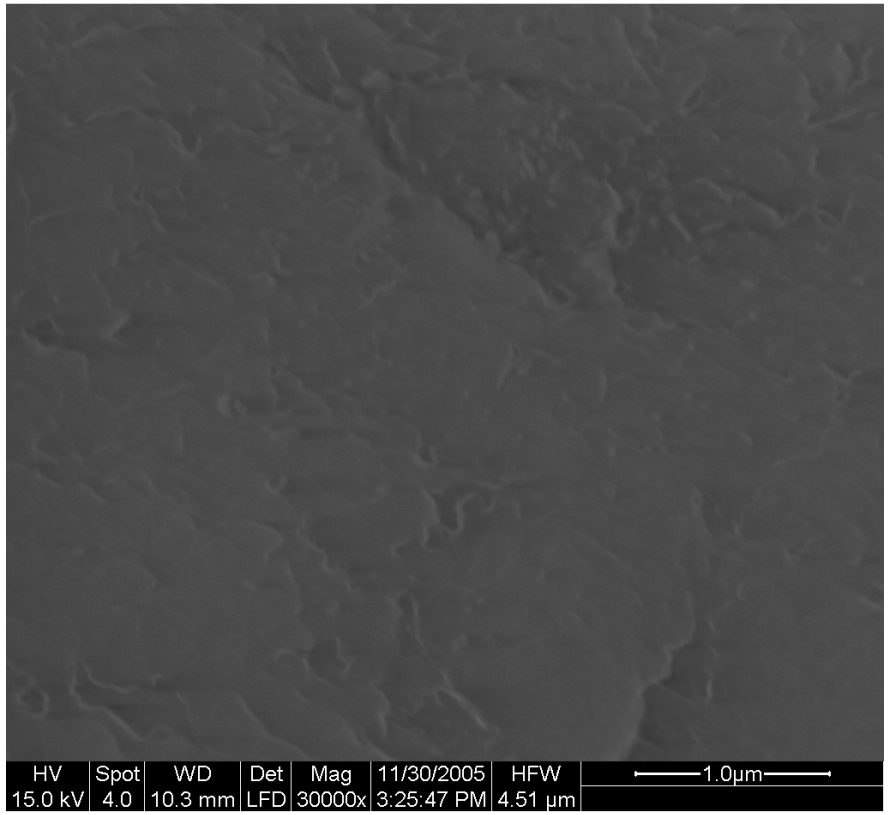

Figure IV-74 Cross Section of New SW 30 membrane at 30 000 magnification

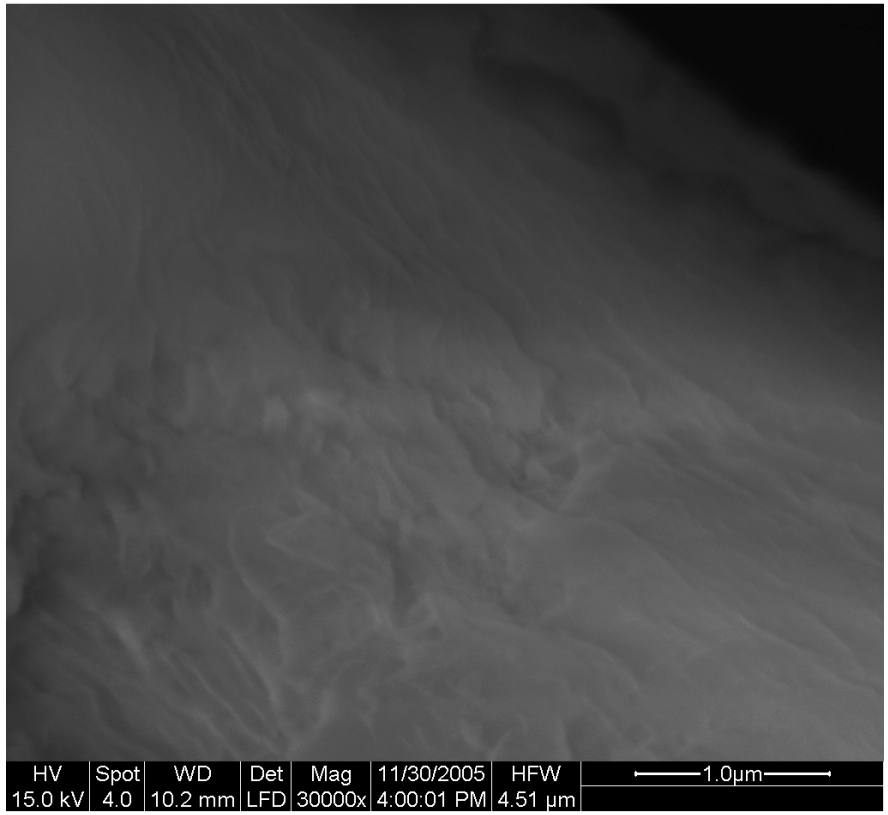

Figure IV-75 Cross Section of New SW 30 membrane at 30 000 magnification

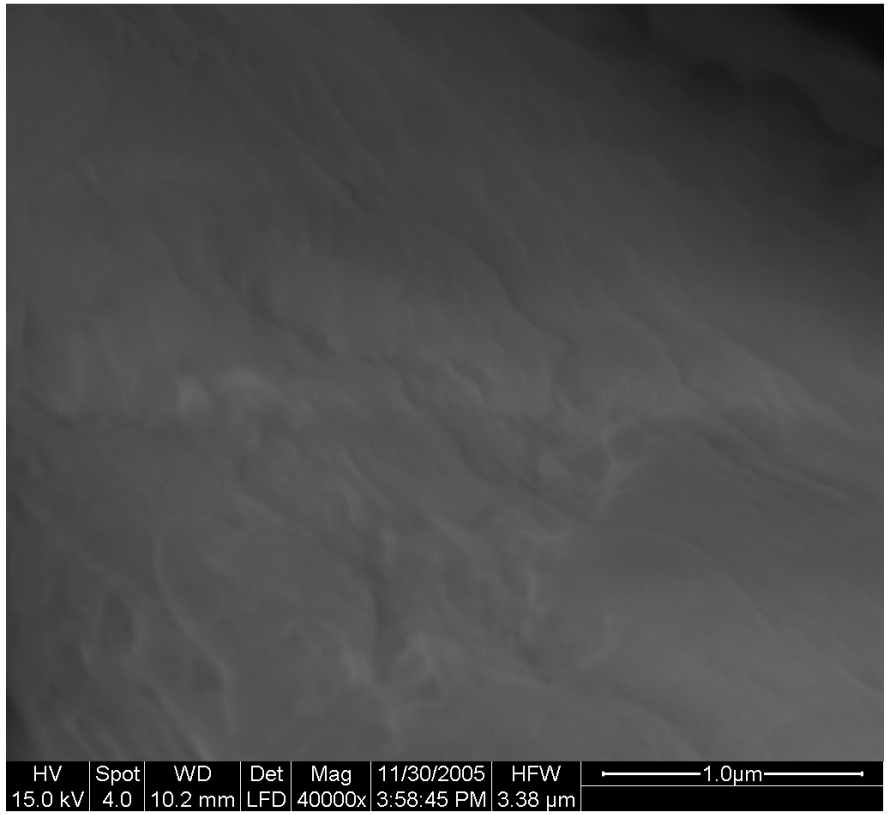

Figure IV-76 Cross Section of New SW 30 membrane at 40 000 magnification

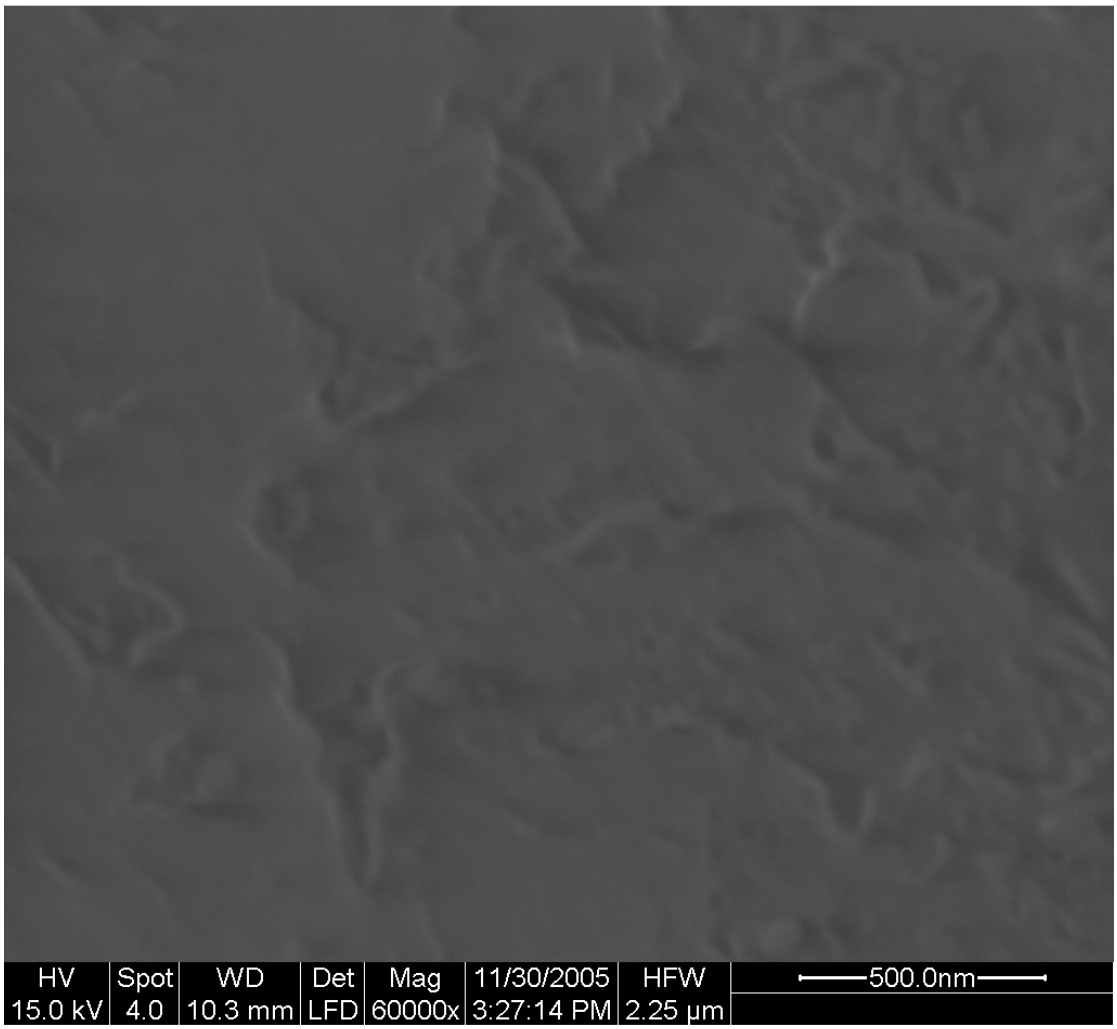

Figure IV-77 Cross Section of New SW 30 membrane at 60 000 magnification

Cross-Section of SW 30 Membrane exposed to pure Hexane

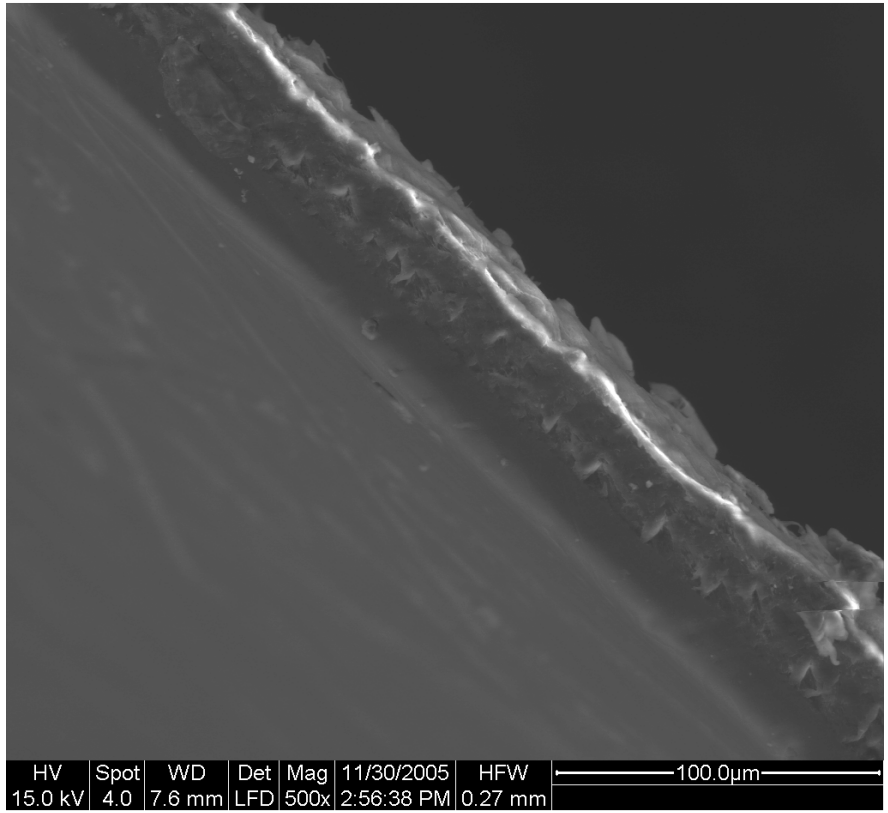

Figure IV-78 Cross Section of SW 30 membrane exposed to Pure Hexane at 500 magnification

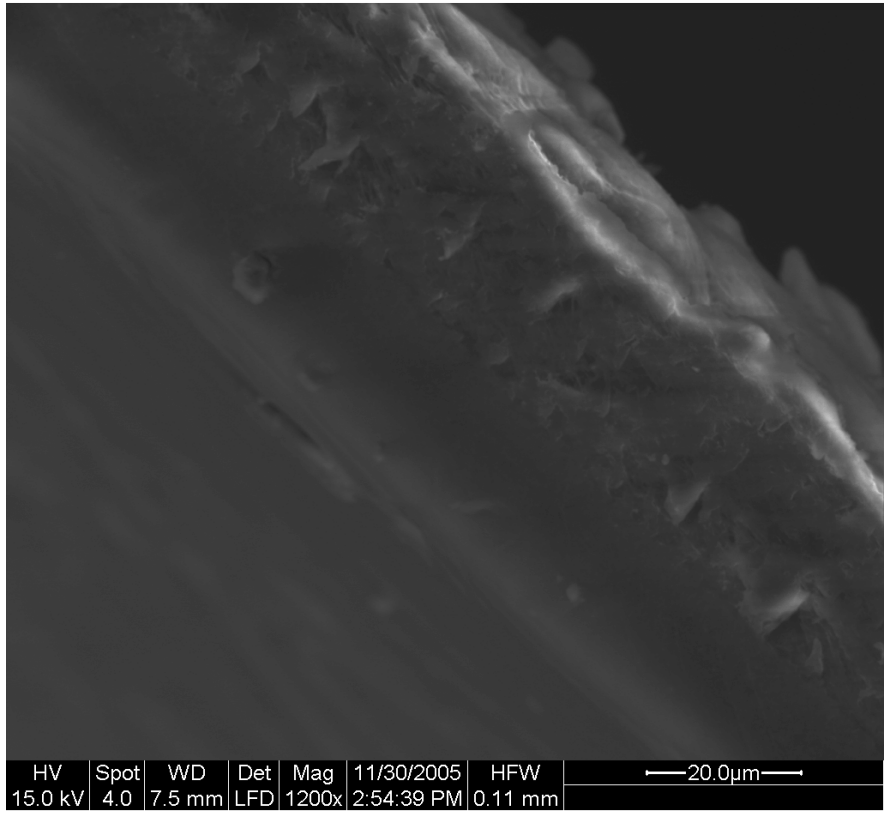

Figure IV-79 Cross Section of SW 30 membrane exposed to Pure Hexane at 1 200 magnification

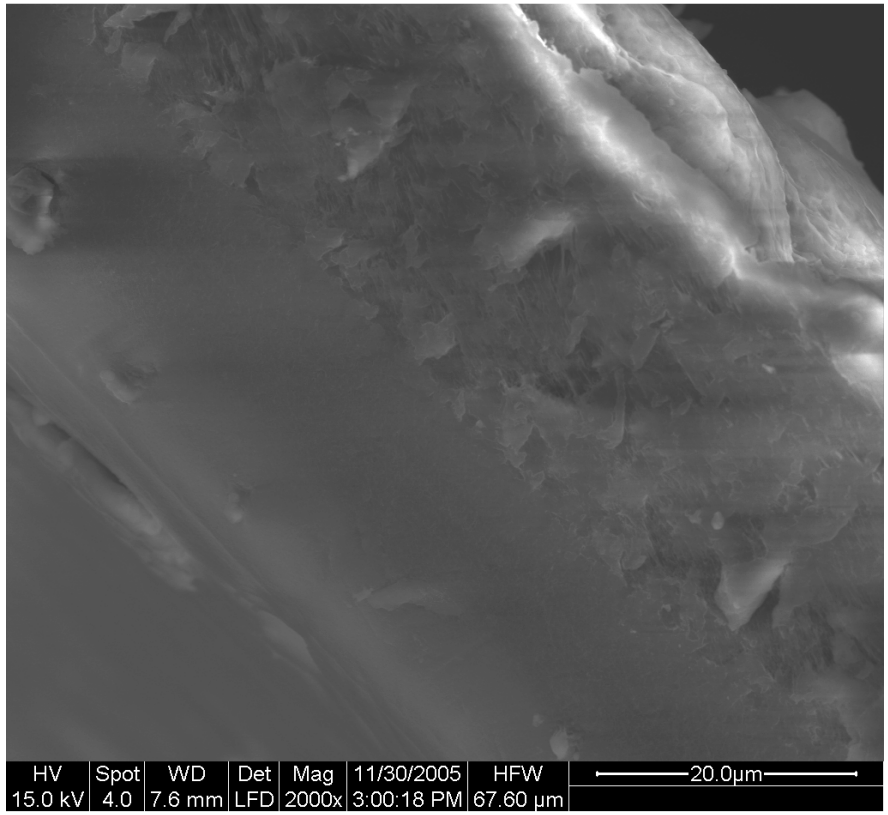

Figure IV-80 Cross Section of SW 30 membrane exposed to Pure Hexane at 2 000 magnification

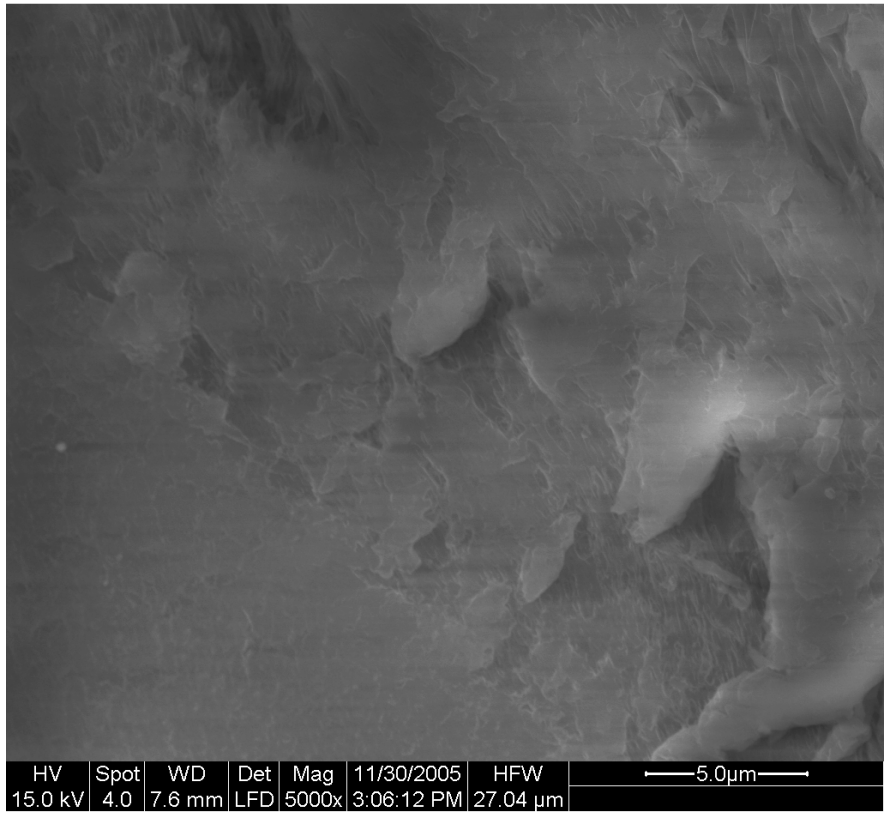

Figure IV-81 Cross Section of SW 30 membrane exposed to Pure Hexane at 5 000 magnification

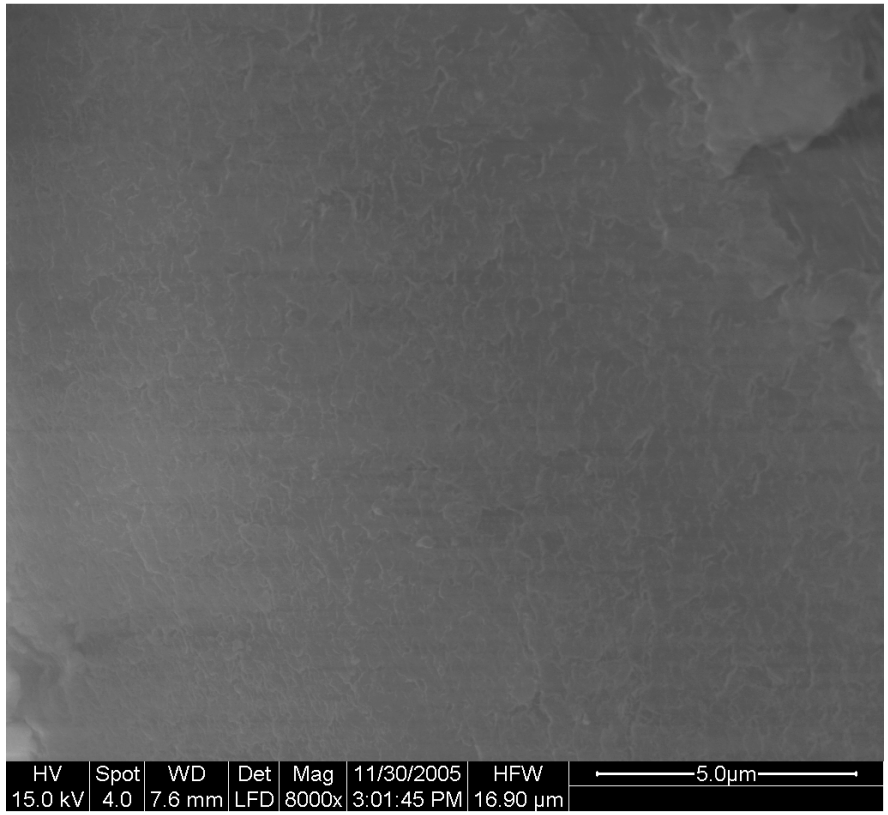

Figure IV-82 Cross Section of SW 30 membrane exposed to Pure Hexane at 8 000 magnification

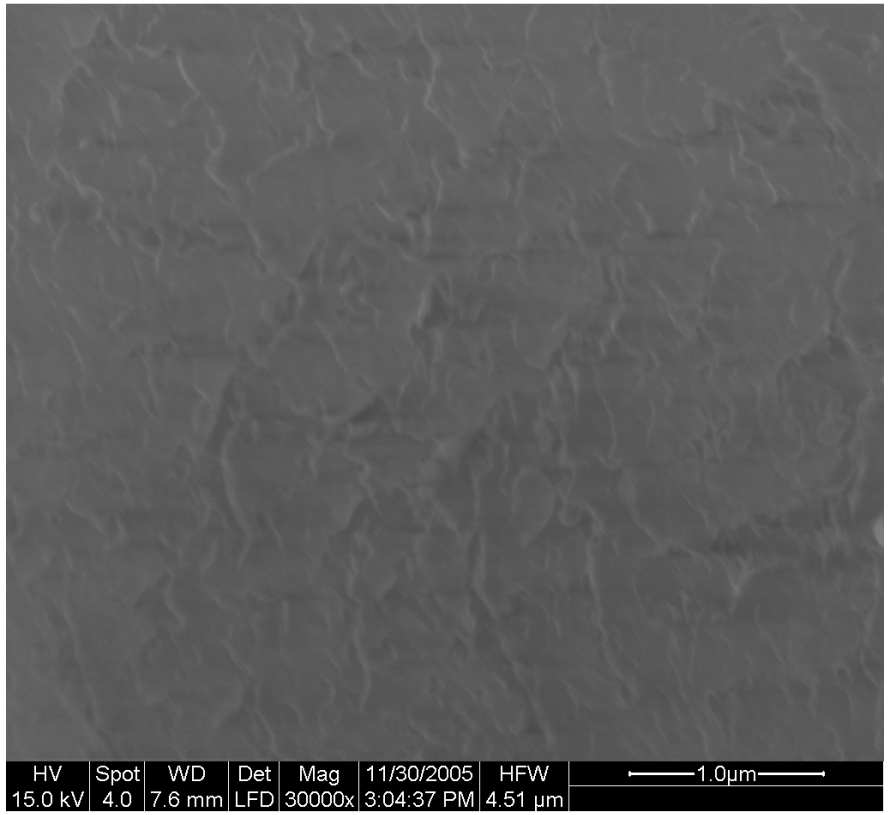

Figure IV-83 Cross Section of SW 30 membrane exposed to Pure Hexane at 30 000 magnification

ACTIVE LAYER OF BW 30 MEMBRANE

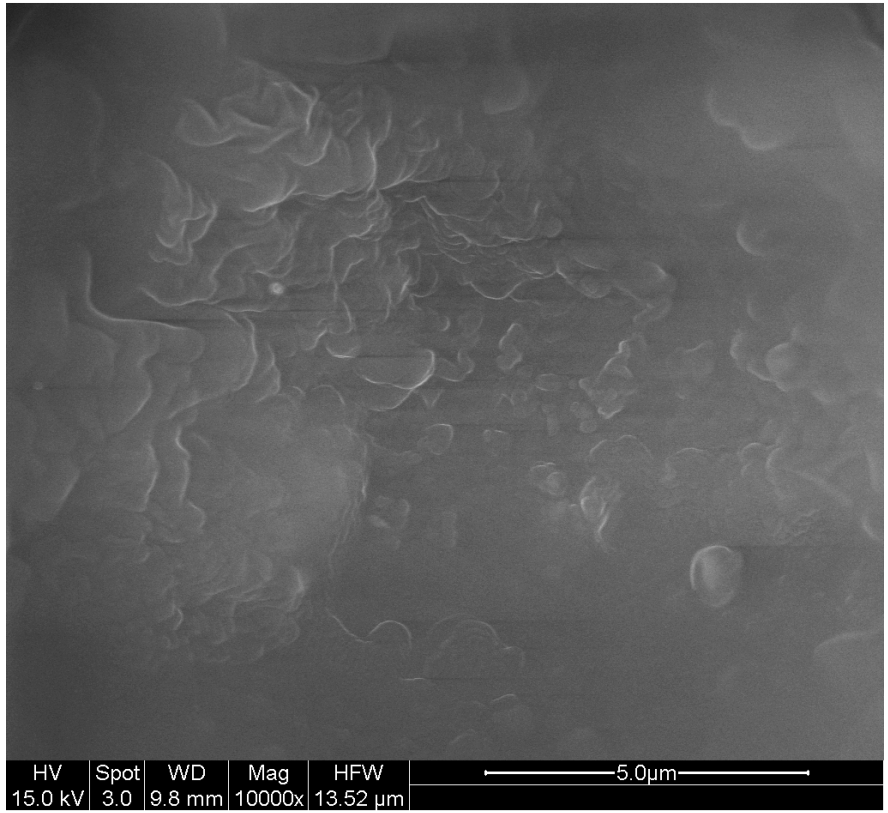

Figure IV-84 Active surface of BW 30 membrane at 10 000 magnification after exposure to Hexane

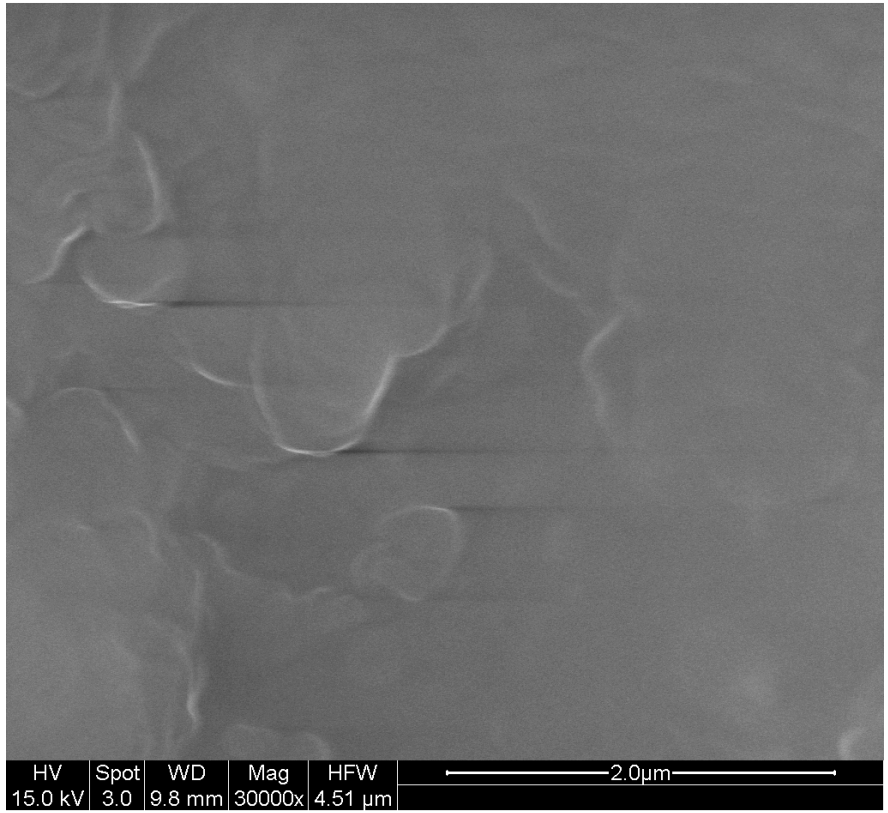

Figure IV-85 Active surface of BW 30 membrane at 30 000 magnification after exposure to Hexane

APPENDIX V: MECHANISM OF DAMAGE.

As postulated in the discussion, it is though that the mechanism of damage to the polysulfone layer of the SW30 seawater membrane involves a softening component as a result of exposure to the hydrocarbon which then leaves the membrane vulnerable to dimensional changes (involving the closure of the pores) with subsequent contact with high pressure feedwater. To confirm this the following test was carried out.

The fibrous backing layer was pealed from a new membrane sample and discarded. The remaining section of the membrane contained the active (polyamide) layer and the inter (polysulfone) layer. This section was then immersed in a container of hexane and sealed for twelve hours.

The membrane was carefully removed and allowed to dry. The sample was then mounted active surface down on a mounting plate and the inter layer of the membrane was then examined using a scanning electron microscope. Figures V-1 and V-2 are what was observed.

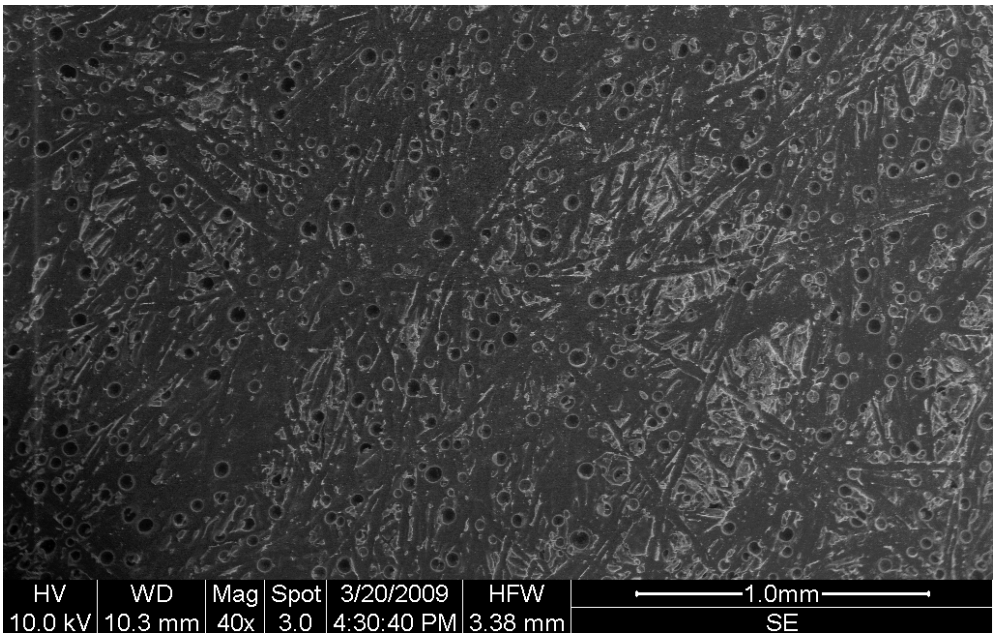

Figure V-1 Surface of treated interlayer of SW 30 membrane at 40 magnification

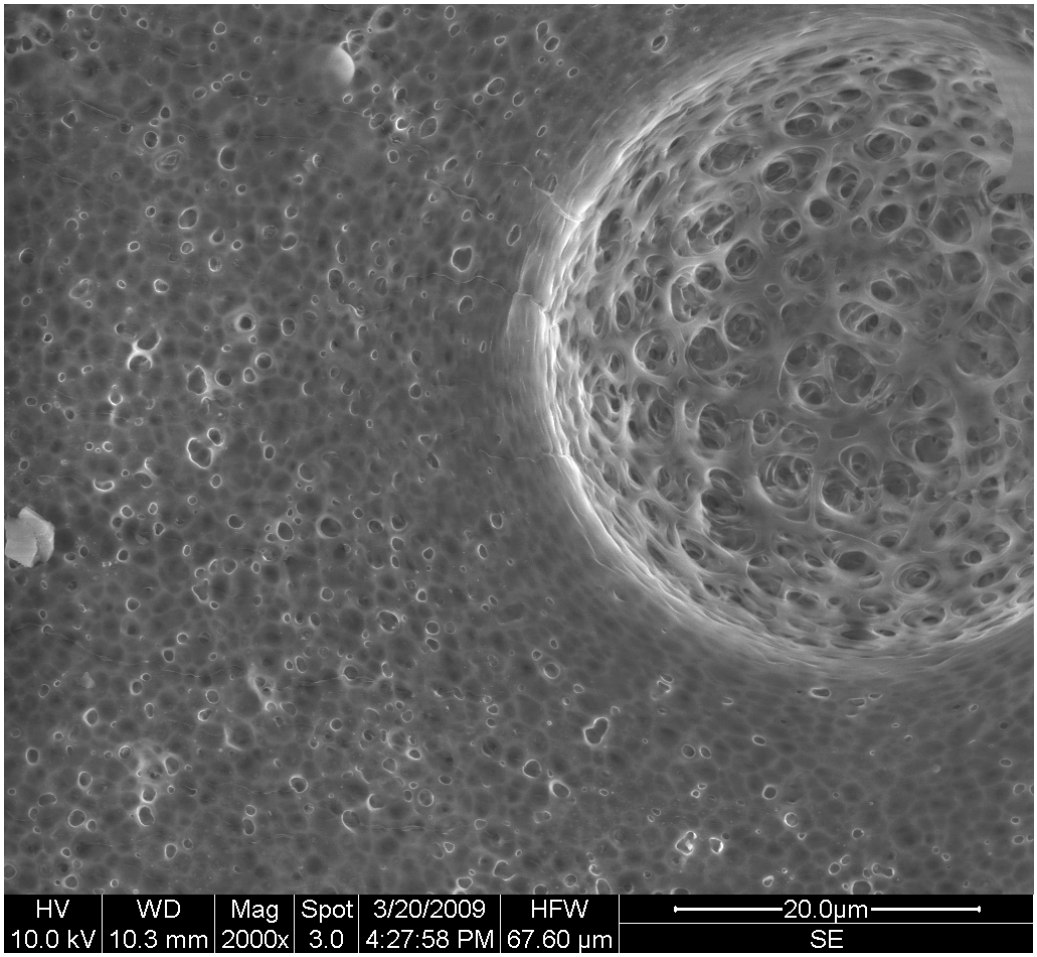

Figure V-2 Surface of treated interlayer of SW 30 membrane at 2000 magnification

It can be seen that the pores both small and large look more or less unaffected. Though the membrane substrate looks more gelatinous when compared to the sample in Figure 8-34 where it has not been exposed to hydrocarbons. This slight change in appearance could have been caused by the softening/swelling of the membrane polymer.

In short the major visible damage only occurs when the high pressure feed is applied to the membrane. In real life this softening of the membrane would occur over an extended period as the membrane is only slightly permeable to hydrocarbons. With the hydrocarbon present in the feed the damage would be gradual leading to the destruction of the useful properties of the membrane.

ABBREVIATIONS

RO	-	Reverse osmosis
SW	-	Sea Water
BW	-	Brackish Water
TFC	-	Thin Film Composite
CA	-	Cellulose acetate
CTA	-	Cellulose TriAcetate
SEM	-	Scanning Electron Microscope
AFM	-	Atomic Force Microscopy
TOC	-	Total Organic Carbon
TDS	-	Total Dissolved Solids
NaCl	-	Sodium Chloride (Salt)
ppm	-	Parts per million

Table 17 Abbreviations

REFERENCES

1 The Water Cycle Diagram, from USGS Water Science for Schools [Internet]. John M. Evans, USGS, Colorado District [cited 2008 September 18] Available from: http://ga.water.usgs.gov/edu/watercyclehi.html

2 Geography 40: Global Environmental Change [Internet]. University of California, Department of Geography; 2008 [cited 2008 Oct 28] Available from: http://geography.berkeley.edu/ProgramCourses/CoursePagesFA2002/Geog40/Geog40.Week11.html

3 Water resources. In Encyclopedia of Climate and Weather. Gleick, P. H.; 1996:, ed. by S. H. Schneider, Oxford University Press, New York, vol. 2, pp.817-823.

4 Aristotle (4th century BC) Meteorologica Book 2 Chapter 3 Quoted in : R. J. Forbes, (1970) “Short History of the Art of Distillation from the Beginnings Up to the Death of Cellier Blumenthal”. Brill Academic Publishers, Leiden, p14,

5 "desalination." Encyclopaedia Britannica. [Internet]. Encyclopaedia Britannica Online; 2008 [cited 2008 04 Aug] Available from http://www.britannica.com/EBchecked/topic/158740/desalination

6 Cardona E, Culotta S, Piacentino A. Energy saving with MSF-RO series desalination plants. Desalination. 2003 Feb ;153(1-3):167-171.

7 The Osmonics Filtration Spectrum [Internet]. [cited 2008 August 04] Available from http://www.liquidfiltration-products.com/LiquidFiltration/Osmonicsfiltraspec.html

8 Wagner Jorgen. Membranes – Materials, Structure, Limits Table 5 'Membrane Filtration Handbook Practical Tips and Hints'. 2nd edition: Osmonics Inc. p14. 2001

9 Glater J. The early history of reverse osmosis membrane development. Desalination. 1998 Sep ;117(1-3):297-309.

10 Farooque AM, Al-Amoudi A, Numata K. Degradation study of cellulose triacetate hollow fine-fiber SWRO membranes. Desalination. 1999 Oct ;123(2-3):165-171.

11 Pure Pak - Water Purification Systems [Internet]. [cited 2008 Oct 21] Available from: http://www.purepak.com/understandro.htm

12 Fujiwara N, Numata K, Kumano A, Ogino Y, Nagai M, Iwahashi H. The effect of heavy metal ions on the oxidation of cellulose triacetate membranes. Desalination. 1994 Jun ;96(1-3):431-439.

13 Dow Water Solutions: Figure 1.10 Schematic cross-section of a FILMTEC thin film composite membrane: Filmtec^{TM} Reverse Osmosis Membranes Technical Manual. p13 Dow Chemical Company.

14 Introduction to Reverse Osmosis, Filmtec membrane Elements Technical Manual, Filmtec Corporation, p10 1995.

15 Bott T R Fouling Notebook. Rugby: Institution of Chemical Engineers. 1990

16 Package assembly for piperazine-based membranes - Patent 7156997 [Internet]. [cited 2008 Oct 24] Available from: http://www.freepatentsonline.com/7156997.html

17 Boerlage SFE, Kennedy MD, Aniye MP, Abogrean EM, Galjaard G, Schippers JC. Monitoring particulate fouling in membrane systems. Desalination. 1998 Sep 20;118(1-3): Conference Membranes in Drinking and Industrial Water Production,131-142.

18 Pervov AG. Scale formation prognosis and cleaning procedure schedules in reverse osmosis systems operation. Desalination. 1991 Sep ;83(1-3):77-118.

19 Lee S, Kim J, Lee C. Analysis of $CaSO_4$ scale formation mechanism in various nanofiltration modules. Journal of Membrane Science. 1999 Oct ;163(1):63-74.

20 Flemming H-, Schaule G, Griebe T, Schmitt J, Tamachkiarowa A. Biofouling--the Achilles heel of membrane processes. Desalination. 1997 Nov 30;113(2-3) , Workshop on Membranes in Drinking Water Production Technical Innovations and Health Aspects:215-225.

21 Sunggyu Lee and Lee Lee, Encyclopedia of Chemical Processing, Published by CRC Press 2005 page 1051

22 Baker JS, Dudley LY. Biofouling in membrane systems — A review. Desalination. 1998 Sep ;118(1-3):81-89.

23 Bos R, van der Mei HC, Busscher HJ. Physico-chemistry of initial microbial adhesive interactions - its mechanisms and methods for study. FEMS Microbiology Reviews. 1999 Apr ;23(2):179-229.

24 Al-Ahmad M, Aleem FAA, Mutiri A, Ubaisy A. Biofuoling in RO membrane systems Part 1: Fundamentals and control. Desalination. 2000 Dec ;132(1-3):173-179.

25 Dow Water Solutions: Section 2.7 Prevention of Fouling by Organics: Filmtec™ Reverse Osmosis Membranes Technical Manual. p63 Dow Chemical Company.

26 Northeastern University [Internet]. The Humic Acid Research Group, Humic Acid, 2004 [cited 2008 Oct 21] SEM Image, Available from http://www.hagroup.neu.edu/haSEM.htm

27 Cornel PK, Summers RS, Roberts PV. Diffusion of humic acid in dilute aqueous solution. Journal of Colloid and Interface Science. 1986 Mar ;110(1):149-164.

28 Uyguner CS, Suph SA, ag, Kerc A, Bekbolet M. Evaluation of adsorption and coagulation characteristics of humic acids preceded by alternative advanced oxidation techniques. Desalination. 2007 Jun ;210(1-3):183-193.

29 Corin N, Backlund P, Wiklund T. Bacterial growth in humic waters exposed to UV-radiation and simulated sunlight. Chemosphere. 1998 Apr ;36(9):1947-1958.

30 Northeastern University (2004) The Humic Acid Research Group, [Internet].About Humic Substances [cited 2008 Oct 21] Available from: http://www.hagroup.neu.edu/abouthafrm.htm

31 Beckett R, Jue Z, Giddings JC. Determination of molecular weight distributions of fulvic and humic acids using flow field-flow fractionation. Environ. Sci. Technol. 1987 Mar 1;21(3):289-295.

32 Yuan W, Zydney AL. Humic acid fouling during microfiltration. Journal of Membrane Science. 1999 May ;157(1):1-12.

33 Almendros G, Sanz J. Structural study on the soil humin fraction—boron trifluoride-methanol transesterification of soil humin preparations. Soil Biology and Biochemistry. 23(12):1147-1154.

34 G. Almendros et al., "Preservation of aliphatic macromolecules in soil humins," Organic Geochemistry 24, no. 6-7 (July 1996): 651-659.

35 Stevenson F.J.: Model structure of Humic Acid, Humus chemistry. Genesis, composition, reactions. John Wiley and Sons. 1982

36 Sarah A. Green, Francois M. M. Morel, and Neil V. Blough, "Investigation of the electrostatic properties of humic substances by fluorescence quenching," Environmental Science & Technology 26, no. 2 (February 1, 1992): 294-302

37 A. Maartens, P. Swart, and E. P. Jacobs, "Humic membrane foulants in natural brown water: characterization and removal," Desalination 115, no. 3 (August 1998): 215-227.

38 Bassam Tawabini, Hraj Kharajian, and Nabil Fayad, "Trihalomethanes (THMs) formation in a distillation process," Desalination 66 (December 1987): 403-414.

39 J.J. Rook , Formation of Haloforms During Chlorination of Natural Waters. Water Trtmt & Exam. 23 (1974), p. 234-243. Quoted in : N. A. Latif, F. M. Al-Awadi, and B. A. Colenutt, "Trihalomethanes (THMs) formation in multi-stage flash (MSF) distillation plants," Desalination 74: 205-226.

40 Stevenson F.J.: Properties of Humic Substances, Humus chemistry. Genesis, composition, reactions. John Wiley and Sons. 1982

41 K. Ghosh and M. Schnitzer, Macromolecular structures of humic substances. Soil Sci. 129 5 (1980), p. 266.

42 Masataka Hiraide et al., "Rapid separation of humic acid in fresh waters by coprecipitation and flotation," Microchimica Acta 92, no. 4 (July 1, 1987): 137-142.

43 Amy E. Childress and Menachem Elimelech, "Effect of solution chemistry on the surface charge of polymeric reverse osmosis and nanofiltration membranes," Journal of Membrane Science 119, no. 2 (October 1996): 253-268.

44 A. I. Schäfer, A. G. Fane, and T. D. Waite, "Nanofiltration of natural organic matter: Removal, fouling and the influence of multivalent ions," Desalination 118, no. 1-3 (September 1998): 109-122.

45 Arza Seidel and Menachem Elimelech, “Coupling between chemical and physical interactions in natural organic matter (NOM) fouling of nanofiltration membranes: implications for fouling control,” Journal of Membrane Science 203, no. 1-2 (June 2002): 245-255.

46 Seungkwan Hong and Menachem Elimelech, “Chemical and physical aspects of natural organic matter (NOM) fouling of nanofiltration membranes,” Journal of Membrane Science 132, no. 2 (September 1997): 159-181.

47 S.G. Yiantsios, D. Sioutopoulos, and A.J. Karabelas, “Colloidal fouling of RO membranes: an overview of key issues and efforts to develop improved prediction techniques,” Desalination 183, no. 1-3 (November 2005): 257-272.

48 J. Lowe and Md.M. Hossain, “Application of ultrafiltration membranes for removal of humic acid from drinking water,” Desalination 218, no. 1-3 (January 2008): 343-354.

49 Raffaele Molinari, Pietro Argurio, and Leonardo Romeo, “Studies on interactions between membranes (RO and NF) and pollutants (SiO_2, NO_3^-, Mn^{++} and humic acid) in water,” Desalination 138, no. 1-3 (September 2001): 271-281.

50 Gary Amy, “Fundamental understanding of organic matter fouling of membranes,” Desalination 231, no. 1-3 (October 2008): 44-51.

51 Amy E. Childress, Shivaji S. Deshmukh "Effect of humic substances and anionic surfactants on the surface change and performance of reverse osmosis membranes." Desalination volume 118, Pages 167-174 (1998).

52 Harvey Winters, “Control of organic fouling at two seawater reverse osmosis plants,” Desalination 66 (December 1987): 319-325.

53 S.A. Al Malek and A.M.O. Mohamed, “Environmental impact assessment of off shore oil spill on desalination plant,” Desalination 185, no. 1-3 (November 2005): 9-30.

54 Mohammadi, T., M. Kazemimoghadam, and M. Saadabadi. "Modeling of membrane fouling and flux decline in reverse osmosis during separation of oil in water emulsions." Desalination 157.1-3 (2003): 369-75.

55 Hodgkiess, T. et al. "Effect of hydrocarbon contaminants on the performance of RO membranes." Desalination 138.1-3 (2001): 283-89.

56 B. Van der Bruggen et al. ”Nanofiltration as a treatment method for the removal of pesticides from ground waters.” Desalination 117 1-3 (1998): 139-147

57 n-Hexane. (2005). Available from <http://www.ilo.org/public/english/protection/safework/cis/products/icsc/dtasht/_icsc02/icsc0279.htm>

58 Diesel Fuel No.2. (2004). Available from <http://www.ilo.org/public/english/protection/safework/cis/products/icsc/dtasht/_icsc15/icsc1561.htm>

59 Vejella V., "Re-commissioning of a RO Test Rig and Performance Analysis of Sulphate Reducing Membrane," M.Sc Course Project Report, Department of Mechanical Engineering, University of Glasgow. (September2006)

60 Marsh, Allyn R. (Eden Prairie, MN, US), Schaffenberg, Russ (Bloomington, MN, US), Jons, Steven D. (Eden Prairie, MN, US), Davis, Roy A. (Midland, MI, US). Package assembly for piperazine-based membranes - Patent 7156997 [Internet]. [cited 2008 Oct 20] Available from: http://www.freepatentsonline.com/7156997.html

61 Maria Tomaszewska et al., "Treatment of bilge water using a combination of ultrafiltration and reverse osmosis," Desalination 185, no. 1-3 (November 2005): 203-212.

62 Chemical Resistance guide p1-3 [Internet]. Liqui-Cel Membrane Contractors. [cited 2008 August 04] Available from http://www.liqui-cel.com/documents/Chemical GD_rev5 10_05.pdf

63 Chemical Resistance Chart [Internet]. K-mac Plastics. [cited 2008 August 04] Available from: http://k-mac-plastics.com/data sheets/PC-PSU-PES-PEEK-PPS-PVDF-Chemical.htm

64 Ali Rafe, Seyed Mohammad Ali Razavi, Water and hexane permeate flux through UF polysulfone amide membrane, Desalination, Volume 236, Issues 1-3, International Membrane Science and Technology Conference 2007, International Membrane Science and Technology Conference 2007, 31 January 2009, Pages 39-45

65 Causserand C. Et al. "Degradation of polysulfone membranes due to contact with bleaching solution" Desalination 199 1-3 (2006) 70-72

66 Cadotte JE, King RS, Majerle RJ, Petersen RJ. Interfacial Synthesis in the Preparation of Reverse Osmosis Membranes. Journal of Macromolecular Science, Part A. 1981 Apr ;Volume 15(Issue 5):727 - 755 .

67 Khaled A. Mohamed, Minimize the negative impact of oil contamination on Abu Dhabi power and desalination plants, Desalination Volume 204, Issues 1-3, , EuroMed 2006 - Conference on Desalination Strategies in South Mediterranean Countries, 5 February 2007, Pages 113-120.